جمهورية العراق
وزارة التعليم العالي و البحث العلمي
جامعة بابل/كلية الهندسة
قسم الهندسة الميكانيكية

التحليل العددي لانتقال الحرارة وجريان المائع المار بشكل متعامد على اسطوانة مهتزة بحساءة

رسالة
مقدمة إلى كلية الهندسة في جامعة بابل

كجزء من متطلبات نيل درجة ماجستير علوم

في الهندسة الميكانيكية

أعدت من قبل

محسن غاوي حمزة الجبوري
بكالوريوس هندسة ميكانيكية، ٢٠٠٣

٢٠٠٧ ميلادي
١٤٢٨هجري

Republic of Iraq
Ministry of Higher Education
and Scientific Research
Babylon University
College of Engineering
Dept. of Mech. Eng.

NUMERICAL ANALYSIS OF HEAT TRANSFER AND FLUID FLOW OVER A RIGIDLY VIBRATING CYLINDER IN CROSS FLOW

A THESIS SUBMITTED TO THE COLLEGE OF ENGINEERING
OF THE UNIVERSITY OF BABYLON IN PARTIAL
FULFILLMENT
OF THE REQUIREMENTS FOR THE

DEGREE OF MASTER OF

SCIENCE IN MECHANICAL

ENGINEERIN

By

MOHSEN GAWY HAMZA AL-GUBOURY

B.Sc., ٢٠٠٣

٢٠٠٧ A.D. **١٤٢٨**
Hijry

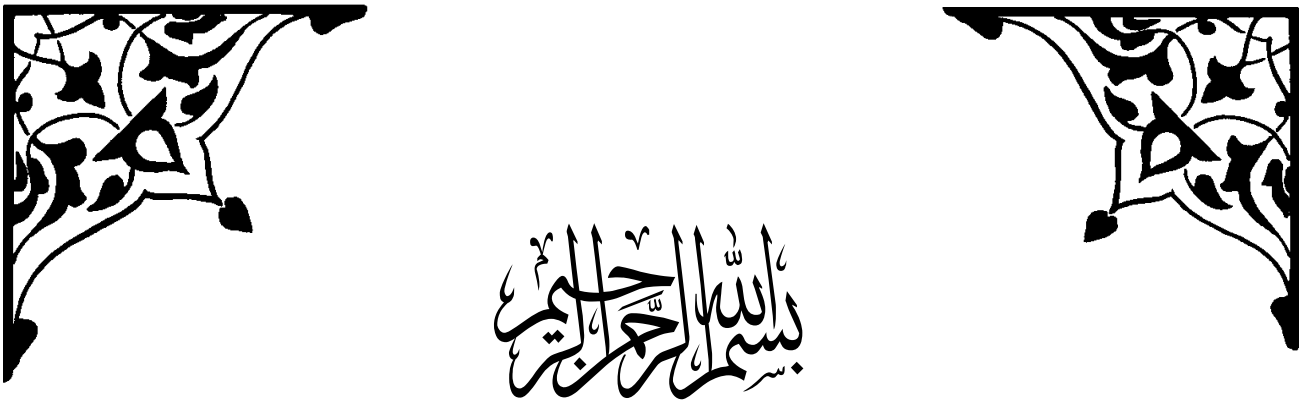

﴿اللهُ نُورُ ٱلسَّمَاوَاتِ والأرض مَثَلُ نُورِهِ كَمِشْكَاةٍ فِيهَا مِصْبَاحٌ ٱلْمِصْبَاحُ فِي

زُجَاجَةٍ ٱلزُّجَاجَةُ كَأَنَّهَا كَوْكَبٌ دُرِّيٌّ يُوقَدُ مِن شَجَرَةٍ مُّبَارَكَةٍ زَيْتُونَةٍ لا شَرْقِيَّةٍ

وَلا غَرْبِيَّةٍ يَكَادُ زَيْتُهَا يُضِيءُ وَلَوْ لَمْ تَمْسَسْهُ نَارٌ نُّورٌ عَلَى نُورٍ يَهْدِي اللهُ

لِنُورِهِ مَن يشاء وَيَضْرِبُ اللهُ ٱلْأَمْثَالَ لِلنَّاسِ وَاللهُ بِكُلِّ شَيْءٍ عَلِيمٌ ﴾

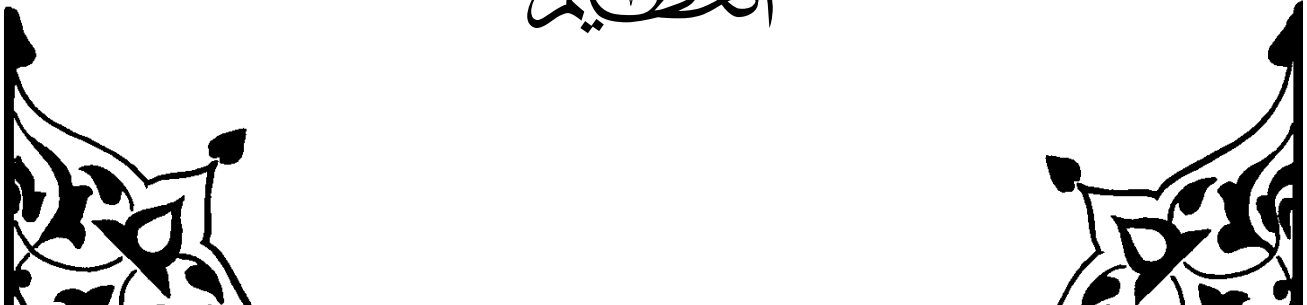

سورة النور/ الآية ٣٥

EXAMINING COMMITTEES CERTIFICATE

We certify that we have read this thesis entitled ***"Numerical Analysis of Heat Transfer and Fluid Flow over a Rigidly Vibrating Cylinder in Cross Flow"*** *and as an examining committee, examined the student,* ***"Mohsen Gawy Hamza"****, in its contents and that in our opinion it meets standard of a thesis for the degree of Master of Science in Mechanical Engineering.*

Signature:

Name: Prof.

Dr. Jalal M. Jalil

(Supervisor)

Date: / / ٢٠٠٧

Signature:

Name: Asst. Prof.

Dr. Adil A. Al-Moosawy

(Supervisor)

Date: / / ٢٠٠٧

Signature:

Name: Asst. Prof.

Dr. Emad S. Ali

(Member)

Date: / / ٢٠٠٧

Signature:

Name: Asst. Prof.

Dr. Ahmed A. Al–Rajihy

(Member)

Date: / / ٢٠٠٧

Signature:

Name: Asst. Prof.

Dr. Haroun A.K. Shahad

(Chairman)

Date: / / ٢٠٠٧

Approval of the Mechanical Engineering Department.

Head of the Mechanical Engineering Department.

Signature:

Name: Asst .Prof.

Dr. Adil A. Al-Moosawy
Date: / / ٢٠٠٧

Approval of the College of Engineering.

Dean of the College of Engineering.

Signature:

Name: Prof.

Dr. Abd Al-Wahid K. Rajih
Date: / / ٢٠٠٧

Supervisors Certificate

We hereby certify that the thesis entitled "**Numerical Analysis of Heat Transfer and Fluid Flow over a Rigidly Vibrating Cylinder in Cross Flow**" prepared by the Engineer(**Mohsen Gawy Hamza**) was carried out under our supervision at the **University of Babylon,** the Mechanical Engineering Department, for the partial fulfillment of the requirements for the degree of Master of Science in Mechanical Engineering (Power Engineering).

Signature:

Name: **Dr. Jalal M. Jalil**

Professor

(Supervisor)

Signature:

Name: **Dr. Adil A. AL-Moosawy**

Assist. Professor

(Supervisor)

NOMENCLATUR

NOTATIONS

Symbol	Description	Unit
a	Amplitude of Oscillation	m
A	Dimensionless Amplitude of Oscillation($A = a / D$)	---
C_f	Dimensionless Friction Factor	---
D	Cylinder Diameter	m
D_{eff}	Effective Cylinder Diameter	m
Dx, Dy	Transforming Coefficients	---
f	Frequency of fluid	١/s
f_w	Frequency of Cylinder	١/s
F	Reduced Frequency of oscillation($F = f_w \cdot D / U_\infty$)	---
h	Local Heat Transfer Coefficient	W/m٢.°C
$\bar{h}$	Average Heat Transfer Coefficient	W/m٢.°C
H	Dimensionless Distance in y–direction	---
J	Jacobain	---
K	Thermal Conductivity	W/m.°C
L	Dimensionless Distance in x–Direction	---
mt	Total Node Number in y–Direction	----
nt	Total Node Number in x–Direction	----
P	Pressure	Pa
t	Time	s
$\bar{t}$	Dimensionless time($\bar{t} = t.U_\infty / D$)	---

T	Fluid Temperature	°C
T_w	Cylinder Surface Temperature	°C
u	Velocity Component in x–Direction	m/s
U	Dimensionless Velocity Component in ζ – Direction(u/U_∞)	----
U_∞	Free Stream Velocity	m/s
v	Velocity Component in y–Direction	m/s
V	Dimensionless Velocity Component in η – Direction(v/U_∞)	---
x, y	Cartesian Coordinates	m
X	Dimensionless x–Coordinate($X = x/D$)	---
Y	Dimensionless y–Coordinate($Y = y/D$)	---

SUBSICRPT AND SUPERSICRPT

Symbol	Description
b	Boundary
i, j	Node symbols indicates position in x ,y direction
max	Maximum Value
n	Time Level τ
$n+1$	Time Level $\tau + \Delta\tau$
o	Old value
w	At The Cylinder Surface

GREEK SYMBOLS

Symbol	Description	Unit
α_f	Thermal Diffusivity	m^2/s
α	Transforming Coefficient	---
β	Transforming Coefficient	---
γ	Transforming Coefficient	---
Δ	Increment	---
ε	Error	---
ζ, η	Computational Coordinates	---
θ	Dimensionless Temperature	---
λ	Transforming Coefficient	---
ν	Kinematics Viscosity of Fluid	m^2/s
π	Constant Ratio=۲۲/۷	---
ρ	Fluid Density	kg/m^3
σ	Transforming Coefficient	---
τ	Dimensionless Time in Moving Grid	---
τ_w	Wall Shear Stress	N/m^2
ϕ	General Variable	---
φ	Stream Function	m^2/s
ψ	Dimensionless Stream Function	---
ω	Dimensionless Vorticity	---
Ω	Vorticity	$1/s$

ABBREVIATIONS

Acronym	Description

AIAA	American Institute of Aeronautics and Astronautics
ASME	American Society of Mechanical Engineers
BFC	Body Fitted Coordinate
CFD	Computational Fluid Dynamics
FDM	Finite Difference Method
inlin	Inline Oscillation Cylinder
it	Iteration
NASA	National Aeronautics and Space Administration
OMAE	Offshore Mechanics and Arctic Engineering
orbit	Orbital Oscillation Cylinder
PC	Personal Computer
PDE	Partial Differential Equation
PDEs	Partial Differential Equation System
RE	Relaxation Factor
SOR	Successive Over–Relaxation
SV	Surface vorticity
statia	Stationary cylinder
trans	Transverse Oscillation Cylinder

DIMENSIONLESS NUMBERS

Symbol	Description	Equation
Gr	Grashof Number	$Gr=\frac{g \cdot \beta.(T-T_w) \cdot D^3}{\nu^2}$
Nu	Local Nusselt Number with Oscillation	$Nu = h \cdot D / K$
$\overline{Nu}$	Average Nusselt Number with Oscillation	$\overline{Nu} = \bar{h} \cdot D / K$

$\overline{Nuo}$	Average Nusselt Number without Oscillation	$=\bar{h}o \cdot D / K$ $\overline{Nuo}$
Pe	Peclet Number	$Pe = \Pr \cdot \mathrm{Re}$
Re	Reynolds Number	$=U_{\infty} \cdot D / \nu$ Re
Pr	Prandtl Number	$=\nu / \alpha_f$ Pr
Str	Stroughl Number	Str=f.D/U

Dedication

To my parents, Who have been
a constant source of inspiration
and whose sincerity and love of
truth have guided my all life.
To my brother and sister, who
bore patience the seemingly
endless hours of work.

Mohsen

٢٠٠٧

Acknowledgments

My first and deepest gratitude goes to "ALLAH" for his uncountable blessings.

I would like to express my deepest thanks and appreciation to my teacher and supervisors: Prof. Dr. Jalal M. Jalil and Asst. Prof. Dr. Adil A. AL-Moosawy for their encouragement, guidance and instructive suggestions without which this thesis would not have come into its present shape.

My greatest thanks to the staff of Mechanical Engineering department in the college of Engineering of Babylon university, and especial thanks to the staff members who taught me during the study course.

I submit my thanks and love to my family that support and help me during the period of the study.

My thanks are extended to the staff of the central library of the university of Technology especially Mrs. Thaurah in the periodical department .

Finally, I would like to thank all lovely people who helped me directly or indirectly to complete this work and to apologize to them for being to mention them by name only in the stillness of my heart.

Mohsen Gawy

٢٠٠٧

Contents

CHAPTER THREE: MATHEMATICAL MODEL

CHAPTER FIVE: RESULTS AND DISCUSSION

Abstract

A numerical simulation is performed to predict the flow structures and heat transfer characteristics of a heated oscillating cylinder in across flow and air forced convection. The variations of the flow and thermal fields classified into a class of moving boundary problems. The fluid is assumed to be incompressible, viscous, two dimensional, laminar unsteady flow. The cylinder have constant wall temperature condition.

The Body Fitted Coordinate system(B.F.C) has been used with the time dependent grid generation technique because of the complexity of physical shape and moving boundary with time of this study since this method enable us to solve the flow equations around the complex bodies without the need to approximate or interpolate at the outside limits of the body, then an internal grid has been generated by solving two elliptic differential equations.

Vorticity-Stream function model has been used in this study. In this model, the governing equations consist of parabolic vorticity and energy equations which are solved by time marching (explicit) method and elliptic stream function equation which is solved by the relaxation method. These equations are solved by using finite difference discretization.

The moving interfaces between the fluid and cylinder have been considered. In fact, to overcome the effect of moving boundary, due to the cylinder oscillation, update the grid at each time step with a new locations and entering a new terms to the vorticity and the energy transport equations,

these terms are treating the effects of this movement of the grid on the computational domain.

The study covers the range of Reynolds numbers (٨٠ to ٦٠٠), reduced frequency (٠.٠ to ٠.٧) and amplitude ratio(٠.٠ to ٠.٩). Single value of Prandtl number(٠.٧) and three types of oscillation, transverse, inline and orbital, and also stationary (fixed) cylinder are used.

Heat transfer is greatly affected by the oscillation of the cylinder. It was found that the average of local Nusselt number in some cases are enhanced by (٣٧٪,٥٧٪ and ٦٤٪) for the transverse, inline and the orbital oscillation respectively. The maximum local Nusselt number for the same cases above are enhanced by (٦٤٪, ٧١٪ and ٧٨٪) for the transverse, inline and the orbital oscillation respectively.

On the other hand, the oscillation significantly affected the heat and momentum transfer characteristics of the air flow over the cylinder. The oscillation affects on density of stream line, isotherm and number of vortex shedding per cycle. The local skin friction coefficient is enhanced in some cases by (٦٣٪,٥٢٪ and ٧٥٪) for the transverse, inline and orbital oscillation respectively. The numerical predictions have been compared with existing data, and good agreement has been found.

الخلاصة

أجريت الدراسة العددية للتكهن بهيكلة الجريان المتعامد مع اسطوانة مهتزة (oscillating)والخواص الحرارية لجريان الهواء عند الحمل القسري . إن التغيرات الناتجة في الجريان والحرارة صنفت ضمن المسائل ذات الحدود المتحركة على فرض أن المائع لا انضغاطي ولزج وان الجريان طباقي ثنائي الأبعاد ومعتمد على الزمن وكذلك أن درجة حرارة سطح الاسطوانة ثابتة.

بسبب التعقيد الموجود في الشكل الفيزيائي وحركة الحدود مع الزمن للدراسة الحالية فقد تم استخدام نظام مطابقة إحداثيات الجسم(B.F.C.) مع أسلوب توليد الشبكة المعتمد على الزمن إذ تمكن هذه الطريقة من حل معادلات الجريان حول الأجسام المعقدة دون الحاجة لأجراء التقريب أو الاستكمال على الحدود الخارجية للجسم, ولقد ولّدت شبكة النقاط الداخلية بحل معادلتين تفاضليتين من نوع القطع الناقص(Elliptic).

استخدمت طريقة(الدوامية–دالة الانسياب) في هذه الدراسة, إن المعادلات الحاكمة في هذه الطريقة تتكون من معادلة قطع ناقص(دالة الانسياب) حيث تم حلها باستخدام طريقة الاسترخاء(Relaxation) ومعادلتي الدوامية والطاقة وهما قطع زائد(Parabolic) وقد تم حلهما باستخدام الزحف الزمني ودالة الفروق البينة. تم تحويل المعادلات الحاكمة من معادلات تفاضلية إلى معدلات جبرية باستخدام الفروق الحدية(Finite difference).

اخذ بنظر الاعتبار التداخل الحاصل بين حركة المائع وحركة الاسطوانة , لغرض التغلب على الحركة المستمرة للحدود الناتجة بسبب اهتزاز الاسطوانة تم تحديث شبكة النقاط لكل خطوة زمنية مع المواقع الجديدة وإدخال حدود جديدة إلى المعدلات الحاكمة(معادلة نقل الدوامية ومعادلة الطاقة), حيث إن تلك الحدود تقوم بمعالجة التأثيرات الناتجة من الحركة المستمرة على المجال الحسابي.

عدد رينولدز المستخدم في الدراسة الحالية ضمن المدى٨٠الى٦٠٠ والتذبذب المخفض٠ إلى ٠.٧ وكذلك السعة اللابعدية ٠ إلى ٠.٩. وقد استخدمت قيمة واحدة لعدد برانتل(٠.٧) وثلاثة أنواع من الاهتزاز (العمودي والأفقي والمداري) بالإضافة إلى الاسطوانة الثابتة.

إن انتقال الحرارة يتأثر بمقدار كبير نتيجة للاهتزاز(Oscillation) الاسطوانة حيث وجد إن عدد نسلت الإجمالي يتعزز في بعض الحالات بنسبة (٣٧%,٥٧%,٦٤%) في حالة الاهتزاز العمودي والأفقي والمدري وعلى الترتيب. كما إن أعظم قيمة لعدد نسلت المحلي لنفس الحالات أعلاه تتعزز بنسبة(٦٤%,٧٠%,٧٨%) للاهتزاز العمودي والأفقي والمداري على الترتيب.

من ناحية أخرى ,إن الاهتزاز يؤثر بشكل ملحوظ على الخواص الحرارية وزخم الهواء المار حول الاسطوانة حيث إن الاهتزاز يؤثر على كثافة خطوط السريان وخطوط ثبوت درجة الحرارة والدوامات المنعزلة من الاسطوانة لكل دورة. حيث وجد إن معامل الاحتكاك المحلي يتعزز في بعض الحالات بنسبة (٦٣%,٥٢%,٧٥%) لكل من الاهتزاز العمودي والأفقي والمداري على الترتيب. لقد تم الحصول على توافق جيد بين النتائج العديدة وما موجود من معلومات عند مقارنتها.

INTRODUCTION

١.١ General

Laminar forced convection is a phenomenon in which a fluid driven by some external force flows over or inside a solid surface such that the streamlines of the flow appear smooth and parallel (**Shih [١]).**

There are three modes of heat transfer by convection from the surface of the heated cylinder. The first mode represents the forced convection which takes place by an external driving force, forcing the fluid to flow across the cylinder, and generally, the rate of heat transfer depends upon the Reynolds number and the Prandtl number. The second type represents the natural convection, where the flow takes place due to a buoyancy force resulting from a reduction in fluid density near the heated surface due to temperature difference. This will cause the fluid to move vertically upwards; and the rate of heat transfer will depend mainly upon Grashof and Prandtl number**.** The third mode, when the forced convection flow in addition to the natural convection flow and neither of them can be neglected. In other words, when the velocity is small and the temperature difference between the surface and the ambient fluid is large, this type of flow and heat transfer is called mixed convection**.**

A phenomenon of vortex shedding induced by a flow passing through a cylinder is important in engineering applications such as heat exchangers,

nuclear reactor, hot–wire anemometers and steel cable suspension bridge. Doubtless, the heat transfer mechanism of the cylinder in the flow of vortex shedding is also interesting and important in many engineer applications

In case of cross flow past stationary cylinder, as Reynolds number exceeds about (٤٠), alternating vortices are shed periodically and arranged downstream in a Karman vortex street. This vortex shedding process is found to cause unsteady flow behavior near the cylinder surface and in turn enhance heat transfer. This shedding process has stimulated the interest of researchers to study the potential of enhancing heat convection using various forms of unsteady excitations. Among these is the use of forced oscillations(**Mahfouz** and **Badr[٢]**).

Understanding heat transfer from oscillating circular cylinders in cross-flow is an important and challenging engineering problem. vortex-induced vibration is known to occur for long, cylindrical elements in tube-bank heat exchangers. This makes it important to understand how oscillations affect the heat transfer so that equipment can be properly designed. The possibility of exploiting oscillation effects in new heat exchanger designs over a wide range of length scale, either through forced or vortex-induced vibrations, also requires that the relationship between oscillations and heat transfer be understood.

Many areas of fluid mechanics are involved in understanding this type of flow. Convective heat transfer, fluid–structure interactions, separated flows and vortex dynamics are all involved in relating cylinder oscillations to heat transfer. This makes for an interesting but challenging problem.

While it is evident from a review of the literature that the wake structure is the connection between oscillations and heat transfer, the mechanism of this

connection is not understood. The theoretical information on oscillation-enhanced heat transfer is still insufficient. The numerical approach becomes necessary to provide further understanding and to clarify some inconsistency in the previous experimental data.

١.٢ Vortex-Induced Vibration

As a fluid particle flows toward the leading edge of a bluff cylinder, the pressure in the fluid particle rises from the free stream pressure to the stagnation pressure. The high fluid pressure near the leading edge impels the development of boundary layers about sides of the cylinder. However, the pressure forces are not sufficient to force the boundary layers around the backside of bluff cylinders at high Reynolds numbers. Near the widest section of the cylinder, the boundary layers separate from each side of the cylinder surface and from two free shear layers that trail aft in the flow. These two free shear layers bound the wake. Since the innermost portion of the free shear layers moves much more slowly than the outermost portion of the layers which are in contact with the free stream, the free shear layers tend to roll up into discrete, swirling, vortices. A regular pattern of vortices is formed in the wake that interacts with the cylinder motion and is the source of the effects called vortex-induced vibration. Periodic forces on the cylinder are generated as the vortices are alternately shed from each side of cylinder. The oscillating forces can cause elastically mounted cylinders to vibrate (**Blevins[٣])**.

١.٣ Interaction between the Flowing Fluid and Moving Body

The flow and thermal fields induced by the interaction between a flowing fluid and a moving body (oscillating cylinder) are very important for application in many engineering problems. From a relative velocity view point, the moving body is traditionally and conveniently regarded as the stationary body in the flowing fluid, in which the relative velocity between the moving body and the fluid is considered. However, the fluid near the body must replenish the vacant space induced by the movement of the body. Strictly speaking, the dynamics problem of the moving body regarded as the stationary body in the flowing fluid is different from that of the body moving in the flowing fluid. Hence, the later situation mentioned above can be classified as a kind of the moving boundary problems(**Fu,W.-S.** and **Yang, S.-J.[٤]**).

previously, most of the researchers investigated the variation of the flow fields only, as will be shown in next chapter. However, in many industrial applications, such as heat exchangers, electric cooling and fluid machinery, the variations of both the flow and thermal fields induced by interaction of fluid and moving body (oscillating cylinder) are important; little attention has been focused on this subject.

Consequently, in this study the moving grid method is adopted to investigate numerically the variation of the flow and thermal fields induced by the cylinder oscillation in transverse direction (having motion), inline direction (surging motion or streamwise) and ,mixed between them, orbital direction(with angle motion) to a flowing fluid. For a treatment the distortion and deformation of the computational meshes due to oscillation of the cylinder

and to prevents the interpolation, the time dependent grid is used and add a new time derivative to convective terms in the governing equations.

١.٤ Objectives of the Present Works

The purpose of the present study is to develop a computational model to investigate the variations of flow and thermal fields of the laminar flow passing over a heated oscillating cylinder. Due to the interaction between the flow and the oscillating cylinder, the variations of the flow and thermal fields become time-dependent and belong to a class of the moving boundary problems. The cylinder is heated with uniform surface temperature. This study will be based on the solution of full Navier-Stokes and energy equations and consequently the solution will be based on the method of Vorticity-Stream function. The study is achieved at constant Prandtl number (Pr=٠.٧) and dimensionless domain distance. The objective of the present study can thus be summarized as follows:

١. Simulate the fluid flow and heat transfer in cross flow over a stationary circular cylinder(two dimensional unsteady flow).
٢. Using time-dependent grid to simulate the fluid flow and heat transfer with moving boundary (cylinder oscillate).
٣. The effects of Reynolds number, amplitude and frequency of oscillating cylinder in multi-direction (transverse, inline and orbital) on the flow structures and heat transfer characteristics are investigated.
٤. Compare the values of Nusselt number between two cases(with oscillation and without oscillation) and investigate the increase when the cylinder oscillate.

١.٥ Organization of the Study

The aforementioned work is organized in the chapters of the present contribution as follows:

Chapter ٢: A literature review of the effort devoted to the concerned field of research is presented.

Chapter ٣: The theory and mathematical modeling is set up.

Chapter٤: Introduces the mathematical and numerical tools required for carrying out the numerical simulation.

Chapter ٥: Presents the results and their discussion.

Chapter ٦: Conclusions are made, and some proposals and suggestions for future work are presented.

LITERATURE SURVEY

٢.١ Introduction

This chapter will deal with literature survey related to this problem. Hence, literature will be of three main sections: the first section is concerned with heat transfer and fluid flow in force convection when the cylinder stationary (non-oscillate), and the important results that can be obtained; the second will deal with fluid flow and/or heat transfer when cylinder oscillate. The third section deals with literature about time dependent grid and moving grid. The Fig.(٢-١) shows the organization chart for literature review .

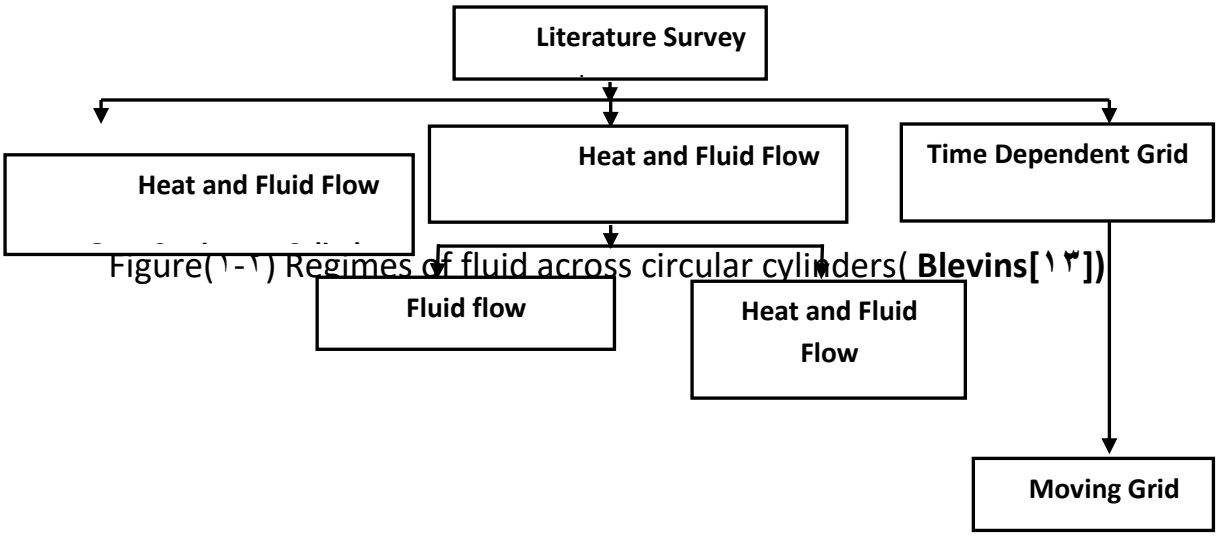

Figure(١-٢) Regimes of fluid across circular cylinders(**Blevins[١٣])**

Fig.(٢-١) Organization chart for Literature Survey

٢.٢ Forced Convection over Stationary Circular Cylinder

There is a large volume of literature devoted to fluid flow and/or heat transfer by force convection from static(stationary) circular cylinder. However, they have received attention for some of these literature.

Dennis and **Chang[٥],** have used finite difference solutions of the equations of motion for steady incompressible flow a round a circular cylinder for a range of Reynolds numbers from Re=٥ to Re=١٠٠. This study was two-dimensional and was carried out by vorticity-stream function model. The flow is assumed to posses symmetry about the x-axis. Calculated values of the drag coefficient, the angle of separation, and the pressure and vorticity distributions over the cylinder surface are presented. They found that the separation has started at Re=٧, and the length of the wake, from the rear of the cylinder to the end of the separated region, increase approximately linearly with Reynolds number over the whole range.

Jain and **Goel[٦],** numerically, investigated the process of shedding of vortices from a circular cylinder by solving an unsteady viscous fluid flow problem at Reynolds number equal to ٢٠٠. The numerical study described the shedding of the equivorticity lines at a different times and Strouhal number is calculated. They found that symmetric eddy pair and a symmetric flow pattern exist for a sufficiently longer time, also they get the shedding process from time=١٠ onwards. After this time the flow in wake has become unsymmetrical. They calculated the value of Strouhal number(dimensionless frequency of fluid flow over cylinder) in their case is approximately (٠.١٧) .

Jain and **Goel[٧],** presented a numerical investigation of an unsteady laminar forced convection from a circular cylinder. The results are obtained at Reynolds numbers ١٠٠ and ٢٠٠, and a Prandtl number of ٠.٧٣. They found that the process of the vortex shedding is accelerated by introducing a perturbation in the wake of the flow at time=٣.٤٧(Re=١٠٠) and time=٦(Re=٢٠٠).The unsymmetrical flow in wake gives rise to an unsymmetrical pattern of the isothermal line at time=٦.٤٢(Re=١٠٠) and time=٩.٤(Re=٢٠٠). The Nusselt number distribution on the surface of cylinder remains almost symmetrical except in wake region where some asymmetry is found due to the presence of the shedding of vortices.

Patel[٨], has used a semi-analytical solution of the Navier-Stokes equation to calculate the two-dimensional, symmetrical, viscous incompressible flow past a circular cylinder. The stream and vorticity functions are expanded in the finite Fourier series and then substituted in the Navier-Stokes equations. The numerical calculation have been performed over half circular cylinder over Reynolds number ٦٠,١٠٠,٢٠٠,٥٠٠,٥٥٠,and ٦٠٠ . He found that the wake continues to grow and so actually the flow field never becomes steady and also a secondary vortex appeared on the surface of the cylinder in case of Reynolds ٥٠٠,٥٥٠,٦٠٠ .

Lin et al.[٩], performed a numerical solution of the Navier-Stokes for separated flows a round a circular cylinder at Reynolds numbers ٤٠,٨٠,and ٢٠٠ . They found that the flow pattern in the recirculating region of a circular cylinder begins to oscillate as the Reynolds number exceeds ٤٠ ,and also, separated flow around a circular cylinder can have a line of symmetry in the wake region only at Reynolds number less than ٤٠ .

Tuann and **Olson [١٠],** numerically have investigated the vorticity, stream and surface pressure of fluid flow over circular cylinder for Reynolds number from ١ to ١٠٠. The numerical method is based on a finite element approximation. They found that the closed wake appears at about Re=٥ and the tendency of wake to become unsteady and wavy in shape at Re≥٤٠ .

Ta Phuoc Loc and **Bouard[١١],** have analysed the flow structure at early times of the impulsively started circular cylinder at Reynolds numbers of ٣٠٠٠ and ٩٥٠٠ . These are analyzed numerically by the direct integration of the Navier-Stokes equations.A fourth-order finite difference scheme is used for the solution of the stream function equation and a second order one for the vorticity transport equation. They found that the secondary vortices, which are stable and confined in the main wake for Re <١٠٠٠, become unstable for greater Reynolds numbers. Also, the increase of Reynolds number involves the multiplication of secondary vortices and the existence of a peak of vorticity at the surface of the cylinder, inside the separation area.

Karniadakis[١٢], has been investigated the forced convection heat transfer from an isolated cylinder in cross flow for Reynolds numbers up to ٢٠٠ by direct numerical simulation of the Navier-Stokes and energy equations using the spectral element method. The numerical results are obtained by using a general-purpose spectral element code, NEKTON has shown that for Reynolds numbers less than approximately(٤٠) the cylinder flow is steady and takes the form of an attached pair of vortices behind the cylinder. It was also shown that a typical streamlines pattern of the unsteady flow, occurs for a Reynolds number greater than ٤٠ . Also, he found the unsteady the local heat transfer coefficient is in excellent agreement with available experimental data.

Rumsey[١٣], has described the application of upwind implicit approximate factorization Navier-Stokes algorithm to the unsteady impulsive start-up flow over a circular cylinder at Reynolds number ١٢٠٠. The complete form of the compressible Navier-Stokes equation is used. The algorithm is a second-order accurate in both space and time. The local maximum drag during the start-up flow is computed to be ١.٤٤ at $\bar{t}$ =١.٦,and the Strouhal number of the periodic flow is ٠.٢٢٢ .

Chun and **Boehm[١٤],** have used various finite difference solutions to developed a numerical model to study forced flow and convection heat transfer over a circular cylinder in cross flow. A constant heat flux or an isothermal wall boundary condition are considered. The formulation of the governing equations uses the stream function-vorticity approach. The range of Reynolds number used is(٤٠ to ٣٤٨٠) and Prandtl(٠.٧). They used either the central difference(CD)or the power law(PL)scheme to discretize the transport equations. They found that the use of (PL) and (CD)schemes are suitable for solution transport equations for low Reynolds numbers(٤٠,٢٠٠,٥٠٠),but the use of the (PL) scheme in conjunction with a non-uniform staggered grid system might be the best approach to use for higher Reynolds numbers.

Lange et al.[١٥], have been presented detailed numerical investigation of the two-dimensional laminar flow of air around a heated circular cylinder. Numerical investigations were carried out for the Reynolds number range ($١٠^{-٤}$ ≤ Re ≤ ٢٠٠). They used finite volume method for the spatial discretization and Crank–Nicolson scheme for the time discretization of the governing equations. They found that the critical Reynolds number where vortex shedding starts to be at Re=٤٥.٩. they also presented correlation for their result of Nusselt number, as (Nusselt=٠.٠٨٢*$Re^{٠.٥}$+٠.٧٣٤*Re^{x}) where: x=٠.٠٥+٠.٢٢٦*$Re^{٠.٠٨٥}$).

Baranyi[١٦], presented a finite difference solution for two dimension, low Reynolds number, unsteady fluid flow around and heat transfer from a stationary circular cylinder placed in a uniform flow. The fluid is assumed to be incompressible and of constant properties. The governing equations are the Navier-Stokes equation, the continuity equation and energy equation. The non-dimensional vortex shedding frequency “Strouhal number”, time-mean values of drag, lift, base pressure and Nusselt number were determined for Reynolds numbers from ٥٠ to ١٨٠. Results were compared with the experimental data and an excellent agreement was obtained. He found that the flow becomes unstable and ٣D effects begin to appear above Re=١٦٠ and the maximum heat transfer rate was located near the upstream stagnation point.

٢.٣ Heat Transfer and Fluid Flow over Oscillating cylinder

This section focuses on literature that dealing with fluid flow and/or heat transfer over oscillating cylinder. The literature about this subject in almost deals with fluid flow over oscillating cylinder and study the phenomena that known as "lock-on" and the effect of oscillation on the characteristics of fluid flow and heat transfer.

٢.٣.١ Fluid Flow over Oscillating Cylinder

This section is dealing with the literature that focused on the fluid flow over an oscillating cylinder.

Hurlbut et al.[١٧], used a finite difference scheme to solve the two-dimensional Navier-Stokes equation for fluid flow around an oscillating circular cylinder. A non-inertial coordinate transformation was used so that the grid mesh remains fixed relative to the accelerating cylinder. Three types of cylinder motion were considered: oscillation in a still fluid, oscillating parallel to a moving stream(inline) and oscillating transverse to a moving stream. Computations are made for Reynolds numbers between(١ to ١٠٠) and amplitude ratio(٠.١ to ٢). They found that the lock-in or wake capture phenomenon occurs when cylinder oscillation is near the natural vortex shedding frequency. Also, detailed computations at Reynolds number of (٨٠) are to be in quantitative agreement with available experimental data for oscillating cylinders.

Lecointe and **Piquet[١٨],**have used the finite difference scheme ,optimized ADI method “Mehrstellen”, for solution of the unsteady incompressible Navier-Stokes equation in their vorticity stream function formulation. These methods were applied to the study of separated flow around a circular cylinder at several Reynolds number. The impulsively started cylinder at Re=٢٠٠,and ٥٥٠, was considered without symmetry restrictions. The Karman vortex street was investigated at Re=٢٠٠ with a uniform flow with superimposed motions(oscillating) of the cylinder. In the last case, a frequency analysis has allowed a critical examination of results pertaining to locked-in situations with respect to confinement effects.

Chilukuri[١٩],used an implicit finite difference scheme to solve the Navier-Stokes equation in terms of primitive variables, to study the transverse oscillation of a cylinder in cross flow at Reynolds number of ٨٠ and ١٤٤ with frequency and amplitude ratio up to ٠.١٨٥ and ١ respectively. The non-inertial

transformation from a stationary frame of reference to a frame that moves with oscillating cylinder is used in a numerical solution. The drag amplification at high amplitude was significantly underestimated in those calculation. Both the mean and fluctuating drag showed and increase with oscillation amplitude.

Ongoren and **Rockwell[٢٠],**studied the flow structure over a cylinder in across flow, subjected to controlled oscillations in the transverse direction. In their experiments, they used a free-surface water channel: cylinders of circular, triangular, and rectangular cross sections: and a hydrogen bubble visualization technique. The range of Reynolds number was used between about ٥٨٤ to ١٣٠٠. They observed two forms of synchronization, or "lock-in". In sub harmonic synchronization, where the frequency of oscillation is half of the natural vortex shedding frequency, vortices of the same sense are shed from the same side of the body, irrespective of whether it moves towards its upper or lower positions. On the other hand, in fundamental synchronization, where the frequency of oscillation is almost equal to that of the natural vortex shedding, vortices of opposite sense are shed from either side of the body, as it alternately moves towards its upper and lower positions in its cycle .

Also, in the fundamental synchronization region, they observed that the vortex formation can undergo a phase switch from the "outer" side to the "inner" side of the cylinder, or vice versa. For a circular cylinder, at frequencies of oscillation higher than the natural vortex shedding frequency, vortices are shed from the "inner" side of the cylinder, while at frequencies equal to or lower than the natural frequency of vortex shedding, vortices are shed from the "outer" side of the body.

Ongoren and **Rockwell[٢١],** studied the wake structure of a circular cylinder forced to oscillate at an angle with respect to the incident cross flow,

at a Reynolds number of ٨٥٥. They used a flow visualization technique in a water channel. The amplitude of oscillation in most of their experiments was set at ١٣٪ of the diameter of the cylinder. They identified a symmetrical vortex shedding mode, and four basic antisymmetrical modes, at synchronization between the vortex shedding and the cylinder motion.

For the symmetrical mode, which they referred to as the(S)mode, two vortices are shed at the same time from the two sides of the cylinder during one oscillation cycle of the cylinder. This mode could occur at any angle of oscillation except angle=٩٠° (pure transverse oscillation). This shedding mode was observed only for frequency ratios of F=٣ and F=٤ ,and for oscillation angles of ٠°,٤٥°, and ٠°,٤٥°,٦٠°, respectively.

In the case of the first antisymmetrical mode, denoted as A-I, there is alternate out-of-phase shedding of two vortices from either side of the cylinder over an oscillation cycle. This is the vortex shedding mode that leads to the well-known Karman vortex street. For(angle=٩٠°), this is the shedding mode observed for all values of excitation frequency ratio at which synchronization occurred. Also, for the frequency ratio F=٠.٥, this mode observed for all values of angle of oscillation. For modes A-II to A-IV(the other three antisymmetrical modes), the period of the vortex pattern is twice the period of cylinder oscillation. Mode A-II was observed for any angle=٠°,٩٠°,and modes A-III and A-IV only for angle=٠°.

Lecointe and **piquet[٢٢],** numerically investigated the vortex shedding characteristics in the wake of a circular cylinder in a two-dimensional cross-flow, under in-line or transverse oscillations at a given amplitude. They solved the Navier-Stokes equation in terms of vorticity and stream-function, using second or fourth order accurate spatial discretization, and ADI time

discretization scheme. A case of in-line oscillation at a frequency ratio of F=٠.٨, amplitude of A/D=٠.٢٥, and Re=٢٠٠ was considered in order to study the effect of an oscillation frequency close to the natural shedding frequency. In this case, an asymmetric shedding was obtained that locked into the cylinder motion. A few test cases for Re=٨٥٥ and A/D=٠.١٣ was simulated at different frequency ratios, and the results were compared with experimental visualizations of **Ongoren** and **Rockwell[٢٠].**

Mittal et al.[٢٣], used a space-time finite element formulation of incompressible flows, including those involving moving boundaries and interface. The results were presented for certain unsteady flows past a circular cylinder. First, flow past a fixed circular cylinder at Reynolds number ١٠٠ was solved. Then, at the same Reynolds number, the cylinder was subjected to forced horizontal oscillations. This leads to a symmetric mode of vortex shedding. The final case studied involves flow past a circular cylinder that is mounted on flexible supports and is free to respond to the fluid forces in the vertical direction. The Reynolds number for this simulation was ٣٢٤ . Depending on the amplitude and frequency, they found that two modes of vortex shedding are possible. Oscillations with a low reduced frequency lead to asymmetric modes of vortex shedding, but for high reduced frequency symmetric vortex shedding was observed.

Mittal and **Tezduyar[٢٤],** used a finite element formulation to simulate, among other problems, the flow over a circular cylinder oscillating longitudinally in a cross flow at Re=١٠٠. The amplitude of oscillation was set at A/D=٠.٥, and the frequency ratio at F=٢. They observed the symmetric mode vortex shedding(for a long period of time)in their simulation.

Mittal and **Kumer[٢٥],** investigated fluid flow, among other problems, over oscillating cylinder by using finite element formulation. The cylinder was allowed to oscillate, both in the inline and in the cross-flow(transverse) direction. The Reynolds number was ٣٢٥ and computation were carried out for various values of reduced frequency including the sub and super harmonics of the natural vortex-shedding frequencies of a stationary cylinder. They observed that their computations are in consistent with work of **Ongeron** and **Rockwell [٢٠,٢١]**.

Blackburn and **Henderson[٢٦],** presented a detailed study of the wake structures and flow dynamics associated with simulated two-dimensional flow past a circular cylinder that is either stationary or in simple harmonic cross-flow oscillation. Results were examined for Re=٥٠٠ and reduced frequency range(٠.٧٥<F<١.٠٥)with a fixed motion amplitude of y/D=٠.٢٥. A spectral element spatial discretization was employed in conjunction with second order time splitting scheme in order to solve the two-dimensional incompressible Navier-Stokes equation. The Navier-Stokes equations was solved in a moving reference frame fixed to the cylinder. They found that phase-switching of vortex shedding is associated with a change in sign of mechanical energy transfer between the cylinder and the flow.

Mittal and **Kumar[٢٧],** have employed finite element methods to investigated fluid flow over vibrating light circular cylinder placed in a uniform flow at Reynolds number in the range $١٠^{٣}$-$١٠^{٤}$ and frequency ratio up to (٠.٧٦). The governing equations for fluid flow was the Navier-Stokes equation for incompressible flow. The cylinder was mounted on lightly damped, flexible supports and allowed to vibrate, both in the in-line and cross flow directions under the action of aerodynamics force. The behavior of the oscillator for

various values of the reduced frequency(F) including those that were super-harmonics of the vortex-shedding frequency for the stationary cylinder have been presented. At higher Reynolds number, the vortex shedding was quite disorganized and the cylinder doesn't reach a temporally periodic solution.

٢.٣.٢ Heat and Momentum Transfer over Oscillating Cylinder

This section is dealing with the literature that focused on the effect of oscillation on heat transfer from an oscillating cylinder.

Heat transfer from transversely oscillating(vibrating) cylinders in cross flow was first studied by **Sreenivasan** and **Ramachandran[٢٨],** over the range ١٥٠٠<Re<٢٥٠٠ in air. They concluded that transverse oscillations had no effect on heat transfer. This is likely because the oscillation frequencies used in their experiments were much lower than the natural shedding frequency. Though they considered amplitude ratio up to ١.٨, the largest value of reduce frequency in their study was (٠.٠٧).

Later experiments have found that heat transfer from a cylinder is enhanced by transverse oscillations near the Strouhal frequency. **Kezios** and **Prasanna[٢٩],** working in the range ٥٥٠٠<Re<١٤٠٠٠, found that heat transfer was enhanced by about ٢٠٪ for small amplitude(٠.٠٢<A <٠.٠٧٥) oscillations at the Strouhal frequency. They found that this enhancement exceeded the expected increase in heat transfer if the effect was only due to the higher effective free stream velocity.

Saxena and **Laird[٣٠],** measured local heat transfer coefficients using thermocouple embedded in the cylinder surface. They conducted experiments at Re=٣٥٠٠ in water over the range ٠.٨٩≤A≤١.٩٩ and ٠.٢٨≤F≤٠.٨٣. Their results indicate that local heat transfer coefficients increase as the oscillation frequency approaches the Strouhal frequency. On the down stream half of the cylinder, local heat transfer coefficients are observed to increase by ٥٠٪ to ٦٠٪ for the highest amplitudes and frequencies. Heat transfer enhancement on the down stream half of the cylinder is consistently about ١٥٪ higher than for the leading half of the cylinder.

Michaelides et al.[٣١], developed an experimental program to examine banks of flexible tubes made of "Teflon" material with air flowing a cross the tubes. The effect of the following parameters on the pressure drop and heat transfer was investigated: Reynolds number of the flow, tube free length, tube temperature and number of rows in the banks. The experimental pressure drop and heat transfer coefficients were reported for Reynolds numbers ranging from ٤٠٠ to ٨٠٠٠ and frequency up to (٣٠Hz) with amplitude exceeded two tube diameter. They observed that tubes vibrated with low frequencies and higher amplitudes in their experiments. Banks of flexible tubes made of "Teflon" material exhibit higher outside heat transfer coefficients than an equivalent array of rigid tubes in cross-flow, due to high fluid mixing.

Chang et al.[٣٢], developed a numerical scheme to calculate the heat transfer coefficients in heat exchangers made of flexible tubes. Calculations are performed with the first tube at positions ranging from ٠.٣٥ to -٠.٣٥ diameters off-center with steps of ٠.٠٥ diameters and Reynolds numbers from ١٣٨ to ١٣٣٩. The vibrating tubes were modeled in a quasi-static way by taking first tube of the row to be in ١٥ asymmetric positions with respect to the rest

of the tube and averaging in time the steady-state solutions corresponding to each one of these geometries. The results show that the eccentricity of the first tubes affects the velocity and temperature profiles significantly. The time averaged heat transfer coefficients is ٢٠-٢٥٪ higher than that of the rigid tubes. The Comparison of the results shows very good agreement with experimental data from flexible tube heat exchangers.

Karanth et al.[٣٣] numerically, computed the fluid flow and heat transfer for Re=٢٠٠ and pr=١ at amplitude ratio of ٠.٢٥ and ٠.٥ for F=٠.٢. They used non-inertial reference frame to simplify the computation. They predicted increases in the time-averaged heat transfer coefficient of ١.٤٪ and ٤.٦٪for the two cases. The location of the highest local heat transfer coefficient was found to vary as a function of time, thought it is always on the leading half of the cylinder. The largest increases in local heat transfer were observed close to the trailing edge.

Cheng et al.[٣٤], conducted experiments at Re=٢٠٠,٥٠٠ and ١٠٠٠ in air. Amplitude ratios of ٠.١٣٨,٠.٣١٤ and ٠.٦٢٨ were explored over the range F≤٠.٣, and heat transfer enhancement of up to ٣٤٪ was observed. Enhancement near the Strouhal frequency was attributed to lock-on, or synchronization of the wake with the cylinder oscillations. High heat transfer coefficients at large amplitude ratios and high F, particularly for the highest Reynolds number, were attributed to a vague “turbulence effect”.

Cheng and **Hong[٣٥],** performed computations at Re=٢٠٠. They examined cases in the range F≤٠.٣ and A≤٠.٧ with Pr=٠.٧١ and ٧.٠. The governing equations are Navier-Stokes and energy equations with non-inertial reference frame technique. For oscillations at the natural shedding frequency, heat transfer was significantly enhanced, and the magnitude of the enhancement

depended on the amplitude ratio. These computational results agreed well with experimental results of **Cheng et al.[٣٤].**

Park[٣٦],conducted experiments in water at Reynolds numbers of ٥٥٠, ٦١٠, ١١٠٠, and ٣٥٠٠. He considered frequencies up to F=١.٠٥ for two amplitude ratios,٠.١and ٠.٢. He found that heat transfer was significantly enhanced at frequencies corresponding to the Strouhal frequency and to ٣ times the Strouhal frequency. For the large amplitude ratio, he also found that heat transfer was enhanced at ٢ times the Strouhal frequency. Using digital particle image thermometry/velocimetry, he was able to show that the heat transfer enhancement was correlated with a shortening of the vortex roll-up distance. He suggested that the closer proximity of the vortices to the cylinder allow hot, stagnant fluid to be moved away from the cylinder base.

Gau et al.[٣٧], performed experiments in air at Reynolds number of ١٦٠٠,٣٢٠٠ and ٤٨٠٠. They measured the local heat transfer coefficient for small amplitude ratios of ٠.٠١٦,٠.٠٣٢ and ٠.٠٦٤ in the range ٠.٥ ≤F≤٣.٠ . A sample of **Gau et al.'s** result is shown in Figure(٢-٢). Heat transfer is significantly enhanced at ١ and ٣ times the Strouhal frequency, and the most significant enhancement occurs near the trailing edge of the cylinder for these cases. This is consistent with the results of other case studies, as well.

Fu and **Tong[٣٨],** performed a numerical simulation, by using finite element formulation, to study the flow structures and heat transfer characteristics of a heated transversely oscillating cylinder in a cross-flow. They examined the effects of Reynolds number, oscillating amplitude, oscillating speed on the flow structures and heat transfer characteristics. They examined cases in the range F≤٠.٤ and amplitude less than ٠.٨ with Reynolds numbers(١٠٠,٢٠٠ and ٥٠٠). They found that the heat transfer rate is enhanced remarkably as the

oscillating frequency of the cylinder approaches the natural shedding frequency and also the heat transfer rate increased apparently when the oscillating velocity of the cylinder and the Reynolds number are increased.

Pottebanm[٣٩], carried out a series of experiments in order to understand the relationship between wake structure and heat transfer for a transversely oscillating circular cylinder in cross-flow and to explore the dynamics of vortex formation process in the wake. The cylinder heat transfer coefficient was determined over a range of oscillation amplitudes up to ١.٥ cylinder diameters and oscillation frequencies up to ٥ times the stationary cylinder natural shedding frequency. The results were compared established relationships between oscillation conditions and wake structure. Digital particle image thermometry/velocimetry was used to measure the temperature and velocity fields in the near-wake for a set of cases chosen to be representative of the variety of wake structure that exist for this type of flow. The experiments were carried out in a water tunnel at a Reynolds number of ٦٩٠.

It was found that wake structure and heat transfer both significantly affect each other. The wake mode, a label indicating the number and type of vortices sheded in each oscillation period, is directly related to the observed heat transfer enhancement. The cylinder's transverse velocity was shown to influence the heat transfer by affecting the circulation of the wake vortices. For a fixed wake structure, the effectiveness of the wake vortices at enhancing heat transfer depends on their circulation. Also, the cylinder's transverse velocity continually changes the orientation of the wake with respect to the source of heat transfer enhancement the vortices near the cylinder base-over a larger portion of the cylinder surface.

Fu and **Tong[٤٠],** performed a numerical simulation to study the influence of an oscillating cylinder on the heat transfer from heated blocks in a channel flow. Finite element formulation was applied to solve the governing equations. They examined the effects of Reynolds number amplitude and frequency of oscillation on the heat transfer characteristics of the heated wall. They simulated cases in the range F≤٠.٤ and amplitude ratio(A≤٠.٤) with Reynolds numbers(١٠٠,٢٥٠ and ٥٠٠). They found that the heat transfer rate could be improved substantially as the cylinder oscillating in the lock-in region(frequency of the cylinder equal or near the natural shedding frequency). Also, the heat transfer rate increase when the Reynolds number increases

٢.٤ Time Dependent Grids

In many application areas the solution domain changes in time due to the movement of boundaries. The movement is either determined by external effects(as in piston-driven flows, oscillating cylinder) or it must be calculated as a part of the solution(for example, in free surface flows)(**Feziger** and **Peric[٤١]).** The time dependent grids can be classified in two case. First: the grids moving due to boundaries move in response to influences of the physical problem, this is known **moving grids**, second: the grids moving due to the system is made to adjust itself to concentrate lines in developing regions of large gradients, this is well known **Adaptive grids.** In this section the focus is on the moving grids only.

٢.٤.١ Moving Grids

The moving grids have been used in many problem that dealing with moving boundary as shown below.

Thompeson et al.[٤٢], presented a numerical technique, among other problems, to perform all computation on the fixed rectangular grid in the transformed plane without any interpolation, when the grid point moves in the physical plane. The movement of grid points due to the boundaries in physical plane have actually moved or may be just to change the concentration of grid points around the boundaries. Thus, although the position of a grid point changes on the physical plane the position in the transformed plane is fixed.

Tannehill et al.[٤٣], presented the time dependent finite difference method to solve the complete set of Navier-Stokes equations over circular cylinder by assuming, two dimensional, viscous, blunt body flows with an impinging shock wave. They used moving coordinate system to follow a bow shock. The coordinate system was regenerated by a shearing transformation to follow a moving bow shock. The grid moves due to the boundary movement with the bow shock as the latter moves toward its “steady state” position. The velocity of movement of grid can be calculated from the local velocity of shock wave and the latter calculated from the shock location from previous time step.

Steger and **Bailey[٤٤],** developed a numerical technique to implicit finite difference with two-layer algebraic eddy viscosity model and exact geometric specification of the airfoil, simulate transonic aileron buzz. Treated an airfoil with an oscillating aileron by first generating a coordinate system for the

undeflected configuration, and then, with the motion of the aileron trailing edge being approximated as normal to the undeflected airfoil chord line, all points aft of the hinge points were simply moved normal to the undeflected chord in proper proportion to the distance from the hinge point as time progressed. This procedure results in a coordinate line discontinuity on the line emanating from the hinge line on each side. The length of the aileron also changes artificially with time since its trailing edge is made to move normal to the undeflected chord. The velocity of grid solved at each time step from the displacement of the aileron and used the later to update the grid generation.

Hindman et al.[٤٥], presented a general method for solving the unsteady two-dimensional Euler equations on multiple flow regions with arbitrarily-shaped and time varying boundaries. The method is applicable to problems with moving boundaries provided the velocity of such movement can be determined or specified. This includes problems with moving pistons, structural deformations, accelerating bodies, moving or stationary discontinuity surfaces such as shocks and slip surfaces, etc. In the case of discontinuity surfaces, the scheme has the capability of capturing any discontinuities whose approximate shape and location is not known a priori provided the strength of such discontinuities is not excessive. In this work the elliptic generating system was differentiated with respect to time. With x and y taken from the previous time step, these equations are linear partial differential equations for X_τ and Y_τ, which were solved by a direct method. New values of x and y were then calculated from X_τ and Y_τ.

Chyu et al.[٤٦], used unsteady grid generation technique suitable for the treatment of moving and deforming airfoils. The outer boundaries of the grid

were help fixed in space and time, while the airfoil position varied in time. The grid, in turn, is deformed as time progressed to follow the motion of the airfoil.

Allowing the airfoil surface to vary within a stationary outer boundary requires that a new grid be generated at each time step of the computation. To reduce the computational effort needed to repeatedly generate the grids, treated a pitching airfoil by first generating grid for the two extreme airfoil positions. Each grid point was then moved along a circular arc between the two extreme positions of the point, the arc radius of curvature being taken equal to the distance from the airfoil rotation axis to one of the extreme positions.

٢.٥ Conclusion of Previous Works

Based on the review of the previous investigations of the fluid flow and heat transfer over stationary cylinder and oscillating cylinder in cross flow, and also the time dependent grid that is used in computational fluid dynamics, the following observations can be made.

First: observation for stationary cylinders

١. For numerical work, most of this work is dealt with low Reynolds number and using almost vorticity–stream model with finite difference except a small number of attempt using primitive variable such as **Lange et al.[١٥]** and **Baranyi[١٦]**

Second: observation for oscillating cylinders.

١. For the experimental works, authors focus on the flow characteristics and lock-on “synchronization” phenomena. And also, dealing with fluid at low Reynolds numbers such as ١٠٠,٢٠٠ and ٣٠٠.

٢. The numerical investigations performed almost by moving reference frame “non-inertia” coordinate and no literature was sited using time-dependent grid technique with finite difference.

٣. For heat transfer, work was performed experimentally except a small number of attempted to simulate this physical phenomena numerically.

In the presents investigation, attempts, by using computational approaches, were made to examine the effects of oscillation on the fluid flow(air) and heat transfer when the cylinder is subjected to an oscillation in the three direction (transverse, inline and orbital). Time dependent grid will be used to treat the moving boundary due to oscillation and also solve the governing equations with general coordinate. The range of Reynolds number is (٨٠ to ٦٠٠), frequency(٠.٠ to ٠.٧) and amplitude (٠.٠ to ٠.٩) and also Prandtl(٠.٧) in all computation.

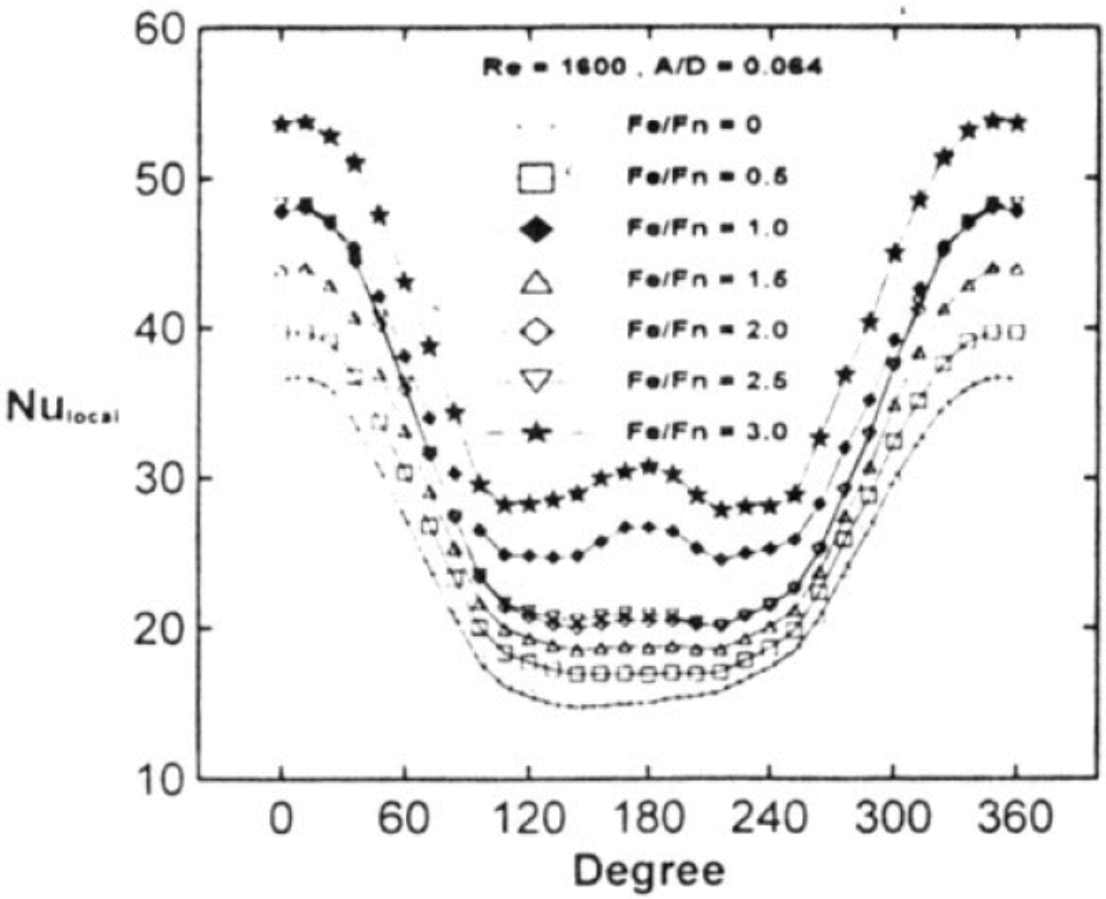

Figure(٢-٢)Local Nusselt number as a function of angular position for various non-dimensional oscillation frequencies at Re=١٦٠٠ and A/D=٠.٠٦٤. From **Gau et al.[٣٧]**

MATHEMITICAL MODEL

٣.١ Introduction

The numerical solution of heat transfer, fluid flow and other related processes can begin when the laws governing these processes have been expressed in mathematical form, generally in term of differential equations, **Patanker**[٤٧].

The present chapter handles three parts: the first part is concerned with the physical characteristics to describe the process of flow and heat transfer over circular cylinder, in two cases; first, when cylinder is stationary(non-oscillating), second, when the cylinder is oscillating, and the assumptions upon which governing equations are based.

The second part, sheds light on initial and boundary conditions that have been assumed depending on the physical characteristics of the problem. The third part, focuses on the grid generation and body fitted coordinate system and the process of equation transform from Cartesian coordinates(x,y)to the general coordinates(ζ,η). Figure(٣-١)shows the road map for calculation fluid flow and heat transfer.

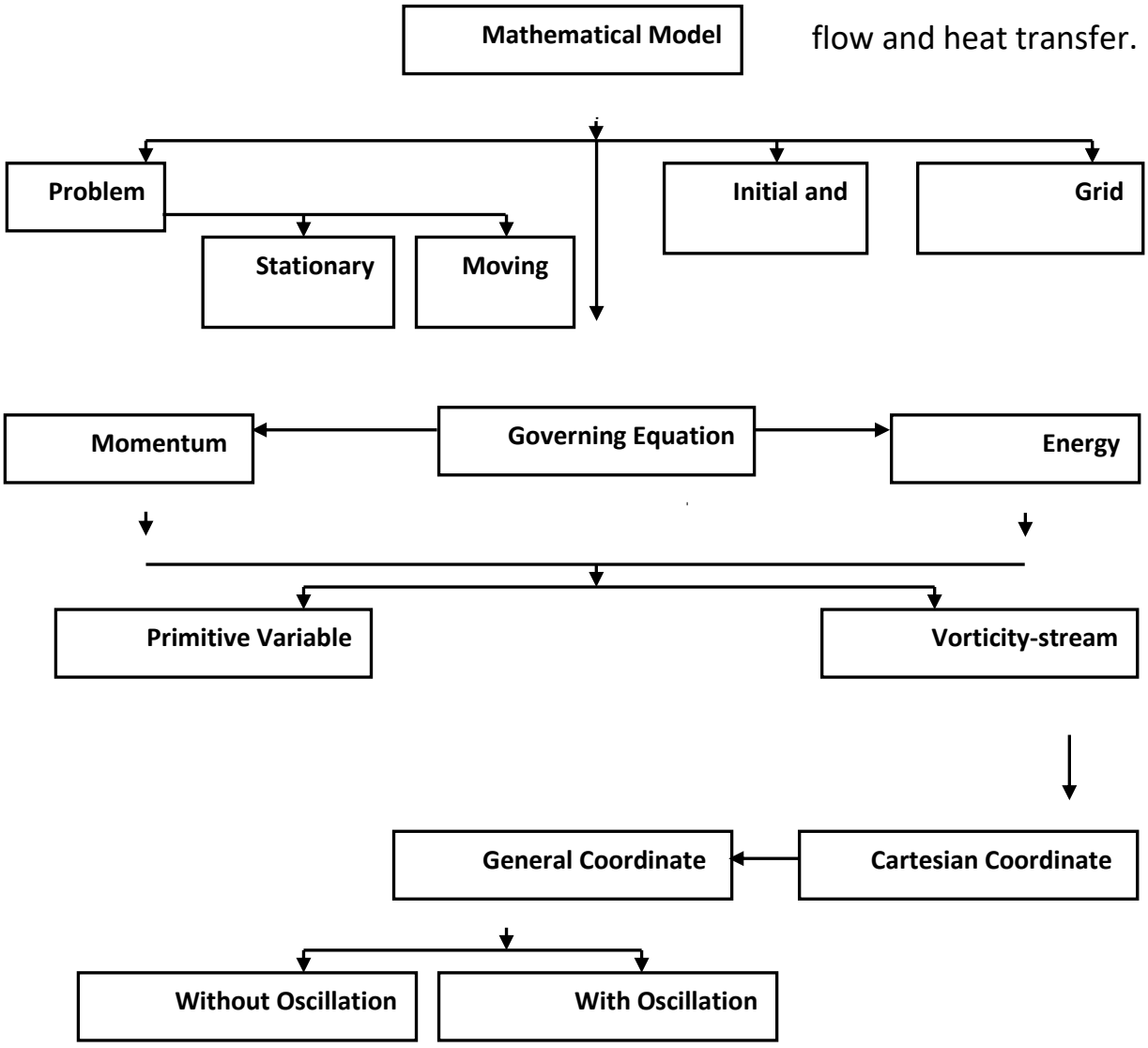

Fig.(٣-١)**Road Map of Mathematical Model**

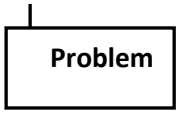

٣.٢ Problem Description

In the present study, there will be a focus on the process of fluid flow and heat transfer by forced convection from circular cylinder in cross flow with, uniform surface temperature is in two cases. First, when cylinder is stationary (fixed), second, when cylinder oscillates, and there is a comparison between them. Figure(٣-٢) shows the geometry and coordinate system.

Some assumptions should be considered to obtain the final form of governing equations and consequently to obtain the numerical solution. These assumptions are:

- Laminar flow
- Unsteady fluid flow
- Incompressible flow of a Newtonian fluid with no body forces and constant properties.
- Very high length to diameter ratios(l/D >٤٠-٤٥)so the outside flow can be considered as two-dimensional, **Chang et al. [٣٢]** and **Pantazopoulos[٤٨].**
- The cylinder end effects on the velocity and temperature fields are neglected (two-dimensions).
- No external heat addition and neglecting the effect of radiation heat transfer.

٣.٣ Physical Model

This part, will describe the governing equations that will be generated based on the above assumptions. In addition, the method of **Vorticity-Stream Function** can be used to express the form of equations. Finally, the governing equations will be transformed into dimensionless form.

٣.٣.١ Governing Equations

The conservation laws of the mass, momentum and energy constitute the governing equations of a fluid flow. The fundamental equations based on the assumptions mentioned in section(٣.٢)are the momentum equations(Navier-stokes) and continuity equation, **Schlichting[٤٩]** and **Yuan[٥٠].**

$$\frac{\partial u}{\partial x}+\frac{\partial v}{\partial y}=0 \qquad \cdots\cdots\cdots(3.1)$$

$$\frac{\partial u}{\partial t}+u\frac{\partial u}{\partial x}+v\frac{\partial u}{\partial y}=\nu\left(\frac{\partial^2 u}{\partial x^2}+\frac{\partial^2 u}{\partial y^2}\right)-\frac{1}{\rho}\frac{\partial p}{\partial x} \qquad \cdots\cdots\cdots(3.2)$$

$$\frac{\partial v}{\partial t}+u\frac{\partial v}{\partial x}+v\frac{\partial v}{\partial y}=\nu\left(\frac{\partial^2 v}{\partial x^2}+\frac{\partial^2 v}{\partial y^2}\right)-\frac{1}{\rho}\frac{\partial p}{\partial y} \qquad \cdots\cdots\cdots(3.3)$$

$$\frac{\partial T}{\partial t}+u\frac{\partial T}{\partial x}+v\frac{\partial T}{\partial y}=\alpha_f\left(\frac{\partial^2 T}{\partial x^2}+\frac{\partial^2 T}{\partial y^2}\right) \qquad \cdots\cdots\cdots(3.4)$$

٣.٣.٢ Vorticity and Stream Function Method

The difficulty associated with determination of pressure has led to methods that eliminate pressure term from the governing equations. Thus, in two dimensions, the elimination of pressure term from the two-momentum equations by cross differentiation leads to a **Vorticity-Transport** equation. This, when combined with the definition of a stream function for steady two-dimensional situations, is the basis of the "**Stream-Function/Vorticity method".**

The stream-function/vorticity method has some attractive features. The pressure makes no appearance, and instead of dealing with continuity equation and two momentum equations, there is the need to solve only two

equations to obtain the stream function and the vorticity. Some of the boundary conditions can be rather easily specified: when an external irrotational flow lies adjacent to the calculation domain, the boundary vorticity can conveniently be set equal **Zero.** However, there are some major disadvantages of stream-function/vorticity method. The value of vorticity at a wall is difficult to specify and can be the cause of trouble in getting a converged solution. Vorticity is a measure of the amount of anticlockwise rotation which the fluid possesses. The stream function is scalar quantity, represented by symbol**(** ψ **),patanker[٤٧]** and **Iatridis[٥١].**

The vorticity equation is derived from the two momentum equations which relate respectively to the momentum in direction(x) and (y); the first is differentiated with respect to(y)and the second is differentiated with respect to(x). Because the one equation contains($\partial^2 p/\partial x\partial y$)and others equation contains ($\partial^2 p/\partial x\partial y$) also, a subtraction removes the pressure entirely. Thus, the first aim of the procedure is swiftly achieved, **patanker[٤٧]**.

Thereafter, introduction of definition of vorticity results in the elimination of most the terms in which differentials of velocity appear, **Iatridis [٥١], Bose[٥٢]** and **Ferziger** and **Peric[٤١].** The resultant equations are:

Momentum equation in x-direction:

$$\frac{\partial u}{\partial t}+u\frac{\partial u}{\partial x}+v\frac{\partial u}{\partial y}=\nu\left(\frac{\partial^2 u}{\partial x^2}+\frac{\partial^2 u}{\partial y^2}\right)-\frac{1}{\rho}\frac{\partial p}{\partial x} \qquad \cdots\cdots\cdots(3.5)$$

Momentum equation in y-direction:

$$\frac{\partial v}{\partial t}+u\frac{\partial v}{\partial x}+v\frac{\partial v}{\partial y}=\nu\left(\frac{\partial^2 v}{\partial x^2}+\frac{\partial^2 v}{\partial y^2}\right)-\frac{1}{\rho}\frac{\partial p}{\partial y} \qquad \cdots\cdots\cdots(3.6)$$

Differentiating the equation(٣.٥)with respect to(y)and differentiating the equation(٣.٦)with respect to(x),can obtain two equations, as follows:

$$\frac{\partial}{\partial t}(\frac{\partial u}{\partial y})+\frac{\partial}{\partial y}(u.\frac{\partial u}{\partial x})+\frac{\partial}{\partial y}(v.\frac{\partial u}{\partial y})=-\frac{1}{\rho}\frac{\partial^2 p}{\partial x\partial y}+\nu\frac{\partial}{\partial y}(\frac{\partial^2 u}{\partial x^2}+\frac{\partial^2 u}{\partial y^2}) \quad \cdots\cdots(3.7)$$

$$\frac{\partial}{\partial t}(\frac{\partial v}{\partial x})+\frac{\partial}{\partial x}(u.\frac{\partial v}{\partial x})+\frac{\partial}{\partial x}(v.\frac{\partial v}{\partial y})=-\frac{1}{\rho}\frac{\partial^2 p}{\partial x\partial y}+\nu\frac{\partial}{\partial x}(\frac{\partial^2 v}{\partial x^2}+\frac{\partial^2 v}{\partial y^2}) \quad \cdots\cdots(3.8)$$

By subtracting equation(٣.٧)from equation(٣.٨)the following equation may be obtained:

$$\frac{\partial}{\partial t}(\frac{\partial v}{\partial x}-\frac{\partial u}{\partial y})+\frac{\partial}{\partial x}(u\frac{\partial v}{\partial x})+\frac{\partial}{\partial x}(v\frac{\partial v}{\partial y})-\frac{\partial}{\partial y}(u\frac{\partial u}{\partial x})-\frac{\partial}{\partial y}(v\frac{\partial u}{\partial y})=$$
$$-\frac{1}{\rho}\frac{\partial^2 p}{\partial x\partial y}+\nu\frac{\partial}{\partial x}(\frac{\partial^2 v}{\partial x^2}+\frac{\partial^2 v}{\partial y^2})+\frac{1}{\rho}\frac{\partial^2 p}{\partial x\partial y}-\nu\frac{\partial}{\partial y}(\frac{\partial^2 u}{\partial x^2}+\frac{\partial^2 u}{\partial y^2})) \quad \cdots\cdots(3.9)$$

Re-arranging equation(٣.٩)becomes:

$$\frac{\partial}{\partial t}(\frac{\partial v}{\partial x}-\frac{\partial u}{\partial y})+u\frac{\partial^2 v}{\partial x^2}+\frac{\partial v}{\partial x}\frac{\partial u}{\partial x}+v\frac{\partial^2 v}{\partial x\partial y}+\frac{\partial v}{\partial y}\frac{\partial v}{\partial x}-u\frac{\partial^2 u}{\partial x\partial y}-\frac{\partial u}{\partial x}\frac{\partial u}{\partial y}$$
$$-\nu\frac{\partial^2 u}{\partial y^2}-\frac{\partial u}{\partial y}\frac{\partial v}{\partial y}=\nu(\frac{\partial^3 v}{\partial x^3}+\frac{\partial^3 v}{\partial x\partial^2 y}-\frac{\partial^3 u}{\partial x^2\partial y}-\frac{\partial^3 u}{\partial y^3}) \quad \cdots\cdots(3.10)$$

Also,

$$\frac{\partial}{\partial t}(\frac{\partial v}{\partial x}-\frac{\partial u}{\partial y})+\frac{\partial u}{\partial x}(\frac{\partial v}{\partial x}-\frac{\partial u}{\partial y})+\frac{\partial v}{\partial y}(\frac{\partial v}{\partial x}-\frac{\partial u}{\partial y})+u\frac{\partial}{\partial x}(\frac{\partial v}{\partial x}-\frac{\partial u}{\partial y})$$
$$+\nu\frac{\partial}{\partial y}(\frac{\partial v}{\partial x}-\frac{\partial u}{\partial y})=\nu\left(\frac{\partial^2}{\partial x^2}(\frac{\partial v}{\partial x}-\frac{\partial u}{\partial y})+\frac{\partial^2}{\partial y^2}(\frac{\partial v}{\partial x}-\frac{\partial u}{\partial y})\right) \quad \cdots\cdots(3.11)$$

From the definition of vorticity, **Anderson et al.[٥٣]**

$$\Omega=\frac{\partial v}{\partial x}-\frac{\partial u}{\partial y} \quad \cdots\cdots(3.12)$$

By the substitution of equation(٣.١٢)into equation(٣.١١)the following equation is obtained:

$$\frac{\partial\Omega}{\partial t}+\frac{\partial u}{\partial x}\Omega+\frac{\partial v}{\partial y}\Omega+u\frac{\partial\Omega}{\partial x}+v\frac{\partial\Omega}{\partial y}=\nu(\frac{\partial^2\Omega}{\partial x^2}+\frac{\partial^2\Omega}{\partial y^2}) \quad \cdots\cdots(3.13)$$

From definition of continuity equation, **Schlichting[٤٩]**

$$\frac{\partial u}{\partial x}+\frac{\partial v}{\partial y}=0 \quad \cdots\cdots(3.14)$$

Re-write equation(٣.١٣)it becomes:

$$\frac{\partial \Omega}{\partial t} + u\frac{\partial \Omega}{\partial x} + v\frac{\partial \Omega}{\partial y} = \nu(\frac{\partial^2 \Omega}{\partial x^2} + \frac{\partial^2 \Omega}{\partial y^2}) \quad \cdots\cdots\cdots(3.15)$$

The definition of stream function that satisfies continuity equation may convert the vertical and horizontal velocity and satisfy continuity equation, **Roache[٥٤]** as follows:

$$u = \frac{\partial \varphi}{\partial y} \quad \cdots\cdots\cdots(3.16)$$

$$v = -\frac{\partial \varphi}{\partial x} \quad \cdots\cdots\cdots(3.17)$$

By substituting equations(٣.١٦) and (٣.١٧)into equation(٣.١٢)lead to a kinematics equation connecting the stream function and the vorticity, **Ferziger and Peric[٤١].**

$$\frac{\partial^2 \varphi}{\partial x^2} + \frac{\partial^2 \varphi}{\partial y^2} = -\Omega \quad \cdots\cdots\cdots(3.18)$$

By substituting equations(٣.١٦) and (٣.١٧)into equation(٣.١٥)the final form of vorticity transport equation may be obtained, **Pozrikidis[٥٥].**

$$\frac{\partial \Omega}{\partial t} + \frac{\partial \varphi}{\partial y}\frac{\partial \Omega}{\partial x} - \frac{\partial \varphi}{\partial x}\frac{\partial \Omega}{\partial y} = \nu(\frac{\partial^2 \Omega}{\partial x^2} + \frac{\partial^2 \Omega}{\partial y^2}) \quad \cdots\cdots\cdots(3.19)$$

٣.٣.٣ Governing Equations in Dimensionless Form

Equations of fluid motion may be nondimensionalized to achieve certain objective. For one, it would provide conditions upon which dynamics and energetic similarity may be obtained for geometrically similar situations. Second, of such equations would usually provide values within limits between **Zero** and **One**, **Hoffmann[٥٦].**

The two equations of stream function and vorticity transport of flow over a circular cylinder may be written in dimensionless form, as follows:

$$\frac{\partial^2\psi}{\partial X^2}+\frac{\partial^2\psi}{\partial Y^2}=-\omega \qquad \cdots\cdots\cdots(3.20)$$

$$\frac{\partial\omega}{\partial\bar{t}}+\frac{\partial\psi}{\partial Y}\frac{\partial\omega}{\partial X}-\frac{\partial\psi}{\partial X}\frac{\partial\omega}{\partial Y}=\frac{1}{\mathrm{Re}}\left(\frac{\partial^2\omega}{\partial x^2}+\frac{\partial^2\omega}{\partial Y^2}\right) \qquad \cdots\cdots\cdots(3.21)$$

Also, the energy equation without heat generation and neglect viscous dissipation is:

$$\frac{\partial\theta}{\partial\bar{t}}+\frac{\partial\psi}{\partial Y}\frac{\partial\theta}{\partial X}-\frac{\partial\psi}{\partial X}\frac{\partial\theta}{\partial Y}=\frac{1}{\mathrm{pe}}\left(\frac{\partial^2\theta}{\partial X^2}+\frac{\partial^2\theta}{\partial Y^2}\right) \qquad \cdots\cdots\cdots(3.22)$$

In these equations,(ψ,ω,θ)represent **Stream Function, Vorticity** and **Temperature** respectively in dimensionless form. Diameter(D)is used as characteristic length and free stream velocity(U_∞)as the characteristic velocity **Lin, et al. [٩].** Also, (T_o) is the characteristic temperature.

The nondimensionalized quantities are defined as follows:

١. Stream function, **Mahfouz** and **Badr[٢]** $\psi=\varphi/U_\infty.D$

٢. Vorticity, **Roache[٥٤]** $\omega=\Omega.D/U_\infty$

٣. Temperature, **Chang et al.[٣٢]** $\theta=\dfrac{(T-T_o)}{(T_w-T_o)}$

Where,(T_w)is the temperature of cylinder and(T_o)is the uniform inlet temperature.

٤. Dimensionless Cartesian coordinates $X=x/D, Y=y/D$

٥. Dimensionless Time**, Anderson et al.[٥٣]** $\bar{t}=t.U_\infty/D$

٦. Reynolds number $\mathrm{Re}=U_\infty.D/\nu$

٧. Prandtl number $\mathrm{Pr}=\nu/\alpha_f$

٨. Peclet number $\mathrm{Pe}=\mathrm{Pr}.\mathrm{Re}$

٩. Dimensionless amplitude of cylinder oscillation $A=a/D$

١٠. Reduced frequency, **Lecointe** and **Piquet[٢٢]** $F = f_w \cdot D/U_\infty$

Also, the vertical and horizontal velocity components may be rewritten in dimensionless form, as follows:

$$U = \frac{\partial \psi}{\partial Y} \qquad \cdots\cdots\cdots(3.23)$$

$$V = -\frac{\partial \psi}{\partial X} \qquad \cdots\cdots\cdots(3.24)$$

The unsteady term in the vorticity transport equation(٣.٢١) and energy equation (٣.٢٢) will remain, since the time marching method will be used in the numerical calculations of fluid and heat transfer problems.

٣.٤ Initial and Boundary Conditions

The describing equations are elliptic requiring boundary conditions to prescribed around all boundaries, **Launder and Massey[٥٧].**

The initial conditions used to solve each of energy , vorticity and the stream functions, these taken at time($\bar{t}$ =٠). Two sets of initial conditions are used one for the stationary and other for oscillating cylinder, differs from each other because the oscillation phenomena. Four types of boundaries will be presented; see Fig.(٣-٣) & Fig.(٣-٤).The boundary conditions similar for stationary and oscillating cylinder.

٣.٤.١ Initial Conditions

In order to begin the computation, some initial conditions have to be set at time($\bar{t}$ =٠).

These initial conditions are specified at all mesh points for temperature (θ),stream function (ψ),vorticity (ω), and hence horizontal(U),vertical(V) velocities.

In the present case, the unsteady solution is highly dependent on these initial conditions.

The present study has two different types of initial conditions:

First: For the stationary cylinder case, the initial conditions are defined to be:

- Temperature $\theta = 0$
- Stream Function $\psi = 0$
- Vorticity $\omega = 0$
- Horizontal velocity $U = 0$
- Vertical Velocity $V = 0$

Second: For the oscillating cylinder case, the unsteady solution for flow past the stationary cylinder is used as an initial conditions for computing the flow past the oscillating cylinder, **Mittal** and **Kumar[٢٥]** and **Mittal** and **Kumar[٢٧]**

٣.٤.٢ Boundary Conditions at the Surface of the Cylinder

The boundary conditions that are imposed upon the body surface are the usual impermeability and no-slip conditions for all time, **Patel[٨].** In the

present case, the value of stream function is chosen to equal **Zero** ($\psi = 0$), while the vorticity is not quite so easily handled since its magnitude depends on the mean velocity gradients at the wall which are unknown until the end of calculation, **Launder and Massey[٥٧],** where the knowledge of its value is considered part of solution. The values of(U)and(V) equal **Zero** because no-slip condition. As the temperature of the cylinder will remain at its maximum value and it is depending on the dimensionless assumptions, it will equal **One (** $\theta = 1$**)**.

٣.٤.٣ Boundary Conditions at Inlet Flow

The stream function value at the upstream is changed linearly between **Zero** and **One,** where it equals to **Zero** at center and **One(١)**and negative **One(-١)** in the upper and lower line respectively ,**Chang et al.[٣٢].** The value of vorticity is supposed to be **Zero**(ω=٠) due to no circulation and the value of temperature depending on the dimensionless assumptions will be **Zero**(θ=٠).

The velocity equals free stream velocity, hence (U =١)and (V =٠).

٣.٤.٤ Boundary Conditions at Outlet Flow

When there is no area change in outlet region, and if this region is sufficiently long and far downstream, the flow may safely be assumed as fully developed, which implies negligible stream wise gradients of all variables.

$$\frac{\partial \phi}{\partial n} = 0, \qquad \phi = \psi, \omega, \theta, U, V \qquad \cdots\cdots\cdots (3.25)$$

where (n)is the coordinate direction normal to the outlet.

٣.٤.٥ Upper and Lower Boundaries

The stream function on the upper and lower boundaries of the solution domain set to a uniform value which corresponds to the mean flow rate per unit length of cylinder, **Launder and Massey[٥٧].** On the other hand, the value of the stream function on the lower boundary will have the same value the upper boundary, but with negative sign. In addition, the vorticity and the gradient of the temperature normal to the upper and lower boundaries are both set to **Zero ,**and also the horizontal and vertical components velocity gradient are set equal to **Zero .**

٣.٥ Computational Model

This part will describe the computational domain and the technique can be used to obtain the governing equations in **Body Fitted Coordinates System**.

٣.٥.١ Body Fitted Coordinates System

When studying and calculating fluid movement, the grid generation is, generally, of critical flow calculations demands. This is due to the nature of numerical calculations of the zone flow; which requires a proper treatment of the boundary conditions. These boundary conditions are sometimes hard to be used when the geometrical shape is complex. Thus, the system which is made to generate a grid, might bring about a slow numerical convergence.

This has encouraged to find other methods to generate the grids. This method includes generation of curvilinear coordinate system with coordinate

lines coincident with all boundaries of physical domain. This is called **Body Fitted Coordinates System.** So, this system will be used in the present study.

In the finite-difference formulation, introduction of the **Body Fitted Coordinate System** has made it possible to use the finite difference method in many situations with complicated geometry, **Bose[٥٢].**

Regardless of the shape of body in physical plane, all the numerical computations are achieved in the form of rectangular grid in computational domain. Since the body fitted coordinate system has coordinate lines coincident with all surfaces in physical domain, all boundary conditions can be expressed at grid points by using finite differences between grid points on coordinate lines, without the need for any interpolation between interior points.

The existing method for the generation of a curvilinear body fitted coordinate system are based on two different principle: conformal mapping and the solution of differential equations of elliptical type (**Papantonis and Athanssiadis[٥٨]).** The present study will use the second type.

٣.٥.٢ Grid Generation

In order to numerically solve the governing partial differential equations (PDEs)of fluid mechanics, approximations to the partial differentials are introduced. These approximations convert the partial derivatives to finite difference expressions which are used to rewrite the PDEs as algebraic equations. The approximate algebraic equations referred to as finite difference equations (FDEs), are subsequently solved at discrete points within the domain

of interest. Therefore, a set of grid points within the domain as well as the boundaries of the domain, must be specified. The creation of such a grid system is known as a grid generation, **Hoffmann[٥٦].**

In this part, the grid generation will be discussed in relation to the establishment of the correspondence between points(X,Y)in the irregular physical domain and points(ζ,η)in the regular computational domain. In practice the grid is generated with a less computational effort by working in the computational domain. Thus, fixing the location of the points on the boundary give $X = X_b(\zeta,\eta)$ and $Y = Y_b(\zeta,\eta)$. The generation of the grid in the interior is expressed as the following boundary value problem: given $X = X_b(\zeta,\eta)$ and $Y = Y_b(\zeta,\eta)$ generate $X = X(\zeta,\eta)$ and $Y = Y(\zeta,\eta)$ in the region(Z)as shown in figure (٣-٥).

Since the interior points in the computational domain form a regular grid and the boundaries coincide with coordinate lines, the determination of $X = X(\zeta,\eta)$, $Y = Y(\zeta,\eta)$ is easier than working in the irregular physical domain, particularly if a partial differential equation is to be solved to generate the solution, $X(\zeta,\eta), Y(\zeta,\eta)$.

In defining the relationship between domains, it is necessary that there must be a one-to-one correspondence. It would be unacceptable for a single point in the physical domain to map into two points in the computational domain, and vice-versa , **Fletcher[٥٩].**

٣.٥.٢.١ Technique Used to Generate the Grid

In order to obtain the computational grid in the present study, the elliptical partial differential equations (PDEs) are solved. In general, partial differential equation that can be used is Laplace's equations, **Anderson[٦٠]**, as follows:

$$\zeta_{xx} + \zeta_{yy} = 0 \qquad \cdots\cdots\cdots(3.26)$$

$$\eta_{xx} + \eta_{yy} = 0 \qquad \cdots\cdots\cdots(3.27)$$

The elliptical equations for the coordinates are solved in the finite difference approximation by **S**uccessive **O**ver **R**elaxation(SOR) iteration, **Thames et al.[٦١].** However, computation must take place in a rectangular domain with uniform grid spacing. Now, in order to do all numerical computations in the rectangular transformed plane, it is necessary to interchange the dependent and independent variables in equations(٣.٢٦)and (٣.٢٧)(**Thompson et al.[٤٢]),**thus:

$$\alpha \cdot X_{\zeta\zeta} - 2 \cdot \beta \cdot X_{\zeta\eta} + \gamma \cdot X_{\eta\eta} = 0 \qquad \cdots\cdots\cdots(3.28)$$

$$\alpha \cdot Y_{\zeta\zeta} - 2 \cdot \beta \cdot Y_{\zeta\eta} + \gamma \cdot Y_{\eta\eta} = 0 \qquad \cdots\cdots\cdots(3.29)$$

Where,

$$\left.\begin{aligned} \alpha &= X_{\eta}^{2} + Y_{\eta}^{2} \\ \beta &= X_{\zeta}.X_{\eta} + Y_{\zeta}.Y_{\eta} \\ \gamma &= X_{\zeta}^{2} + Y_{\zeta}^{2} \end{aligned}\right\} \qquad \cdots\cdots\cdots(3.30)$$

The system of elliptic equations(٣.٢٨)and(٣.٢٩) will be solved in the computational domain(ζ,η)in order to provide the grid points locations in the physical space(X,Y). The distribution of points in computational domain is shown in figure (٣-٥).

٣.٥.٣ Governing Equations in Body Fitted Coordinates System

To enhance the efficiency and accuracy of a numerical scheme and to simplify implementation of boundary conditions, a transformation from physical space to computational space is performed. This transformation allows clustering of grid points in regions where flow variables undergo high gradients and grid point motion when required. The computational domain is a rectangular shape which is divided into an equally spaced grid system. In order to solve the governing equations of motion in computational space, a transformation of the equations from physical space into computational space is required **Hoffmann[٥٦].** In this section, investigates generalized coordinate transformation of the governing equations of fluid dynamics, expressed in the Cartesian coordinate system (X,Y),from physical space to computational space($\zeta.\eta$).

٣.٥.٣.١ Generalized Coordinate Transformation

The governing equation are transformed from the physical space($X,Y,\bar{t}$) to the computational space(ζ,η,τ)by the following relations, **Anderson[٦٠], Steger[٦٢].**

$$\zeta = \zeta(X,Y,\bar{t}) \quad \cdots\cdots\cdots(3.31)$$
$$\eta = \eta(X,Y,\bar{t}) \quad \cdots\cdots\cdots(3.32)$$
$$\tau = \bar{t} \quad \cdots\cdots\cdots(3.33)$$

Which can be used to transform the governing equations from the physical domain(X,Y)to the computational domain(ζ,η). Differentiating equations (٣.٣١) and (٣.٣٢) partially with respect to(ζ)and(η)respectively, the following four equations are produced.

$$\zeta_x \cdot X_\zeta + \zeta_y \cdot Y_\zeta = 1 \quad \cdots\cdots\cdots(3.34)$$

$$\zeta_x \cdot X_\eta + \zeta_y \cdot Y_\eta = 0 \quad \cdots\cdots\cdots(3.35)$$

$$\eta_x \cdot X_\zeta + \eta_y \cdot Y_\zeta = 0 \quad \cdots\cdots\cdots(3.36)$$

$$\eta_x \cdot X_\eta + \eta_y \cdot Y_\eta = 1 \quad \cdots\cdots\cdots(3.37)$$

From the above equations the following relations are obtained :

$$\zeta_x = \frac{1}{J} Y_\eta \quad \cdots\cdots\cdots(3.38)$$

$$\zeta_y = -\frac{1}{J} X_\eta \quad \cdots\cdots\cdots(3.39)$$

$$\eta_x = -\frac{1}{J} Y_\zeta \quad \cdots\cdots\cdots(3.40)$$

$$\eta_y = \frac{1}{J} X_\zeta \quad \cdots\cdots\cdots(3.41)$$

where,

$$J = X_\zeta . Y_\eta - X_\eta . Y_\zeta \quad \cdots\cdots\cdots(3.42)$$

and is defined as the Jacobian transformation.

The physical meaning of metrics($\zeta_x, \zeta_y, \eta_x, \eta_y$) is that, it represents the ratio of arc length in the computational space to that of the physical space. Also, the Jacobian(J) transformation, it is defined as the ratio of the volumes in the physical space to that of the computational space.

٣.٥.٣.٢ Transforming Derivatives of Function

The process of transforming derivatives of the first and the second degree from Cartesian coordinate to general coordinate by using chain rule, will be achieved. Before transforming these derivatives, general variable will be applied to all equations, that is (ϕ).

Transforming the derivative of the first degree with respect to(X)and with respect to(Y), **Anderson[٦٠],** as follow:

$$\frac{\partial \phi}{\partial X} = \phi_x = (\phi_\zeta . Y_\eta - \phi_\eta . Y_\zeta)/J \qquad \cdots\cdots\cdots(3.43)$$

$$\frac{\partial \phi}{\partial Y} = \phi_y = (-\phi_\zeta . X_\eta + \phi_\eta . Y_\zeta)/J \qquad \cdots\cdots\cdots(3.44)$$

Transforming the derivatives of the second degree with respect to(X)and with respect to(Y), **Petrovic** and **Stupar[٦٣]**, as follow:

$$\frac{\partial^2 \phi}{\partial X^2} = \phi_{xx} = \frac{\partial}{\partial X}(\phi_x) \qquad \cdots\cdots\cdots(3.45)$$

$$\begin{aligned}\frac{\partial^2 \phi}{\partial X^2} = \phi_{xx} = {} & (Y_\eta^2 \cdot \phi_{\zeta\zeta} - 2.Y_\zeta . Y_\eta \phi_{\zeta\eta} + Y_\zeta^2 . \phi_{\eta\eta})/J^2 \\ & + [(Y_\eta^2 . Y_{\zeta\zeta} - 2.Y_\zeta . Y_\eta . Y_{\zeta\eta} + Y_\zeta^2 . Y_{\eta\eta})(X_\eta . \phi_\zeta - X_\zeta . \phi_\eta) \\ & + (Y_\eta^2 . X_{\zeta\zeta} - 2.Y_\zeta . Y_\eta X_{\zeta\eta} + Y_\zeta^2 X_{\eta\eta})(Y_\zeta . \phi_\eta - Y_\eta . \phi_\zeta)]/J^3 \end{aligned} \qquad \cdots\cdots\cdots(3.46)$$

$$\frac{\partial^2 \phi}{\partial Y^2} = \phi_{yy} = \frac{\partial}{\partial Y}(\phi_y) \qquad \cdots\cdots\cdots(3.47)$$

$$\begin{aligned}\frac{\partial^2 \phi}{\partial Y^2} = \phi_{yy} = {} & (X_\eta^2 \cdot \phi_{\zeta\zeta} - 2.X_\zeta . X_\eta \phi_{\zeta\eta} + X_\zeta^2 . \phi_{\eta\eta})/J^2 \\ & + [(X_\eta^2 . Y_{\zeta\zeta} - 2.X_\zeta . X_\eta . Y_{\zeta\eta} + X_\zeta^2 . Y_{\eta\eta})(X_\eta . \phi_\zeta - X_\zeta . \phi_\eta) \\ & + (X_\eta^2 . X_{\zeta\zeta} - 2.X_\zeta . X_\eta X_{\zeta\eta} + X_\zeta^2 X_{\eta\eta})(Y_\zeta . \phi_\eta - Y_\eta . \phi_\zeta)]/J^3 \end{aligned} \qquad \cdots\cdots\cdots(3.48)$$

General form has been used to give the orthogonal with interior points in transforming a derivative of the first degree, which is related to the boundary conditions, **Broughton** and **Oliver[٦٤].**

$$\frac{\partial \phi}{\partial n} = (\alpha . \phi_\zeta - \beta . \phi_\eta)/J\sqrt{\alpha} \qquad (\eta = \text{constant line}) \qquad \cdots\cdots\cdots(3.49)$$

$$\frac{\partial \phi}{\partial n} = (\gamma . \phi_\eta - \beta . \phi_\zeta)/J\sqrt{\gamma} \qquad (\zeta = \text{constant line}) \qquad \cdots\cdots\cdots(3.50)$$

٣.٥.٣.٣ Substitute Derivatives in Governing Equations

In this part, the equations will be transformed continuously, to the conservative form that will be used in solving equations by the numerical methods.

There will be a transformation of convection term which is found in two equations of vorticity transport and energy, that consist of derivatives of first degree and it follows:

$$(\frac{\partial \psi}{\partial Y}\cdot\frac{\partial \phi}{\partial X})-(\frac{\partial \psi}{\partial X}\cdot\frac{\partial \phi}{\partial Y})=\psi_y.\phi_x-\psi_x.\phi_y$$

$$\psi_y.\phi_x-\psi_x.\phi_y=(-\psi_\zeta.\phi_\eta+\psi_\eta.\phi_\zeta)/J \qquad \cdots\cdots\cdots(3.51)$$

In contrast, the second transformation focuses on Laplace equation that represents the left side of the stream function. It represents the diffusion term in both equations of the vorticity transport and energy.

$$\frac{\partial^2 \phi}{\partial X^2}+\frac{\partial^2 \phi}{\partial Y^2}=\phi_{xx}+\phi_{yy}$$

$$\phi_{xx}+\phi_{yy}=(\lambda.\phi_\zeta+\sigma.\phi_\eta+\alpha.\phi_{\zeta\zeta}-2.\beta.\phi_{\zeta\eta}+\gamma.\phi_{\eta\eta})/J^2 \qquad \cdots\cdots\cdots(3.52)$$

$$\left.\begin{aligned}\alpha&=X_\eta^2+Y_\eta^2\\ \beta&=X_\zeta.X_\eta+Y_\zeta.Y_\eta\\ \gamma&=X_\zeta^2+Y_\zeta^2\end{aligned}\right\} \qquad \cdots\cdots\cdots(3.53)$$

$$\left.\begin{aligned}\lambda&=(X_\eta.Dy-Y_\eta.Dx)/J\\ \sigma&=(Y_\zeta.Dx-X_\zeta.Dy)/J\end{aligned}\right\} \qquad \cdots\cdots\cdots(3.54)$$

where :

$$\left.\begin{aligned}Dx&=\alpha.X_{\zeta\zeta}-2.\beta.X_{\zeta\eta}+\gamma.X_{\eta\eta}\\ Dy&=\alpha.Y_{\zeta\zeta}-2.\beta.Y_{\zeta\eta}+\gamma.Y_{\eta\eta}\end{aligned}\right\} \qquad \cdots\cdots\cdots(3.55)$$

Now, by using the final representative by the two equations(٣.٥١)and(٣.٥٢), the governing equations(٣.٢٠),(٣.٢١)and(٣.٢٢)may be written with Cartesian coordinates into general coordinates, **Broughton** and **Oliver[٦٤], Thames et al [٦١]** and **Rangwalla** and **Munson [٦٥].**

$$(\lambda.\psi_{\zeta}+\sigma.\psi_{\eta}+\alpha.\psi_{\zeta\zeta}-2.\beta.\psi_{\zeta\eta}+\gamma.\psi_{\eta\eta})/J^{2}=-\omega \qquad \cdots\cdots\cdots(3.56)$$

$$\omega_{\tilde{t}}+(-\psi_{\zeta}.\omega_{\eta}+\psi_{\eta}.\omega_{\zeta})/J=(\lambda.\omega_{\zeta}+\sigma.\omega_{\eta}+\alpha.\omega_{\zeta\zeta}$$
$$-2.\beta.\omega_{\zeta\eta}+\gamma.\omega_{\eta\eta})/(J^{2}.\mathrm{Re}) \qquad \cdots\cdots\cdots(3.57)$$

$$\theta_{\tilde{t}}+(-\psi_{\zeta}.\theta_{\eta}+\psi_{\eta}.\theta_{\zeta})/J=(\lambda.\theta_{\zeta}+\sigma.\theta_{\eta}+\alpha.\theta_{\zeta\zeta}$$
$$-2.\beta.\theta_{\zeta\eta}+\gamma.\theta_{\eta\eta})/(J^{2}.\mathrm{Pe}) \qquad \cdots\cdots\cdots(3.58)$$

The velocity components are calculated from the equations below:

$$U=\frac{\partial\psi}{\partial Y}=\psi_{y} \qquad \cdots\cdots\cdots(3.59)$$

$$V=-\frac{\partial\psi}{\partial X}=-\psi_{x} \qquad \cdots\cdots\cdots(3.60)$$

Hence, these equations in general coordinate are:

$$U=\frac{\partial\psi}{\partial Y}=\psi_{\zeta}.\zeta_{y}+\psi_{\eta}.\eta_{y} \qquad \cdots\cdots\cdots(3.61)$$

$$V=-\frac{\partial\psi}{\partial X}=-(\psi_{\zeta}.\zeta_{x}+\psi_{\eta}.\eta_{x}) \qquad \cdots\cdots\cdots(3.62)$$

The final form of velocity components, **Thames el at.[٦١]** and **Rangwalla**

and **Munson [٦٥]** are:

$$U=(X_{\zeta}.\psi_{\eta}-X_{\eta}.\psi_{\zeta})/J \qquad \cdots\cdots\cdots(3.63)$$

$$V=(Y_{\zeta}.\psi_{\eta}-Y_{\eta}.\psi_{\zeta})/J \qquad \cdots\cdots\cdots(3.64)$$

٣.٥.٤ Time Dependent Coordinate Systems

A coordinate system may need to be time dependent because the boundaries move, either of themselves or in response to influences of the physical problem, or because the system is made to adjust itself to concentrate lines in developing regions of large gradients. The simplest procedure is to regenerate the coordinate system at each time step using the new boundary locations, or other factors, from the physical solution at previous time step, the solution for the new coordinate at each time step thus being done separately from the physical solution at that step. Alternatively, the equations for the

coordinate system can be added to the system of physical solution equations and the entire set of equations are solved simultaneously at each time step.

In any case, with the partial time derivatives(at fixed “X” and “Y”)in the physical solution equations replaced by partial time derivatives at fixed values of the curvilinear coordinates, the grid in the transformed plane is fixed even though the coordinate system in the physical plane is in motion. This introduces time derivatives of the Cartesian coordinates into the transformed physical solution equations, in the rate of additional convective terms, **Thompson et al. [٦٦].**

٣.٥.٤.١ Governing Equations in Moving Grid

Now, when the coordinate system changes with time i.e, the grid point move in the physical Plane. Ordinarily such movement of the physical grid points would require interpolation among the grid points to produce values of the dependent variables at the new locations of the grid points. It is possible to perform all computation on the fixed rectangular grid in the transformed plane without any interpolation no matter how the grid points move in the physical plane as time progresses, **Thompson et al. [٤٢].** To perform the solution with moving grid and without any interpolation the time derivative transformed to the transformed plane as shown below, **Steger** and **Bailey[٤٤]** and **Anderson [٦٠].**

$$\frac{\partial \phi}{\partial \bar{t}} = \frac{\partial \phi}{\partial \tau} + \zeta_{\bar{t}} \frac{\partial \phi}{\partial \zeta} + \eta_{\bar{t}} \frac{\partial \phi}{\partial \eta} \qquad \cdots\cdots\cdots(3.65)$$

where,

$$\zeta_{\bar{t}} = -X_\tau \zeta_x - Y_\tau . \zeta_y = \frac{1}{J}(-X_\tau . Y_\eta + Y_\tau . X_\eta) \qquad \cdots\cdots\cdots(3.66)$$

$$\eta_{\bar{t}} = -X_\tau . \eta_x - Y_\tau . \eta_y = \frac{1}{J}(X_\tau . Y_\zeta - Y_\tau . X_\zeta) \qquad \cdots\cdots\cdots(3.67)$$

The physical meaning of($\zeta_{\bar{t}}$) is the time rate of change of(ζ)at fixed(X,Y)location in the physical plane. Similarly, the physical meaning of ($\eta_{\bar{t}}$)is the time rate of change of(η)at fixed(X,Y) location in the physical plane **Anderson [٦٠].**

By the substitution of equations (٣.٦٦) and (٣.٦٧) in equation (٣.٦٥) the following equation is obtained:

$$\frac{\partial \phi}{\partial \bar{t}} = \frac{\partial \phi}{\partial \tau} + \frac{\partial \phi}{\partial \zeta}\left(\frac{1}{J}(-X_\tau . Y_\eta + Y_\tau . X_\eta)\right) + \frac{\partial \phi}{\partial \eta}\left(\frac{1}{J}(X_\tau . Y_\zeta - Y_\tau . X_\zeta)\right) \qquad \cdots\cdots\cdots(3.68)$$

Re-arrange Equation(٣.٦٨)becomes:

$$\frac{\partial \phi}{\partial \bar{t}} = \phi_\tau + \left(\phi_\zeta(-X_\tau . Y_\eta + Y_\tau . X_\eta) + \phi_\eta(X_\tau . Y_\zeta - Y_\tau . X_\zeta)\right)/J \qquad \cdots\cdots\cdots(3.69)$$

By the substitution of the Equation(٣.٦٩)in general governing Equations (٣.٥٧)and(٣.٥٨)and re-arrange the final form **Vorticity Transport** equation and **Energy Transport** equation may be obtained:

$$\omega_\tau + (\omega_\zeta(-X_\tau . Y_\eta + Y_\tau . X_\eta) + \omega_\eta(X_\tau . Y_\zeta - Y_\tau . X_\zeta) + (-\psi_\zeta . \omega_\eta + \psi_\eta . \omega_\zeta))/J$$
$$= (\lambda . \omega_\zeta + \sigma . \omega_\eta + \alpha . \omega_{\zeta\zeta} - 2.\beta . \omega_{\zeta\eta} + \gamma . \omega_{\eta\eta})/(J^2 . \mathrm{Re}) \qquad \cdots\cdots\cdots(3.70)$$

$$\theta_\tau + (\theta_\zeta(-X_\tau . Y_\eta + Y_\tau . X_\eta) + \theta_\eta(X_\tau . Y_\zeta - Y_\tau . X_\zeta) + (-\psi_\zeta . \theta_\eta + \psi_\eta . \theta_\zeta))/J$$
$$= (\lambda . \theta_\zeta + \sigma . \theta_\eta + \alpha . \theta_{\zeta\zeta} - 2.\beta . \theta_{\zeta\eta} + \gamma . \theta_{\eta\eta})/(J^2 . \mathrm{Pe}) \qquad \cdots\cdots\cdots(3.71)$$

The quantities(X_τ)and(Y_τ)represent the grid point speed in horizontal and vertical direction respectively in physical space(**Thompson et al. [٦٦]).** The speed of grid existent dependent on the direction of oscillation, in which the(X_τ) and (Y_τ) coexist in case of orbital oscillation and incase of transverse or

inline oscillation only one exist (in case of transverse X_τ =۰, in case of inline Y_τ =۰)

In this study, the grid moves due to the movement of boundary which moves due to oscillation of the cylinder. The oscillating cylinder have harmonics sine wave motion governed by the following equations.

$$Y = A \cdot \sin(2 \cdot \pi \cdot F \cdot \tau) \quad \cdots\cdots\cdots(3.72)$$

$$X = A \cdot \sin(2 \cdot \pi \cdot F \cdot \tau) \quad \cdots\cdots\cdots(3.73)$$

Where,

:Dimensionless Amplitude. A

:Reduced Frequency. F

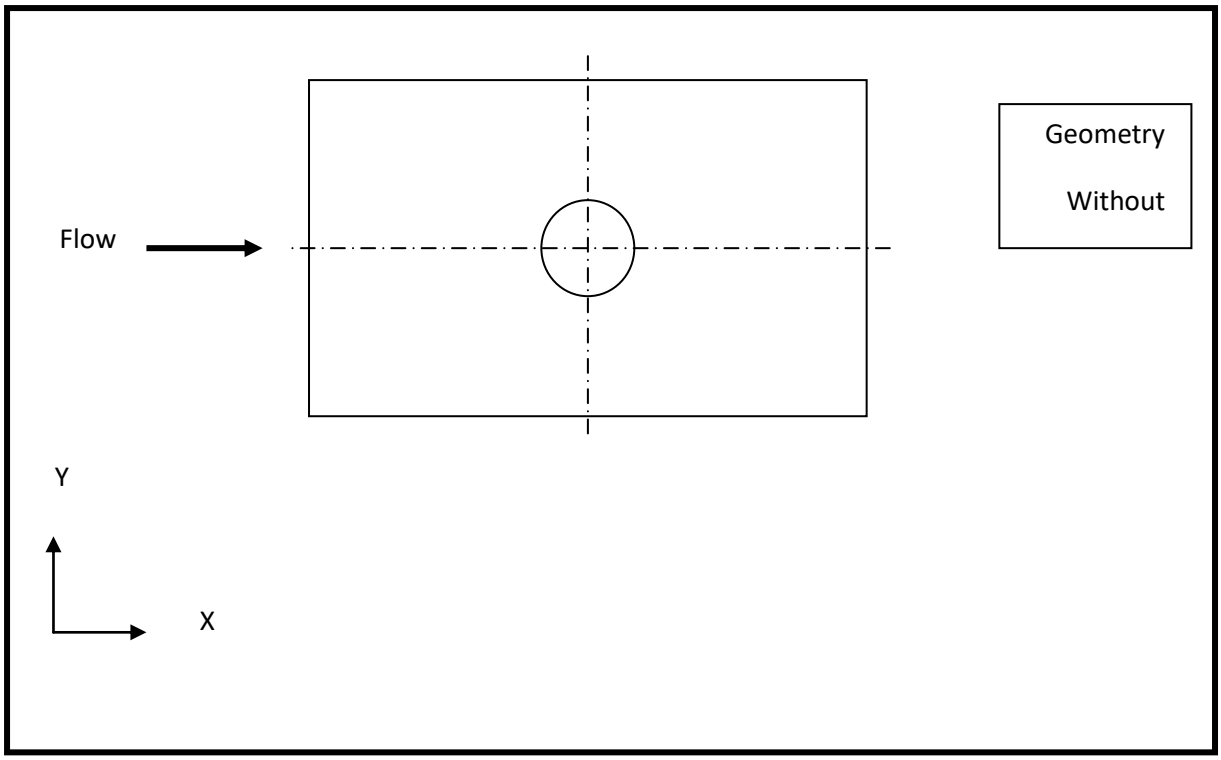
Flow
Geometry
Without
Y
X

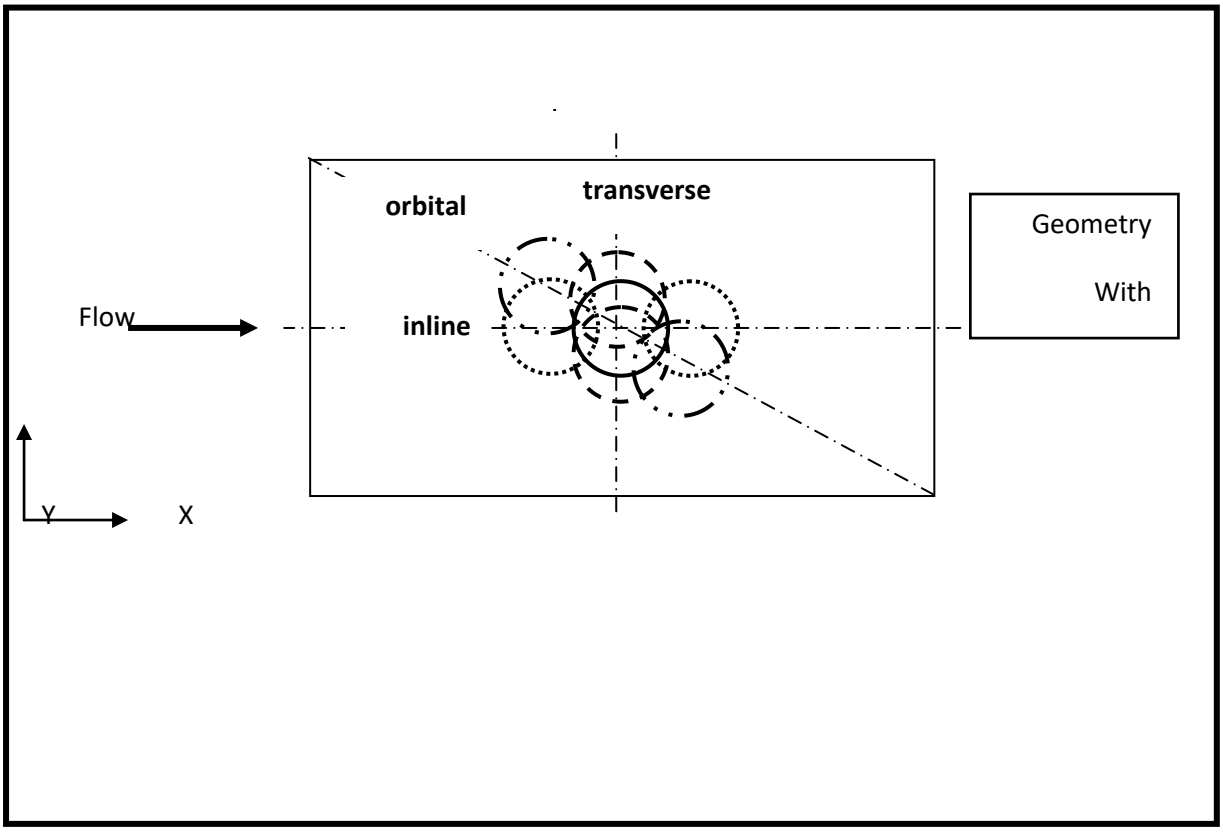
orbital
transverse
inline
Flow
Geometry
With
Y
X

Fig.(٣-٢)Geometry and coordinate system

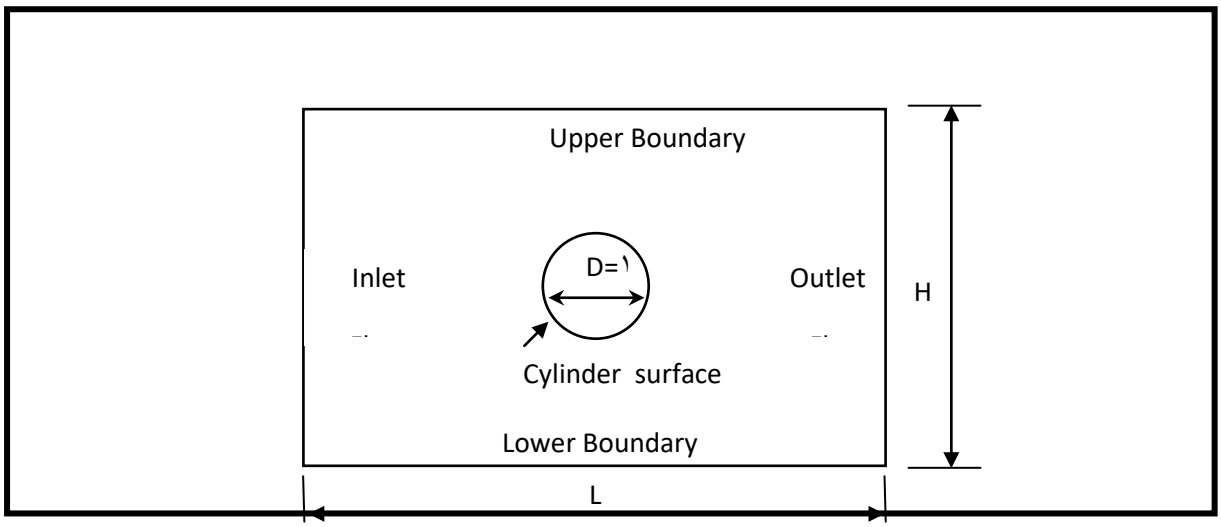

Fig.(٣-٣)The Physical Domain for the Present Study

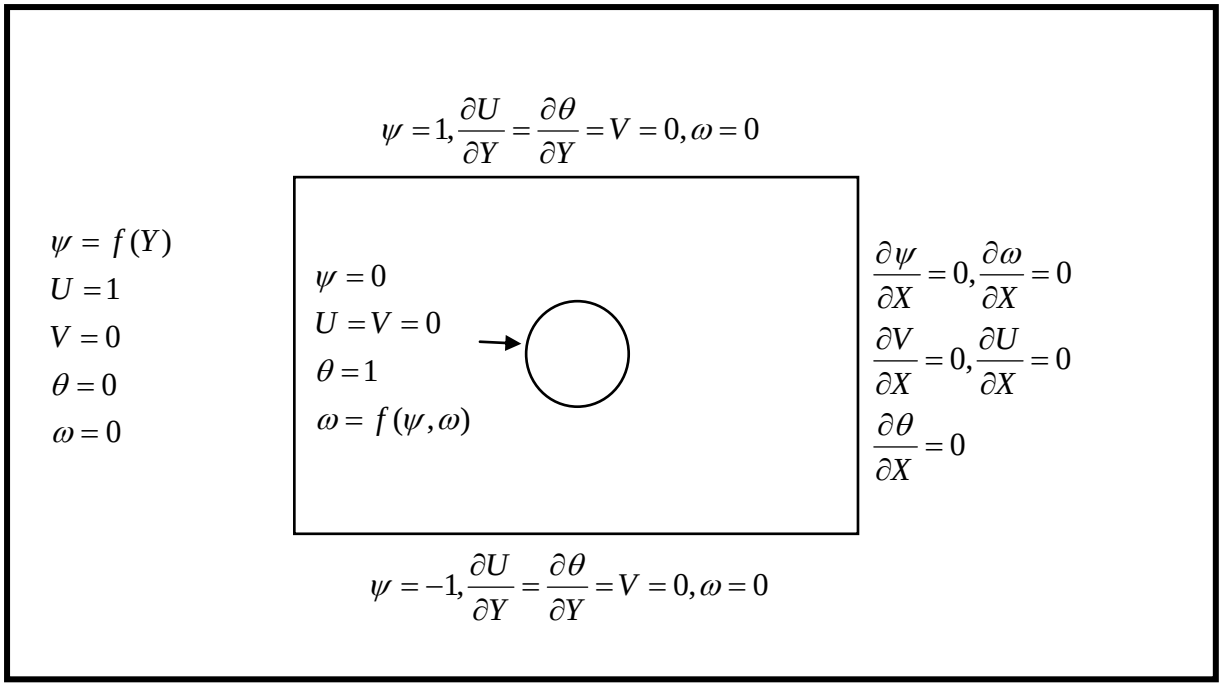

Fig.(٣-٤)The Computational Domain with Boundary Conditions

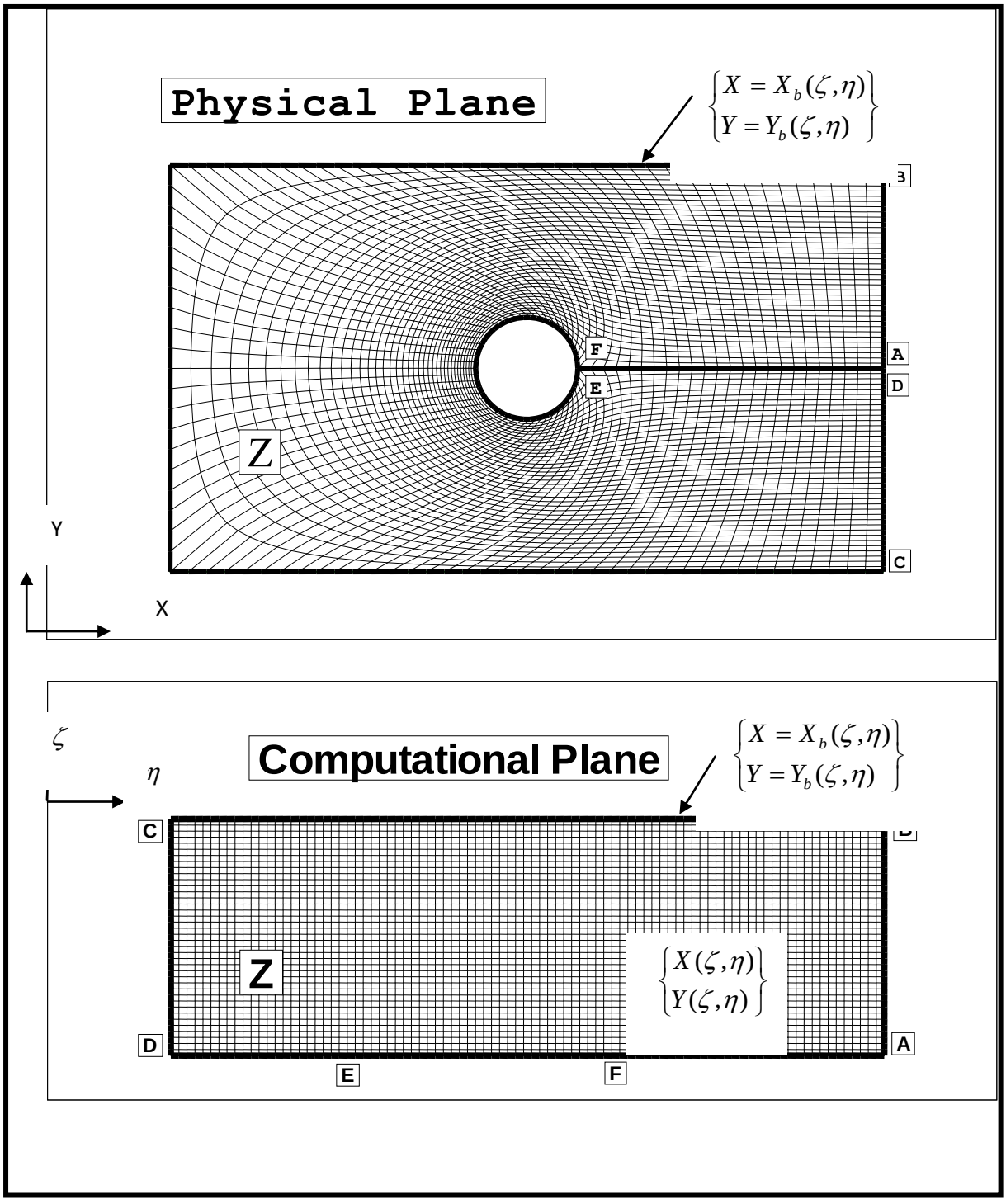

Fig.(٣-٥)Two-Dimensional Grid in Physical

NUMERICAL SOLUTION

٤.١ Introduction

The task of obtaining solutions to the governing equations of fluid mechanics represents one of the most challenging problems in science and engineering. In most instances, the mathematical formulations of fundamental laws of fluid mechanics are expressed as partial differential equations(PDE). Second-order partial differential equations appear frequently and, therefore, they are of particular interest in fluid mechanics and heat transfer. The governing equations of fluid mechanics form a set of coupled, nonlinear PDEs which must be solved with an irregular domain subject various initial and boundary conditions.

In many instances, analytical solutions of equations of fluid mechanics are limited. This is further restricted due to the imposed boundary conditions. For example, a PDE subjected to a Neumann boundary condition may not have an analytical solution.

Experimental fluid mechanics can provide some information regarding a particular flow field. However, the limitation on the hardware, such as the model and tunnel size and the difficulty in adequately simulating the prototype flow field, makes it an impractical means of obtaining flow fields for many problems.

A technique that has gained popularity in recent years is computational (numerical) fluid dynamics. Numerical analysis has been around for many years. However, improvements in computer hardware, resulting in increased memory and efficiency, have made it possible to solve equations in fluid mechanics using a variety of numerical techniques, **Hoffmann[٥٦].**

This chapter reveals the accurate details for the way of numerical solution and explains it completely, starting, with the operation of transforming the nonlinear governing differential equation to linear algebraic equations by using the method of finite differences that is considered the base for the numerical solution. Figure(٤-١) shows the road map of this chapter.

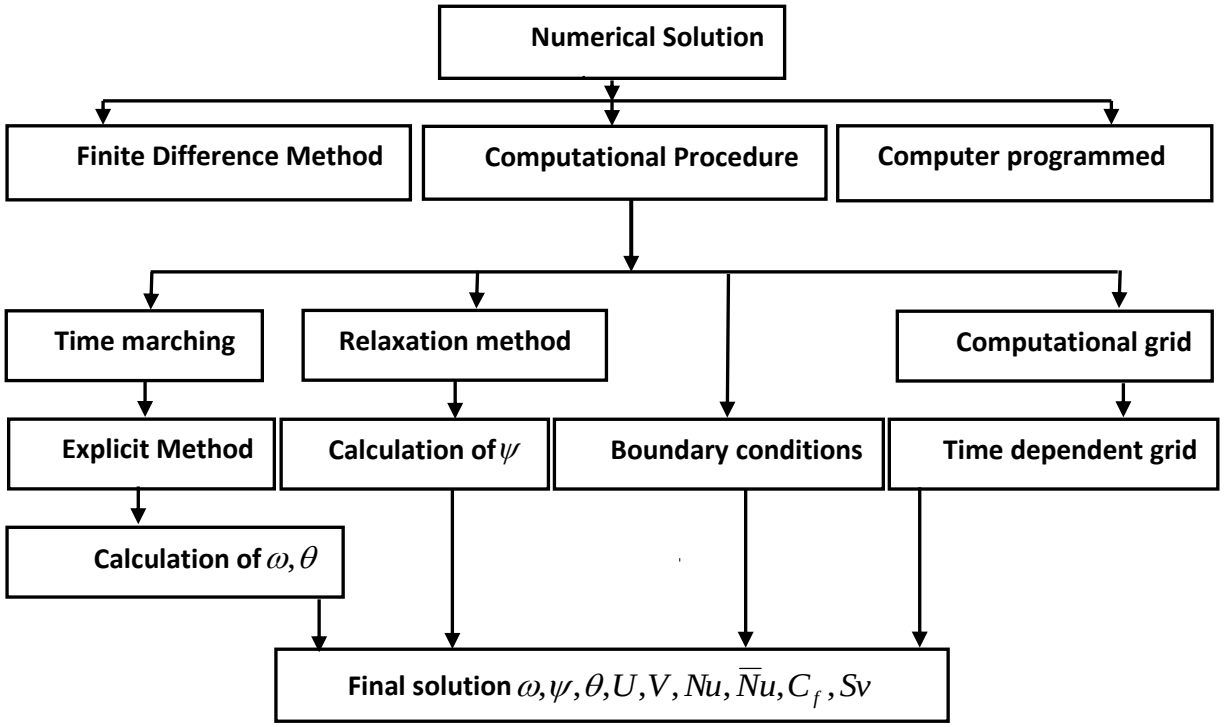

Fig.(٤-١) Road map of numerical solution

٤.٢ Finite Difference Method

The finite difference method is one of the most widely used numerical method for decades. Its popularity may be due to the fact that the mathematical concept of its discretization is relatively simple. Here, discretization is defined as an approximation procedure in which a continuous domain is replaced with a network or mesh of discrete points and the field unknowns are sought only at those discrete points rather than everywhere in the domain, **Shih[١].**

Equilibrium problems usually result is a system of algebraic equations, which must be solved simultaneously throughout the problem domain in conjunction with specified boundary values. Marching problem results in algebraic equations, which usually, can solve one at the time although it is often convenient to solve several of them at a time, **Roache[٥٤].**

One of the first steps to be taken in establishing a finite difference procedure for solving a PDE is to replace the continuous problem domain by a finite difference mesh or grid. For example, PDE is supposed to be solved for which $\psi(\zeta,\eta)$ is the dependent variable in the square domain $0<\zeta<1,0<\eta<1.$ A grid on the domain is established by replacing $\psi(\zeta,\eta)$ by $\psi(i\Delta\zeta, j\Delta\eta).$ Points can be located according to the values of i and j so different equations are usually written in terms of the general point(i, j) and its neighbors, **Anderson et al. [٥٣].**

The idea is that a finite difference representation for a derivative can be introduced by recalling the definition of the derivative the function $\psi(\zeta,\eta)$ at $\zeta=\zeta_o$, $\eta=\eta_o$.

$$\frac{\partial\psi}{\partial\zeta}=\lim_{\Delta\zeta\to 0}\frac{\psi(\zeta_o+\Delta\zeta,\eta_o)-\psi(\zeta_o,\eta_o)}{\Delta\zeta}$$

Here,if ψ is continuous, it is expected that the term[$\psi(\zeta_o+\Delta\zeta,\eta_o)-\psi(\zeta_o,\eta_o)]/\Delta\zeta$ will be a reasonable approximation to $(\partial\psi/\partial\zeta)$ for a sufficiently small but finite $\Delta\zeta$, **Anderson et al. [٥٣]**.

The finite difference approximations for the stream function derivative are, as follows:

First center difference formula:

$$\frac{\partial\psi}{\partial\zeta}=\frac{\psi_{i+1,j}-\psi_{i-1,j}}{2.\Delta\zeta}$$
$$\frac{\partial\psi}{\partial\eta}=\frac{\psi_{i,j+1}-\psi_{i,j-1}}{2.\Delta\eta}$$

and second center difference formula:

$$\frac{\partial^2\psi}{\partial\zeta^2}=\frac{\psi_{i+1,j}-2.\psi_{i,j}+\psi_{i-1,j}}{\Delta\zeta^2}$$
$$\frac{\partial^2\psi}{\partial\eta^2}=\frac{\psi_{i,j+1}-2.\psi_{i,j}+\psi_{i,j-1}}{\Delta\eta^2}$$

similarly for vorticity ω and temperature θ.

٤.٣ Computational Procedure

The purpose of this section is to outline all of the computational works, which take place and to explain in details the mathematical model. It consists of two parts, the first is concerned with vorticity transport and energy equations that their solution will be achieved by using the time marching technique, and the second part is concerned with the stream function that will be solved by relaxation method.

٤.٣.١ Time Marching Method

Time marching is a comparatively new method of calculating flow in turbo-machinery developments. The method has become more and more popular for the calculation of inviscid, transonic flows. The main reason for this evolution is that the partial differential equation describing a time dependent flow are hyperbolic with respect to time in both subsonic and supersonic flow regions and hence the same finite difference operator can be used over the complete flow field.

Another important factor is the physical understanding that can be obtained from the solutions. With the time marching method the steady flow is calculated after a sufficient long time of the solution of the modeling of the flow enables the user to perform numerical experiments and to obtain solutions where he has no prior knowledge of the flow pattern.

Another attraction is the comparative ease with which such method is extendable to compute fully three dimensional flows.

The basic principle of time marching is to start from an initial guess of the flow pattern. Then the method solves the unsteady continuity, momentum and

energy equations for the evolution of the flow in time until thermal equilibrium is established.

Basically, the flow region is divided into a grid network so that different terms in the governing equations are defined at each grid point. The flow field is then solved from the governing equations in finite difference form subjected to the imposed boundary conditions.

With the flow equations applied to each grid point in turn, the solution becomes closer to the steady state solution for each time step.

The new vorticities associated with each grid points are solved from the stream function/vorticity equation by using the old values of vorticities. The temperatures are calculated from the energy equation. The iteration process is repeated until the solution reaches steady state.

The procedure with the time dependent technique consists of writing the unsteady differential equations in a suitable form, and then solving the finite difference analogue of these equations as a function of time. The solution of this difference analogue should tend to the solution of the differential equations when the differential problem is well posed, the difference formulation is consistent and the computation is stable, **Iatridis[٥١].**

٤.٣.١.١ Explicit Method

An explicit scheme is one for which only one unknown appears in the difference equation in a manner which permits evaluation in terms of known quantities, **Anderson et al.[٥٣].** The explicit method include the calculation of the vorticity or temperature for a next time($\tau + \Delta\tau$)for interior node in terms of

the vorticity or temperature at previous time(τ) for the same node and to its neighboring node that in each node in the grid the temperature and vorticity will be known at the time($\tau = 0$)in initial condition to the problem. So, the vorticity and temperature for each node will be obtained at new time by marching out in time.

As it is indicated previously, there will be a use of finite differences method to transform both vorticity transport and energy equations to approximate algebraic equations. These equations include a number of terms; terms on the left side of equation are called convection terms, while the terms on the right side are called diffusion terms in addition to unsteady terms.

As for the transform of the time derivative for vorticity, the forward differences will be used to change the vorticity that takes place at the location (i, j), and through the periodic time from the time(τ)to time ($\tau + \Delta\tau$)that it is possible to put the time derivative for the vorticity, as in the following:

$$\frac{\partial \omega}{\partial \tau} = \frac{\omega_{i,j}^{n+1} - \omega_{i,j}^{n}}{\Delta \tau} \qquad \cdots\cdots\cdots(4.1)$$

where:

$\omega_{i,j}^{n+1}$:represents the vorticity at $(\tau + \Delta\tau)$.

$\omega_{i,j}^{n}$:represents the vorticity at (τ)

with respect to transform convection terms on the left, central differences will be used, as follow:

$$\frac{\partial \psi}{\partial \zeta}\cdot\frac{\partial \omega}{\partial \eta}=\frac{\psi_{i+1,j}-\psi_{i-1,j}}{2.\Delta\zeta}\cdot\frac{\omega^{n}_{i,j+1}-\omega^{n}_{i,j-1}}{2.\Delta\eta} \quad \cdots\cdots\cdots(4.2)$$

$$\frac{\partial \psi}{\partial \eta}\cdot\frac{\partial \omega}{\partial \zeta}=\frac{\psi_{i,j+1}-\psi_{i,j-1}}{2.\Delta\eta}\cdot\frac{\omega^{n}_{i+1,j}-\omega^{n}_{i-1,j}}{2.\Delta\zeta} \quad \cdots\cdots\cdots(4.3)$$

In case of oscillation it has another terms in convection part of governing equation. These terms are solved by central finite difference .

$$\frac{\partial \omega}{\partial \zeta}(-X_{\tau}\cdot Y_{\eta}+Y_{\tau}\cdot X_{\eta})=\frac{\omega^{n}_{i+1,j}-\omega^{n}_{i-1,j}}{2\cdot\Delta\zeta}[-(\frac{X^{n+1}_{i,j}-X^{n}_{i,j}}{\Delta\tau})\cdot Y_{\eta(i,j)}+(\frac{Y^{n+1}_{i,j}-Y^{n}_{i,j}}{\Delta\tau})\cdot X_{\eta(i,j)}]\cdots\cdots(4.4)$$

$$\frac{\partial \omega}{\partial \eta}(X_{\tau}\cdot Y_{\zeta}-Y_{\tau}\cdot X_{\zeta})=\frac{\omega^{n}_{i,j+1}-\omega^{n}_{i,j-1}}{2\cdot\Delta\eta}[(\frac{X^{n+1}_{i,j}-X^{n}_{i,j}}{\Delta\tau})\cdot Y_{\zeta(i,j)}-(\frac{Y^{n+1}_{i,j}-Y^{n}_{i,j}}{\Delta\tau})\cdot X_{\zeta(i,j)}]\cdots\cdots\cdots(4.5)$$

Also, the central difference will be used to transform the diffusion term, as follows:

$$\frac{\partial \omega}{\partial \zeta}=\frac{\omega^{n}_{i+1,j}-\omega^{n}_{i-1,j}}{2.\Delta\zeta} \quad \cdots\cdots\cdots(4.6)$$

$$\frac{\partial \omega}{\partial \eta}=\frac{\omega^{n}_{i,j+1}-\omega^{n}_{i,j-1}}{2.\Delta\eta} \quad \cdots\cdots\cdots(4.7)$$

$$\frac{\partial^{2} \omega}{\partial \zeta^{2}}=\frac{\omega^{n}_{i+1,j}-2.\omega^{n}_{i,j}+\omega^{n}_{i-1,j}}{\Delta\zeta^{2}} \quad \cdots\cdots\cdots(4.8)$$

$$\frac{\partial^{2} \omega}{\partial \eta^{2}}=\frac{\omega^{n}_{i,j+1}-2.\omega^{n}_{i,j}+\omega^{n}_{i,j-1}}{\Delta\eta^{2}} \quad \cdots\cdots\cdots(4.9)$$

$$\frac{\partial^{2} \omega}{\partial \zeta\partial \eta}=\frac{\omega^{n}_{i+1,j+1}-\omega^{n}_{i+1,j-1}-\omega^{n}_{i-1,j+1}+\omega^{n}_{i-1,j-1}}{4.\Delta\zeta.\Delta\eta} \quad \cdots\cdots\cdots(4.10)$$

By the substitution of equations(٤.١,٢,٣,٦,٧,٨,٩,١٠)in the vorticity transport (٣.٥٧) the following linear equation may obtained:

$$\begin{aligned}\omega^{n+1}_{i,j}=\omega^{n}_{i,j}+\Delta\bar{t}[&(\frac{\psi_{i+1,j}-\psi_{i-1,j}}{2.\Delta\zeta}\cdot\frac{\omega^{n}_{i,j+1}-\omega^{n}_{i,j-1}}{2.\Delta\eta}-\frac{\psi^{n}_{i,j+1}-\psi^{n}_{i,j-1}}{2.\Delta\eta}\cdot\frac{\omega^{n}_{i+1,j}-\omega^{n}_{i-1,j}}{2.\Delta\zeta})/J_{(i,j)}\\&+(\lambda_{(i,j)}\cdot\frac{\omega^{n}_{i+1,j}-\omega^{n}_{i-1,j}}{2.\Delta\zeta}+\sigma_{(i,j)}\cdot\frac{\omega^{n}_{i,j+1}-\omega^{n}_{i,j-1}}{2.\Delta\eta}+\alpha_{(i,j)}\cdot\frac{\omega^{n}_{i+1,j}-2.\omega^{n}_{i,j}+\omega^{n}_{i-1,j}}{\Delta\zeta^{2}}\\&-2\cdot\beta_{(i,j)}\cdot\frac{\omega^{n}_{i+1,j+1}-\omega^{n}_{i+1,j-1}-\omega^{n}_{i-1,j+1}+\omega^{n}_{i-1,j-1}}{4.\Delta\zeta.\Delta\eta}\\&+\gamma_{(i,j)}\frac{\omega^{n}_{i,j+1}-2.\omega^{n}_{i,j}+\omega^{n}_{i,j-1}}{\Delta\eta^{2}})/\mathrm{Re}.J^{2}_{(i,j)}]\end{aligned} \quad \cdots\cdots\cdots(4.11)$$

Either with respect to the energy equation the same procedure may be used

in transforming convection and diffusion terms in addition to unsteady terms from differential form into algebraic equation.

Now, the energy Equation(٣.٥٨)will be transformed into linear equation, as follows:

$$\theta_{i,j}^{n+1}=\theta_{i,j}^{n}+\Delta\bar{t}[(\frac{\psi_{i+1,j}-\psi_{i-1,j}}{2.\Delta\zeta}\cdot\frac{\theta_{i,j+1}^{n}-\theta_{i,j-1}^{n}}{2.\Delta\eta}-\frac{\psi_{i,j+1}^{n}-\psi_{i,j-1}^{n}}{2.\Delta\eta}\cdot\frac{\theta_{i+1,j}^{n}-\theta_{i-1,j}^{n}}{2.\Delta\zeta})/J_{(i,j)}$$
$$+(\lambda_{(i,j)}\cdot\frac{\theta_{i+1,j}^{n}-\theta_{i-1,j}^{n}}{2.\Delta\zeta}+\sigma_{(i,j)}\cdot\frac{\theta_{i,j+1}^{n}-\theta_{i,j-1}^{n}}{2.\Delta\eta}+\alpha_{(i,j)}\cdot\frac{\theta_{i+1,j}^{n}-2.\theta_{i,j}^{n}+\theta_{i-1,j}^{n}}{\Delta\zeta^{2}}$$
$$-2\cdot\beta_{(i,j)}\cdot\frac{\theta_{i+1,j+1}^{n}-\theta_{i+1,j-1}^{n}-\theta_{i-1,j+1}^{n}+\theta_{i-1,j-1}^{n}}{4.\Delta\zeta.\Delta\eta}$$
$$+\gamma_{(i,j)}\frac{\theta_{i,j+1}^{n}-2.\theta_{i,j}^{n}+\theta_{i,j-1}^{n}}{\Delta\eta^{2}})/\mathrm{Pe}.J^{2}{}_{(i,j)}] \qquad \cdots\cdots\cdots(4.12)$$

In case of time dependent grid the vorticity transport and energy equation will be transformed into linear equation by the same manner that used in the above equations, as follows:

By substitution of Equations(٤.١ to ٤.١٠)in the vorticity transport(٣.٧٠) the following linear equation may be obtained:

$$\omega_{i,j}^{n+1}=\omega_{i,j}^{n}+\Delta\tau[\frac{\omega_{i+1,j}^{n}-\omega_{i-1,j}^{n}}{2\cdot\Delta\zeta}\cdot(-Y_{\eta(i,j)}\cdot\frac{X_{i,j}^{n+1}-X_{i,j}^{n}}{\Delta\tau}+X_{\eta(i,j)}\cdot\frac{Y_{i,j}^{n+1}-Y_{i,j}^{n}}{\Delta\tau})$$
$$+\frac{\omega_{i,j+1}^{n}-\omega_{i,j-1}^{n}}{2\cdot\Delta\eta}\cdot(Y_{\zeta(i,j)}\cdot\frac{X_{i,j}^{n+1}-X_{i,j}^{n}}{\Delta\tau}-X_{\zeta(i,j)}\cdot\frac{Y_{i,j}^{n+1}-Y_{i,j}^{n}}{\Delta\tau})$$
$$+(\frac{\psi_{i+1,j}-\psi_{i-1,j}}{2.\Delta\zeta}\cdot\frac{\omega_{i,j+1}^{n}-\omega_{i,j-1}^{n}}{2.\Delta\eta}-\frac{\psi_{i,j+1}^{n}-\psi_{i,j-1}^{n}}{2.\Delta\eta}\cdot\frac{\omega_{i+1,j}^{n}-\omega_{i-1,j}^{n}}{2.\Delta\zeta})/J_{(i,j)}$$
$$+(\lambda_{(i,j)}\cdot\frac{\omega_{i+1,j}^{n}-\omega_{i-1,j}^{n}}{2.\Delta\zeta}+\sigma_{(i,j)}\cdot\frac{\omega_{i,j+1}^{n}-\omega_{i,j-1}^{n}}{2.\Delta\eta}+\alpha_{(i,j)}\cdot\frac{\omega_{i+1,j}^{n}-2.\omega_{i,j}^{n}+\omega_{i-1,j}^{n}}{\Delta\zeta^{2}}$$
$$-2\cdot\beta_{(i,j)}\cdot\frac{\omega_{i+1,j+1}^{n}-\omega_{i+1,j-1}^{n}-\omega_{i-1,j+1}^{n}+\omega_{i-1,j-1}^{n}}{4.\Delta\zeta.\Delta\eta}$$
$$+\gamma_{(i,j)}\frac{\omega_{i,j+1}^{n}-2.\omega_{i,j}^{n}+\omega_{i,j-1}^{n}}{\Delta\eta^{2}})/\mathrm{Re}.J^{2}{}_{(i,j)}] \qquad \cdots\cdots\cdots(4.13)$$

Also, the energy equation will be transformed into linear equation by substituted the same equation in the above into the Equation(٣.٧١)as follows:

$$\theta_{i,j}^{n+1} = \theta_{i,j}^{n} + \Delta\tau[\frac{\theta_{i+1,j}^{n} - \theta_{i-1,j}^{n}}{2\cdot\Delta\zeta}\cdot(-Y_{\eta(i,j)}\cdot\frac{X_{i,j}^{n+1} - X_{i,j}^{n}}{\Delta\tau} + X_{\eta(i,j)}\cdot\frac{Y_{i,j}^{n+1} - Y_{i,j}^{n}}{\Delta\tau})$$

$$+\frac{\theta_{i,j+1}^{n} - \theta_{i,j-1}^{n}}{2\cdot\Delta\eta}\cdot(Y_{\zeta(i,j)}\cdot\frac{X_{i,j}^{n+1} - X_{i,j}^{n}}{\Delta\tau} - X_{\zeta(i,j)}\cdot\frac{Y_{i,j}^{n+1} - Y_{i,j}^{n}}{\Delta\tau})$$

$$+(\frac{\psi_{i+1,j} - \psi_{i-1,j}}{2.\Delta\zeta}\cdot\frac{\theta_{i,j+1}^{n} - \theta_{i,j-1}^{n}}{2.\Delta\eta} - \frac{\psi_{i,j+1}^{n} - \psi_{i,j-1}^{n}}{2.\Delta\eta}\cdot\frac{\theta_{i+1,j}^{n} - \theta_{i-1,j}^{n}}{2.\Delta\zeta})/J_{(i,j)}$$

$$+(\lambda_{(i,j)}\cdot\frac{\theta_{i+1,j}^{n} - \theta_{i-1,j}^{n}}{2.\Delta\zeta} + \sigma_{(i,j)}\cdot\frac{\theta_{i,j+1}^{n} - \theta_{i,j-1}^{n}}{2.\Delta\eta} + \alpha_{(i,j)}\cdot\frac{\theta_{i+1,j}^{n} - 2.\theta_{i,j}^{n} + \theta_{i-1,j}^{n}}{\Delta\zeta^{2}}$$

$$-2\cdot\beta_{(i,j)}\cdot\frac{\theta_{i+1,j+1}^{n} - \theta_{i+1,j-1}^{n} - \theta_{i-1,j+1}^{n} + \theta_{i-1,j-1}^{n}}{4.\Delta\zeta.\Delta\eta}$$

$$+\gamma_{(i,j)}\frac{\theta_{i,j+1}^{n} - 2.\theta_{i,j}^{n} + \theta_{i,j-1}^{n}}{\Delta\eta^{2}})/\mathrm{Pe}.J^{2}{}_{(i,j)}] \qquad \cdots\cdots\cdots(4.14)$$

where, $\Delta\zeta = \Delta\eta = 1$

٤.٣.٢ Relaxation Method

In the iterative solution of the algebraic equation or in the overall iterative scheme employed for handling nonlinearly, it is often desirable to speed up or to slowdown the changes, from iteration to iteration, in the values of the dependent variable. This process is called over relaxation or under relaxation .

The Relaxation method, in general, is a traditional technique of solving a system of finite difference equations. It is suitable for use with a coarse mesh and permits the solution to be effected by means of hand calculations. Application of the method is facilitated by the following procedure **,Iatridis[٥١].**

I. After identifying lines of symmetry and establishing the nodal network for the system, the appropriate finite difference equation is written for each node at which the stream function is unknown. The residual for the node should appear on the right hand side of each equation.

II. Values are then assumed for each of the unknown nodal stream function. To minimize subsequent computations, efforts are made to guess values that are close to the actual stream function.

III. Using the assumed stream function, the residual is then calculated at each node for which the actual stream function is desired.

IV. The largest residual is identified, and the relaxation process is initiated. This is done by adjusting the nodal stream function to the largest residual by an amount which will relax this residual to zero. Since changing the stream function of one node will alter the residuals of neighboring nodes, the values of these residuals must be recomputed.

V. The node now having the largest residual is identified.

VI. Repeated the process until all residuals have been related to values that are small enough to insure achievement of desired accuracy.

Under relaxation, now, is a very useful device for nonlinear problems. It is often employed, also in the present case, to avoid divergence in the iterative solution of strongly nonlinear equations.

Working with the stream function (٣.٥٦) as follow:

$$(\lambda.\psi_{\zeta} + \sigma.\psi_{\eta} + \alpha.\psi_{\zeta\zeta} - 2.\beta.\psi_{\zeta\eta} + \gamma.\psi_{\eta\eta}) / J^2 = -\omega \qquad \cdots\cdots\cdots(4.15)$$

the following equation is derived, in which the finite difference approximations have been introduced:

$$\lambda_{(i,j)} \frac{\psi_{i+1,j} - \psi_{i-1,j}}{2.\Delta\zeta} + \sigma_{(i,j)} \frac{\psi_{(i,j+1)} - \psi_{(i,j-1)}}{2.\Delta\eta} + \alpha_{(i,j)} \frac{\psi_{i+1,j} - 2.\psi_{i,j} + \psi_{i-1,j}}{\Delta\zeta^2}$$
$$+\gamma_{(i,j)} \frac{\psi_{i,j+1} - 2.\psi_{i,j} + \psi_{i,j-1}}{\Delta\eta^2} - 2.\beta_{(i,j)} \frac{\psi_{i+1,j+1} - \psi_{i+1,j-1} - \psi_{i-1,j+1} + \psi_{i-1,j-1}}{4.\Delta\zeta\Delta\eta}$$
$$+J_{(i,j)} \cdot \omega_{(i,j)} = Error = 0 \qquad \cdots\cdots\cdots(4.16)$$

The equation is solved by substituting in the current values of ψ and (ω)where upon the right-hand side $Error$ will be non Zero. In order to solve the

equation, the $Error$ has to be subtracted from both sides. Thus, if a small change $(\Delta\psi_{i,j})$ is made to the centre point value $(\psi_{i,j})$ to do this, the following equation is obtained:

$$(-\frac{2.\alpha_{(i,j)}}{\Delta\zeta^2}-\frac{2.\gamma_{(i,j)}}{\Delta\eta^2})\cdot\Delta\psi_{i,j}=-Error \qquad \cdots\cdots\cdots(4.17)$$

$$\Delta\psi_{i,j}=\frac{Error}{2.(\frac{\alpha_{(i,j)}}{\Delta\zeta^2}+\frac{\gamma_{(i,j)}}{\Delta\eta^2})} \qquad \cdots\cdots\cdots(4.18)$$

can then be calculated from $\psi(it)$ from the previous iteration as: $\psi(it+1)$

$$\psi(it+1)=\psi(it)+RF\cdot\Delta\psi_{i,j} \qquad \cdots\cdots\cdots(4.19)$$

where RF is the relaxation factor which would be equal to(١) .

However, more rapid convergence can often be obtained by employing a higher value of relaxation factor up to a maximum of (٢). Conversely it is sometimes necessary to use values less then (١) in order to maintain computational stability.

It should be noted that, when the iterations converge, that is, when $\psi(it+1)$ becomes equal to $\psi(it)$,equation(٤.١٩) implies that the converged values of(ψ)do satisfy the equation(٤.١٦).

٤.٣.٣ Assessment of Boundary Conditions

This article shows how to calculate the boundary conditions that are used in numerical solution for physical problem.

٤.٣.٣.١ Calculation of Vorticity on the Cylinder Surface

The appropriate evaluation of the vorticity at a wall(on the surface of cylinder)is very crucial, since the success of a stream function-vorticity scheme, more or less, lies on the resolution of the boundary vorticities, **Chun** and **Boehm[١٤].**

The vorticity is determined in the customary manner, by expanding(ψ)out from the walls in a Taylor series and invoking the no-slip condition, **Roache** and **Mueller[٦٨]** and **Roache[٥٤].** The first-order form is computed as follow, where,O is order of magnitude:

$$\psi_{i,w+1} = \psi_{i,w} + \left.\frac{\partial \psi}{\partial Y}\right)_{i,w} \cdot \Delta Y + \frac{1}{2} \cdot \left.\frac{\partial^2 \psi}{\partial Y^2}\right)_{i,w} \cdot \Delta Y^2 + O \cdot \Delta Y^3 \qquad \cdots\cdots\cdots(4.20)$$

where $\psi_{i,w}$ node is located on the cylinder wall and $\psi_{i,w+1}$ node is located near the cylinder wall.

The value of $\left.\frac{\partial \psi}{\partial Y}\right)_{i,w}$ may be equal to **Zero**, because of horizontal velocity,$U_{i,w}$, which can be dependent on the cylinder wall where no-slip occurs.

$$\left.\frac{\partial \psi}{\partial Y}\right)_{i,w} = 0 \qquad \cdots\cdots\cdots(4.21)$$

Since the vorticity at wall is:

$$\omega_{i,j} = \left(\frac{\partial V}{\partial X} - \frac{\partial U}{\partial Y}\right)_{i,w} \qquad \cdots\cdots\cdots(4.22)$$

Because of the vertical velocity(V) is constant along wall.

$$\left.\frac{\partial V}{\partial X}\right)_{i,w} = 0 \qquad \cdots\cdots\cdots(4.23)$$

Equation(٤.٢٢)becomes:

$$\omega_{i,j} = -\left(\frac{\partial U}{\partial Y}\right)_{i,w} \qquad \cdots\cdots\cdots(4.24)$$

From definition of the stream function it may be obtained:

$$U = \frac{\partial \psi}{\partial Y}\Bigg)_{i,w} \Rightarrow$$

$$\frac{\partial U}{\partial Y}\Bigg)_{i,w} = \frac{\partial^2 \psi}{\partial Y^2}\Bigg)_{i,w} \qquad \cdots\cdots\cdots(4.25)$$

substitution of Equation(٤.٢٥)into Equation(٤.٢٤)becomes:

$$\omega_{i,w} = -\frac{\partial^2 \psi}{\partial Y^2}\Bigg)_{i,w} \qquad \cdots\cdots\cdots(4.26)$$

The substitution of the equations (٤.٢١) and (٤.٢٦) into equation(٤.٢٠) gives:

$$\psi_{i,w+1} = \psi_{i,w} - \frac{1}{2}\omega_{i,w} \cdot \Delta Y^2 \qquad \cdots\cdots\cdots(4.27)$$

Also, the value of boundary vorticity is, **Pozrikidis[٥٥]**.

$$\omega_{i,w} = -2 \cdot \frac{\psi_{i,w+1} - \psi_{i,w}}{\Delta Y^2} \qquad \cdots\cdots\cdots(4.28)$$

Equation(٤.٢٨)can be rewritten in the form of general coordinate(ζ,η),**Broughton** and **Oliver[٦٤].**

$$\omega_{i,w} = -2 \cdot \gamma_{(i,w)} \cdot (\psi_{i,w+1} - \psi_{i,w}) / J^2{}_{(i,w)} \qquad \cdots\cdots\cdots(4.29)$$

٤.٣.٣.٢ Calculation of the Values of Vorticity, Stream Function and Temperature at Flow Exit:

Depending on the boundary conditions at flow exit, hence.

$$\frac{\partial \phi}{\partial X} = 0 \qquad \cdots\cdots\cdots(4.30)$$

where(ϕ): may represent vorticity(ω),stream(ψ)and temperature(θ).

Transformation of equation(٤.٣٠)into general form(ζ,η)depending on Equation(٣.٤٩) is done, as follows:

$$\frac{\partial \phi}{\partial X} = (\alpha \cdot \phi_{\zeta} - \beta \cdot \phi_{\eta}) / J \cdot \sqrt{\alpha} = 0 \qquad \cdots\cdots\cdots(4.31)$$

$$\alpha \cdot \phi_{\zeta} - \beta \cdot \phi_{\eta} = 0 \qquad \cdots\cdots\cdots(4.32)$$

Central finite difference are used for($\partial\phi/\partial\eta$)and third order backward differences are used for ($\partial\phi/\partial\zeta$) ,**Hoffmann[٥٦])** and **Petrovic** and **Stupar [٦٣],** as follows:

$$\alpha_{(i,j)} \cdot \frac{11 \cdot \phi_{i,j} + 18 \cdot \phi_{i-1,j} + 9 \cdot \phi_{i-2,j} - 2 \cdot \phi_{i-3,j}}{6 \cdot \Delta\zeta} - \beta_{(i,j)} \frac{\phi_{i,j+1} - \phi_{i,j-1}}{2.\Delta\eta} = 0 \qquad \cdots\cdots\cdots(4.33)$$

where, $\Delta\zeta = \Delta\eta = 1$

Rearranging:

$$\phi_{i,j} = (3 \cdot \beta_{(i,j)} \cdot \frac{\phi_{i,j+1} - \phi_{i,j-1}}{\alpha_{(i,j)}} + 18 \cdot \phi_{i-1,j} - 9 \cdot \phi_{i-2,j} + 2 \cdot \phi_{i-3,j}) / 11 \qquad \cdots\cdots\cdots(4.34)$$

$\phi_{i,j}$ = represents the vorticity or temperature or stream function at exit.

٤.٣.٣.٣ Boundary Condition at the Cuts in the C-Grid

When C-type grids are used, there will be a branch cut across the wake region to maintain a simple connected region. Since physically the flow variables are continuous across this cut, the properties on this cut are specified as averages of the variables one point above and one point below the cut line.

٤.٣.٤ Calculation of Horizontal and Vertical Velocity

The velocity components are calculated from the equations(٣.٥٩)and(٣.٦٠) which in the transformed plane become as equations(٣.٦٣) and(٣.٦٤):

$$U = (X_\zeta \cdot \psi_\eta + X_\eta \cdot \psi_\zeta)/J = [X_{\zeta(i,j)} \cdot (\frac{\psi_{i,j+1} - \psi_{i,j-1}}{2 \cdot \Delta\eta}) - X_{\eta(i,j)} (\frac{\psi_{i+1,j} - \psi_{i-1,j}}{2 \cdot \Delta\zeta})]/J_{(i,j)} \cdots\cdots(4.35)$$

$$V = (Y_\zeta \cdot \psi_\eta - Y_\eta \cdot \psi_\zeta)/J = [Y_{\zeta(i,j)} \cdot (\frac{\psi_{i,j+1} - \psi_{i,j-1}}{2 \cdot \Delta\eta}) - Y_{\eta(i,j)} \cdot (\frac{\psi_{i+1,j} - \psi_{i-1,j}}{2 \cdot \Delta\zeta})]/J_{(i,j)} \cdots\cdots\cdots(4.36)$$

velocities in the interior of the field may be obtained from these relations using second-order central difference expressions for all derivatives as given above.

On the cylinder surface, $\psi_\zeta = 0.0$, **Thames et al.[٦١]**,so that these expressions reduce to:

$$U = X_\zeta \cdot \psi_\eta / J = X_{\zeta(i,j)} \cdot (\frac{\psi_{i,j+1} - \psi_{i,j-1}}{2 \cdot \Delta\eta})/J_{(i,j)} \qquad \cdots\cdots\cdots(4.37)$$

$$V = Y_\zeta \cdot \psi_\eta / J = Y_{\zeta(i,j)} \cdot (\frac{\psi_{i,j+1} - \psi_{i,j-1}}{2 \cdot \Delta\eta})/J_{(i,j)} \qquad \cdots\cdots\cdots(4.38)$$

٤.٣.٥ Calculation of Heat Transfer Coefficients

Heat transfer rate and the temperature distribution around cylinder are very important in most engineering applications. So, the heat transfer coefficient may be expressed by dimensionless form by local Nusselt number, as follows:

The rate of heat transfer from the cylinder surface is ,**Hornbeck[٦٩]**

$$q_w = -k \frac{\partial T}{\partial n}\Big)_w \qquad \cdots\cdots\cdots(4.39)$$

Now, heat transfer by convection is equal to heat transfer by conduction.

$$h \cdot (T_w - T_o) = -k \frac{\partial T}{\partial n}\Big)_w \qquad \cdots\cdots\cdots(4.40)$$

Rearranging:

$$h = -k\frac{\partial T}{\partial n}\cdot\frac{1}{T_w - T_o} \qquad \cdots\cdots\cdots(4.41)$$

Where, the value of Nusselt number is, **Incropera** and **Dewitt[٧٠]**

$$Nu = \frac{h.D}{k} \qquad \cdots\cdots\cdots(4.42)$$

substitution of equation(٤.٤١)into Equation(٤.٤٢)get the definition of local Nusselt number in differential form, **Cebeci** and **Bradshaw[٧١].**

$$Nu = -\frac{D}{T_w - T_o}\cdot\frac{\partial T}{\partial n} \qquad \cdots\cdots\cdots(4.43)$$

In term of dimensionless form:

$$Nu = -\frac{\partial \theta}{\partial n}\Big)_w \qquad \cdots\cdots\cdots(4.44)$$

Depending on Equation (٣.٥٠) Equation(٤.٤٤)is transformed into general coordinate (ζ,η),as follows:

$$Nu = -(\gamma\cdot\theta_\eta - \beta\cdot\theta_\zeta)/J\cdot\sqrt{\gamma} \qquad \cdots\cdots\cdots(4.45)$$

Since the temperature along the cylinder wall may be constant.

$$\frac{\partial\theta}{\partial\zeta} = 0 \qquad \cdots\cdots\cdots(4.46)$$

Rearranging:

$$Nu = -\gamma\cdot\theta_\eta / J\cdot\sqrt{\gamma} \qquad \cdots\cdots\cdots(4.47)$$

A second-order forward difference is used, **Hornbeck[٦٩]**, as follows:

$$Nu_{(i,j)} = -(\gamma_{(i,j)}\frac{-3\cdot\theta_{i,j} + 4\cdot\theta_{i,j+1} - \theta_{i,j+2}}{2\cdot\Delta\eta})/J_{(i,j)}\cdot\sqrt{\gamma_{(i,j)}} \qquad \cdots\cdots\cdots(4.48)$$

Nusselt number in equation(٤.٤٨)is the local Nusselt number. To find the average Nusselt, the local Nusselt number should be integrated, as follows:

$$\overline{Nu} = \frac{\int Nu\cdot ds}{\int ds} \qquad \cdots\cdots\cdots(4.49)$$

Now, by using numerical integration depending on the Simpson rule, **Chapra** and **Canale[٧٢],**as follows:

$$\overline{Nu} = \frac{\Delta X}{3}(Nu_{(i,j)} + 4 \cdot Nu_{(i+1,j)} + 2.Nu_{(i+2,j)} + \cdots\cdots\cdots + Nu_{(i+n,j)}) \quad \cdots\cdots\cdots(4.50)$$

٤.٣.٦ Evaluation Friction Coefficients

The Friction Coefficients is evaluated by using the following equation; **,Dennis** and **Chang[٥]** and **Chun** and **Boehm[١٤].**

$$C_f = -\frac{4}{\mathrm{Re}} \cdot \omega \Big)_w \quad \cdots\cdots\cdots(4.51)$$

٤.٣.٧ Numerical Solution of Computational Grid

The two differential Equations(٣.٢٨)and(٣.٢٩)in chapter three that deal with grid generation will be solved by using the finite difference with S.O.R. method **Thompson et al. [٤٢],** as follows:

$$\alpha \cdot X_{\zeta\zeta} - 2 \cdot \beta \cdot X_{\zeta\eta} + \gamma \cdot X_{\eta\eta} = 0 \quad \cdots\cdots\cdots(4.52)$$

$$\alpha \cdot Y_{\zeta\zeta} - 2 \cdot \beta \cdot Y_{\zeta\eta} + \gamma \cdot Y_{\eta\eta} = 0 \quad \cdots\cdots\cdots(4.53)$$

To solve equation (٤.٥٢) the central finite differences will be used **,Hoffmann[٥٦].** as follows:

$$\alpha = X_\eta^2 + Y_\eta^2 = [(X_{i,j+1} - X_{i,j-1})^2 + (Y_{i,j+1} - Y_{i,j-1})^2]/4 \cdot \Delta\eta^2 \quad \cdots\cdots\cdots(4.54)$$

$$\beta = X_\zeta \cdot X_\eta + Y_\zeta \cdot Y_\eta = [(X_{i+1,j} - X_{i-1,j}) \cdot (X_{i,j+1} - X_{i,j-1}) + (Y_{i+1,j} - Y_{i-1,j}) \cdot (Y_{i,j+1} - Y_{i,j-1})]/4 \cdot \Delta\zeta \cdot \Delta\eta \quad \cdots\cdots\cdots(4.55)$$

$$\gamma = X^2\zeta + Y^2\zeta = [(X_{i+1,j} - X_{i-1,j})^2 + (Y_{i+1,j} - Y_{i-1,j})^2]/4 \cdot \Delta\zeta^2 \quad \cdots\cdots\cdots(4.56)$$

$$X_{\zeta\zeta} = (X_{i+1,j} - 2 \cdot X_{i,j} + X_{i-1,j})/\Delta\zeta^2 \quad \cdots\cdots\cdots(4.57)$$

$$X_{\zeta\eta} = (X_{i+1,j+1} - X_{i+1,j-1} - X_{i-1,j+1} + X_{i-1,j-1})/4 \cdot \Delta\zeta \cdot \Delta\eta \quad \cdots\cdots\cdots(4.58)$$

$$X_{\eta\eta} = (X_{i,j+1} - 2 \cdot X_{i,j} + X_{i,j-1})/\Delta\eta^2 \quad \cdots\cdots\cdots(4.59)$$

In the above equations each form i, j represents grid point in ζ and η coordinate respectively. Now, by substituting Equations(٤.٥٤ to ٤.٥٩) into

Equation(٤.٥٢) and by using S.O.R. method the following equation may be obtained **,Fletcher[٥٩]** and **Petrovic** and **Stupar [٦٣].**

$$X_{i,j} = (1-RF)\cdot X^{o}_{i,j} + RF\cdot[\frac{\alpha_{(i,j)}}{\Delta\zeta^{2}}(X_{i+1,j}+X_{i-1,j}) + \frac{\gamma_{(i,j)}}{\Delta\eta^{2}}(X_{i,j+1}+X_{i,j-1})$$
$$\frac{\beta_{(i,j)}}{2\cdot\Delta\zeta\cdot\Delta\eta}(X_{i+1,j+1}-X_{i-1,j+1}-X_{i+1,j-1}+X_{i-1,j-1})]/(\frac{2\cdot\alpha_{(i,j)}}{\Delta\zeta^{2}}+\frac{2\cdot\gamma_{(i,j)}}{\Delta\eta^{2}}) \quad \cdots\cdots\cdots(4.60)$$

The same procedure is used to solve equation(٤.٥٣):

$$Y_{i,j} = (1-RF)\cdot Y^{o}_{i,j} + RF\cdot[\frac{\alpha_{(i,j)}}{\Delta\zeta^{2}}(Y_{i+1,j}+Y_{i-1,j}) + \frac{\gamma_{(i,j)}}{\Delta\eta^{2}}(Y_{i,j+1}+Y_{i,j-1})$$
$$\frac{\beta_{(i,j)}}{2\cdot\Delta\zeta\cdot\Delta\eta}(Y_{i+1,j+1}-Y_{i-1,j+1}-Y_{i+1,j-1}+Y_{i-1,j-1})]/(\frac{2\cdot\alpha_{(i,j)}}{\Delta\zeta^{2}}+\frac{2\cdot\gamma_{(i,j)}}{\Delta\eta^{2}}) \quad \cdots\cdots\cdots(4.61)$$

Where RF is the relaxation factor. The optimum over-relaxation coefficient is greater than (١.٥),**Petrovic** and **Stupar[٦٣].** $\Delta\zeta$ and $\Delta\eta$ is equal(١) in all computation.

The above equation is used to generate C-mesh for the present simulation. This type of mesh is ideally suited for simulating wake flows since better streamwise resolution can be provided in the wake region. The use of a C-mesh also simplifies the application of out flow boundary conditions, **Baek** and **Sung [٧٣] .**

٤.٣.٧.١ Calculation of Time Dependents Grid

In the pervious section equation (٤.٦٠)and (٤.٦١) are used to generate C-grid for computational representation. This grid is generated after specification of boundary of the domain, and also it is generated for one time in all computation because the boundary is static(non-oscillating cylinder), but in case of oscillating cylinder(moving boundary) the grid must move always. This is performed by the following step:

١. define the ζ and η directions, and set the number of grid lines in both directions(i.e set $\zeta_{\max}$ and $\eta_{\max}$).

٢. define the(X,Y) for each grid point(ζ,η) along the initial boundaries. In the present work, a uniform spacing of grid points along the boundaries was used.

٣. guess an initial(X,Y)for each internal grid points.

٤. calculate the inverse metric coefficients(α,β,γ)using central difference based on the current grid point.

٥. solve Equation(٤.٦٠)and(٤.٦١) to calculate a new X and Y value for each internal grid point .

٦. return to step ٤ and repeat until convergence is achieved.

In the present work, the convergence criteria used were based on the maximum change in X and Y between two successive iterations ,k, and k+١ throughout the entire field.

$$\left.\begin{aligned} abs(X_{i,j}^{K+1} - X_{i,j}^{k}) < 0.001 \\ abs(Y_{i,j}^{K+1} - Y_{i,j}^{K}) < 0.001 \end{aligned}\right\} \quad \cdots\cdots\cdots(4.62)$$

٧. in case of oscillation, update the location of boundaries because the boundaries are time dependent. This is performed by knowing the time and oscillation frequency and amplitude, as follows.

- In case of the transverse (cross-flow)oscillation.

$$Y = A \cdot \sin(2 \cdot \pi \cdot F \cdot \tau) \quad \cdots\cdots\cdots(4.63)$$
$$X = 0 \quad \cdots\cdots\cdots(4.64)$$

- In case of the in-line(streamwise)oscillation.

$$X = A \cdot \sin(2 \cdot \pi \cdot F \cdot \tau) \quad \cdots\cdots\cdots(4.65)$$
$$Y = 0 \quad \cdots\cdots\cdots(4.66)$$

- In case of with-angle(orbital)oscillation.

$$X = A \cdot \sin(2 \cdot \pi \cdot F \cdot \tau) \quad \cdots\cdots\cdots(4.67)$$
$$Y = A \cdot \sin(2 \cdot \pi \cdot F \cdot \tau) \quad \cdots\cdots\cdots(4.68)$$

٨. return to the step ٣ .
٩. repeat the same procedure to generate mesh in each time step when the time developed. Figure(٤-٢) shows the flowchart.

٤.٤ Computer Program

The computer program is a general program for calculating unsteady, two-dimensional laminar flow without compressibility effects. The computer code which developed is applicable to the computation of fluid flow and heat transfer around a stationary or oscillating cylinder.

The programming language is FORTRAN ٩٠ and the program can be run on PC machines. The program is teaching oriented and it is written in very simple and straightforward form which is readily amenable.

Computer code has been built to perform the numerical solution to the equations mentioned previously. Constant has been introduced in the program that includes the dimensionless distance of computational domain in both directions, a number of nodal points in both directions, maximum value of error and the suitable value of time step that achieve the stability of numerical solution.

This program consists of two main part. The first, solve the fluid flow and heat transfer when the cylinder stationary(non-oscillating), this part has the time marching and interior iteration(subroutine). In subroutine, the stream function will be calculated. Exit from this iteration occurs when the value of error is less than (٠.٠٠١). After the exit from this iteration, it will return to the time marching to obtain the vorticity and temperature. When the result from

time marching have been oscillated in the wake after the cylinder, the solution exits from the first part of program. The results from the first part will become the initial condition for the next part of the program. The second part has also time marching and interior iteration, and also time dependent mesh generation subroutine. Interior iteration calculated the stream function with same manner in the first part of the program. After exiting from this iteration, it will return to the time marching to obtain the vorticity and temperature. The time marching updates the mesh generation network always because the cylinder oscillation and this lead to the moving boundary. The update grid is performed by subroutine dependent on the time, amplitude and frequency and this grid is generated by another interior iteration(S.O.R.). It is possible to summarize the procedure of the numerical solution as follows:

١. Calculating suitable body-fitted coordinates(X,Y) both of which have been calculated by subroutine using S.O.R. method. This is performed when the cylinder is stationary(non-oscillate).
٢. Calculating transforming factors(metrics), by subroutine using central finite difference ($\alpha,\beta,\gamma,\lambda,\sigma$).
٣. Specify initial values for ω,ψ,θ , at time equals to Zero.
٤. Specify the boundary conditions for θ,ψ .
٥. calculating the values of stream function by subroutine using relaxation method depending on the previous values of vorticity that are calculated at time($\bar{t}$),and consequently, the value of stream function at time($\bar{t}+\Delta\bar{t}$)is obtained.
٦. After that there will be a return to the main program to calculate the values of vorticity and temperature at interior grid using time-

marching(explicit method). The calculation of vorticity and temperature depends on the values of the calculated stream function at time($\bar{t} + \Delta\bar{t}$).

٧. Determine the value of ω on the boundaries using ψ and ω values at interior points.

٨. Then, the three previous steps(٥,٦,٧) will be repeated until the fluid flow after this stationary cylinder begins move with fluctuation motion. This will be used as initial conditions for oscillating cylinder.

٩. Now, the cylinder is oscillate. In this case the program will be calculate the location of the cylinder boundary, at each time step when time progress by using subroutine, that depends on the frequency, amplitude and time.

١٠. When calculate the new location the program remeshing the grid network at each time step and calculate the displacement and velocity grid movement.

١١. After update the mesh generation of the domain, the vorticity transport equation is solved by time marching and stream function is solved by relaxation method and also temperature is solved by time marching at($\tau + \Delta\tau$), with insert the effect of grid movement in the calculation(ζ_τ, η_τ).

١٢. Repeat the three previous steps to reach to the time that is limited previously.

١٣. Calculating the velocity component dependent on the final values of stream function.

١٤. Calculating the local Nusselt number depending on the final values of temperature. In addition, calculating the average Nusselt number depending on the local Nusselt number.

١٥. Calculating the friction coefficient and the surface vorticity depending on the final values of vorticity.

١٦. Save all output data($\omega,\psi,\theta,Nu,\overline{Nu},U,V,C_f,SV$) in files and preparation to plotting by TECPLOT ٧ software.

Figure(٤-٣) indicates the sequence of operation(Flowchart).

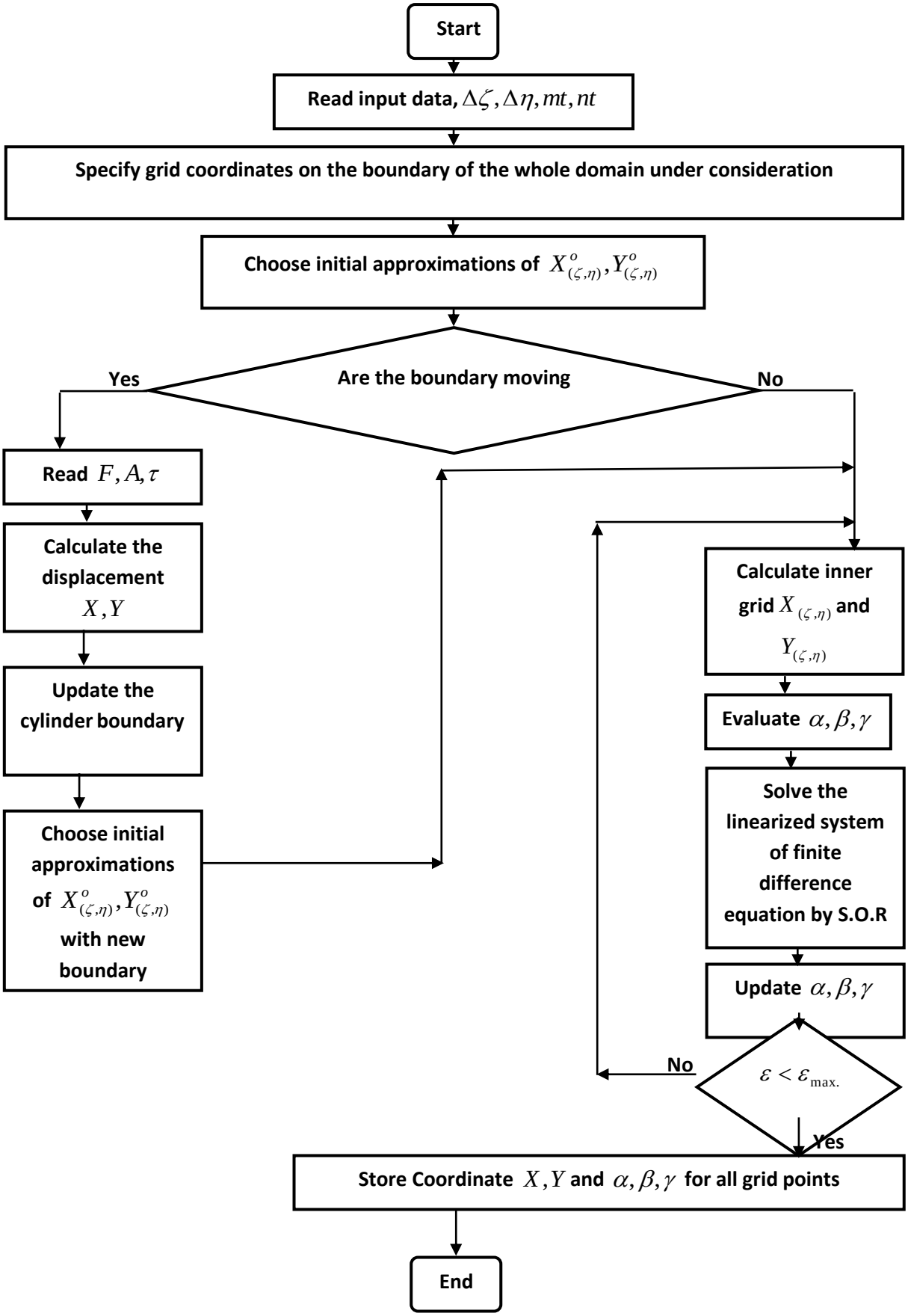

Figure(٤-٢)Flowchart of subroutine for grid generation

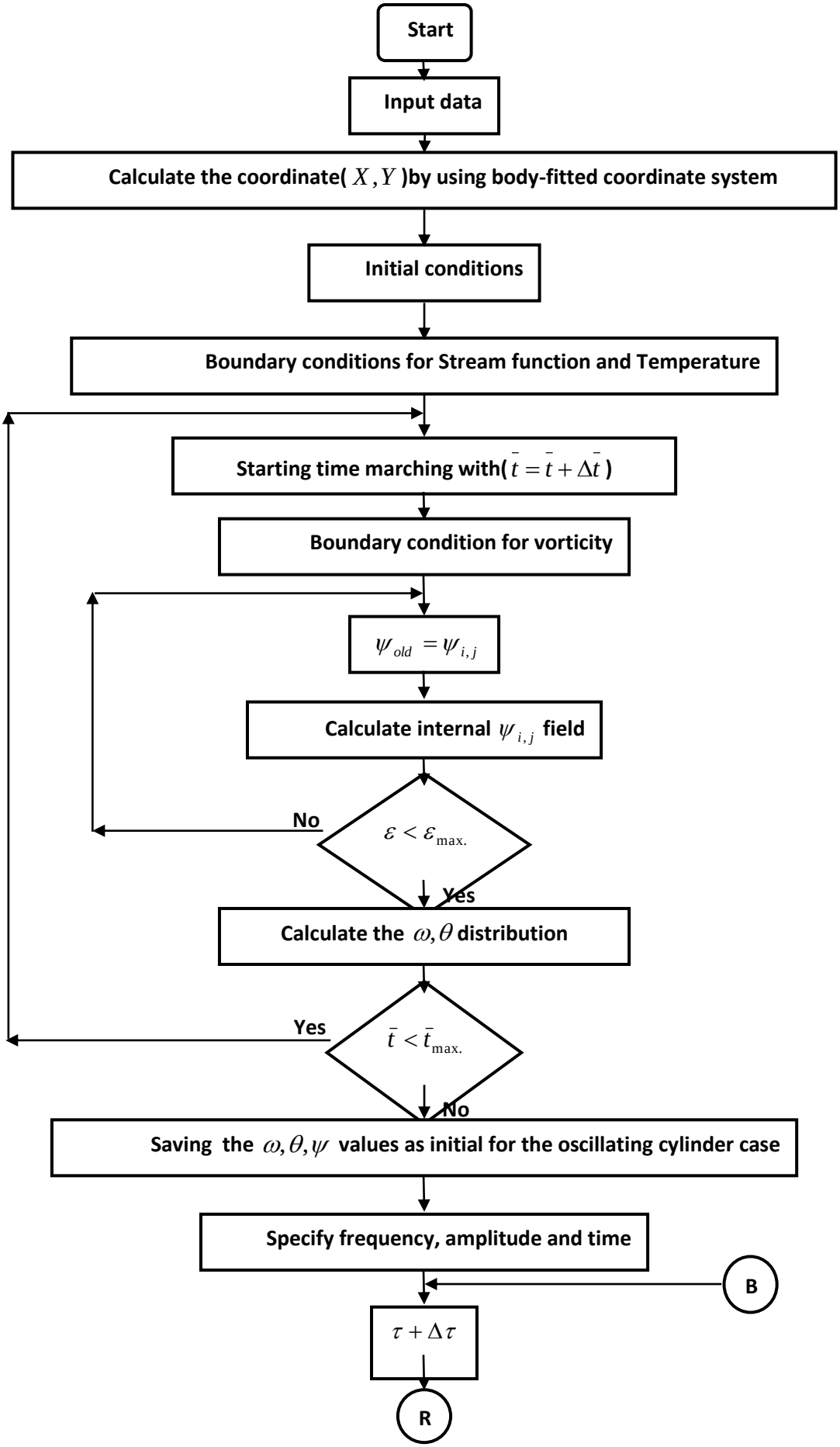

Figure(٤-٣)Flowchart of main computer program

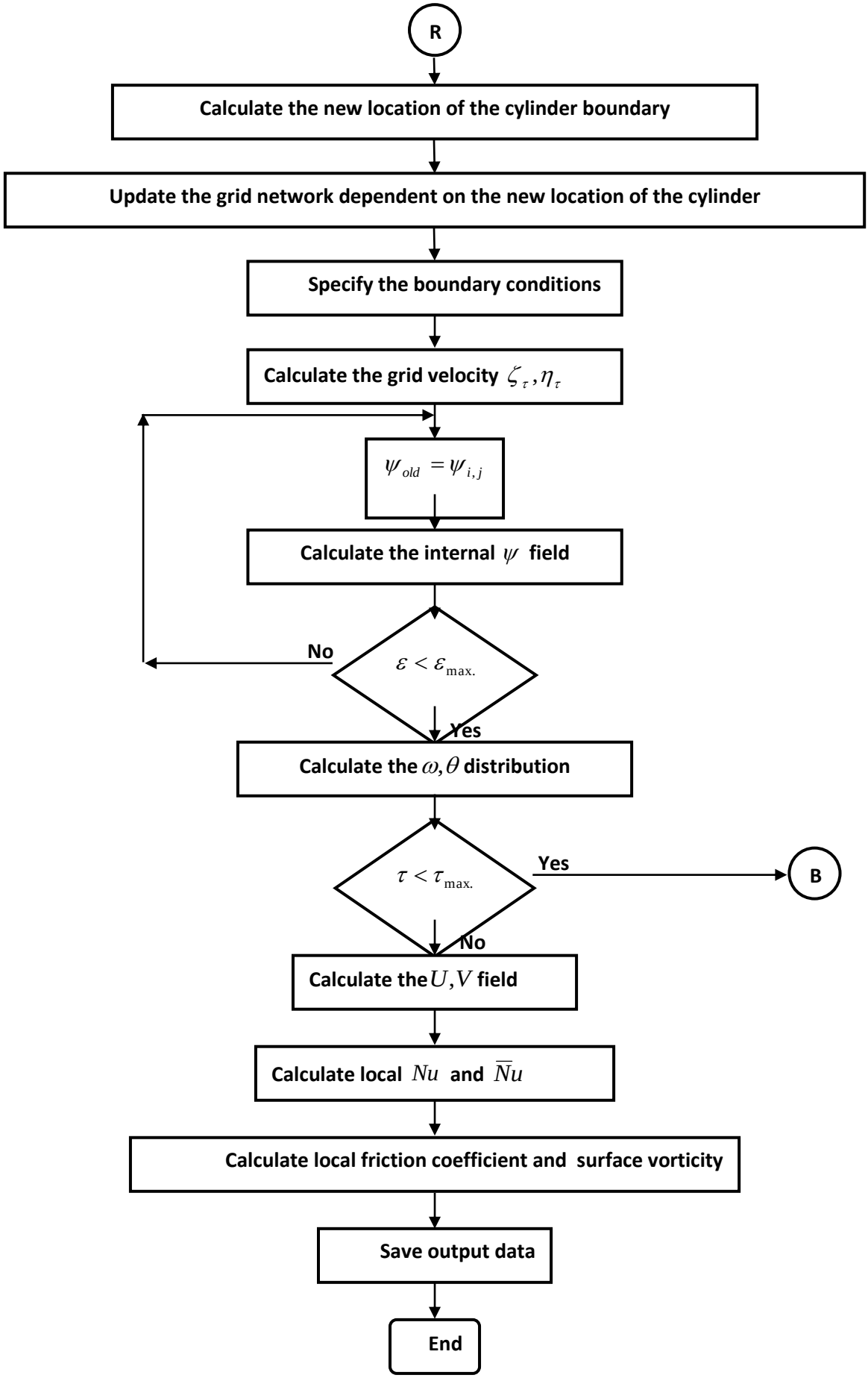

Figure(٤-٣)continue

RESULTS AND DISCUSSION

٥.١ Introduction

After completing the numerical solution, the obtained numerical results will be exposed and discussed to indicate the reasons behind such results. The beginning of the present chapter is to compare the results with the literature review. Then, there will be an exposition to the main results of the present study that are related to the flow behavior and the heat transfer by forced convection over oscillating cylinder, Reynolds number range is (٨٠ to ٦٠٠), and reduce frequency range is(٠.٠ to ٠.٧) and also dimensionless amplitude (٠.٠ to ٠.٩). After this the value of local Nusselt Number are compared for the three case of oscillating(Transverse, Inline and Orbital or with angle) with the case of stationary (fixed) cylinder.

The time step used in all computation will be selected equal to(dt=٠.٠١). This time step is suitable to guarantee the stability of the solution. Note that "time", amplitude and frequency in all figures and discussion means dimensionless time (τ), dimensionless amplitude(A) and reduced frequency(F) respectively.

The computational grid dimensions in two directions (X,Y) are ($L=7D, H=4D$) respectively. The node number that considered, in this study, for covering the computational domain are(mt=٩٩,nt=٤٠).

٥.٢ Comparison of the Results

In order to verify the numerical results that are obtained in the present study, and also in order to a certain that computational code and mathematical model developed in this study is correct, it is necessary to compare these results with the results from previous work. The flow pattern for oscillating cylinder is compared with work of **Hurlbut et al[١٧]** at Reynolds (٨٠) for transverse oscillation at frequency (F=٠.١٤) and amplitude (A=٠.١٤). Fig.(٥-١A,B) shows this comparison. Good agreement have been obtained. Also, the flow pattern is compared with work of **Cheng** and **Hong[٣٥]** at Reynolds number(٨٠)for transverse oscillation at frequency(F=٠.١٥٥)and amplitude(A=٠.١٤)for complete cycle. Figure(٥-٢)shows this comparison. Good agreement has been obtained.

The results are compared in relation to the value of the ratio of average Nusselt number with oscillation (Nu) and without oscillation (Nuo), for transverse oscillating cylinder with forced convection, with experimental works of **Park[٣٦]** and **Pottebaum[٣٩]**. Figure (٥-٣) indicates this comparison. The difference between the present work and experimental work is with(٢%)when amplitude(A=٠.١)with work of **Pottebaum**, and(٣.٣%),(٩%)at amplitude (A=٠.٢) with work of **Park** and **Pottebaum** respectively.

The average Nusselt number compare with empirical correlation in **Waqar[٧٤]** for stationary(fixed) cylinder($Nuo=٠.٤٤٩٣*Re^{٠.٥}$). Figure (٥-٤) indicates this comparison. The difference between the two is within(٨%).

Also, the results of surface vorticity and local skin friction coefficients distribution for stationary cylinder are compared with the work of **Dennis** and

Chang[٥] and **Chun** and **Boehm[١٤],** respectively. Small difference will be shown between the present work and the previous work, that may be come from they are assume symmetry flow after cylinder and solve upper half flow of the cylinder. Figure(٥-٥)shows the surface vorticity and Figure(٥-٦)shows the local skin friction coefficient.

٥.٣ Streamline Field Analysis

This section, presents and discusses the flow pattern around oscillating cylinder with forced convection in three cases(transverse, inline and orbital)of oscillation, as shown below.

٥.٣.١ Transverse Oscillating(Having motion) Cylinder

Figures(٥-٧) to (٥-١١) illustrate the stream line contours for the forced convection with oscillating cylinder in transverse(cross flow)direction, at Reynolds number (٨٠,١٠٠,١٢٠,٢٠٠ and ٣٠٠) and also frequency (٠.٠ to ٠.٥٥) and amplitude (٠.٠ to ٠.٤٣). In general, it can be seen from these figures that the size and orientation of wake region are completely dependent on frequency (F) and amplitude (A) and also Reynolds number(Re). Also, the flow has periodic motion.

At(Re=٨٠, F=٠.٢ and A=٠.٠ to ٠.٤٣) as shown in Fig.(٥-٧) the circulation fluid zone in wake occurs and fluid separation from alternating side of the cylinder surface, but the vortices roll-up are very close to the base of the cylinder in case of oscillation when compare with stationary (fixed) cylinder,

Fig.(٥-٧a), because of entrainment of free stream fluid into the wake region. As(A) increase, the rolled-up vortices appear to be more circular and the vortices are scattered in the flow due to the drastic swing of the cylinder.

At(Re=٢٠٠,F=٠.٢ and A=٠.٠ to ٠.٢٥),as shown in figure(٥-٨), the vortices become more and small in size in case of oscillation when compare with stationary cylinder case, because the large recirculation zone behind the cylinder are difficult to maintain their original situations, which causes the large recirculation zones to be split into small vortices and to flow to the down stream.

At(Re=١٠٠,A=٠.٢ and F=٠.٠ to ٠.٥), as shown in Fig.(٥-٩), the circulating zone in wake appear and the vortices increase in size when the frequency becomes more due to increase the effective speed of flow and the wake width increase laterally. Also, the vortex shedding becomes two after the frequency equals(٠.٢), due to increase in speed of cylinder with increase of frequency and this leads to scatter the vortices in the down stream. The point of vortex shedding is alternating from up to down at each(٠.٠٥)due to inverse the direction of cylinder oscillation at each half cycle.

The same comment will be drawn on figure(٥-١٠) when (Re=٣٠٠,A=٠.١ and F=٠.٠ to ٠.٥٥) except the two shedding vortex become after frequency (F=٠.١)because the relative velocity between the cylinder and fluid flow become considerable after frequency(F=٠.١).

Figure(٥-١١) shows the streamline contours for the cylinder oscillating transversely with(F=٠.٢,A=٠.٣ and Re=١٢٠) for complete cycle of oscillation. As shown in Fig.(٥-١١a) the cylinder at zero displacement location and moves upward. The fluid near the top region of the cylinder will be pressed by the

surface of the cylinder. Conversely, the fluid near the bottom region of the cylinder simultaneously replenishes the vacant space due to the continuity of the flow. The cylinder turns downward as it reaches the maximum upper amplitude. As shown in Fig.(٥-١١b), the cylinder is on the way to move downward. Since the moving direction of the cylinder is changed, the fluid near the top region of the cylinder will replenish the vacant space and cause a new recirculation zone form around the rear of the cylinder. After ward, the fluid near the bottom region of the cylinder is continuously pressed by the cylinder, as shown in Fig.(٥-١١c). As the cylinder reaches the maximum downward amplitude, the cylinder returns upward immediately shown in figures(٥-١١d,e).

٥.٣.٢ Inline Oscillating(Surging Motion) Cylinder

The stream line contours for fluid flow around circular cylinder with inline(streamwise) oscillation at Reynolds number(٨٠,١٠٠,١٢٠,٢٠٠,٣٠٠), frequency range(٠.٠ to ٠.٧) and amplitude (٠.٠ to ٠.٩) can be seen in figures (٥-١٢) to (٥-١٦).

In general, it can be seen from these figures that the size and orientation of the wake and also the shape and size of circulation zone are dependent on frequency (F), amplitude(A), displacement and Reynolds number(Re).

At (Re=٨٠,F=٠.٢,A=٠.٠ to ٠.٩) and (Re=٢٠٠,F=٠.٢ and A=٠.٠ to ٠.٦٥), as shown in Fig.(٥-١٢) and Fig.(٥-١٣), the circulation zone in wake occurs and the bubble of fluid separated from each side of the cylinder, also the fluid flow has symmetry shape after the cylinder because the cylinder move parallel with the fluid. As the amplitude increases, the lateral spacing of vortices decrease, Fig.(٥-١٢e,f) and Fig.(٥-١٣b,c). Further increase will result in breakdown of

vortices and appearance of secondary vortices, Fig.(٥-١٣f,g,h), because the fluid after the cylinder replenish the vacant space due to continuity when the cylinder oscillating parallel to the flow.

At(Re=١٠٠,A=٠.٥ and F=٠.٠ to ٠.٧), as shown in figure (٥-١٤), in this figure the fluid flow has symmetric shape after cylinder. When the frequency increase the wake region increase and the vortices elongated. The new phenomenon observed in this figure, is the small vortices exist before the cylinder, because the increase of frequency lead to increase the velocity of the cylinder with respect to the flow at which the fluid replenish the vacant space and generated the new vortices before the cylinder as shown in Fig.(٥-١٤f,h). The same comment is shown in Fig.(٥-١٥)when the (Re=٣٠٠,A=٠.٢٥ and F=٠.٠ to ٠.٥), but the vortices appear only after the cylinder and disappear before it due to the velocity of the cylinder small with respect to the fluid flow.

Figure(٥-١٦) shows the fluid flow over cylinder for a complete one cycle of oscillation at (Re=١٢٠, F=٠.٢ and A=٠.٤). As shown in this figure, the cylinder moving forward and backward inside the fluid flow. The fluid flow has four vortices in the beginning and ending of the cycle, Fig.(٥-١٦a,e). When the moving in the same direction of the fluid(backward) the fluid flow has less turbulence compared with the cylinder moving against the fluid flow direction, as shown in Fig.(٥-١٦b,d).

٥.٣.٣ Orbital (with angle) Oscillating Cylinder

Orbital oscillating can be defined as the motions that are not limited to one direction, i.e they oscillate in both transverse and inline directions. Oscillation in two directions can result in an orbital motion of the body(**Baranyi[٧٥]).**

The stream line contours of fluid flow around circular cylinder with orbital oscillation at Reynolds(٨٠,١٢٠,١٠٠), frequency (٠.٠ to ٠.٦٥) and amplitude (٠.٠ to ٠.٤) can be seen in figures(٥-١٧) to (٥-١٩). The angle used in all computation is (٤٥°)from the leading edge of the cylinder.

Figure(٥-١٧) shows the fluid flow over cylinder at orbital oscillating at(Re=٨٠, F=٠.٣, A=٠.٠ to ٠.٤) the same observation on the wake and circulation after the cylinder of the case of transverse oscillation figure.(٥-٧)will be drawn in this case, but the flow pattern more fluctuation than the case of transverse oscillation and also, the size of the circulation zone greater in comparison with this case because the cylinder covering more region in moving with angle inside the fluid.

In the figure (٥-١٨) when the(Re=١٠٠,A=٠.٢٥ and F=٠.٠ to A=٠.٦٥), the characteristics of flow the same as the previous figure, but, the flow seems more turbulent when the frequency increases and the circulation zone increasing in number from two in fixed(stationary) case, Fig.(٥-١٨a) to the three, Fig.(٥-١٨g,h) because the cylinder moving with high vigorous motion lead to high turbulence in fluid and more vortices shedding from the cylinder.

Figure (٥-١٩), shows the fluid flow over oscillating cylinder for a complete one cycle of orbital oscillation at (Re=١٢٠,F=٠.٢,A=٠.٤). This case is a mixture between transverse and inline cases and the behavior of the fluid is changing continually when the cylinder moving with oscillating motion. The stream lines pressed when the cylinder at extreme maximum location, Fig.(٥-١٩b,d) and also the fluid replenish the vacant space due to the continuity of the flow.

٥.٤ Velocity Vector Distribution

In this section, the numerical results for velocity vector distribution over oscillating cylinder in cross flow are presented. The velocity vector is obtained by indirect calculation, this is performed by solving the relation between the velocity and stream function.

The velocity vector and corresponding stream lines contours of the fluid flow over stationary and oscillating cylinder in(transverse, inline and orbital)direction at Reynolds(Re=٤٠٠), frequency(F=٠.٢)and amplitude(A=٠.١), can be seen in figure(٥-٢٠).

It is clear from vector plots the gradient of velocity start from zero at the surface of the cylinder to maximum at faraway from the cylinder surface due to the fluid is assume viscous. The velocity distribution in the wake gradient from low inside the center of vortices and maximum at outer boundaries of vortices. The fluid flow in inline case, Fig.(٥-٢٠c١,c٢)has characteristics less vigorous and more close to the stationary cylinder, Fig.(٥-٢٠ a١,a٢), because the cylinder moving parallel to the fluid flow, when comparison with the transverse and orbital cases, Fig.(٥-٢٠ b١,b٢, d١,d٢).

٥.٥ Temperature Distribution

In this part, the temperature distribution around the cylinder surface will be discussed. The temperature distribution obtained by the time marching with moving grid technique to solve energy equation with an assumption of the incompressible flow.

Isotherm maps are presented in figures(٥-٢١) to (٥-٣٣) and corresponding streamline contours are shown previously in figures(٥-٧) to (٥-١٩). In all the cases the working fluid is air the Prandtl number has been taken as(Pr=٠.٧).

In general, the isothermal lines are unsymmetrical about line of symmetry and heat transfer rate depends on both temperature difference between the cylinder and the around fluid and velocity. As the wake in the rear stagnation point region gets elongated and increase in breadth, the pattern of the isotherm also gets elongated and becomes broader in the region.

The process of the vortex shedding takes place at a rate which is slower than the rate at which the outer streamlines on the periphery of the wake moves into main stream. The fluid along streamlines passing in the neighborhood of the cylinder gets heated and these streamlines usually form S-shaped patterns in the wake. Thus, the fluid in the wake region gets more heated than in the outer flow region.

In case of oscillating cylinder, the entrainment process of the free stream into the wake is main reason to increase heat transfer rate. This entrainment has the effect of bending the temperature contours, thereby creating a steeper temperature gradient in the cylinder base region, as shown in figures(٥-٢١),(٥-٢٢),(٥-٢٣),(٥-٢٤),(٥-٢٥),(٥-٣١),(٥-٣٢) and (٥-٣٣).

By observing the pattern of the isotherms, one finds that an unsymmetrical flow in the wake gives rise to an unsymmetrical pattern of the isotherms. From figures(٥-٢١),(٥-٢٢), and (٥-٣١) it is observed that the isotherm becomes more asymmetric as the amplitude increase because the fluid flow become more asymmetric. Also, in case of inline oscillation, figures(٥-٢٦) and (٥-٣٠) are nearest to the symmetry when comparing with the transverse and orbital

oscillating cases figures(٥-٢١), (٥-٢٢) and (٥-٣١) due to the cylinder moving parallel to the fluid flow .

The variation of the thermal fields usually corresponds to the variation of the fluid flow fields. The distribution of the isothermal lines is dense near the surface of the leading edge of the cylinder, as shown in all figures of isotherm, except some cases as shown in figure(٥-٢٨), in these cases, the isotherm less dense at the cylinder leading edge because the vortices appear before the cylinder, as shown in figure(٥-١٤).

٥.٦ The Local Nusselt Number

In most engineering applications, the local Nusselt number is used to express the rate of heat transfer. Local Nusselt number can be defined as dimensionless heat transfer coefficient ratio of convection heat transfer to conduction in fluid layer.

In general, the peak of local Nusselt number located at the upstream stagnation point(angular position equals zero for fixed (stationary) cylinder and deviation from this position when oscillation occurs). This is anticipated, since thin boundary layer presented at that point(i.e. maximum heat transfer rate). As the boundary layer thickens, the local Nusselt number decreases steeply, since the downstream growth of a thermal boundary layer would certainly increase the thermal resistance. In forced convection, the thermal boundary layer thickness around the heated cylinder surface is very thin(i.e. low thermal resistance) and its effects on the heat transfer coefficient can be neglected. In this case, the Nusselt number is a function of Reynolds number

and Prandtl number. Thus, any increase in the flow Reynolds number, produces an increase in the Nusselt number.

The Nusselt number will increase, if the heated cylinder is allowed to oscillate with any amplitude of oscillation. The reason for this increase in the local Nusselt number is due to the increase of the effective diameter this leads to the increases of the effective area, subjected to the air flow, with increase amplitude, so effective diameter equal(D_{eff})=(D+A). And also, the oscillation increase the fluid mixing and turbulence this lead to enhance Nusselt number. When the cylinder oscillate the vortices roll-up close to the cylinder base and this lead to increase heat transfer rate. The reason behind the increased heat transfer when the vortices roll-up close to the cylinder is that the vortices are able scrub away the hot fluid at the base of the cylinder. In case of a stationary cylinder, there is a region of stagnant fluid just behind the cylinder which does not convect any heat away from base of the cylinder, but in case of oscillating cylinder this region convecting heat transfer at the cylinder base. The overall heat transfer, therefore increases when the heat transfer rate at the normally low region at the base of the cylinder is increased.

The oscillating velocity(function of "A" and " F" of oscillating cylinder) can affect heat transfer enhancement in two ways. First, it can increase the circulation of the forming vortices by increasing the vorticity flux in the shear layers. Second, it can allow the vortices to affect a larger portion of the cylinder surface area.

Figures(٥-٣٤) to (٥-٤٦) show the local Nusselt number distribution around circular cylinder with and without oscillation at (Re=٨٠ to ٦٠٠), amplitude (٠.٠ to ٠.٥) and frequency (٠.٠ to ٠.٥٥).

At(Re=٨٠, ١٢٠,١٦٠,٢٠٠)and constant frequency and amplitude(F=٠.٢ and A=٠.٢) with three case of oscillation(transverse, inline and orbital),as shown in figure(٥-٣٤). The average Nusselt number enhancement of up(٢٢٪,٢٨٪,٣٣٪ and ٣٧٪) for transverse oscillation and for inline the enhancement up to(٤٢%,٤٩٪,٥٣٪ and ٥٧٪) and also for orbital oscillation the enhancement up to(٤٩%,٥٦٪,٦١٪ and ٦٤٪) this when compare with stationary cylinder due to the influence of oscillation of the cylinder on the fluid structure, as mention in above . Also, it's observed that maximum Nusselt number in case of transverse and orbital oscillation deviation from it is position when compared with stationary cylinder because the change is in the location of leading stagnation point. The maximum improvement at stagnation point for transverse, inline and orbital oscillation are(٥٠%, ٥٧% ٦٢% and ٦٤%), (٦١٪,٦٨٪,٦٩٪ and ٧١٪) and (٦٨٪,٧٣٪,٧٦٪ and ٧٨٪) respectively.

At(Re=١٠٠,A=٠.٢, and F=٠.٠٢ to ٠.٥٥),as shown in figures(٥-٣٥)and (٥-٣٦), show that the effect of frequency increases on the local Nusselt number. In case of transverse oscillation, figure(٥-٣٥) the increase of frequency leads to increase Nusselt number(due to increase of oscillating velocity and fluid mixing) and the angular position of maximum Nusselt changes at each(٠.٠٥)added due to change of location of stagnation point for each half of oscillation cycle. The oscillation frequency(F=٠.٠٢) represented the threshold of the effects of the transverse oscillation on heat transfer coefficient, greater than this frequency the Nusselt number will be affected by transverse oscillation and vise versa. And also the same observation will be drawn on the case of the orbital oscillation, as shown in figure(٥-٣٦).

At(Re=١٠٠,F=٠.٢,and A=٠.٠١ to ٠.٥), as shown in figures(٥-٣٧),(٥-٣٨), (٥-٣٩), it presents the effect of amplitude increases on local Nusselt number. In

case of transverse oscillation, figure(٥-٣٧) the Nusselt number enhances with the increase of the amplitude due to increase of effected area and oscillating velocity. The same results will be obtained at inline and orbital oscillation, figures(٥-٣٨)and (٥-٣٩), in which the Nusselt number enhances with the increase amplitude. Also, in case of inline the local Nusselt number symmetry about zero angular position because the cylinder oscillate parallel to the fluid flow. The threshold of amplitude equal to(٠.٠٤,٠.٠١ and ٠.٠١) for transverse, inline and orbital oscillation respectively.

Figures(٥-٤٠),(٥-٤١),(٥-٤٢), show the local Nusselt number distribution for complete one cycle of oscillation for cylinder oscillate in transverse, inline and orbital respectively and corresponding streamlines and isothermal are shows in figures(٥-١١),(٥-١٦),(٥-١٩) and (٥-٢٥),(٥-٣٠),(٥-٣٣) respectively. The maximum Nusselt number distribution occur at the beginning and ending of the cycle due to high temperature rate because the vortex is close enough to induce flow around the base of the cylinder an carry away heat from the base of cylinder. Always the Nusselt number greater than of the stationary cylinder case excepted in inline oscillation case, in which the Nusselt number decreases in some locations because the low temperature rate in these locations as shown in figure(٥-٤١).

Figures(٥-٤٣),(٥-٤٤)and (٥-٤٥), show the local Nusselt number distribution for Re(١٠٠ to ٦٠٠, F=٠.٢ and A=٠.١) when the cylinder oscillation in (transverse , inline and orbital) and also stationary cylinder. Observed from these figures the local Nusselt number increase with increase of the Reynolds number in all cases because the Nusselt number is a function of Reynolds number, as well. Also, can gets the same value of Nusselt number for high

Reynolds, in case of stationary cylinder, from oscillating cylinder case with less Reynolds number.

٥.٧ Average Nusselt Number

Figure(٥-٤٦)shows the average Nusselt number without oscillation (stationary) and with oscillation cylinder(transverse, inline and orbital)at frequency(F=٠.٢)and amplitude(A=٠.١). It is found that the average Nusselt number in case of oscillating cylinder is greater than the case of the stationary cylinder. The ratio of enhancement of the Nusselt number is(١٦%, ٤٥% and ٤٩%) in transverse, inline and orbital oscillating respectively. Also, in all cases, fixed, transverse, inline and orbital the Nusselt number increases with the increase Reynolds number because Nusselt is function of Reynolds number and Prandtl.

٥.٨ Surface Vorticity Distribution

Figures(٥-٤٧) to (٥-٥٣) show the surface vorticity distribution around a circular cylinder with and without oscillation at (Re=٨٠,١٠٠,١٢٠,١٦٠,٢٠٠), frequency (٠.٠٢ to ٠.٥٥) and amplitude (٠.٠١ to ٠.٥).

At(Re=٨٠,١٢٠,١٦٠,٢٠٠, F=٠.٢ and A=٠.٢), figure(٥-٤٧) shows three cases of oscillation(transverse, inline and orbital), and also the stationary case. The surface vorticity increases with oscillation in the lower half of cylinder by ratio(٤٥٪,٥٣٪,٥٨% and ٦٣٪) in transverse,(٣٨٪,٤٤٪,٤٨٪ and ٥٢٪) in case of inline and(٦١٪,٦٧٪,٧٢٪ and ٧٥٪) in the orbital oscillation respectively. The kink of vorticity lines become less pronounced at angular positions near (-

١٢٠°,٠°,١٢٠°)and vanished completely at these points because the velocity gradients at these points vanish.

The development of the vorticity distribution around the surface of the cylinder at(Re=١٠٠, A=٠.٢ and F=٠.٠٢ to ٠.٥٥)is shown in figures(٥-٤٨),(٥-٤٩), (٥-٥٠). It will be seen that the vorticity over the surface develops a kink in the separating region when the frequency increases. At transverse oscillation, figure(٥-٤٨), the kink eventually becomes less pronounced in angular position (-١٥° to ١٥°). In case of inline oscillation, figure(٥-٤٩), all vorticity line intersect at zero angular position(stagnation point). And also, in the orbital oscillation, figure(٥-٥٠)the surface vorticity line intersect at points near to(٠° ,٥٠° and ١٠٥°) angular position.

The effect of amplitude increase on the surface vorticity is presented in figures (٥-٥١), (٥-٥٢) and (٥-٥٣). It is clear from these figures that the surface vorticity increases with the increase of the amplitude (due to increase the vorticity gradients) and developed a kink of line intersect in some points in angular position(-١٣٠°,-١٥°,١٥°,١١٠°) in case of transverse,(-١٣٠°,-١٠٠°,٠°,١٠٠°,١٣٠°)in case of inline and (-١٢٥°,٥°,٦٠°,١٢٠°) in case of orbital oscillation.

٥.٩ Local Skin Friction Coefficient Distribution

Figures(٥-٥٤) to (٥-٦٠)show the local skin friction coefficient distribution on the cylinder surface without and with oscillation at (Re=٨٠,١٠٠,١٢٠,١٦٠,٢٠٠), frequency(F=٠.٠٢ to ٠.٥٥)and amplitude(A=٠.٠١ to ٠.٥) with three cases of oscillation(transverse, inline and orbital). It is found that the local skin friction coefficient(C_f) is greater when compared with a stationary cylinder, as shown

in figure(٥-٥٦), in which these increments up to(٤٥٪,٥٣٪,٥٨٪ and ٦٣٪), (٣٨٪,٤٤٪,٤٨٪ and ٥٢٪) and (٦١٪,٦٧٪,٧٢٪ and ٧٥٪) when the cylinder oscillate in transverse, inline and orbital direction respectively.

Because the local skin friction coefficient is a function of surface vorticity as shown previously, the same observation, behavior and influences on the surface vorticity will be drawn on the skin friction, as shown in the figures(٥-٤٧)to (٥-٥٣).

٥.١٠ Computer Run Times

The present numerical model which was implemented on the Personal Computer has properties(CPU ٢.٤GHz, Cache memory ٢٥٦k and ٢٥٦ MB of RAM memory).

Computer average run times for these simulation were(١٨٠)seconds for each one time unit developed in case of oscillating cylinder and in case of stationary cylinder each one time unit needs(١.٣)seconds. These difference between the two cases are due to the program in case of oscillating cylinder need re-meshing the domain and calculates the grid velocity and metrics($\alpha, \beta, \gamma, \sigma, \lambda$) at each time step because the boundary is moving with time.

transverse oscillation,Re=80,F=0.14, A=0.14
present work

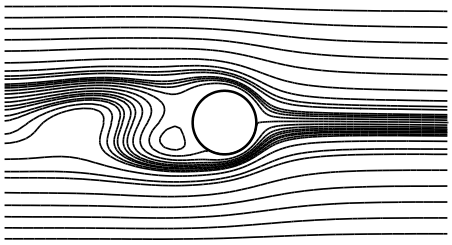

a1

transverse oscillation,Re=80,F=0.14, A=0.14
Hurlbut et al

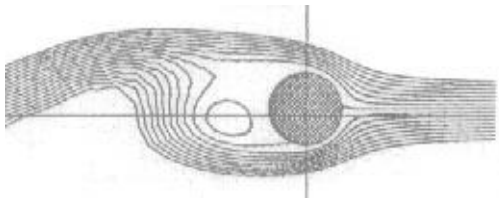

a2

transverse oscillation,Re=80,F=0.14, A=0.14
present work

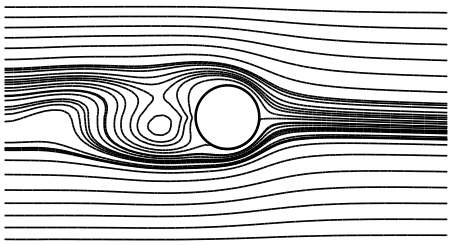

b1

transverse oscillation,Re=80,F=0.14, A=0.14
Hurlbut et al

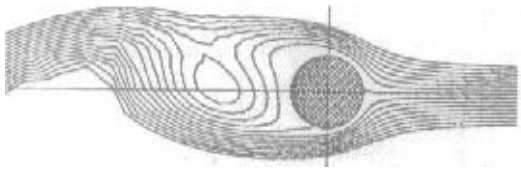

b2

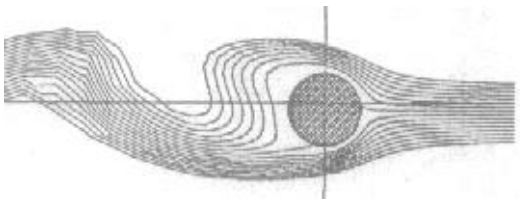

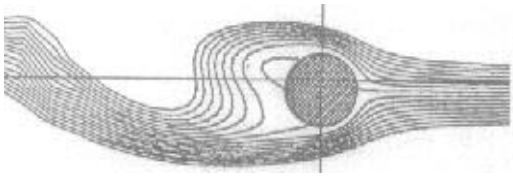

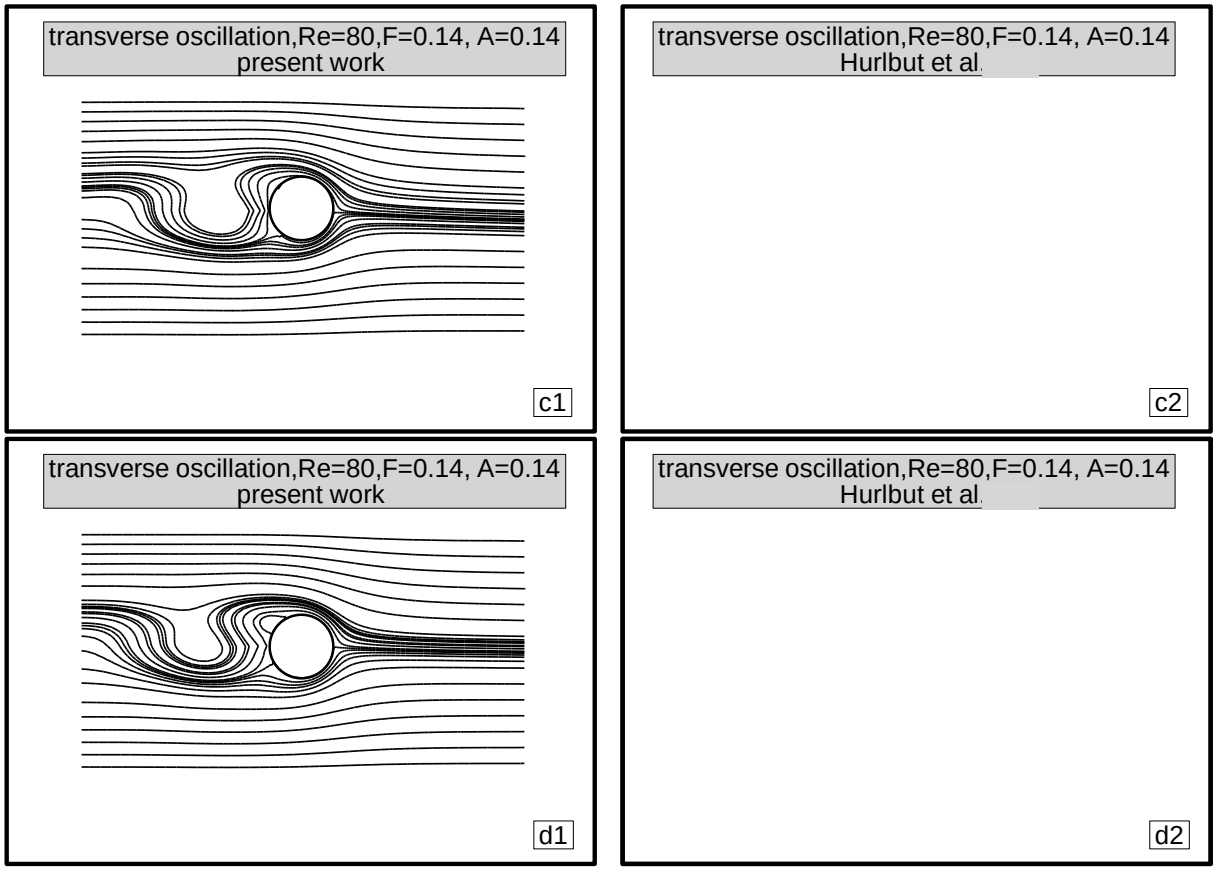

Fig.(٥-١A)Compare the flow pattern with previous work by **Hurlbut etal.[١٧]** at Reynolds number=٨٠ for transverse oscillation cylinder every one-eighth cycle

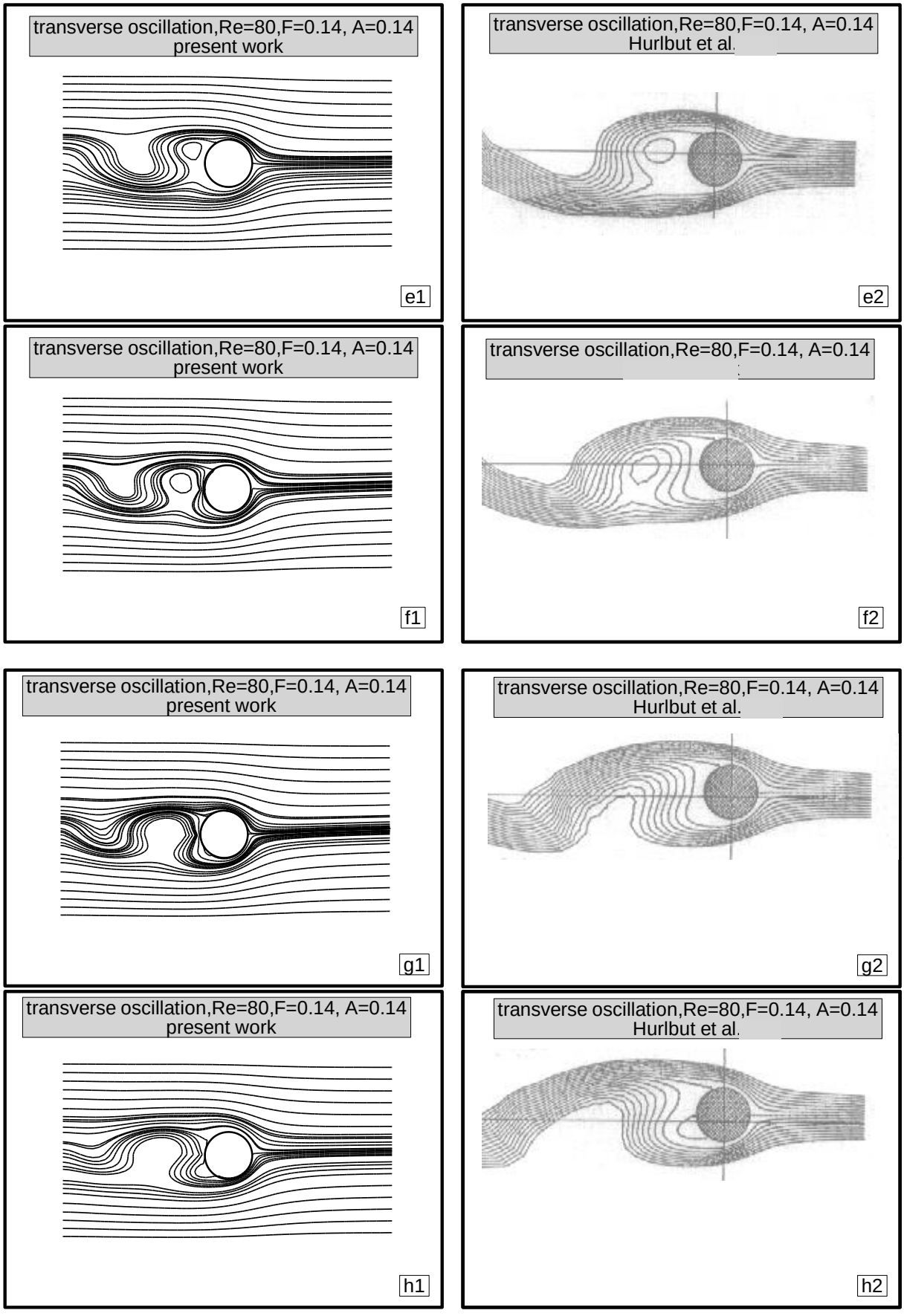

Fig.(٥-١B)Compare the flow pattern with previous work by **Hurlbut etal.[١٧]** at Reynolds number=٨٠ for transverse oscillation cylinder every one-eighth cycle

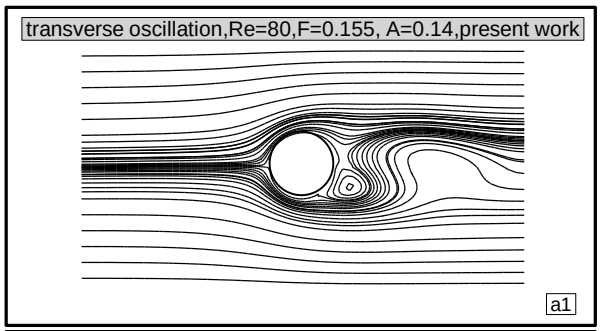
transverse oscillation,Re=80,F=0.155, A=0.14,present work
a1

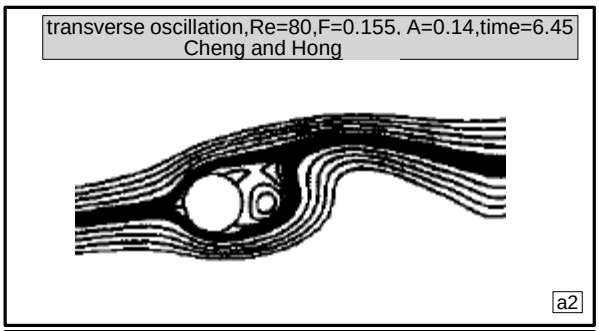
transverse oscillation,Re=80,F=0.155, A=0.14,time=6.45
Cheng and Hong
a2

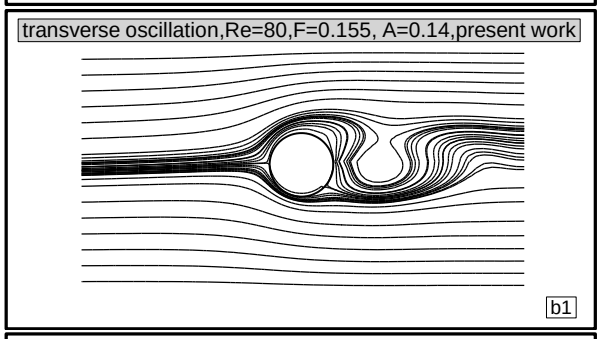
transverse oscillation,Re=80,F=0.155, A=0.14,present work
b1

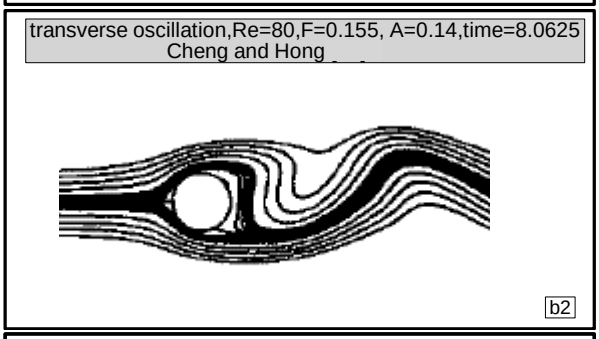
transverse oscillation,Re=80,F=0.155, A=0.14,time=8.0625
Cheng and Hong
b2

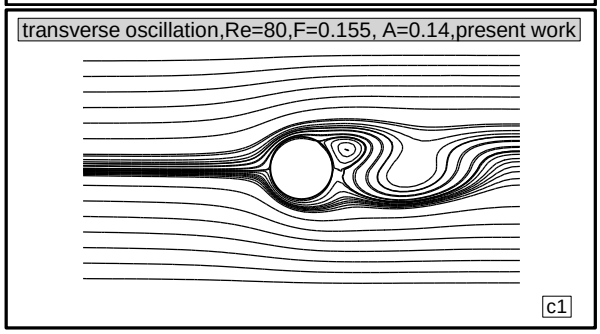
transverse oscillation,Re=80,F=0.155, A=0.14,present work
c1

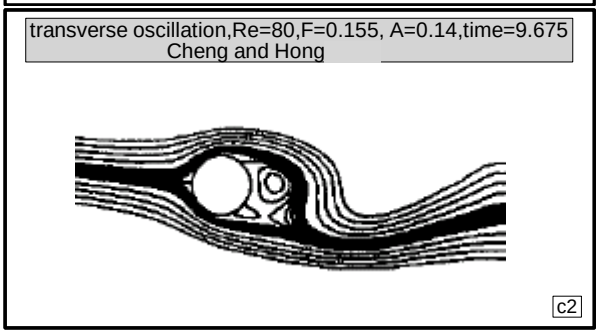
transverse oscillation,Re=80,F=0.155, A=0.14,time=9.675
Cheng and Hong
c2

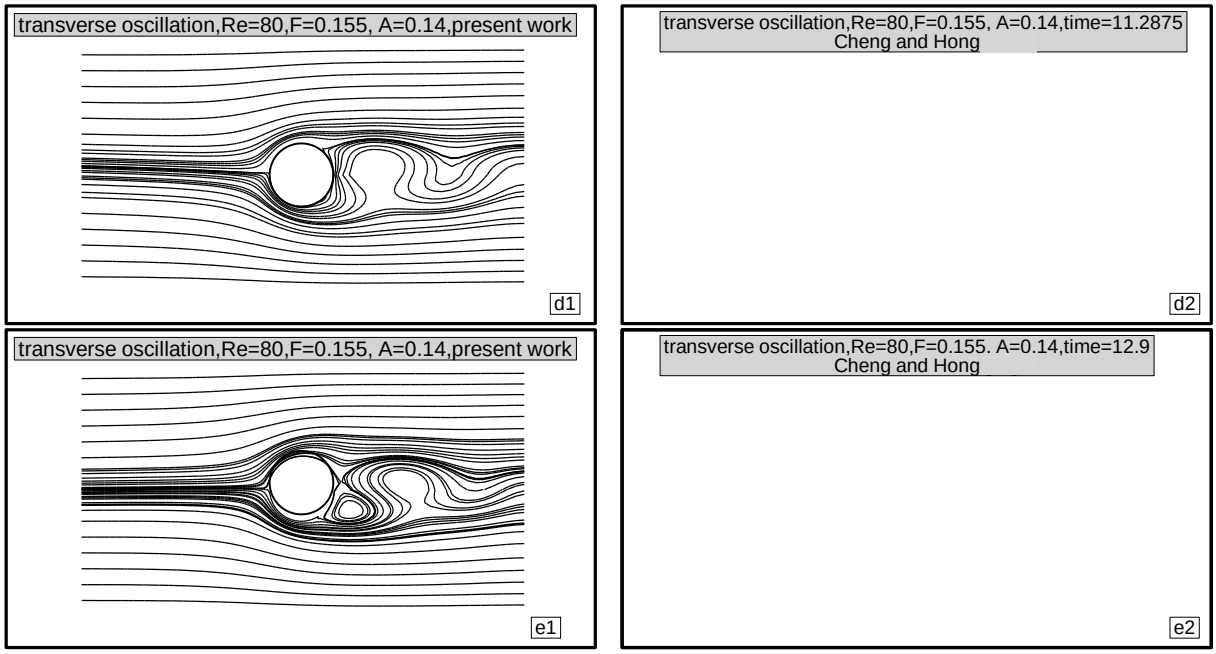

Fig.(٥-٢)Compare the flow pattern with previous work by **Cheng** and **Hong[٣٥]** at Reynolds number=٨٠ for transverse oscillation cylinder for complete cycle

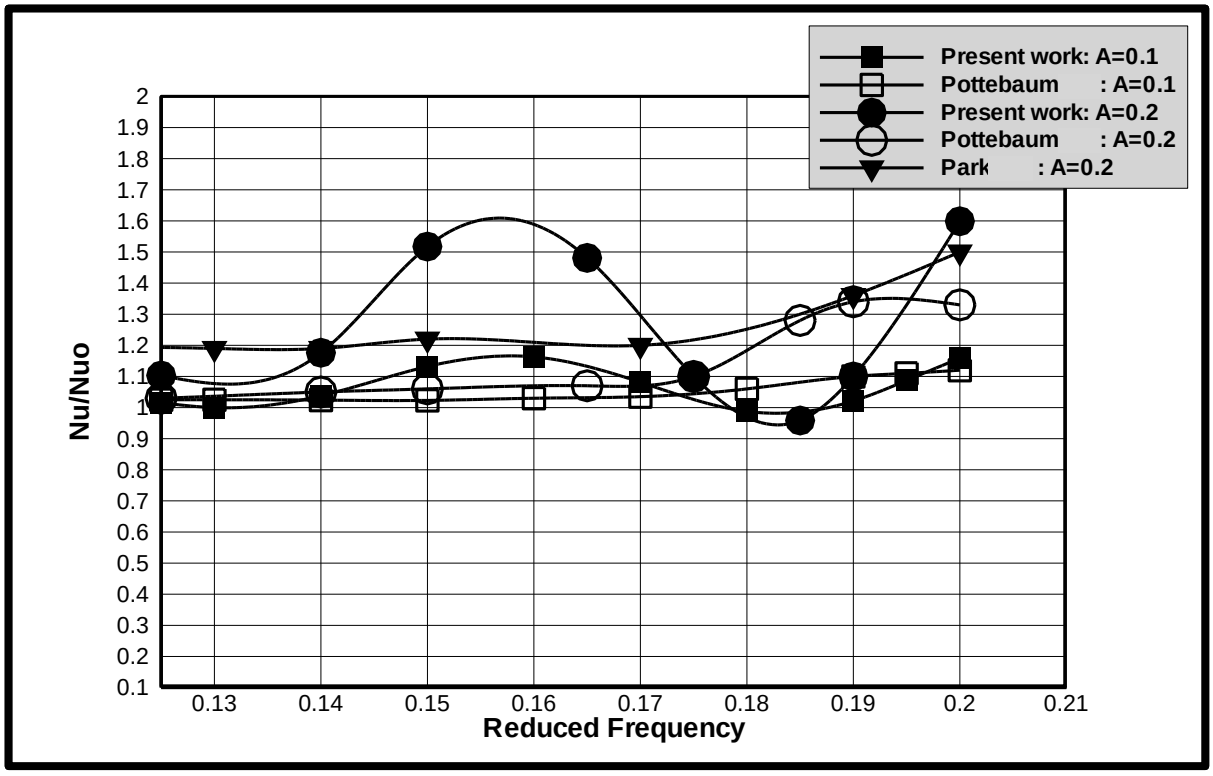

Fig.(٥-٣)Compare the ratio of Nusselt number with previous work by **Park[٣٦]** and **Pottebaum[٣٩]** for transverse oscillating cylinder at (A=٠.١ and A=٠.٢)

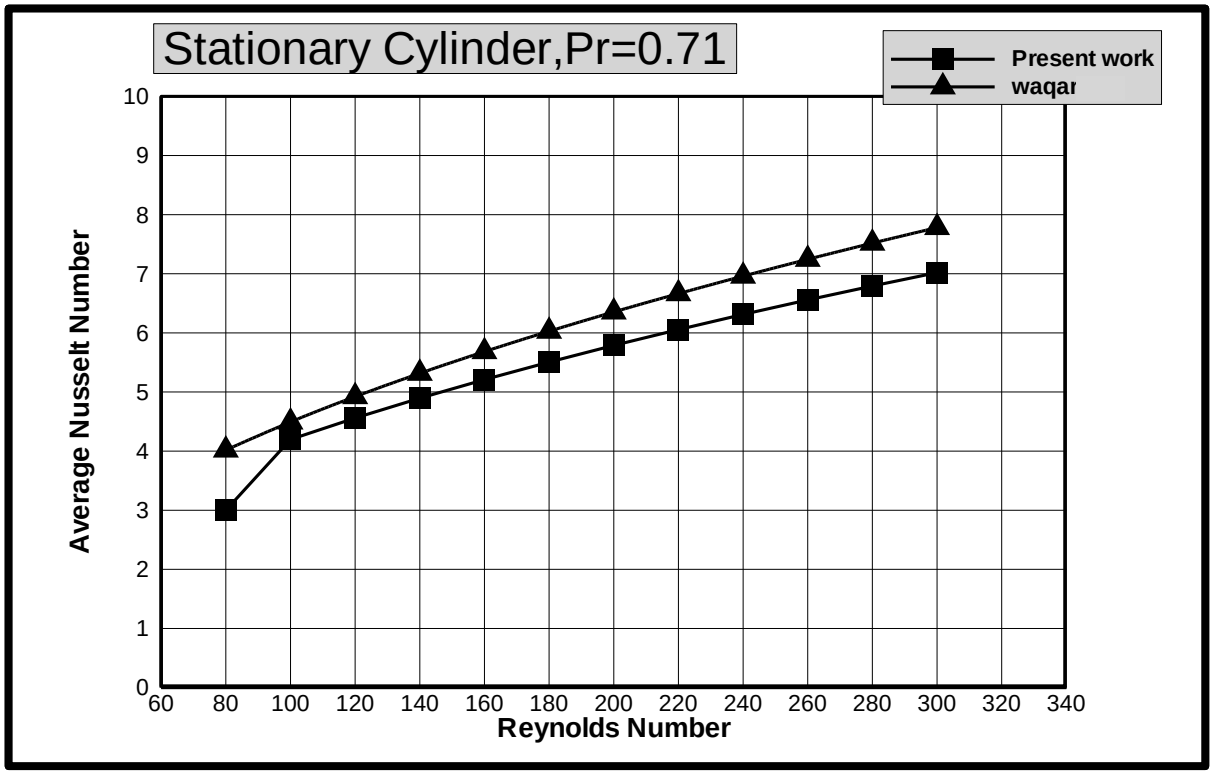

Fig.(٥-٤)Compare the average Nusselt number with empirical correlation by **Waqar[٧٤]** for stationary cylinder

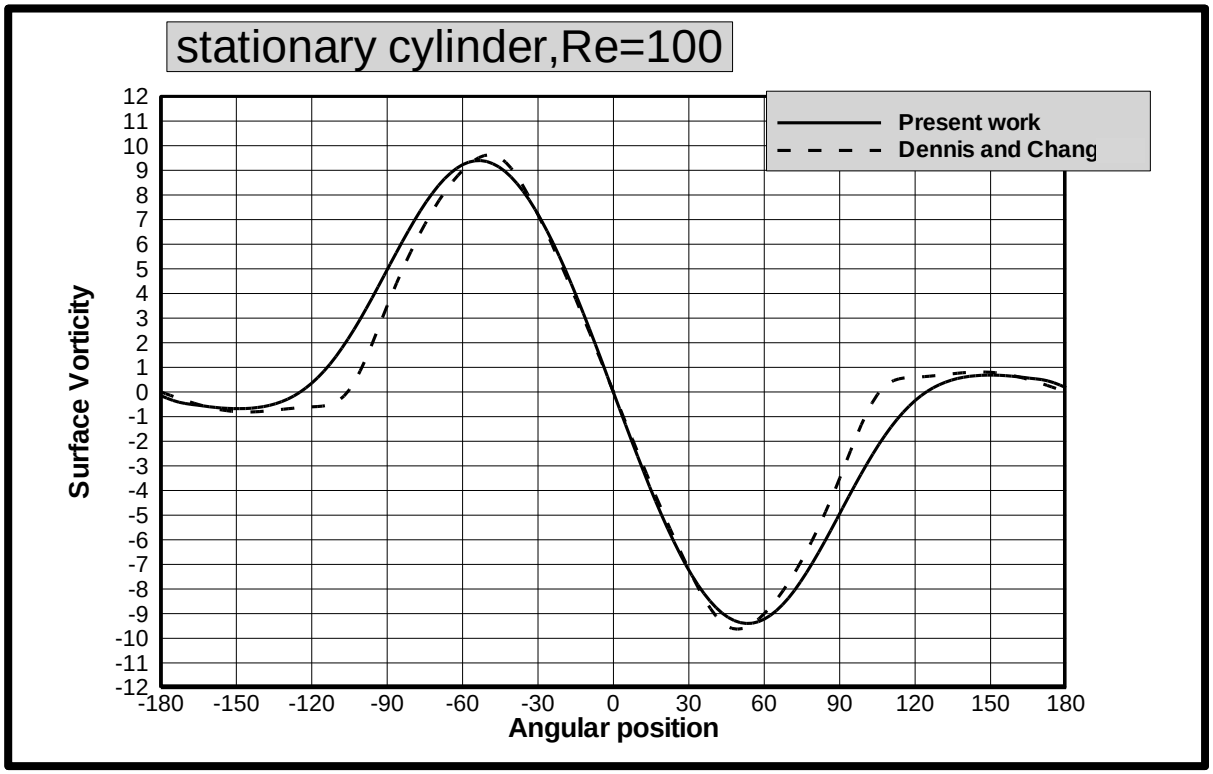

Fig.(٥-٥)Compare the surface vorticity with steady state solution in **Dennis** and **Chang[٥]** for stationary cylinder

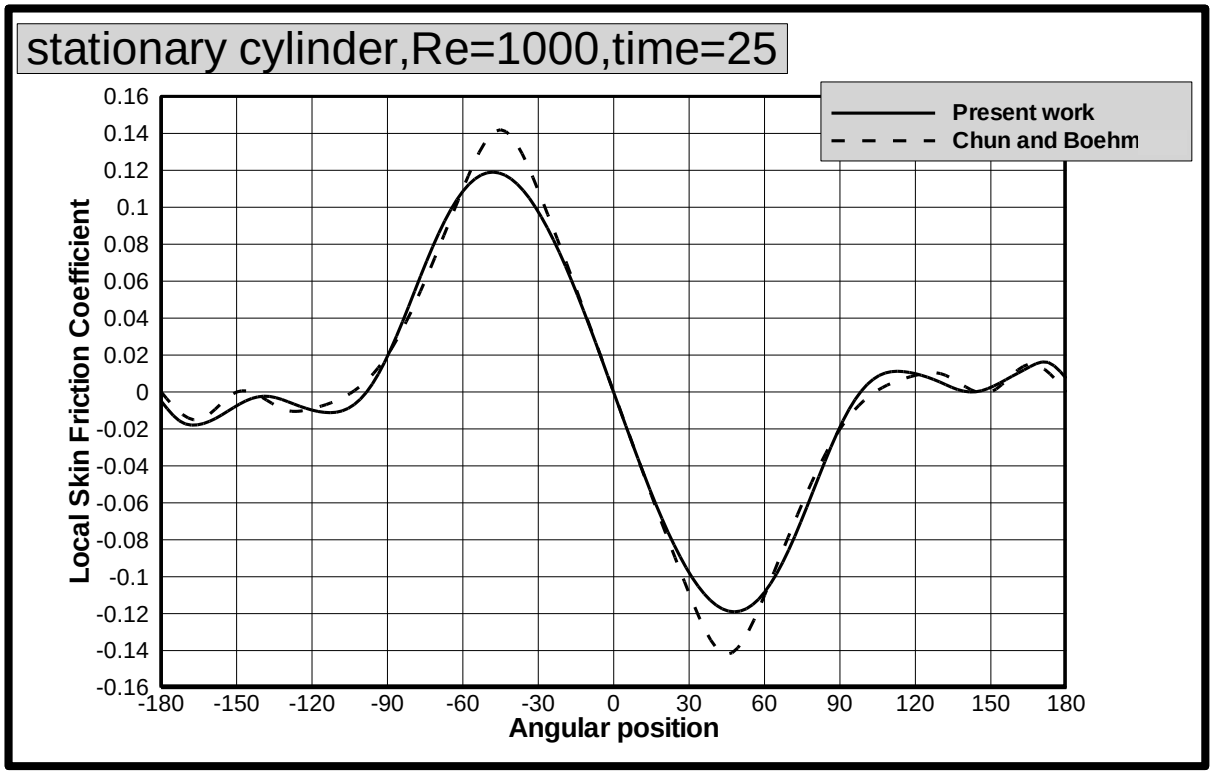

Fig.(٥-٦)Compare the local skin friction coefficient with previous work of **Chun** and **Boehm[١٤]** for stationary cylinder

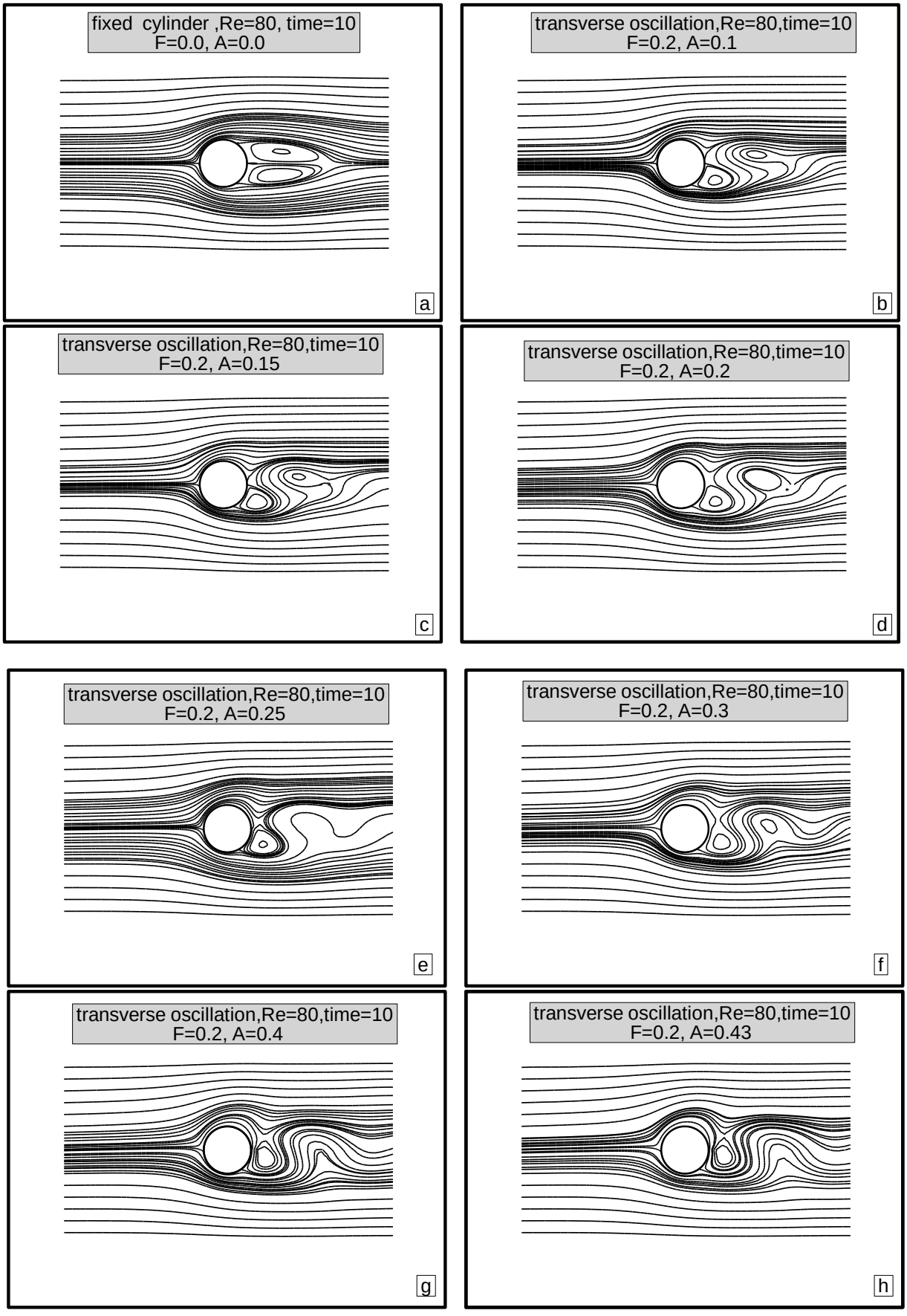
fixed cylinder ,Re=80, time=10
F=0.0, A=0.0
a
transverse oscillation,Re=80,time=10
F=0.2, A=0.1
b
transverse oscillation,Re=80,time=10
F=0.2, A=0.15
c
transverse oscillation,Re=80,time=10
F=0.2, A=0.2
d
transverse oscillation,Re=80,time=10
F=0.2, A=0.25
e
transverse oscillation,Re=80,time=10
F=0.2, A=0.3
f
transverse oscillation,Re=80,time=10
F=0.2, A=0.4
g
transverse oscillation,Re=80,time=10
F=0.2, A=0.43
h

Fig.(٥-٧)Stream lines contours for transverse oscillating cylinder at Re=٨٠ and F=٠.٢ with multi-amplitude.

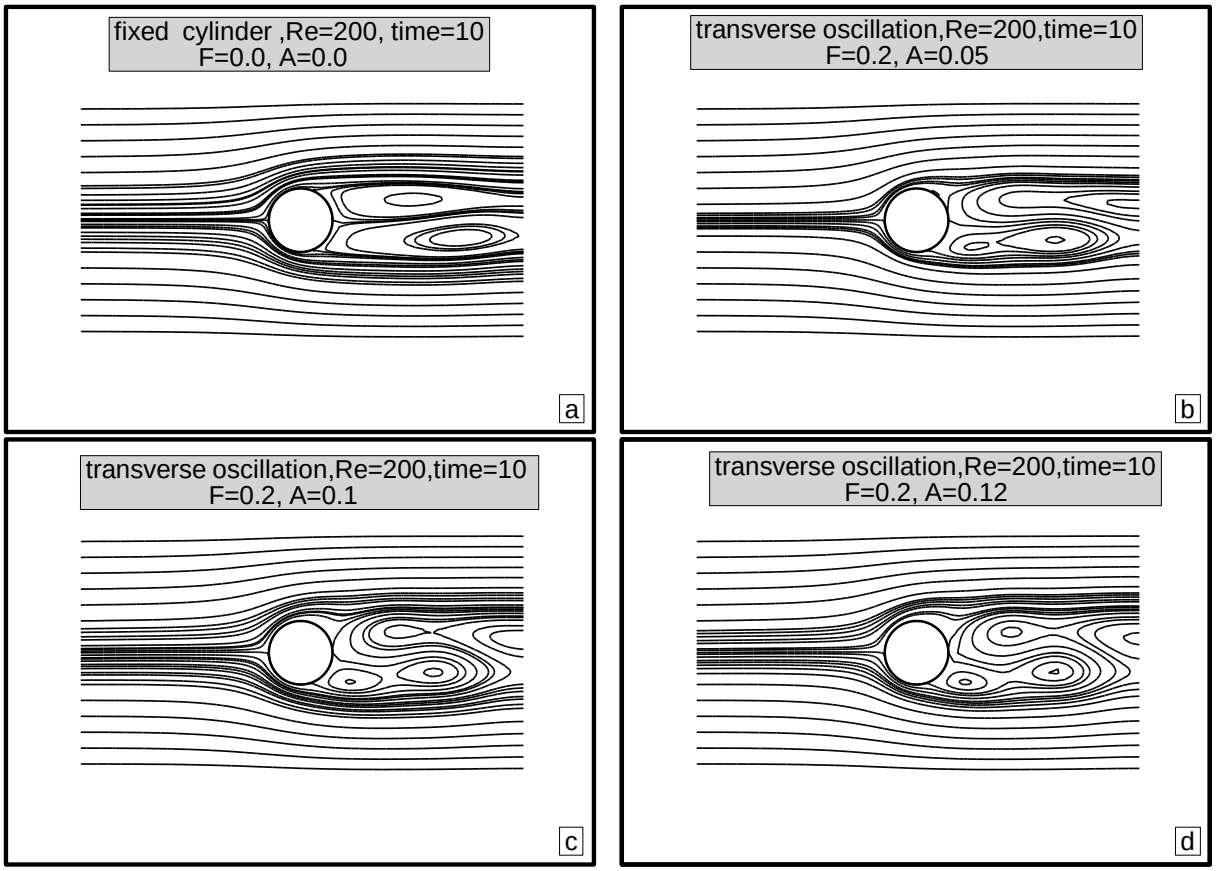

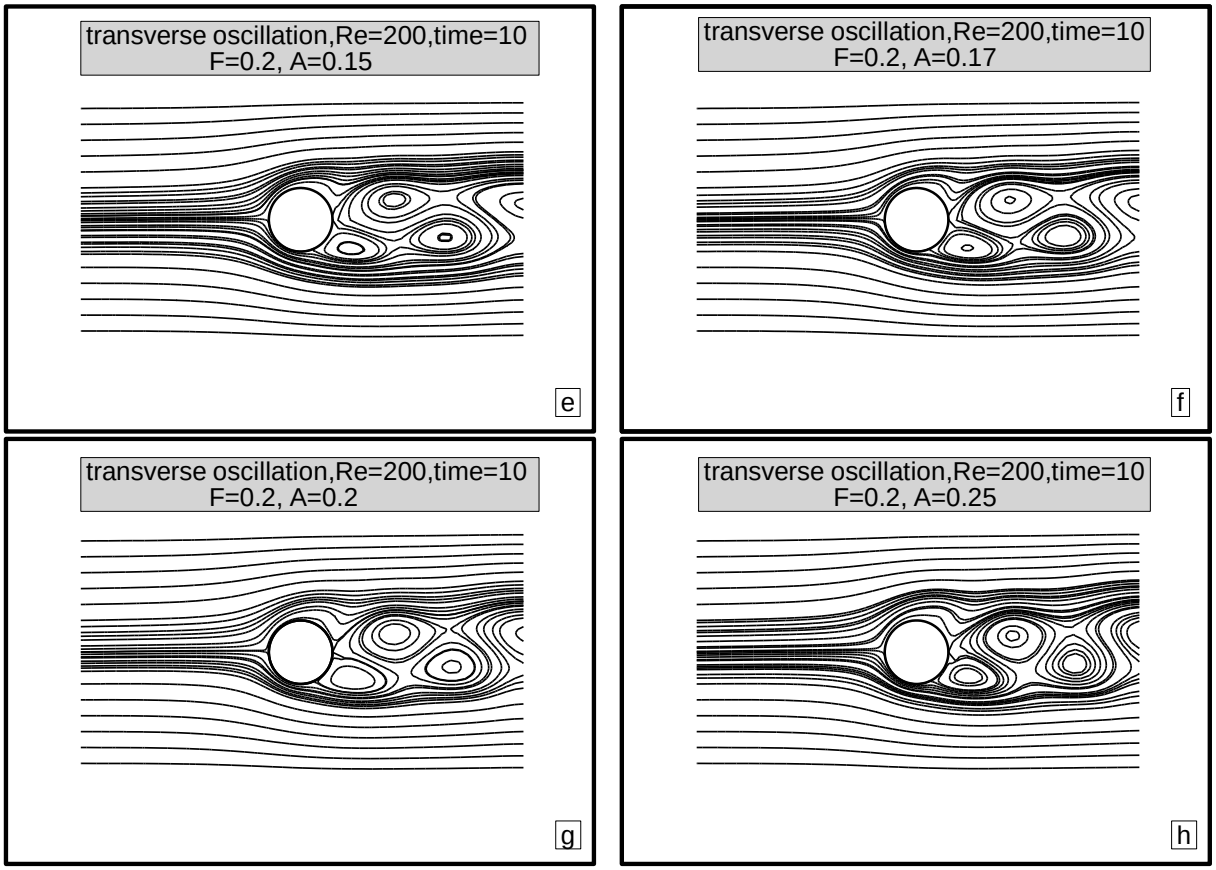

Fig.(٥-٨)Stream lines contours for transverse oscillating cylinder at Re=٢٠٠ and F=٠.٢ with multi-amplitude.

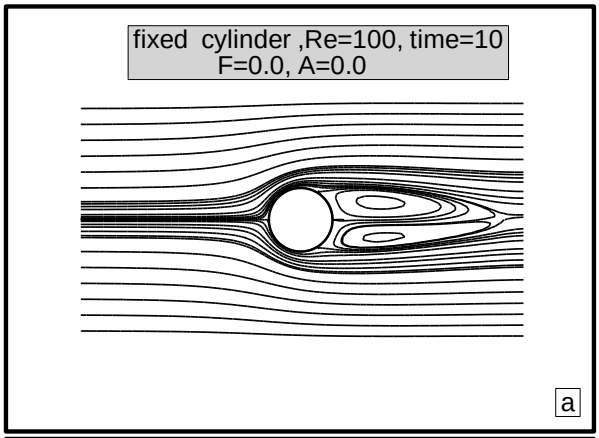
fixed cylinder ,Re=100, time=10
F=0.0, A=0.0
a

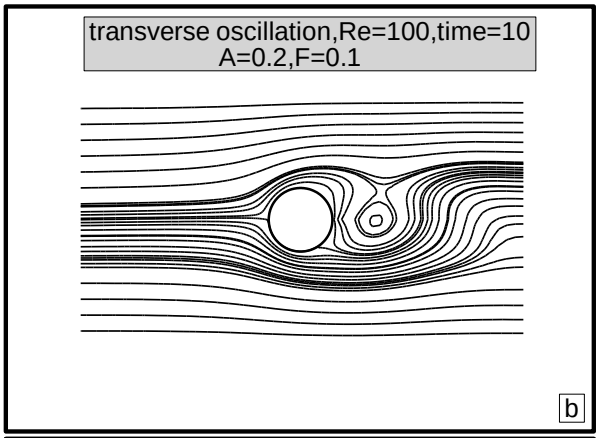
transverse oscillation,Re=100,time=10
A=0.2,F=0.1
b

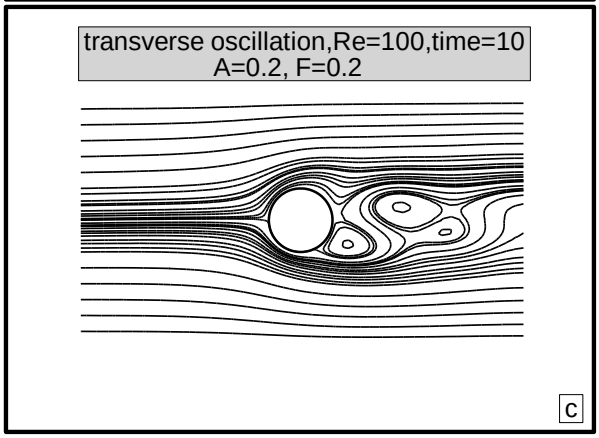
transverse oscillation,Re=100,time=10
A=0.2, F=0.2
c

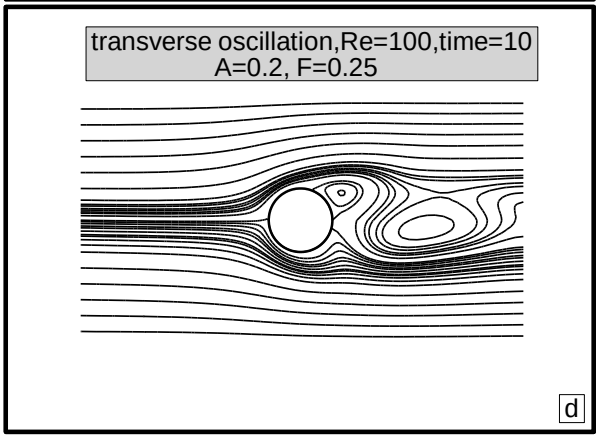
transverse oscillation,Re=100,time=10
A=0.2, F=0.25
d

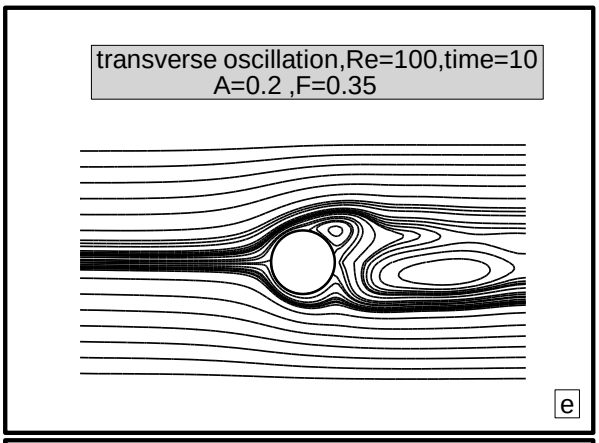
transverse oscillation,Re=100,time=10
A=0.2 ,F=0.35
e

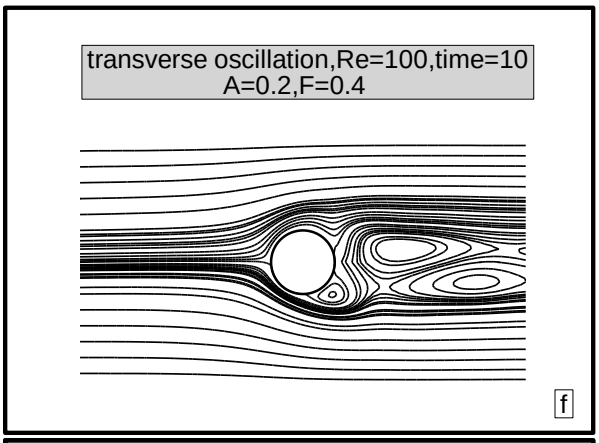
transverse oscillation,Re=100,time=10
A=0.2,F=0.4
f

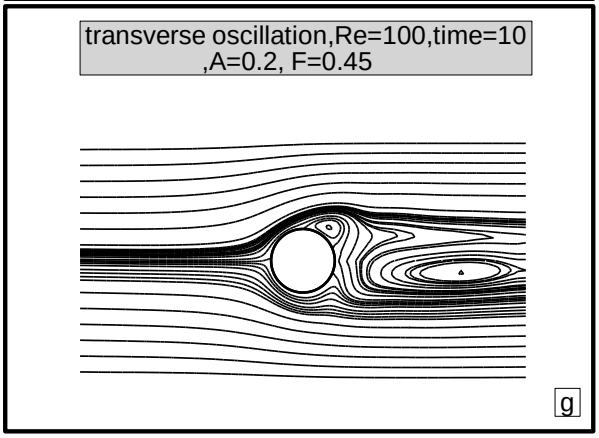
transverse oscillation,Re=100,time=10
,A=0.2, F=0.45
g

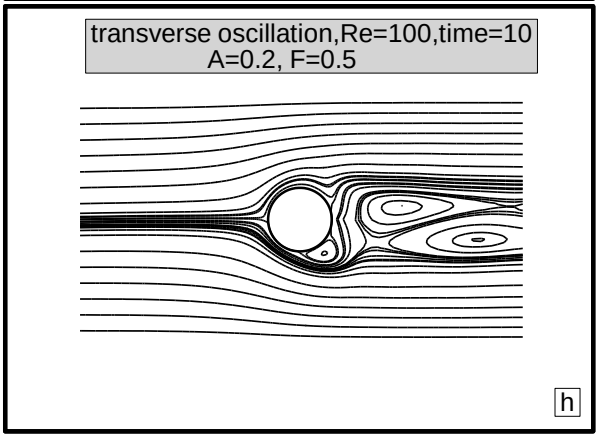
transverse oscillation,Re=100,time=10
A=0.2, F=0.5
h

Fig.(٥-٩)Stream lines contours for transverse oscillating cylinder at Re=١٠٠ and A=٠.٢ with multi-frequency.

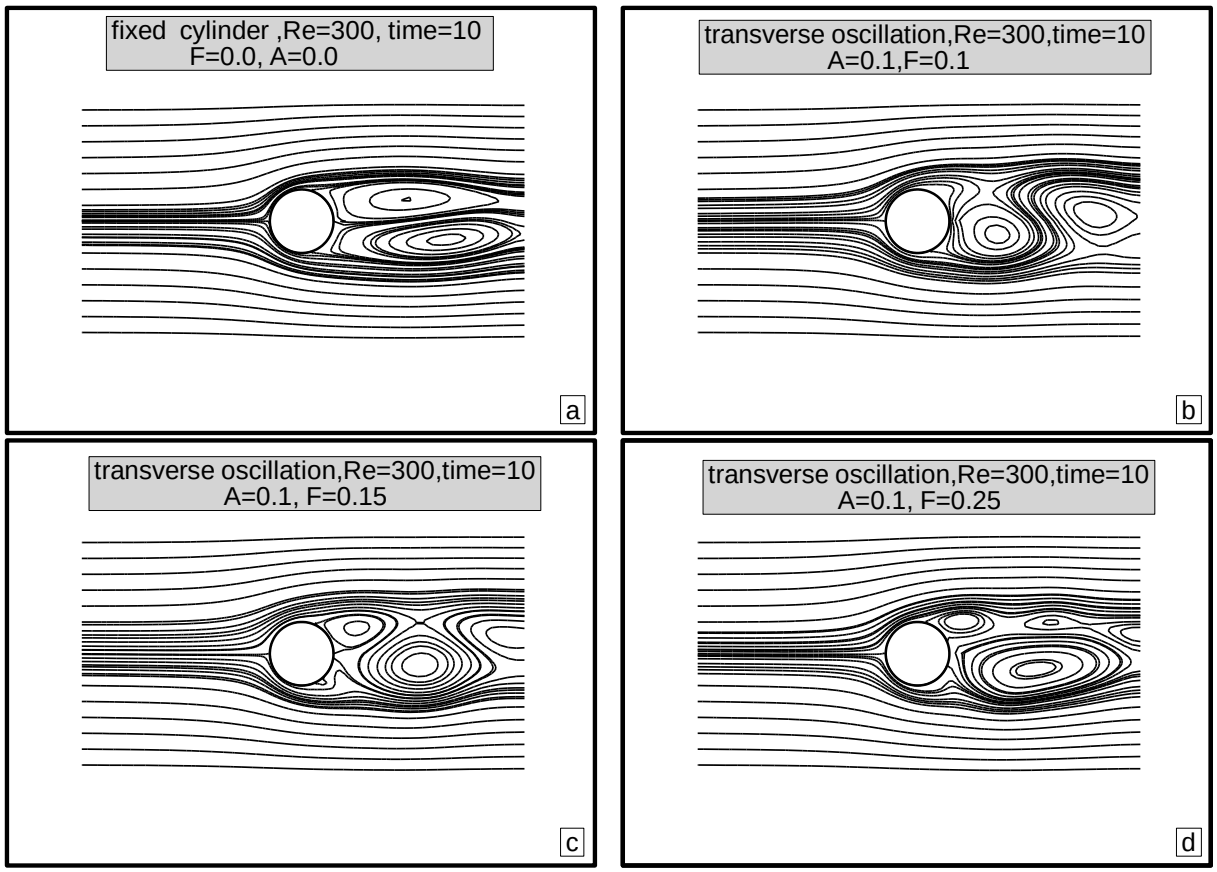

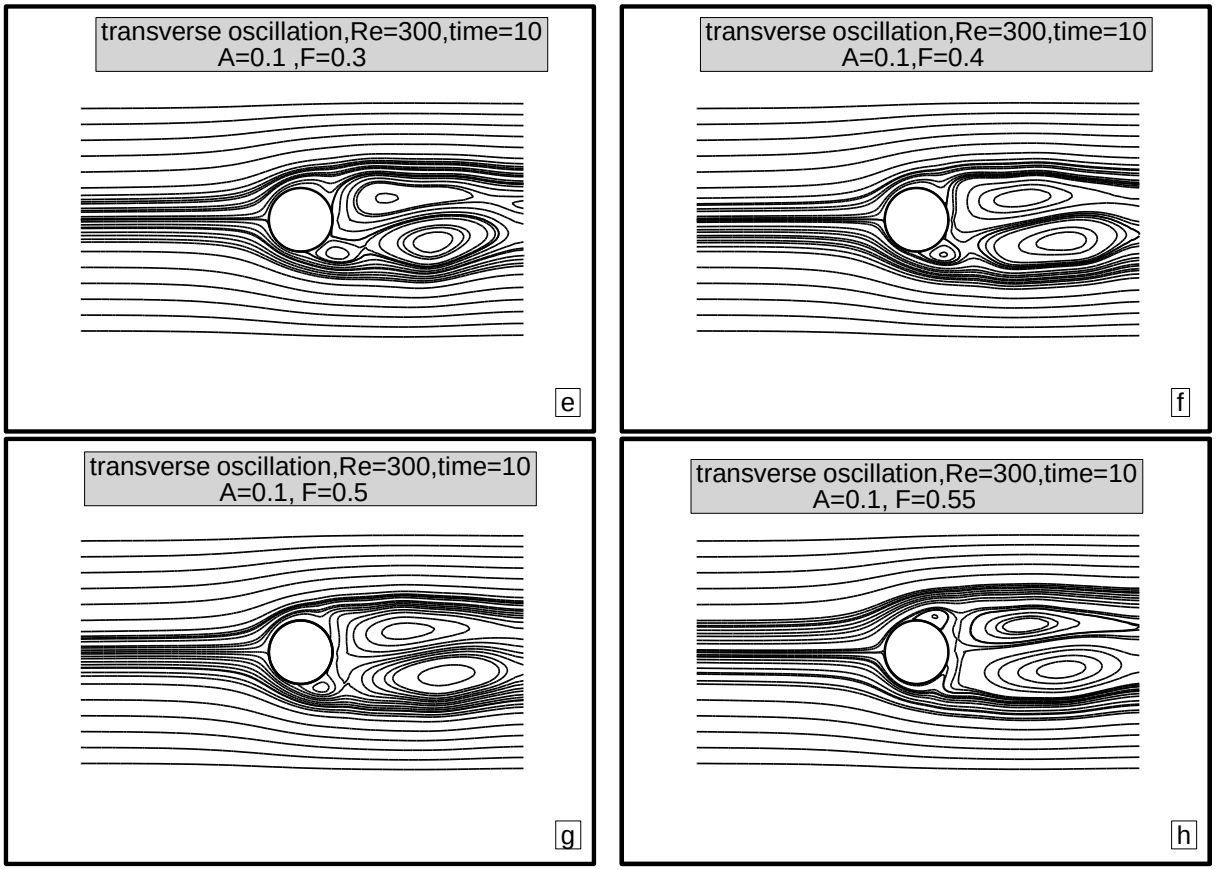

Fig.(٥-١٠)Stream lines contours for transverse oscillating cylinder at Re=٣٠٠ and A=٠.١ with multi-frequency.

transverse oscillation, Re=120, time=10
A=0.3,F=0.2

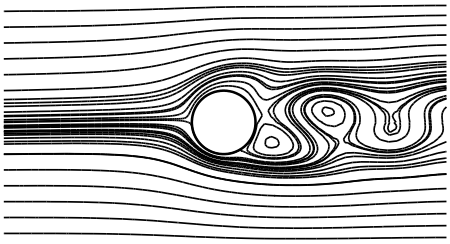

a

transverse oscillation, Re=120, time=11.25
A=0.3,F=0.2

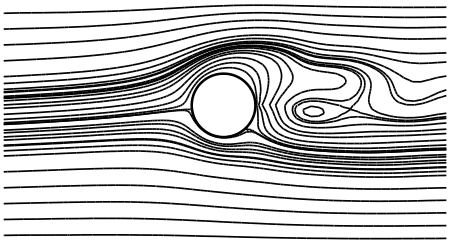

b

transverse oscillation, Re=120, time=12.5
A=0.3,F=0.2

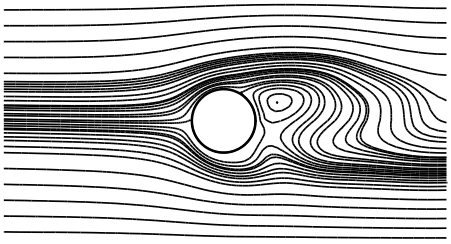

c

transverse oscillation, Re=120, time=13.75
A=0.3,F=0.2

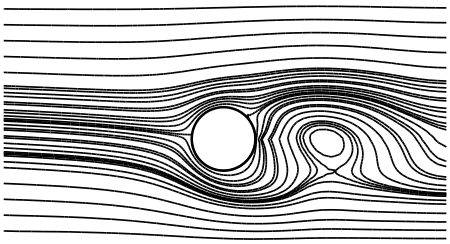

d

transverse oscillation, Re=120, time=15
A=0.3,F=0.2

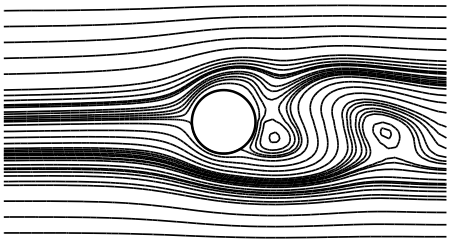

e

transverse oscillation,complete cycle,A=0.3,F=0.2

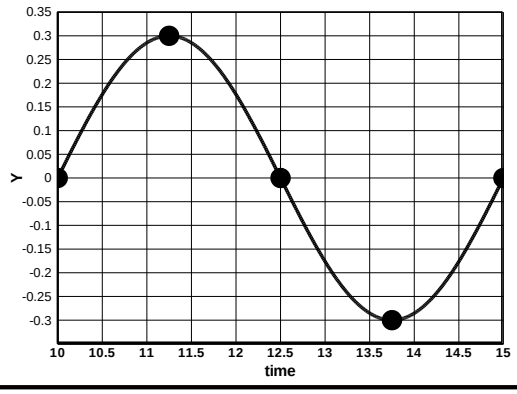

f

Fig.(٥-١١)Stream lines contours for transverse oscillating cylinder at Re=١٢٠,F=٠.٢ and A=٠.٣ for complete cycle

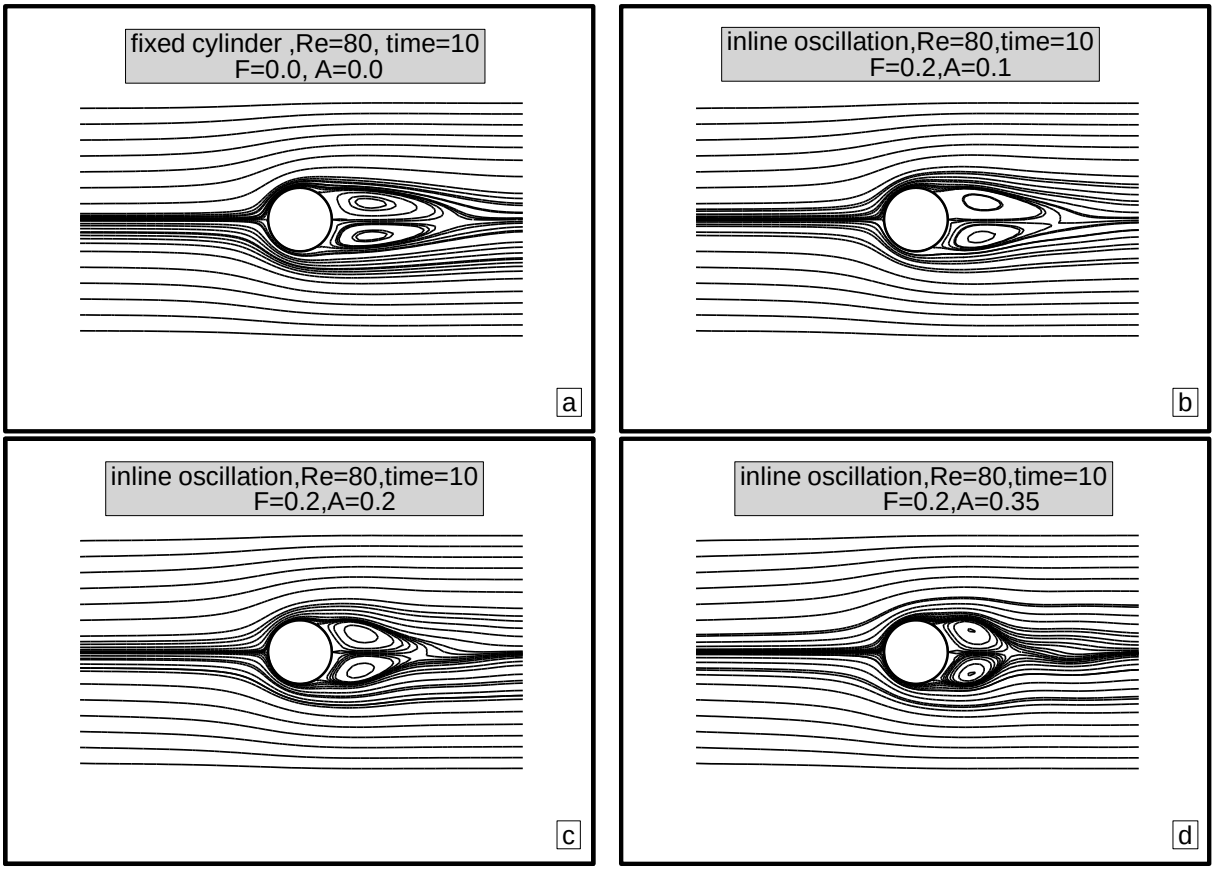

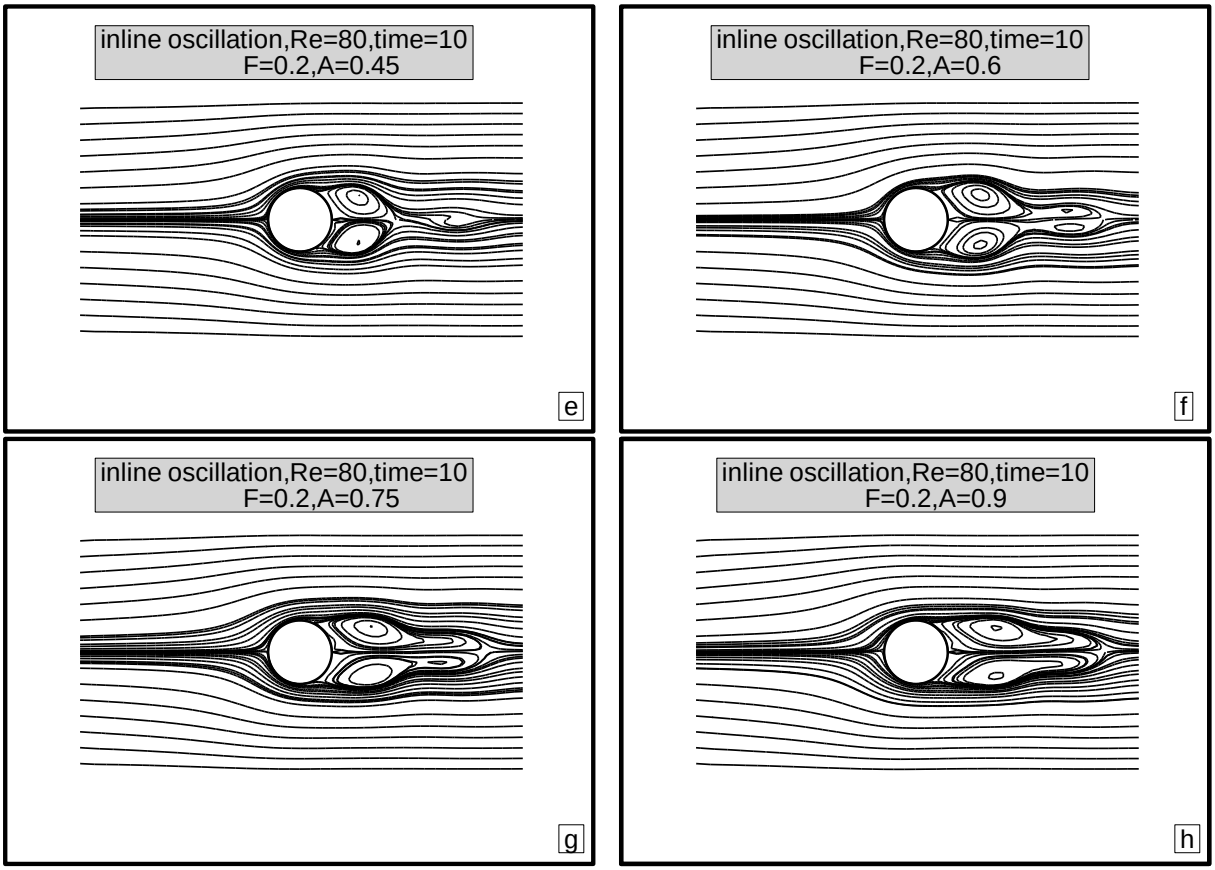

Fig.(٥-١٢)Stream lines contours for inline oscillating cylinder at Re=٨٠ and F=٠.٢ with multi-amplitude.

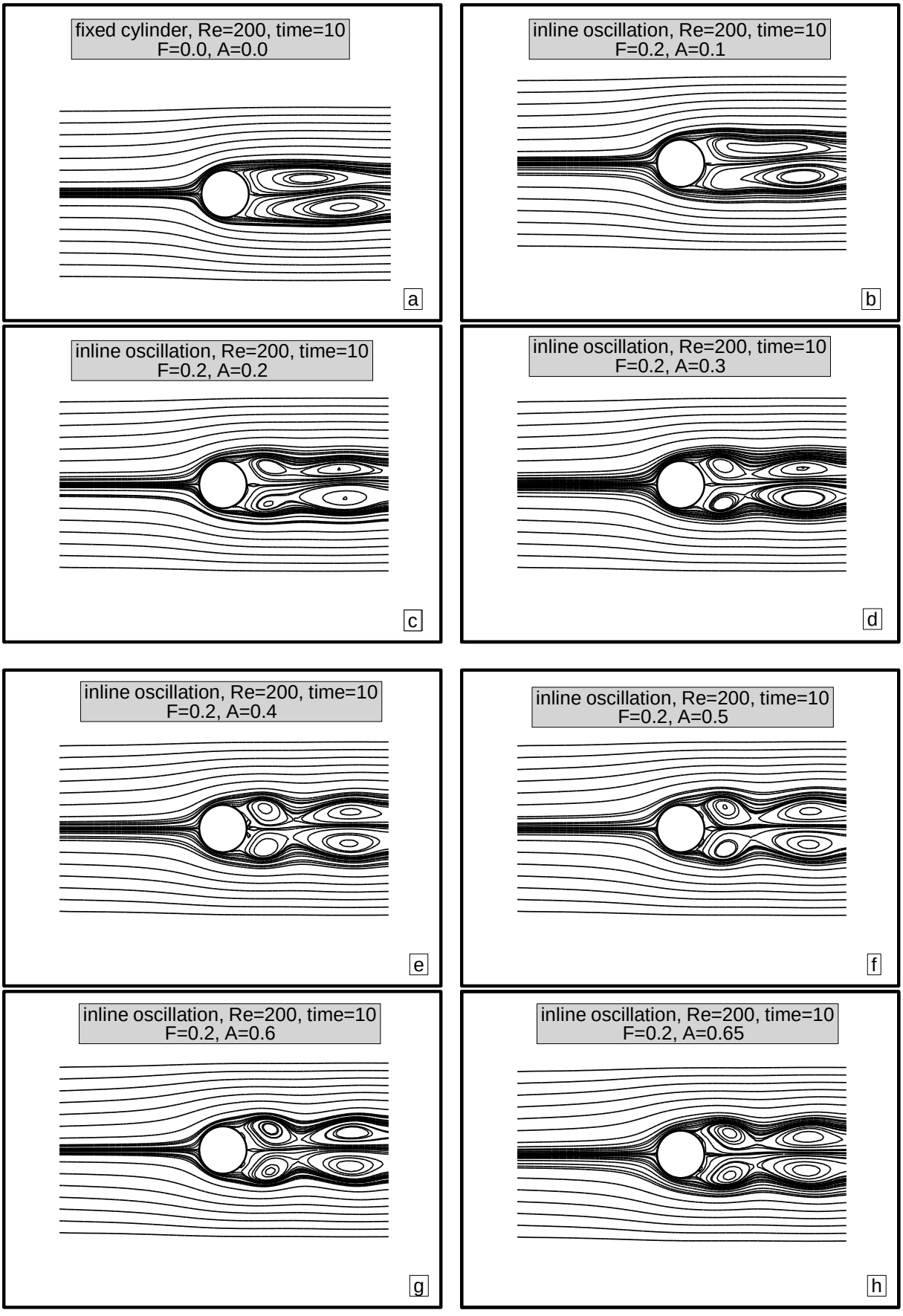
fixed cylinder, Re=200, time=10
F=0.0, A=0.0
a
inline oscillation, Re=200, time=10
F=0.2, A=0.1
b
inline oscillation, Re=200, time=10
F=0.2, A=0.2
c
inline oscillation, Re=200, time=10
F=0.2, A=0.3
d
inline oscillation, Re=200, time=10
F=0.2, A=0.4
e
inline oscillation, Re=200, time=10
F=0.2, A=0.5
f
inline oscillation, Re=200, time=10
F=0.2, A=0.6
g
inline oscillation, Re=200, time=10
F=0.2, A=0.65
h

Fig.(٥-١٣)Stream lines contours for inline oscillating cylinder at Re=٢٠٠ and F=٠.٢ with multi-amplitude.

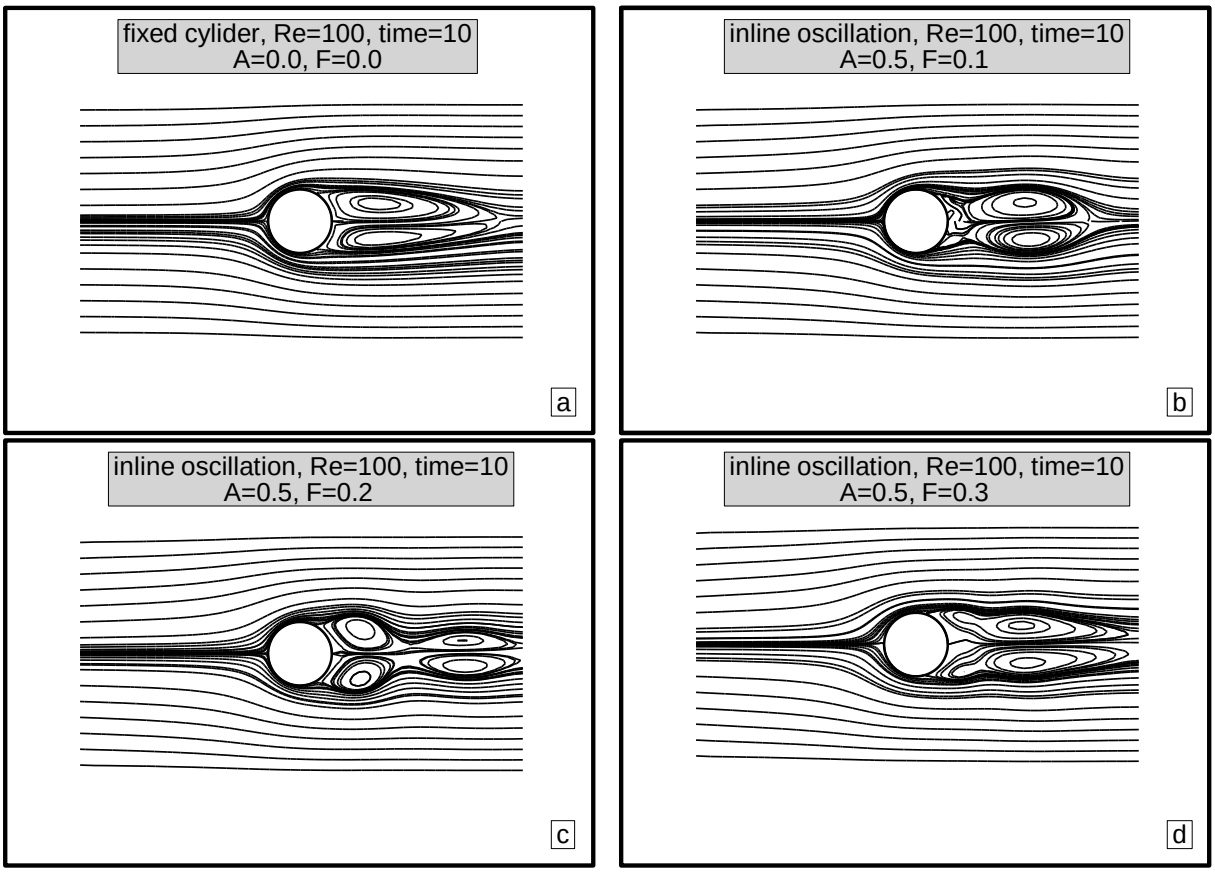

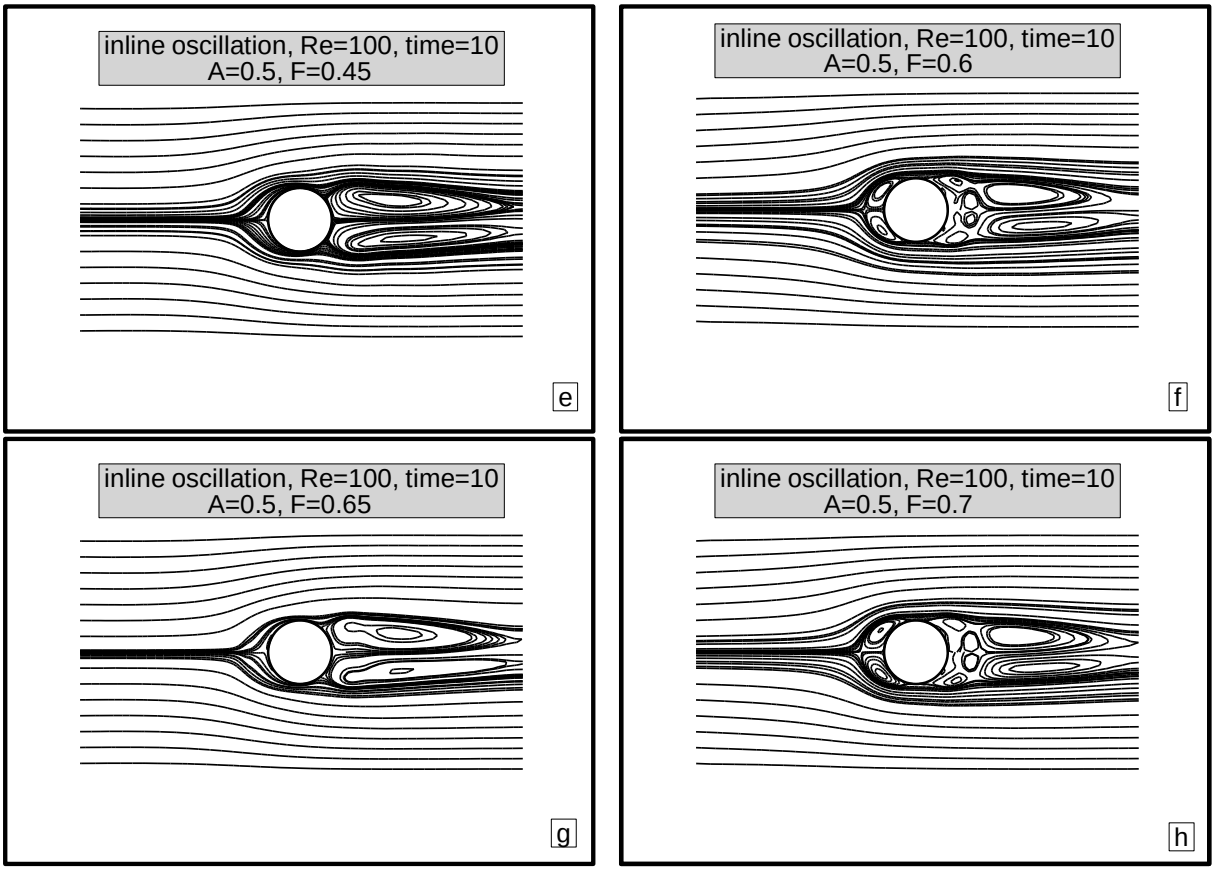

Fig.(٥-١٤)Stream lines contours for inline oscillating cylinder at Re=١٠٠ and A=٠.٥ with multi-frequency.

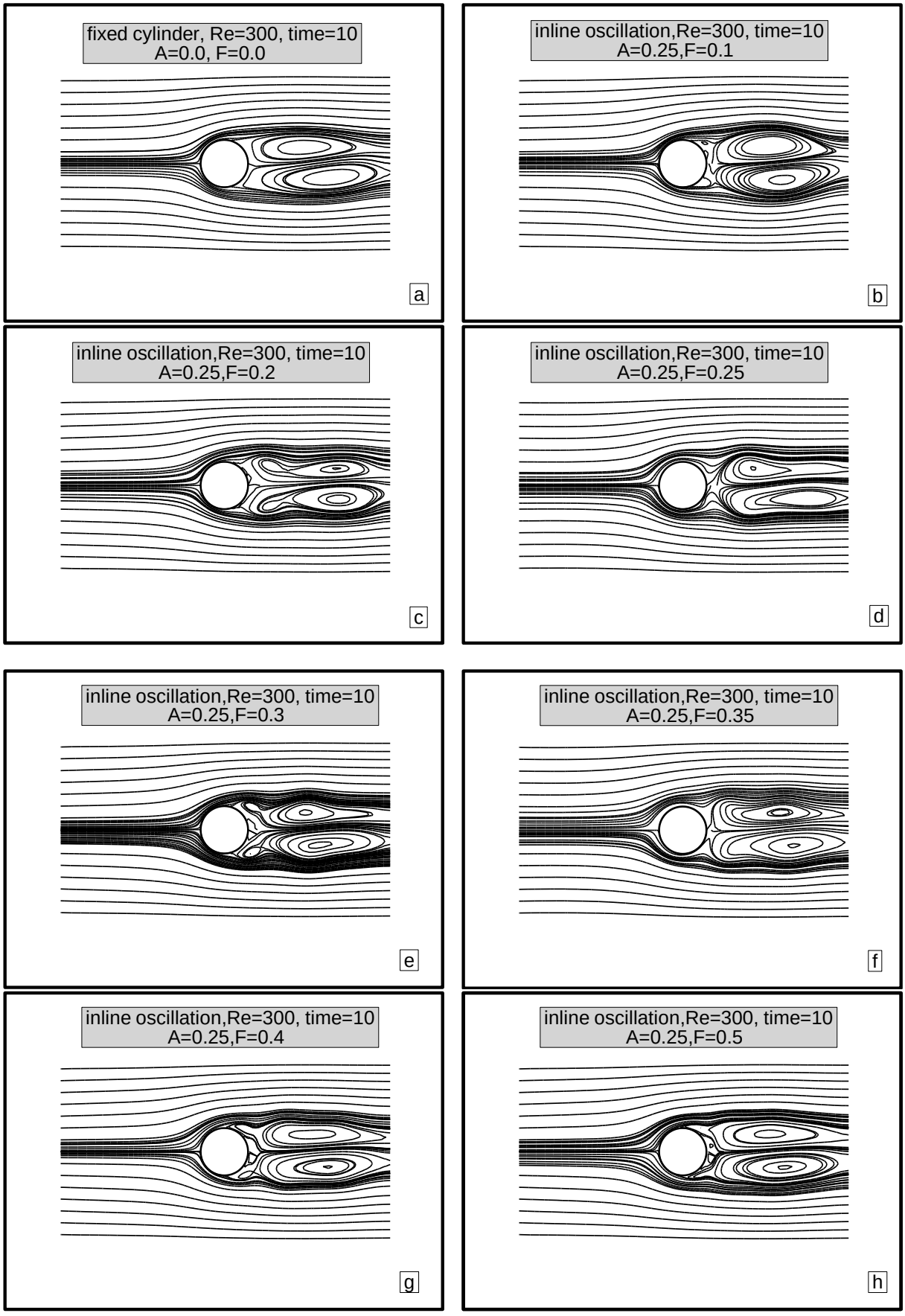
fixed cylinder, Re=300, time=10
A=0.0, F=0.0
a
inline oscillation,Re=300, time=10
A=0.25,F=0.1
b
inline oscillation,Re=300, time=10
A=0.25,F=0.2
c
inline oscillation,Re=300, time=10
A=0.25,F=0.25
d
inline oscillation,Re=300, time=10
A=0.25,F=0.3
e
inline oscillation,Re=300, time=10
A=0.25,F=0.35
f
inline oscillation,Re=300, time=10
A=0.25,F=0.4
g
inline oscillation,Re=300, time=10
A=0.25,F=0.5
h

Fig.(٥-١٥)Stream lines contours for inline oscillating cylinder at Re=٣٠٠ and A=٠.٢٥ with multi-frequency.

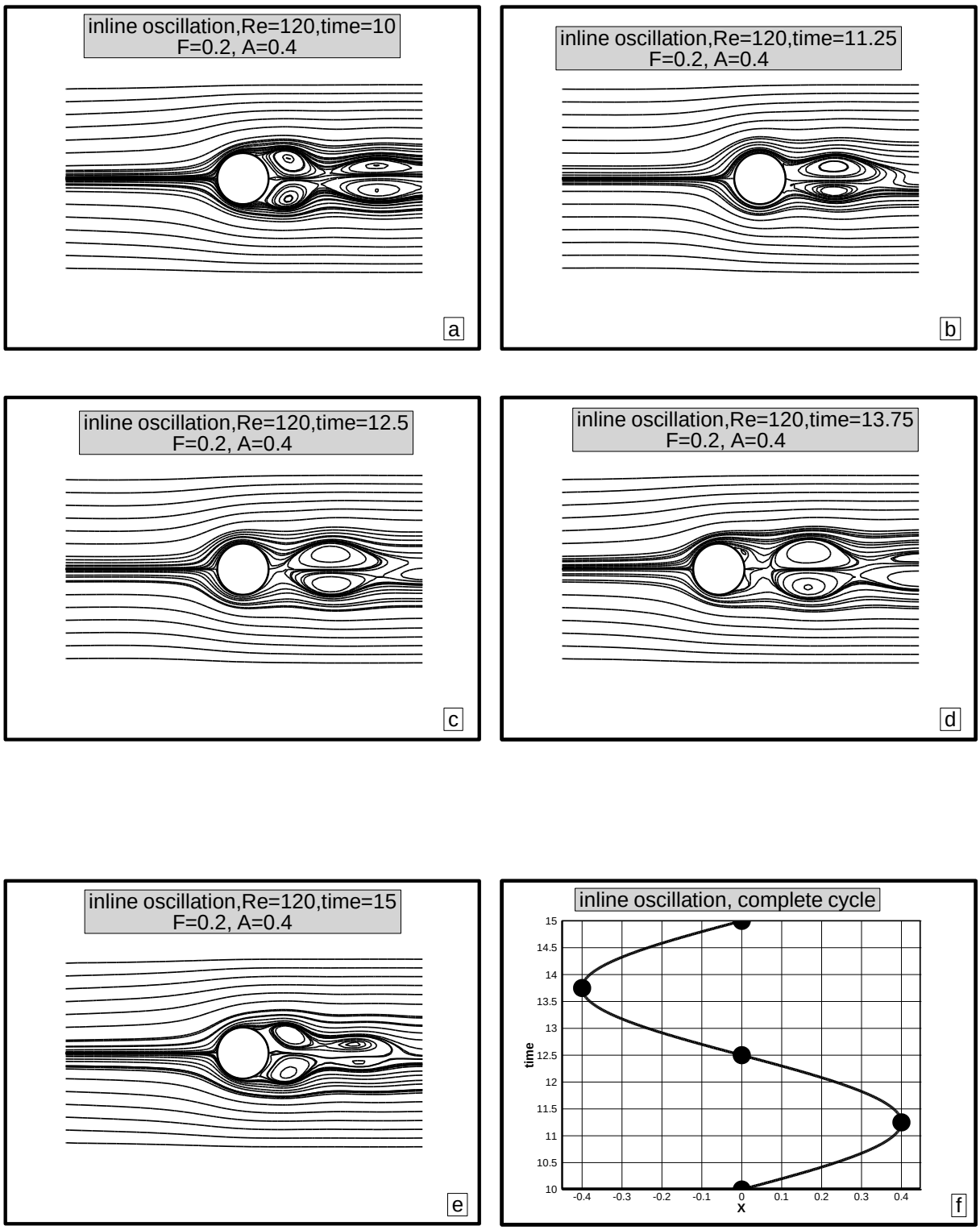

Fig.(٥-١٦)Stream lines contours for inline oscillating cylinder at Re=١٢٠,F=٠.٢ and A=٠.٤ for complete cycle

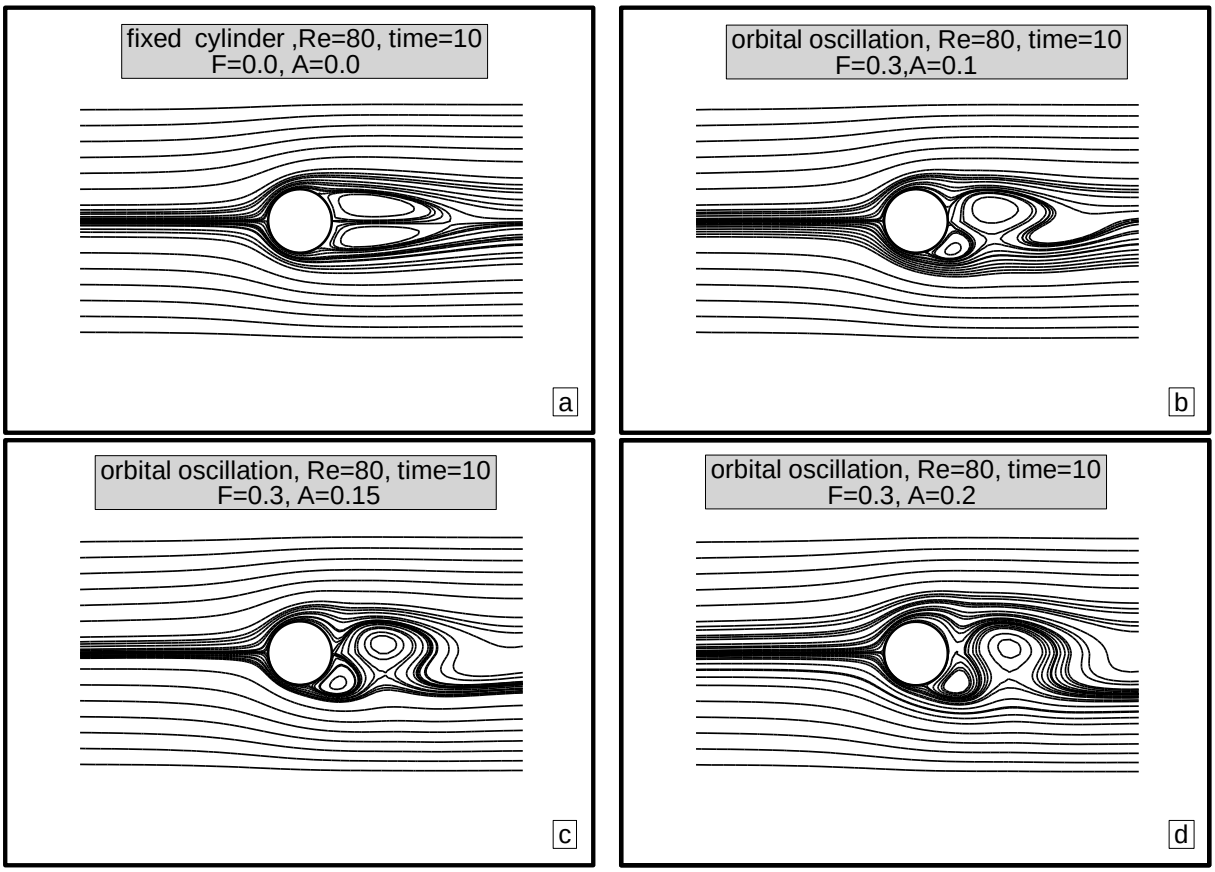

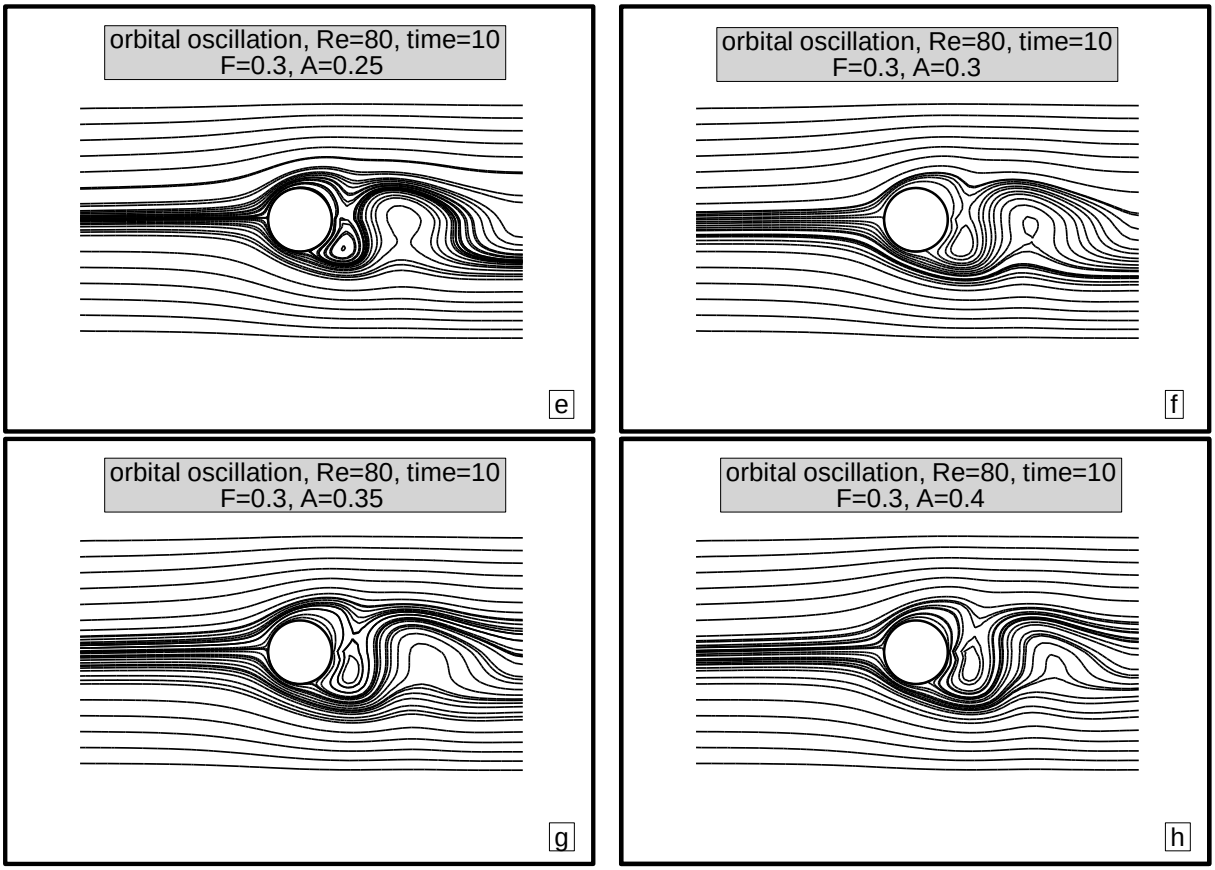

Fig.(٥-١٧)Stream lines contours for orbital oscillating cylinder at Re=٨٠ and F=٠.٣ with multi-amplitude.

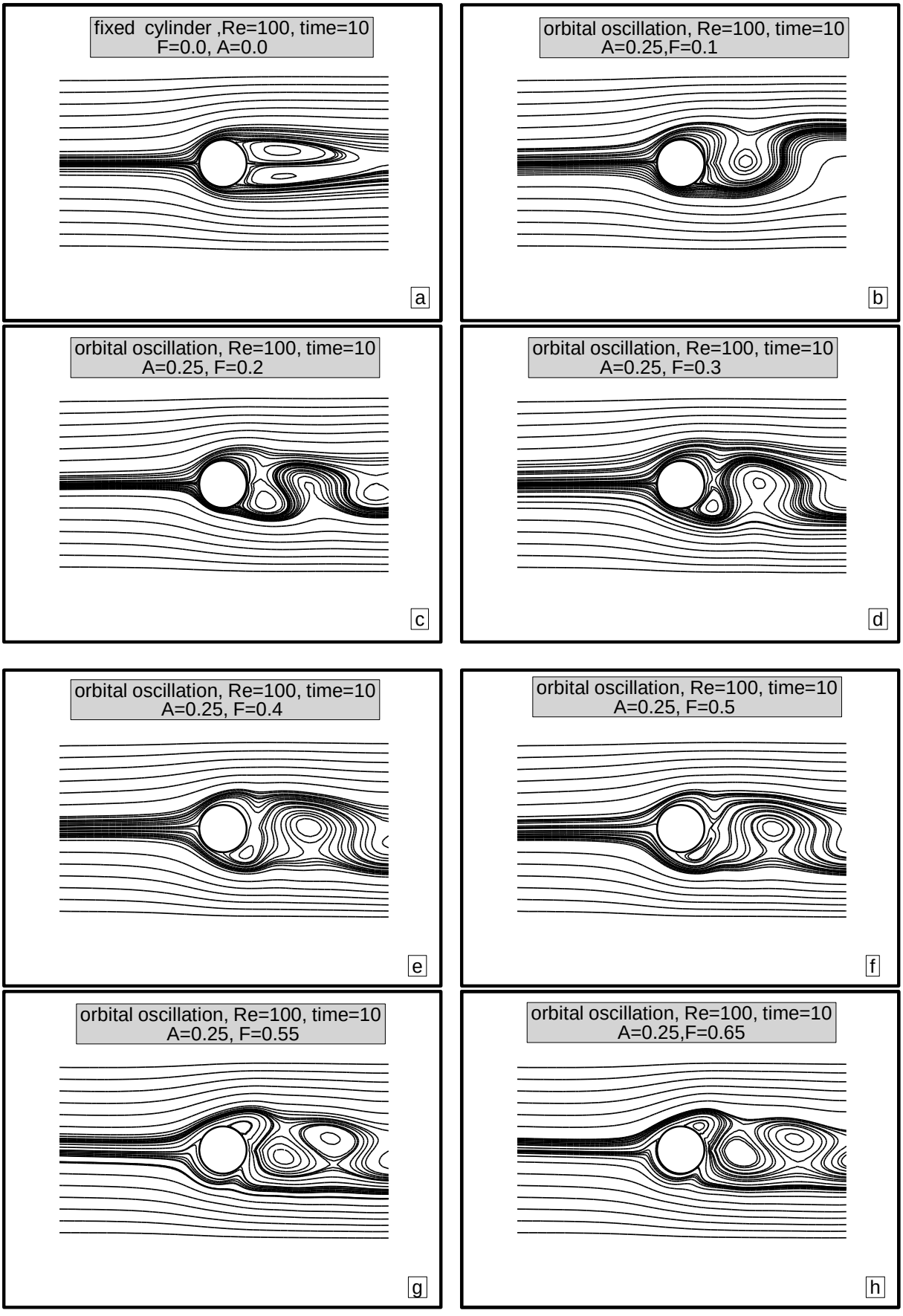
fixed cylinder ,Re=100, time=10
F=0.0, A=0.0
a
orbital oscillation, Re=100, time=10
A=0.25,F=0.1
b
orbital oscillation, Re=100, time=10
A=0.25, F=0.2
c
orbital oscillation, Re=100, time=10
A=0.25, F=0.3
d
orbital oscillation, Re=100, time=10
A=0.25, F=0.4
e
orbital oscillation, Re=100, time=10
A=0.25, F=0.5
f
orbital oscillation, Re=100, time=10
A=0.25, F=0.55
g
orbital oscillation, Re=100, time=10
A=0.25,F=0.65
h

Fig.(٥-١٨)Stream lines contours for orbital oscillating cylinder at Re=١٠٠ and A=٠.٢٥ with multi-frequency.

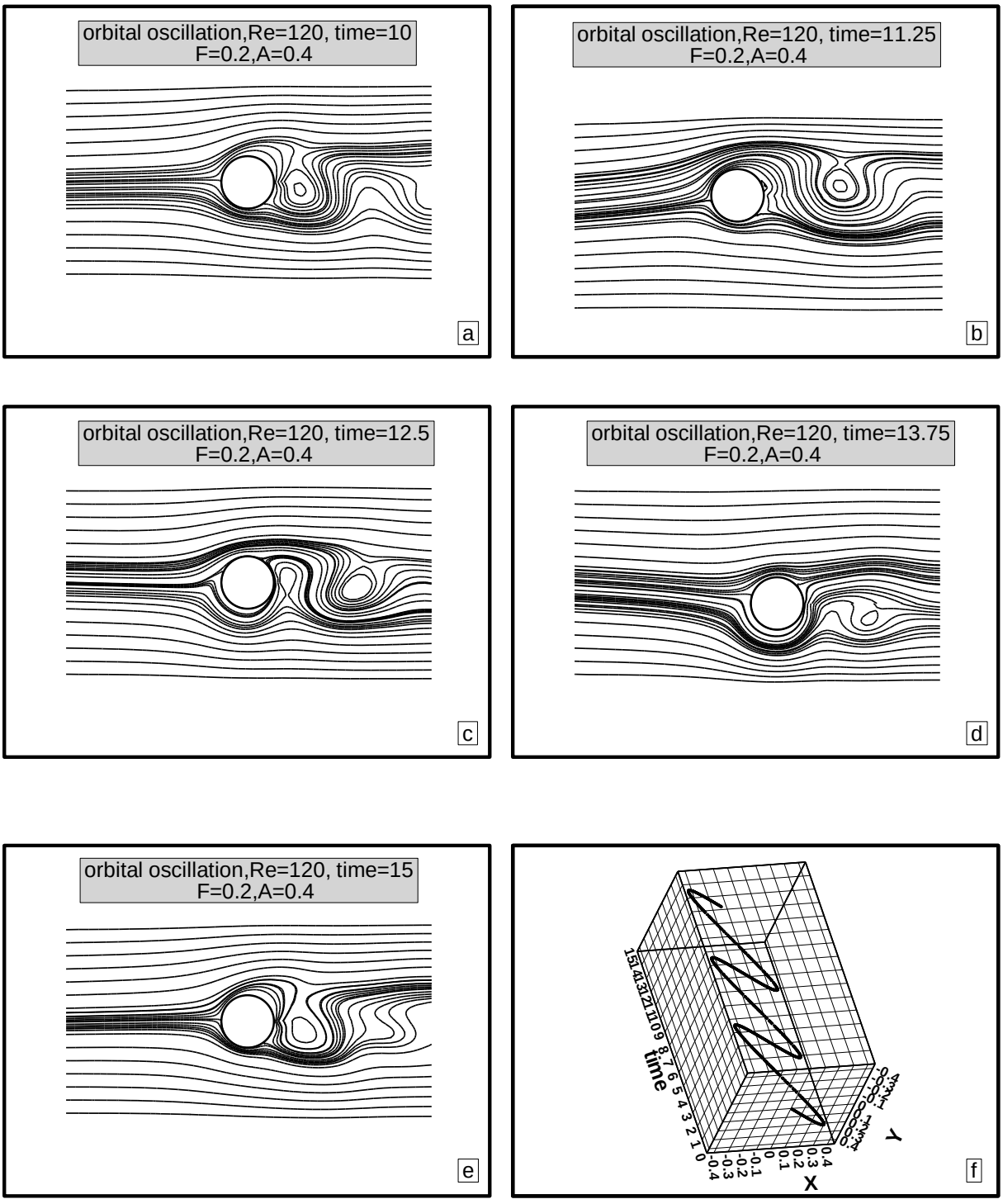

Fig.(٥-١٩)Stream lines contours for orbital oscillating cylinder at Re=١٢٠,F=٠.٢ and A=٠.٤ for complete cycle

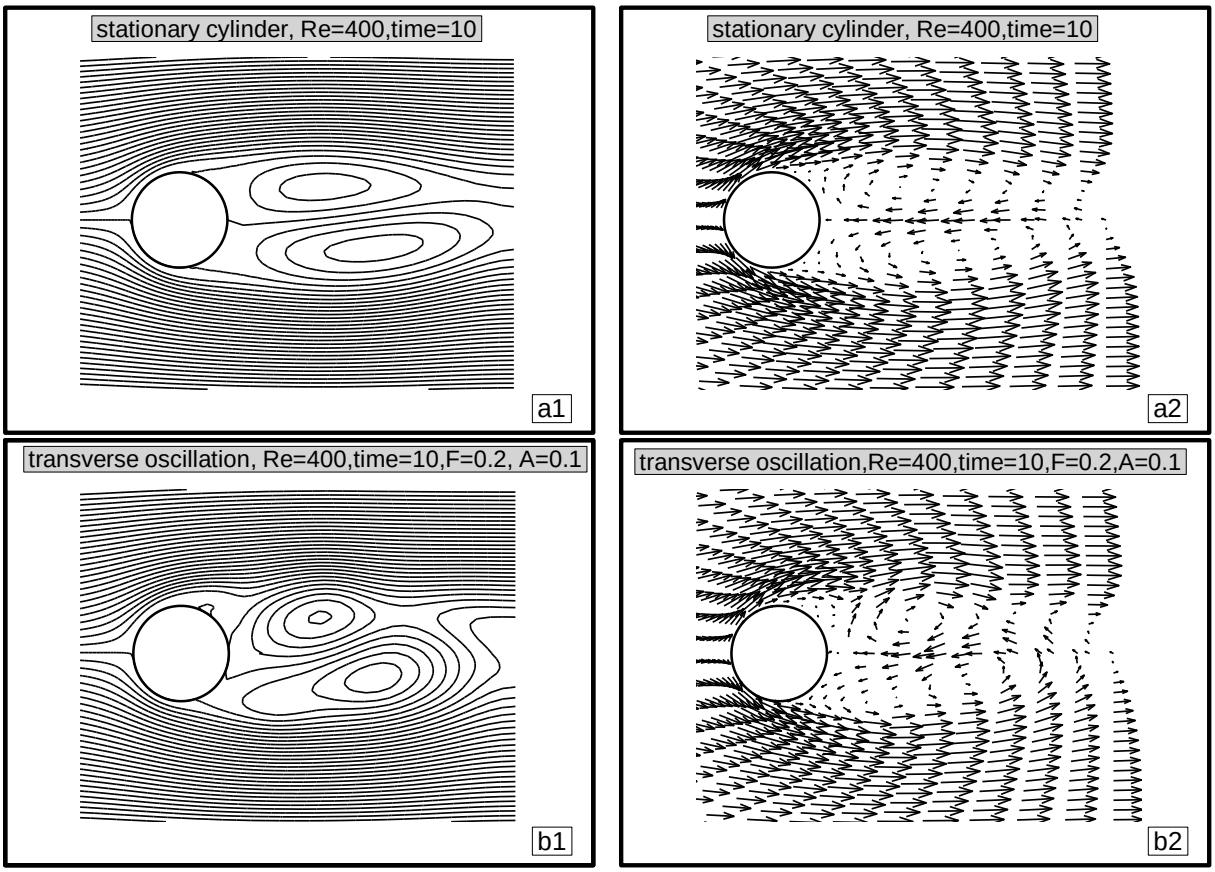

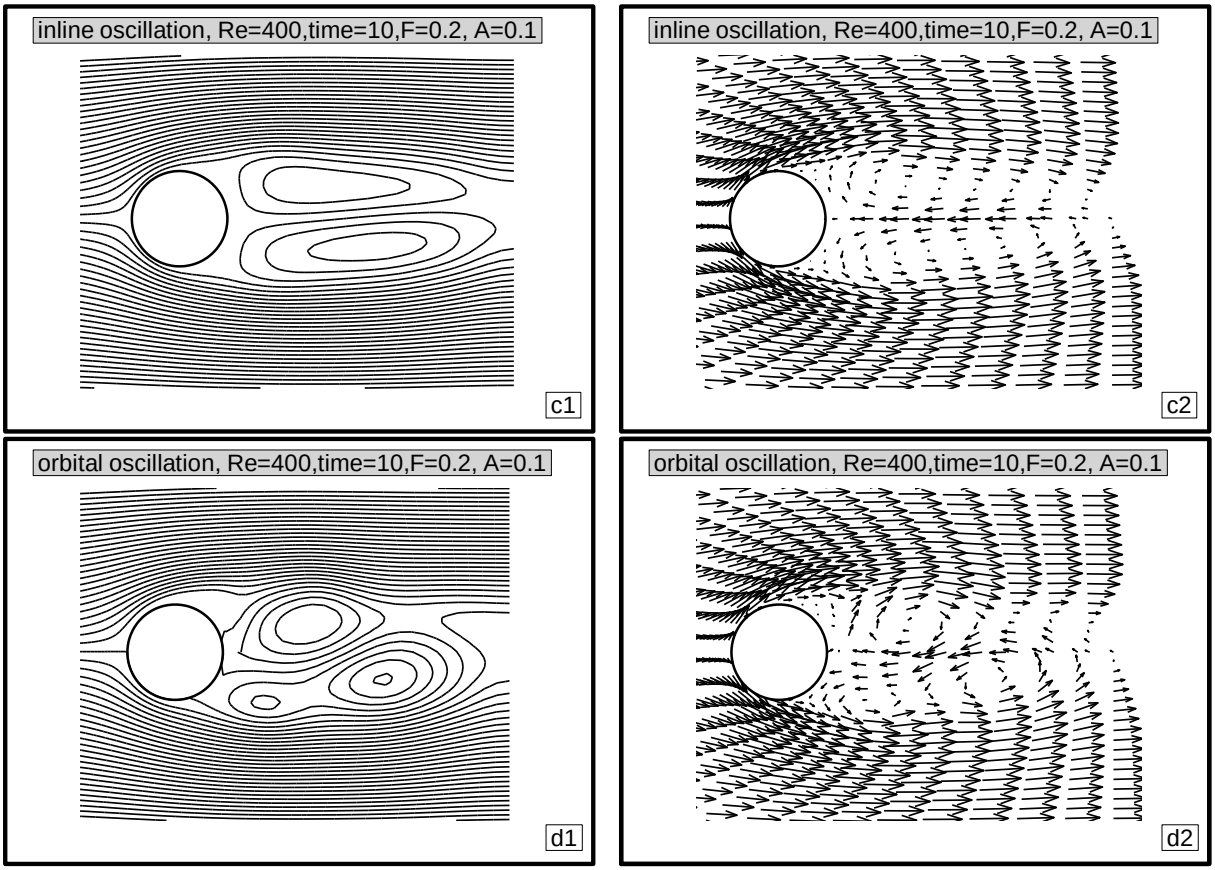

Fig.(٥-٢٠)Stream lines contours and velocity vector field for oscillating and stationary cylinder at Re=٤٠٠, F=٠.٢ and A=٠.١.

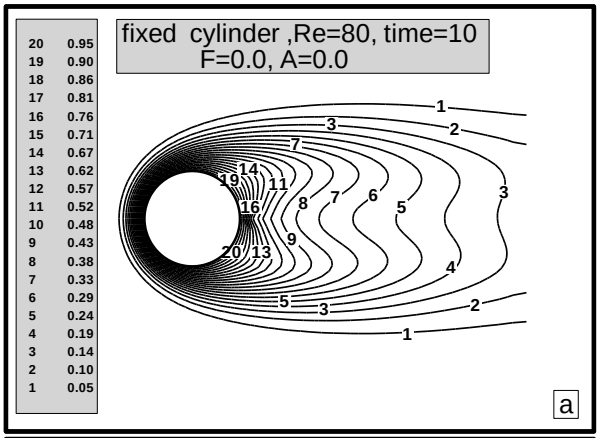
fixed cylinder ,Re=80, time=10
F=0.0, A=0.0
a

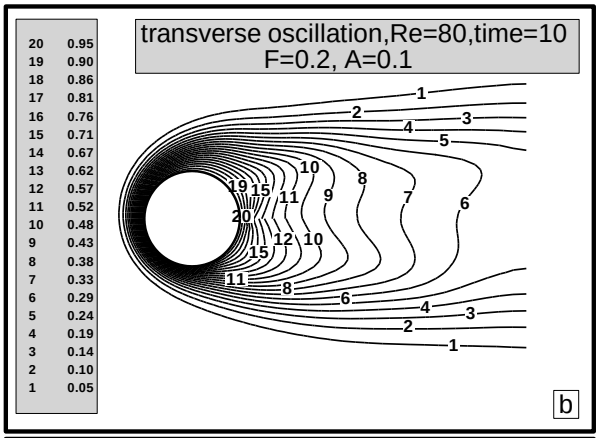
transverse oscillation,Re=80,time=10
F=0.2, A=0.1
b

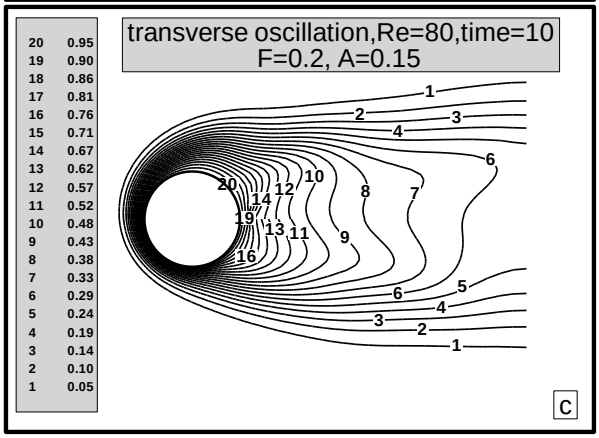
transverse oscillation,Re=80,time=10
F=0.2, A=0.15
c

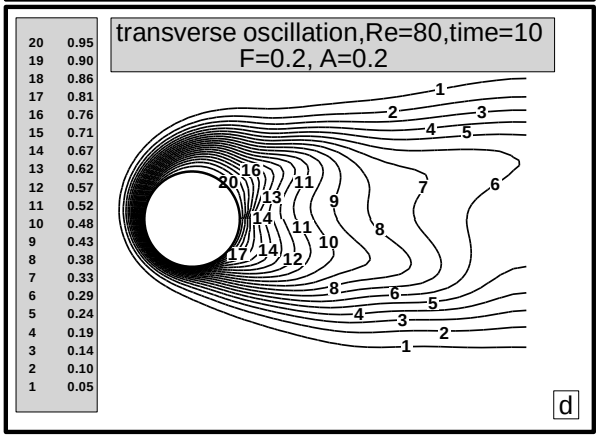
transverse oscillation,Re=80,time=10
F=0.2, A=0.2
d

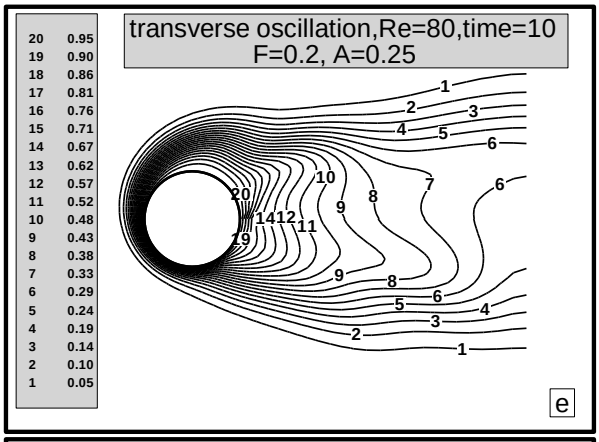
transverse oscillation,Re=80,time=10
F=0.2, A=0.25
e

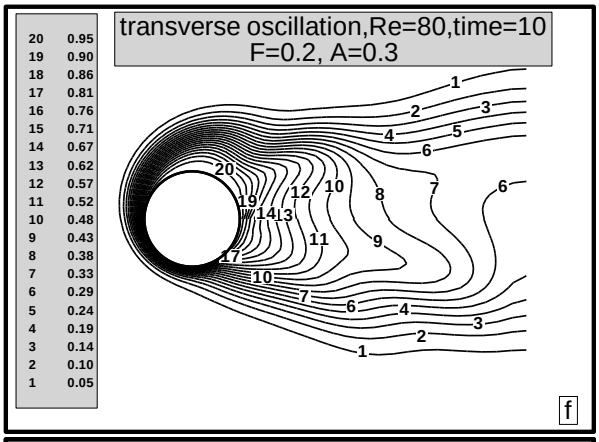
transverse oscillation,Re=80,time=10
F=0.2, A=0.3
f

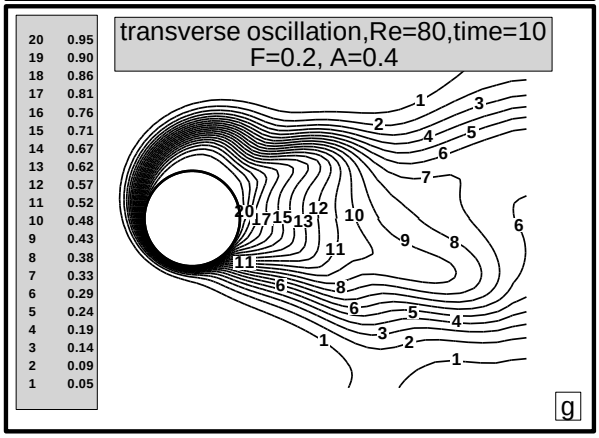
transverse oscillation,Re=80,time=10
F=0.2, A=0.4
g

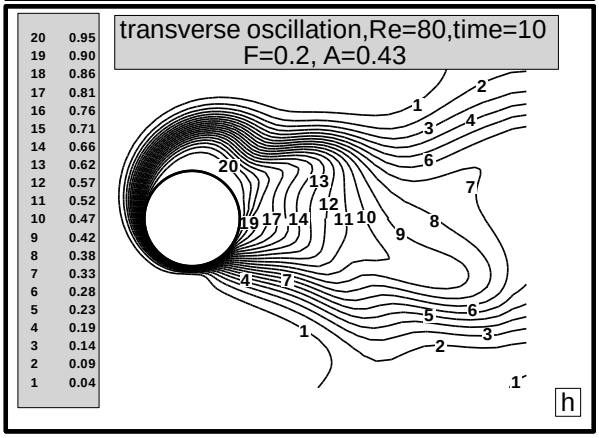
transverse oscillation,Re=80,time=10
F=0.2, A=0.43
h

Fig.(٥-٢١)Isothermal contours for transverse oscillating cylinder at Re=٨٠ and F=٠.٢ with multi-amplitude

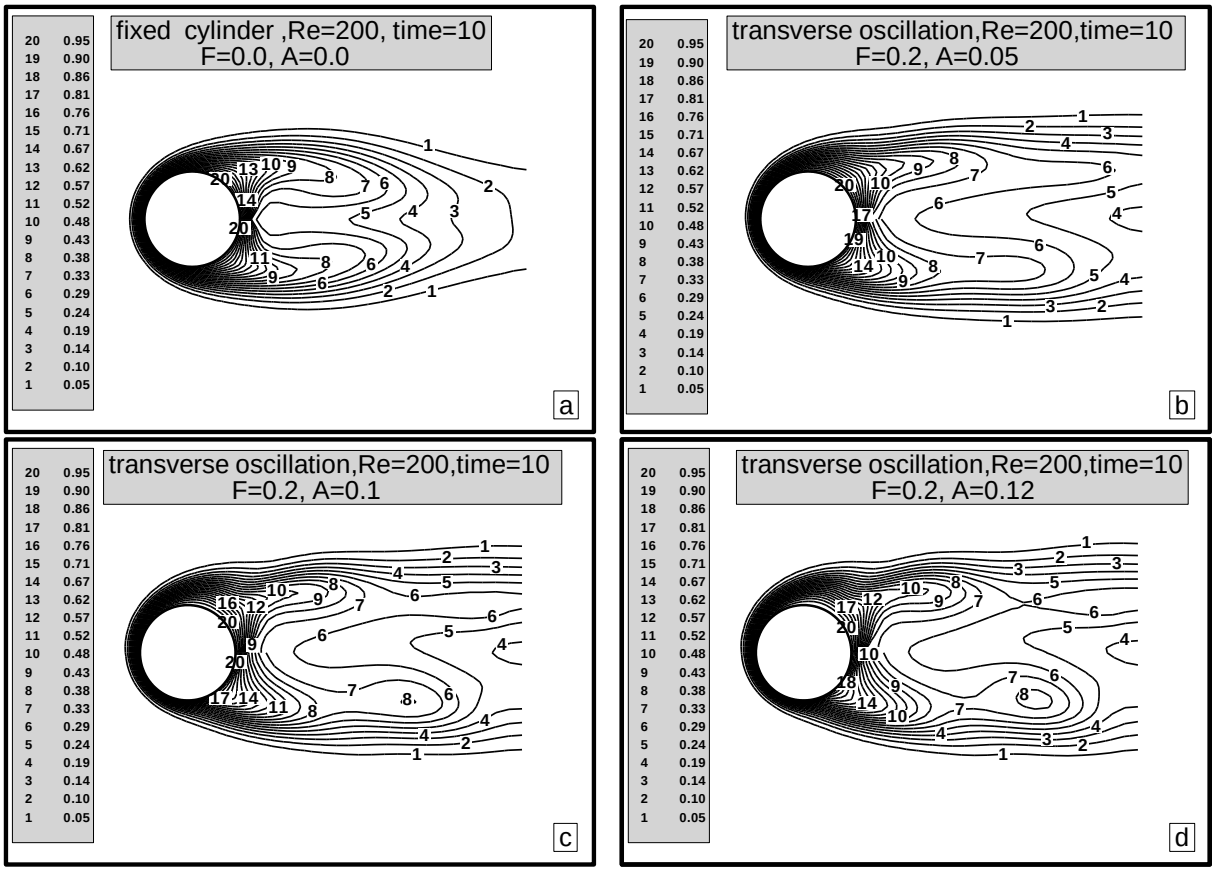

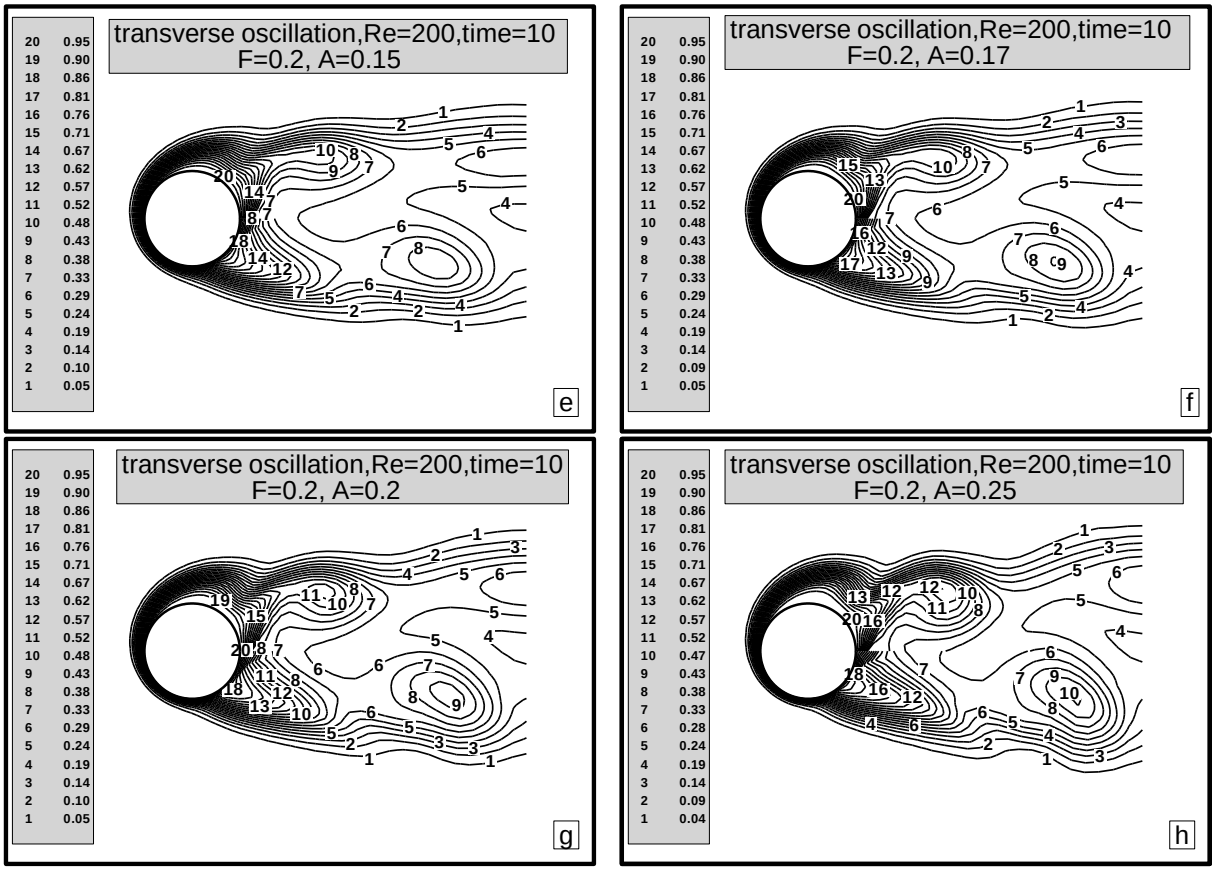

Fig.(٥-٢٢)Isothermal contours for transverse oscillating cylinder at Re=٢٠٠ and F=٠.٢ with multi-amplitude

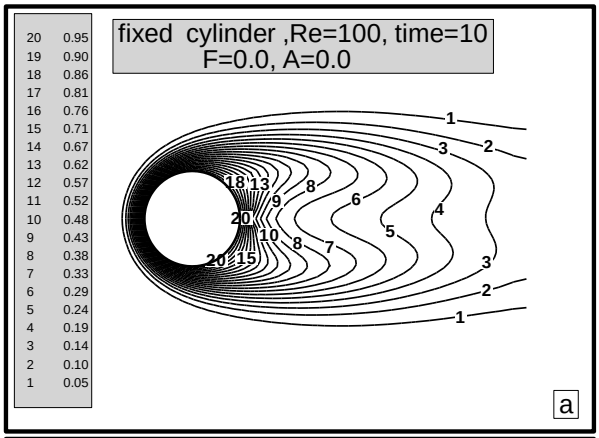
20 0.95
19 0.90
18 0.86
17 0.81
16 0.76
15 0.71
14 0.67
13 0.62
12 0.57
11 0.52
10 0.48
9 0.43
8 0.38
7 0.33
6 0.29
5 0.24
4 0.19
3 0.14
2 0.10
1 0.05
fixed cylinder ,Re=100, time=10
F=0.0, A=0.0
a

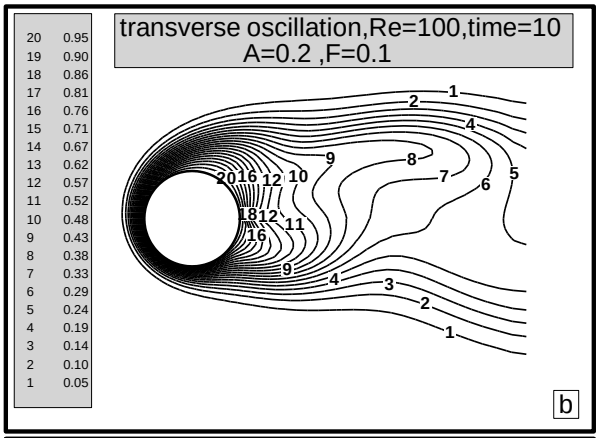
20 0.95
19 0.90
18 0.86
17 0.81
16 0.76
15 0.71
14 0.67
13 0.62
12 0.57
11 0.52
10 0.48
9 0.43
8 0.38
7 0.33
6 0.29
5 0.24
4 0.19
3 0.14
2 0.10
1 0.05
transverse oscillation,Re=100,time=10
A=0.2 ,F=0.1
b

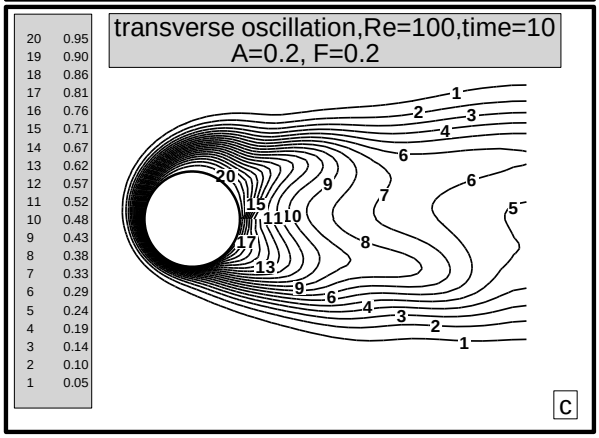
20 0.95
19 0.90
18 0.86
17 0.81
16 0.76
15 0.71
14 0.67
13 0.62
12 0.57
11 0.52
10 0.48
9 0.43
8 0.38
7 0.33
6 0.29
5 0.24
4 0.19
3 0.14
2 0.10
1 0.05
transverse oscillation,Re=100,time=10
A=0.2, F=0.2
c

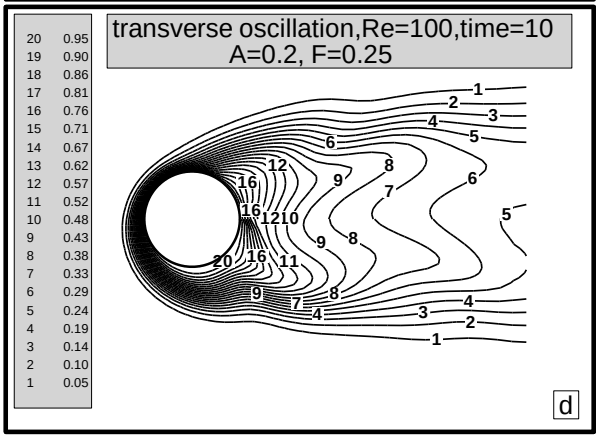
20 0.95
19 0.90
18 0.86
17 0.81
16 0.76
15 0.71
14 0.67
13 0.62
12 0.57
11 0.52
10 0.48
9 0.43
8 0.38
7 0.33
6 0.29
5 0.24
4 0.19
3 0.14
2 0.10
1 0.05
transverse oscillation,Re=100,time=10
A=0.2, F=0.25
d

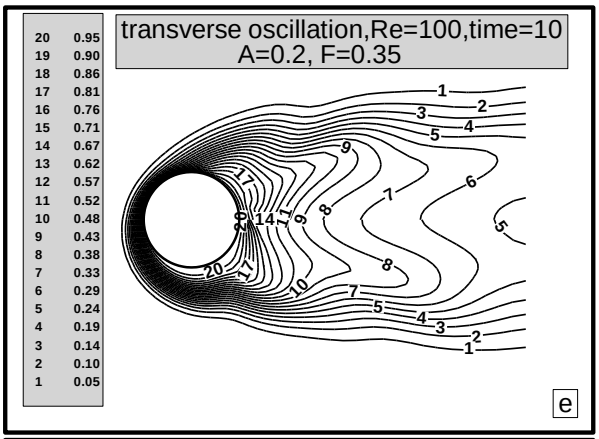
20 0.95
19 0.90
18 0.86
17 0.81
16 0.76
15 0.71
14 0.67
13 0.62
12 0.57
11 0.52
10 0.48
9 0.43
8 0.38
7 0.33
6 0.29
5 0.24
4 0.19
3 0.14
2 0.10
1 0.05
transverse oscillation,Re=100,time=10
A=0.2, F=0.35
e

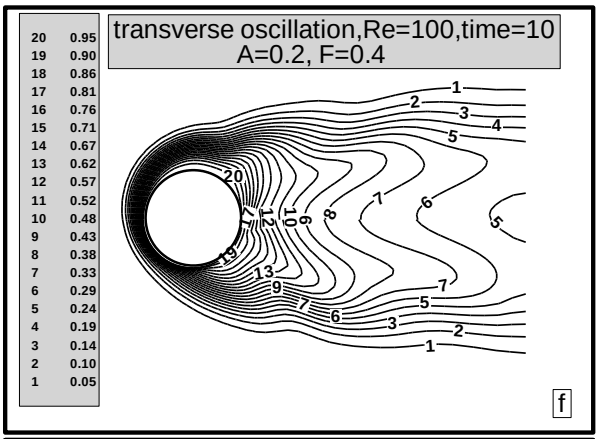
20 0.95
19 0.90
18 0.86
17 0.81
16 0.76
15 0.71
14 0.67
13 0.62
12 0.57
11 0.52
10 0.48
9 0.43
8 0.38
7 0.33
6 0.29
5 0.24
4 0.19
3 0.14
2 0.10
1 0.05
transverse oscillation,Re=100,time=10
A=0.2, F=0.4
f

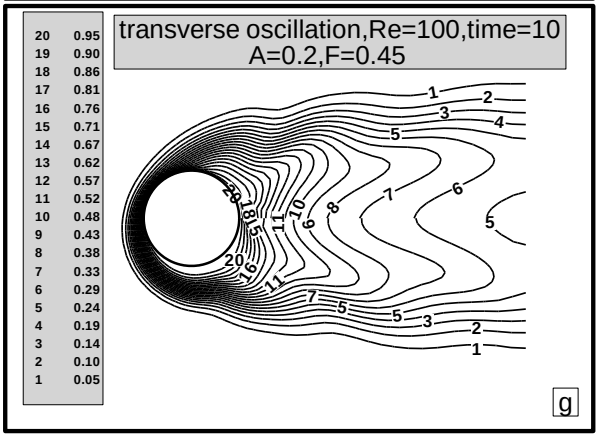
20 0.95
19 0.90
18 0.86
17 0.81
16 0.76
15 0.71
14 0.67
13 0.62
12 0.57
11 0.52
10 0.48
9 0.43
8 0.38
7 0.33
6 0.29
5 0.24
4 0.19
3 0.14
2 0.10
1 0.05
transverse oscillation,Re=100,time=10
A=0.2,F=0.45
g

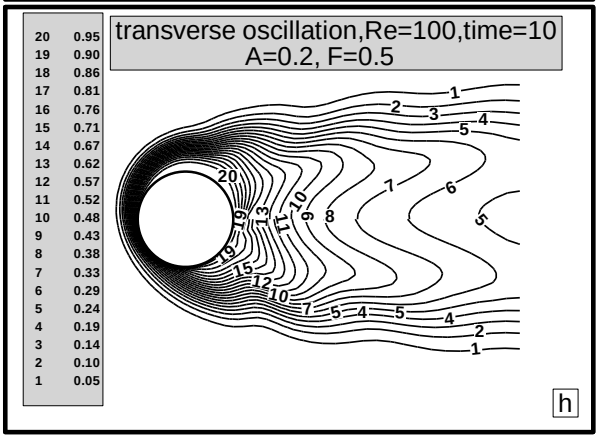
20 0.95
19 0.90
18 0.86
17 0.81
16 0.76
15 0.71
14 0.67
13 0.62
12 0.57
11 0.52
10 0.48
9 0.43
8 0.38
7 0.33
6 0.29
5 0.24
4 0.19
3 0.14
2 0.10
1 0.05
transverse oscillation,Re=100,time=10
A=0.2, F=0.5
h

Fig.(٥-٢٣)Isothermal contours for transverse oscillating cylinder at Re=١٠٠ and A=٠.٢ with multi-frequency

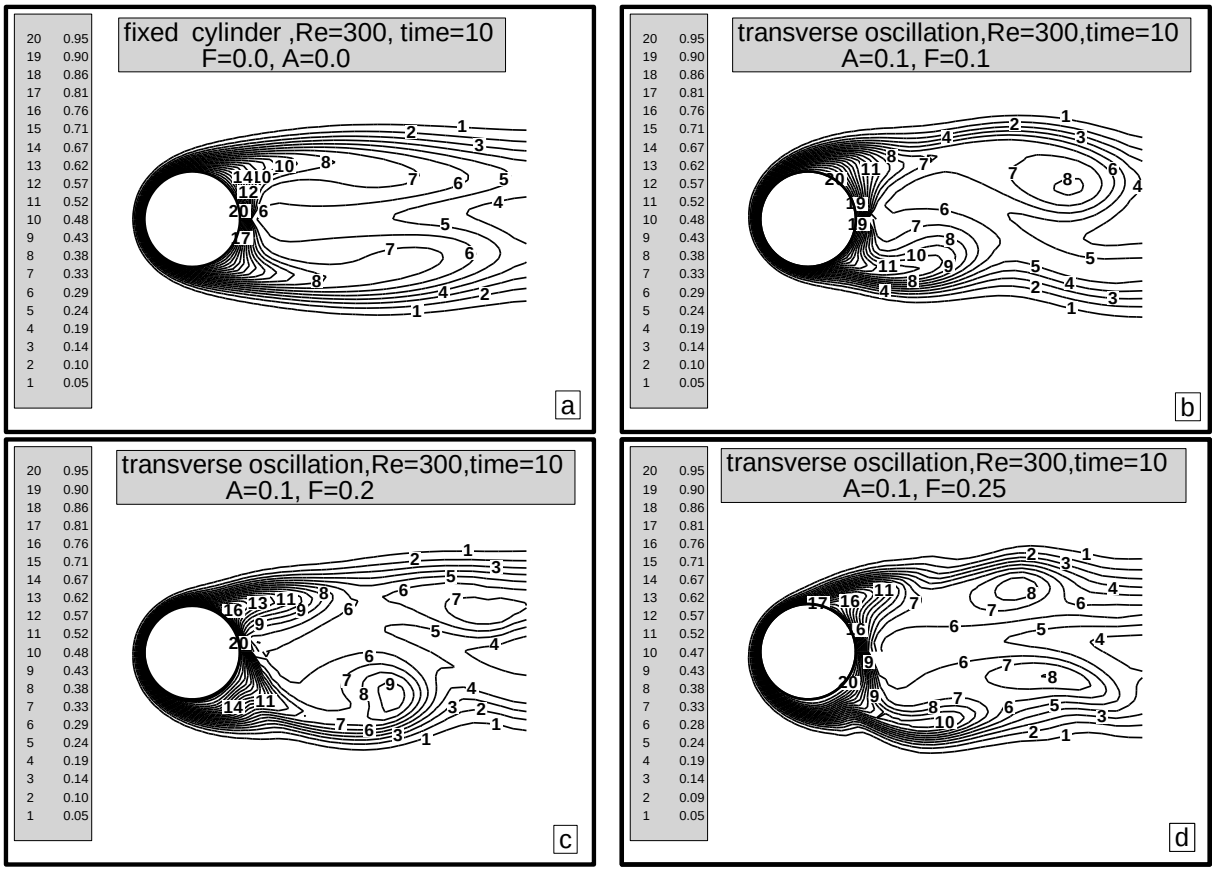

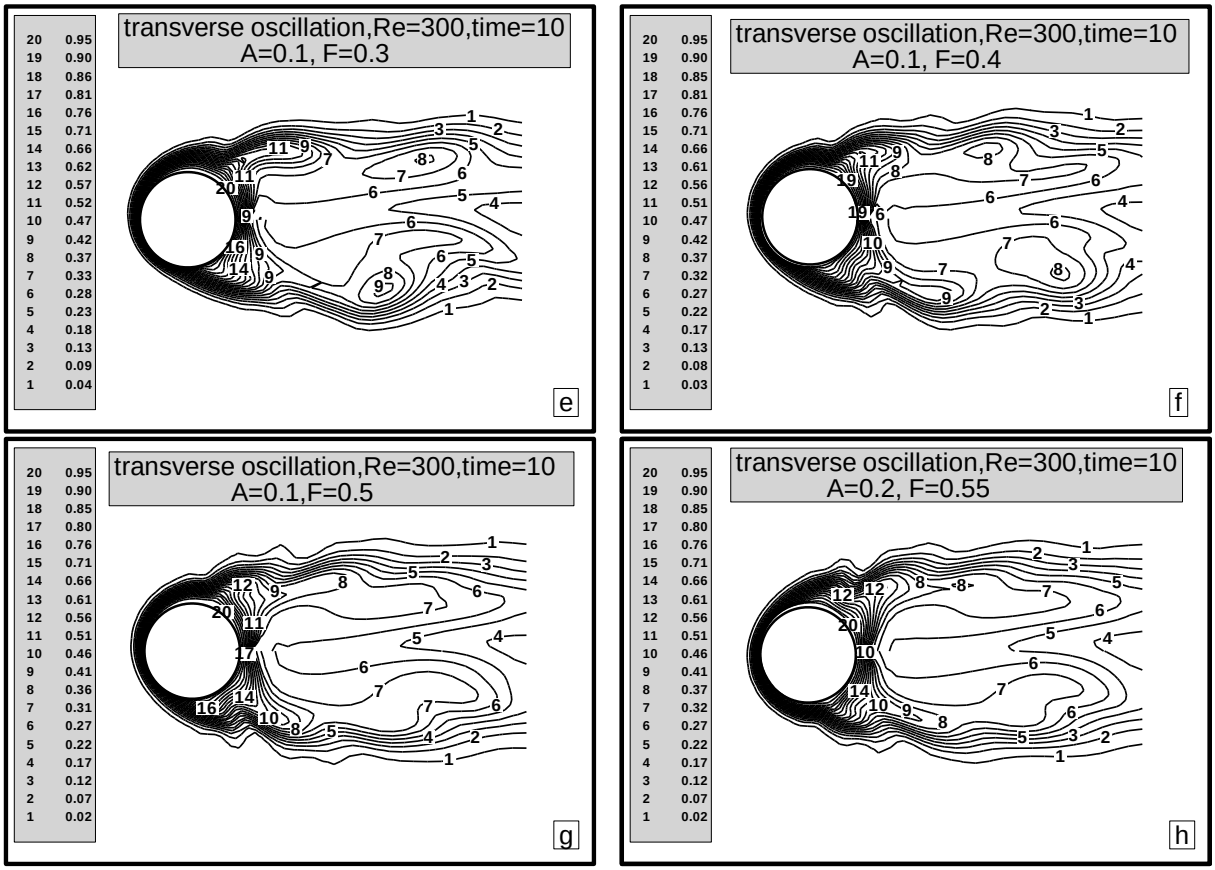

Fig.(٥-٢٤)Isothermal contours for transverse oscillating cylinder at Re=٣٠٠ and A=٠.٢ with multi-frequency

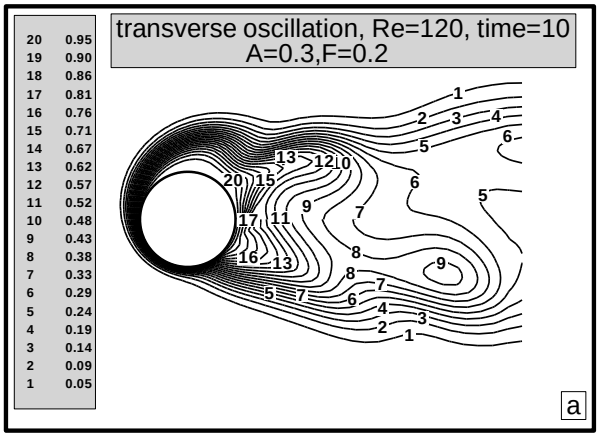
transverse oscillation, Re=120, time=10
A=0.3,F=0.2
a

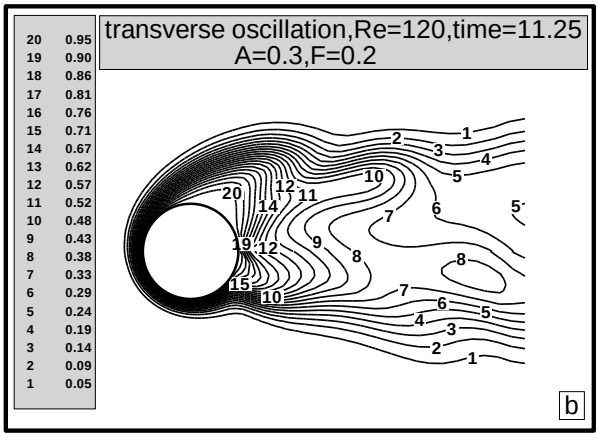
transverse oscillation,Re=120,time=11.25
A=0.3,F=0.2
b

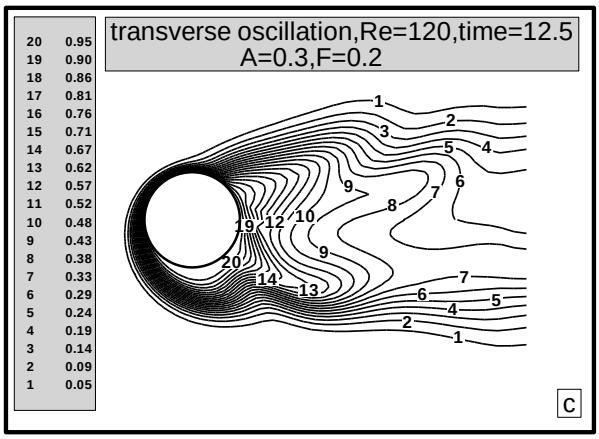
transverse oscillation,Re=120,time=12.5
A=0.3,F=0.2
c

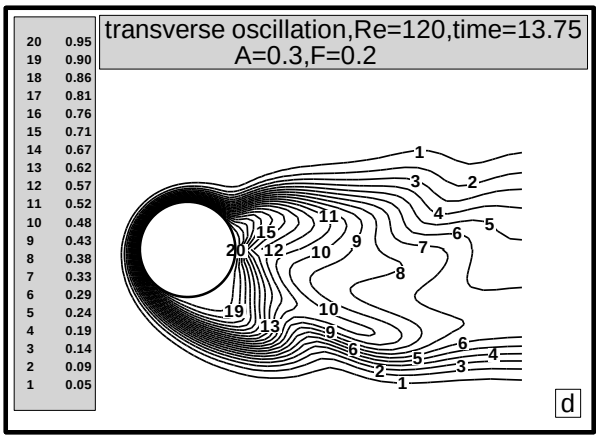
transverse oscillation,Re=120,time=13.75
A=0.3,F=0.2
d

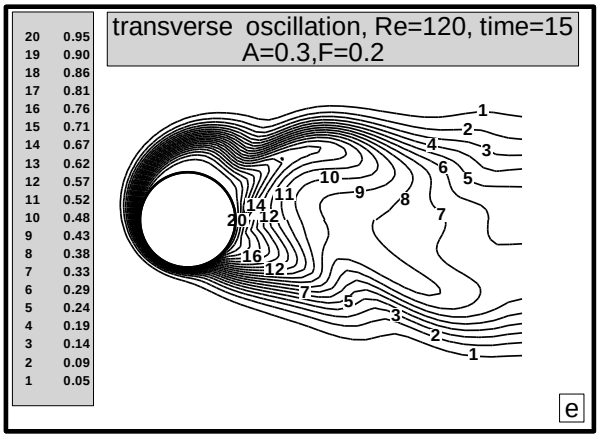
transverse oscillation, Re=120, time=15
A=0.3,F=0.2
e

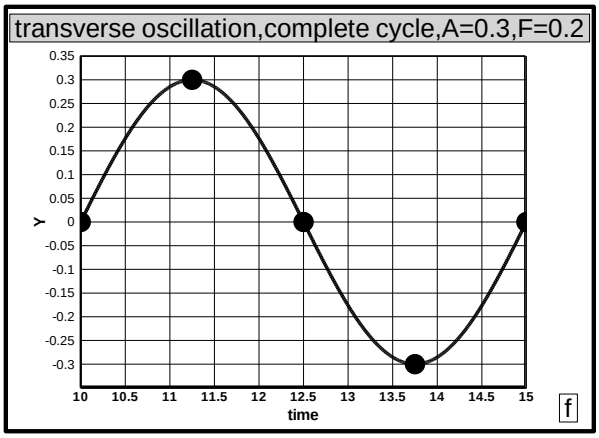
transverse oscillation,complete cycle,A=0.3,F=0.2
Y
time
f

Fig.(٥-٢٥)Isothermal contours for transverse oscillating cylinder at Re=١٢٠,F=٠.٢ and A=٠.٣ for complete cycle

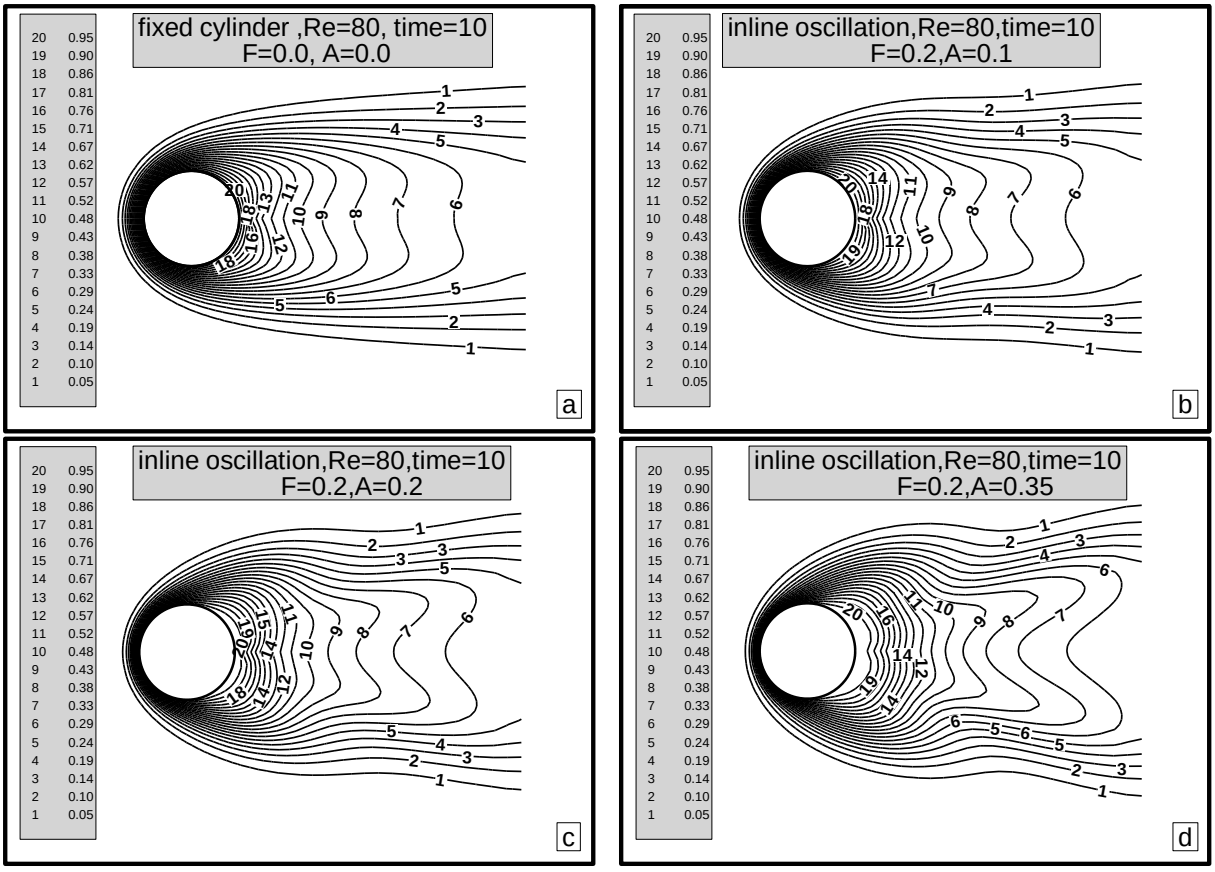

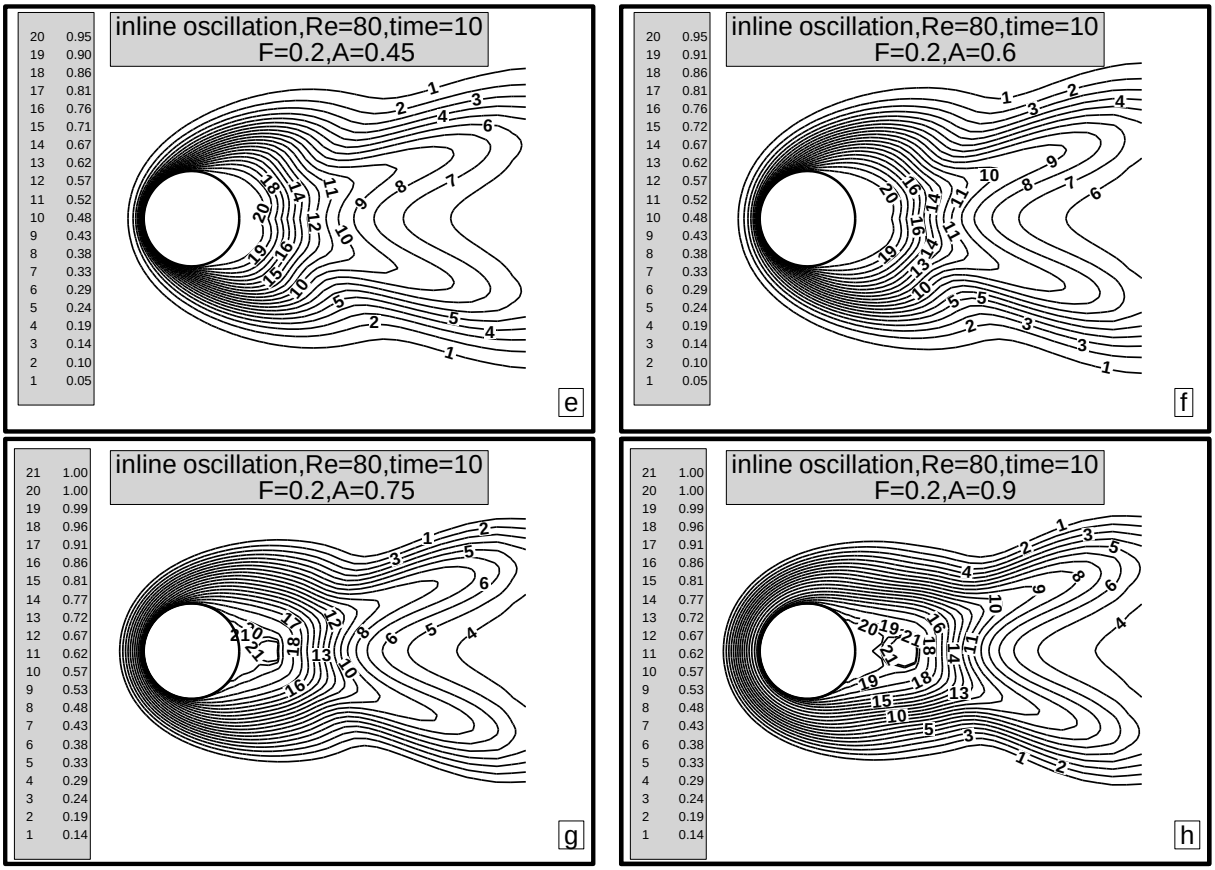

Fig.(٥-٢٦)Isothermal contours for inline oscillating cylinder at Re=٨٠ and F=٠.٢ with multi-amplitude.

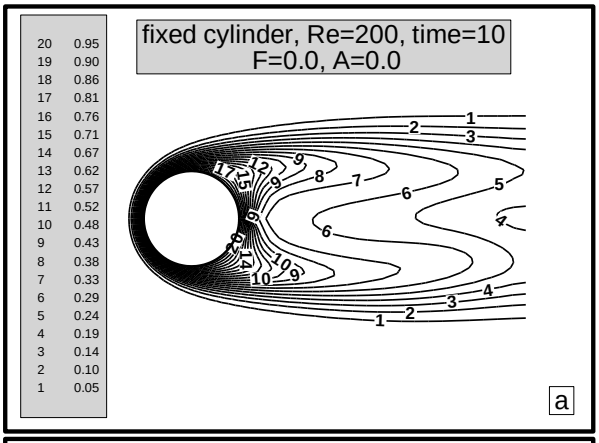
20 0.95
19 0.90
18 0.86
17 0.81
16 0.76
15 0.71
14 0.67
13 0.62
12 0.57
11 0.52
10 0.48
9 0.43
8 0.38
7 0.33
6 0.29
5 0.24
4 0.19
3 0.14
2 0.10
1 0.05
fixed cylinder, Re=200, time=10
F=0.0, A=0.0
a

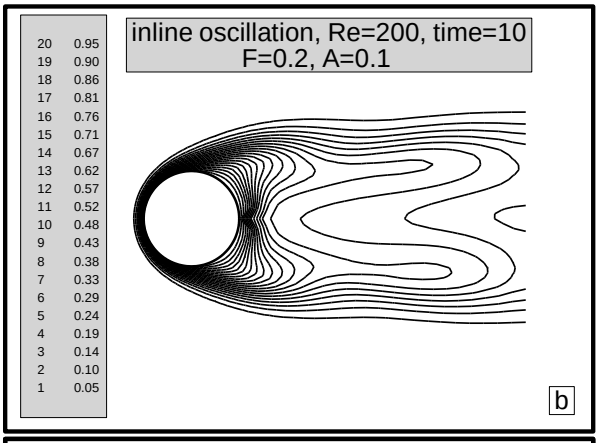
20 0.95
19 0.90
18 0.86
17 0.81
16 0.76
15 0.71
14 0.67
13 0.62
12 0.57
11 0.52
10 0.48
9 0.43
8 0.38
7 0.33
6 0.29
5 0.24
4 0.19
3 0.14
2 0.10
1 0.05
inline oscillation, Re=200, time=10
F=0.2, A=0.1
b

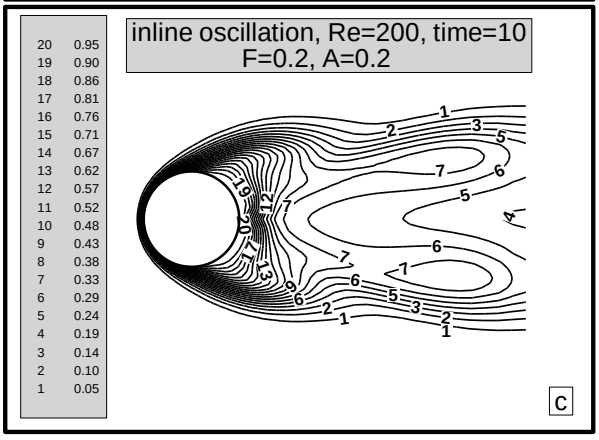
20 0.95
19 0.90
18 0.86
17 0.81
16 0.76
15 0.71
14 0.67
13 0.62
12 0.57
11 0.52
10 0.48
9 0.43
8 0.38
7 0.33
6 0.29
5 0.24
4 0.19
3 0.14
2 0.10
1 0.05
inline oscillation, Re=200, time=10
F=0.2, A=0.2
c

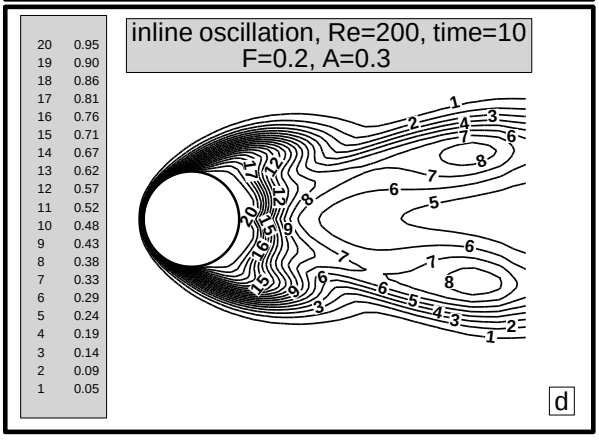
20 0.95
19 0.90
18 0.86
17 0.81
16 0.76
15 0.71
14 0.67
13 0.62
12 0.57
11 0.52
10 0.48
9 0.43
8 0.38
7 0.33
6 0.29
5 0.24
4 0.19
3 0.14
2 0.09
1 0.05
inline oscillation, Re=200, time=10
F=0.2, A=0.3
d

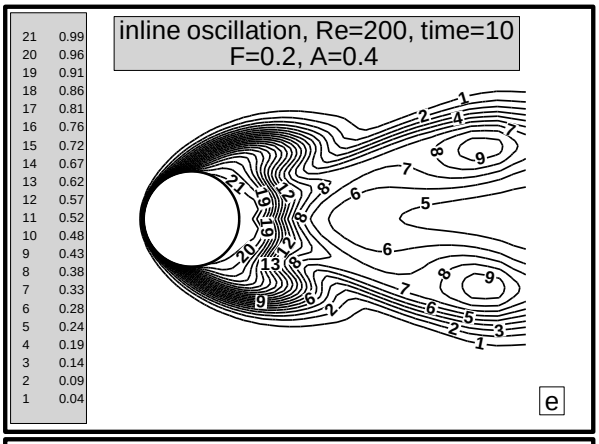
21 0.99
20 0.96
19 0.91
18 0.86
17 0.81
16 0.76
15 0.72
14 0.67
13 0.62
12 0.57
11 0.52
10 0.48
9 0.43
8 0.38
7 0.33
6 0.28
5 0.24
4 0.19
3 0.14
2 0.09
1 0.04
inline oscillation, Re=200, time=10
F=0.2, A=0.4
e

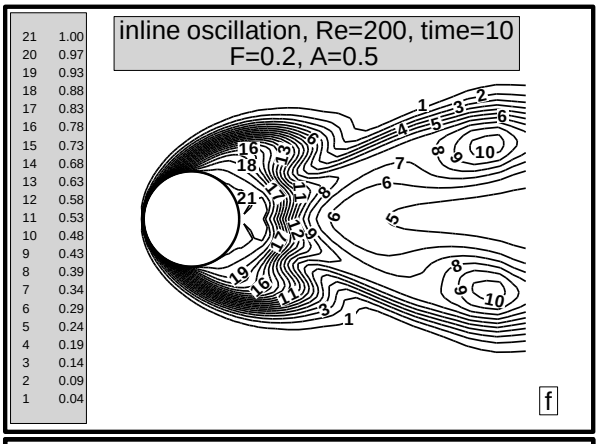
21 1.00
20 0.97
19 0.93
18 0.88
17 0.83
16 0.78
15 0.73
14 0.68
13 0.63
12 0.58
11 0.53
10 0.48
9 0.43
8 0.39
7 0.34
6 0.29
5 0.24
4 0.19
3 0.14
2 0.09
1 0.04
inline oscillation, Re=200, time=10
F=0.2, A=0.5
f

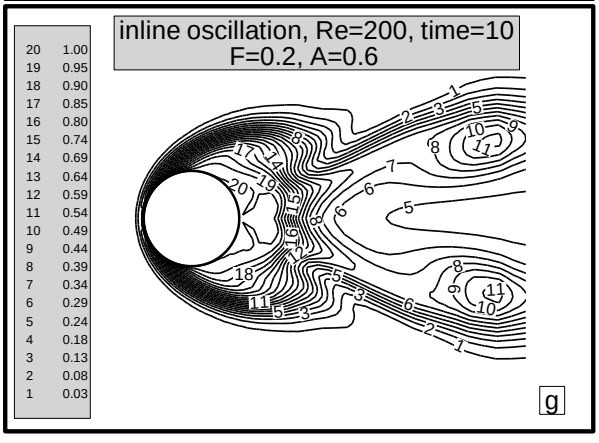
20 1.00
19 0.95
18 0.90
17 0.85
16 0.80
15 0.74
14 0.69
13 0.64
12 0.59
11 0.54
10 0.49
9 0.44
8 0.39
7 0.34
6 0.29
5 0.24
4 0.18
3 0.13
2 0.08
1 0.03
inline oscillation, Re=200, time=10
F=0.2, A=0.6
g

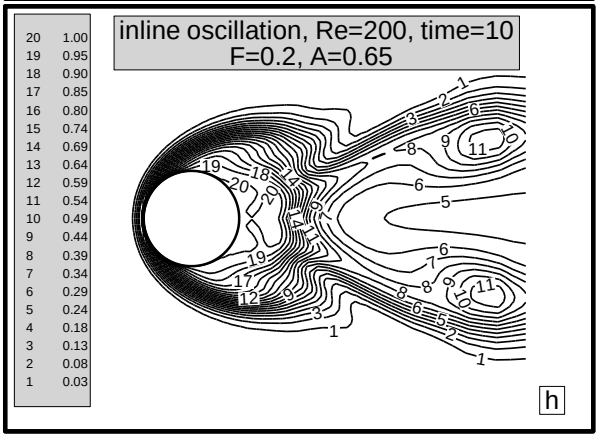
20 1.00
19 0.95
18 0.90
17 0.85
16 0.80
15 0.74
14 0.69
13 0.64
12 0.59
11 0.54
10 0.49
9 0.44
8 0.39
7 0.34
6 0.29
5 0.24
4 0.18
3 0.13
2 0.08
1 0.03
inline oscillation, Re=200, time=10
F=0.2, A=0.65
h

Fig.(٥-٢٧)Isothermal contours for inline oscillating cylinder at Re=٢٠٠ and F=٠.٢ with multi-amplitude.

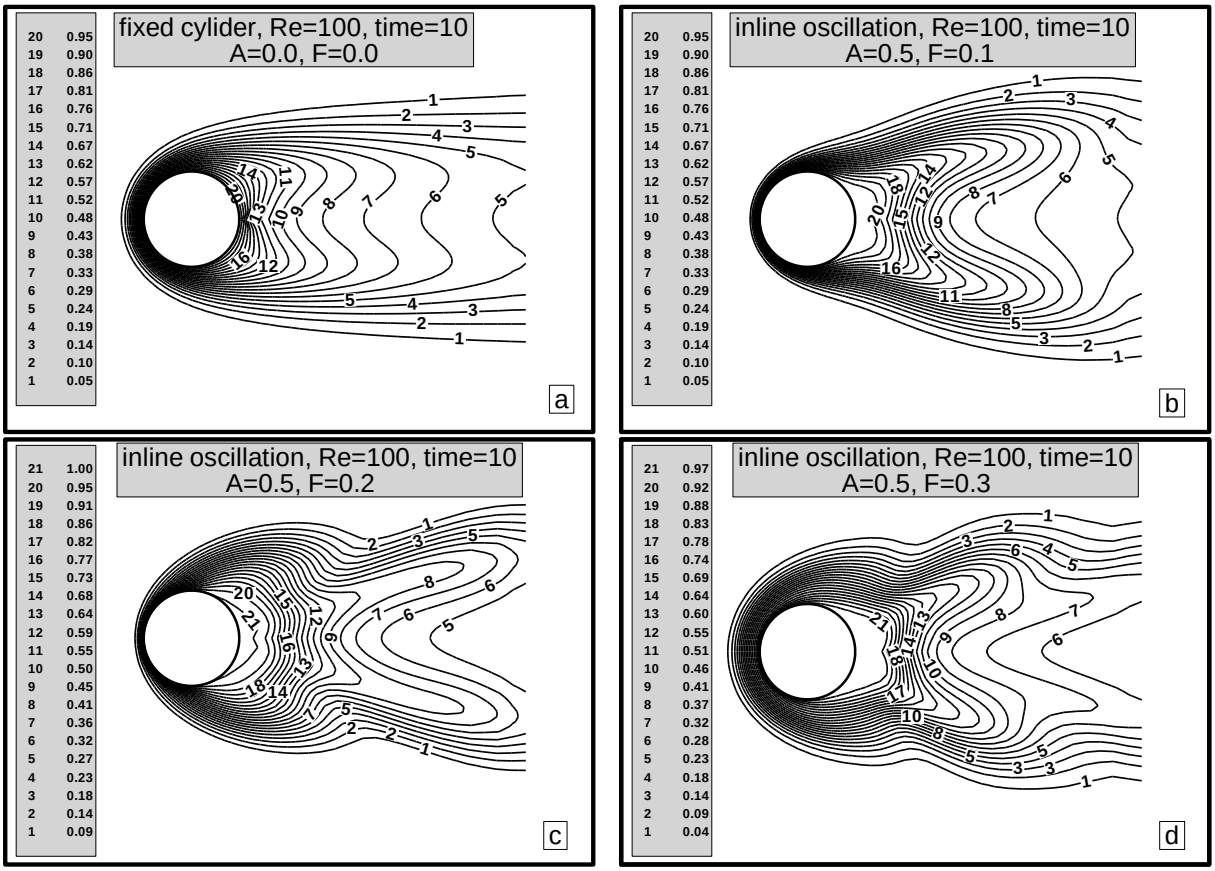

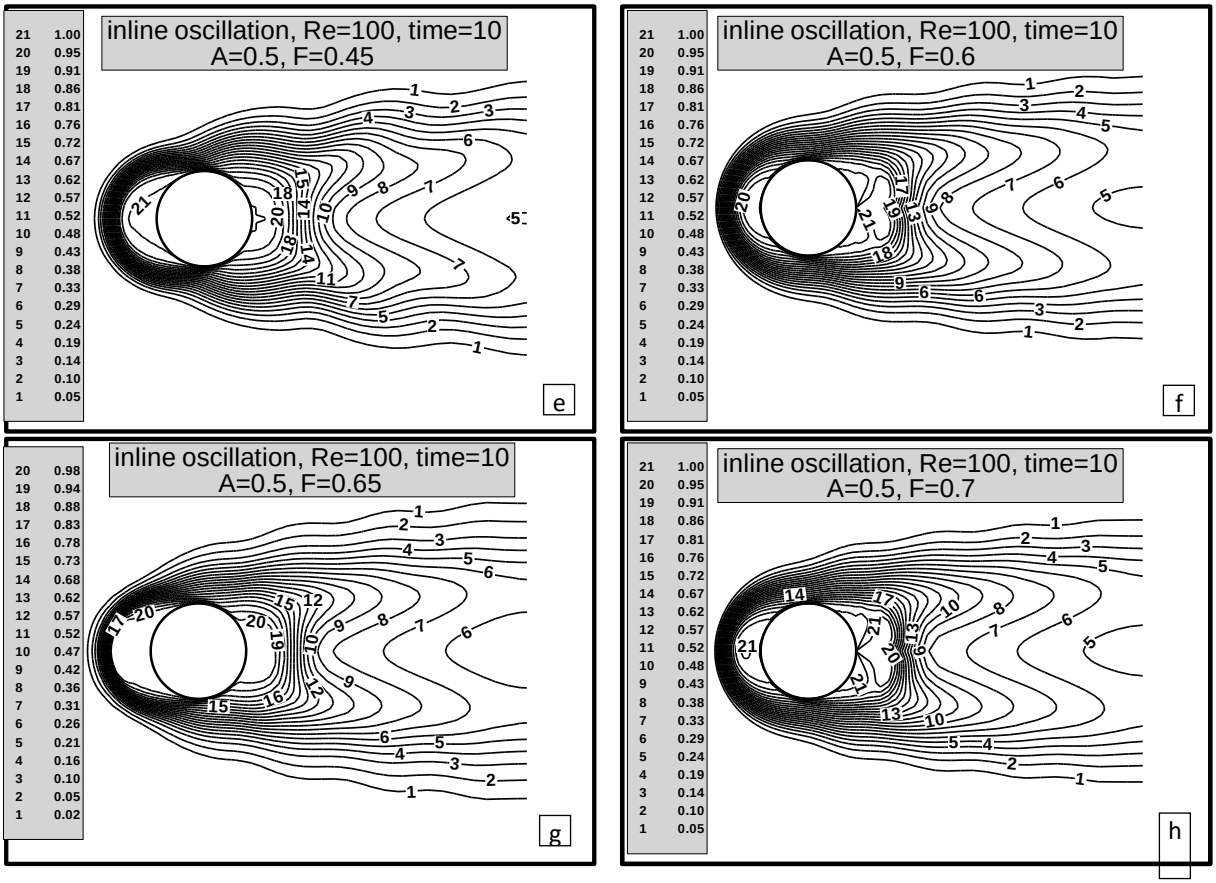

Fig.(٥-٢٨)Isothermal contours for inline oscillating cylinder at Re=١٠٠ and A=٠.٥ with multi-frequency.

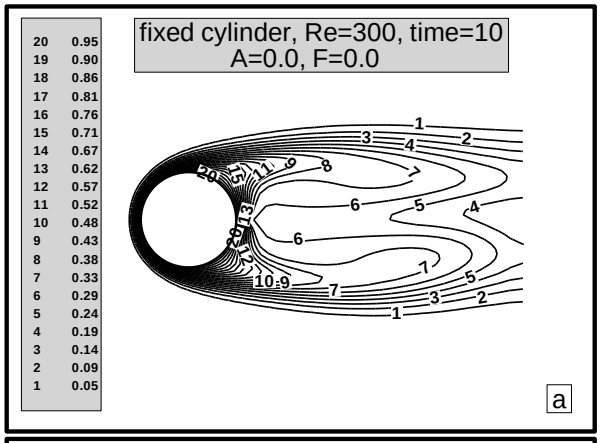
20 0.95
19 0.90
18 0.86
17 0.81
16 0.76
15 0.71
14 0.67
13 0.62
12 0.57
11 0.52
10 0.48
9 0.43
8 0.38
7 0.33
6 0.29
5 0.24
4 0.19
3 0.14
2 0.09
1 0.05
fixed cylinder, Re=300, time=10
A=0.0, F=0.0
a

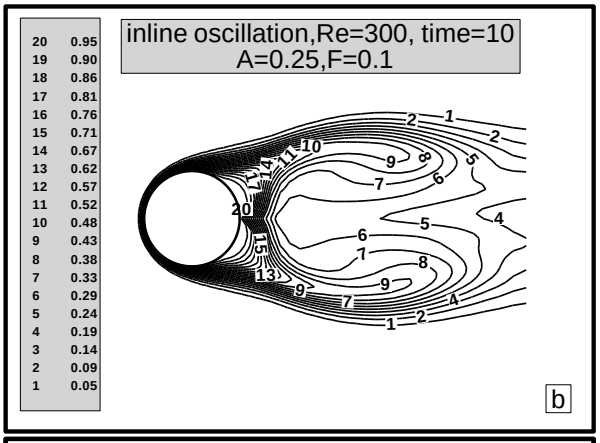
20 0.95
19 0.90
18 0.86
17 0.81
16 0.76
15 0.71
14 0.67
13 0.62
12 0.57
11 0.52
10 0.48
9 0.43
8 0.38
7 0.33
6 0.29
5 0.24
4 0.19
3 0.14
2 0.09
1 0.05
inline oscillation,Re=300, time=10
A=0.25,F=0.1
b

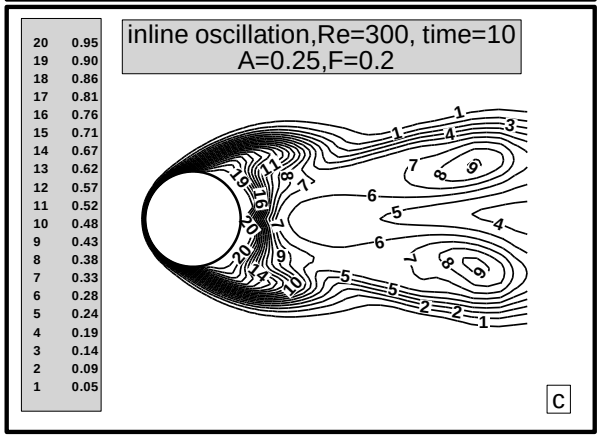
20 0.95
19 0.90
18 0.86
17 0.81
16 0.76
15 0.71
14 0.67
13 0.62
12 0.57
11 0.52
10 0.48
9 0.43
8 0.38
7 0.33
6 0.28
5 0.24
4 0.19
3 0.14
2 0.09
1 0.05
inline oscillation,Re=300, time=10
A=0.25,F=0.2
c

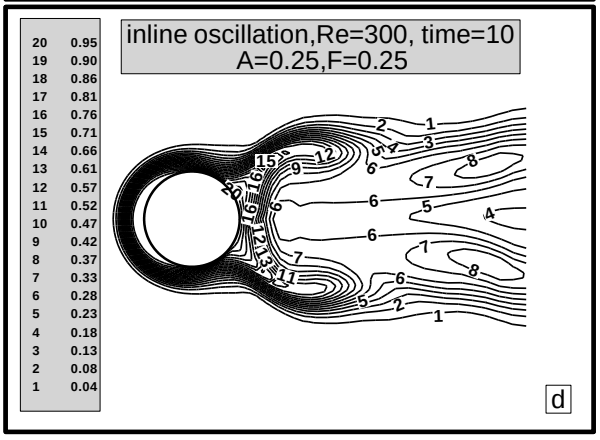
20 0.95
19 0.90
18 0.86
17 0.81
16 0.76
15 0.71
14 0.66
13 0.61
12 0.57
11 0.52
10 0.47
9 0.42
8 0.37
7 0.33
6 0.28
5 0.23
4 0.18
3 0.13
2 0.08
1 0.04
inline oscillation,Re=300, time=10
A=0.25,F=0.25
d

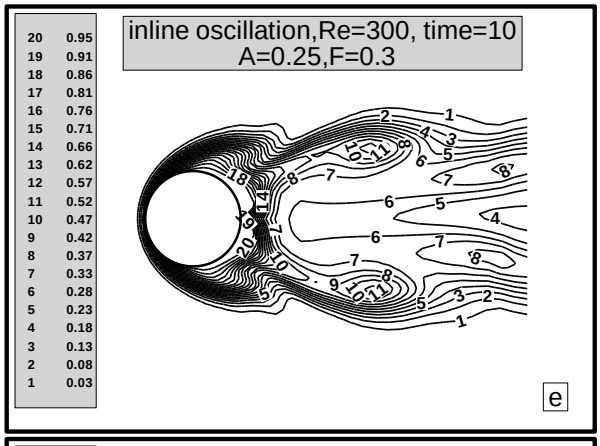
20 0.95
19 0.91
18 0.86
17 0.81
16 0.76
15 0.71
14 0.66
13 0.62
12 0.57
11 0.52
10 0.47
9 0.42
8 0.37
7 0.33
6 0.28
5 0.23
4 0.18
3 0.13
2 0.08
1 0.03
inline oscillation,Re=300, time=10
A=0.25,F=0.3
e

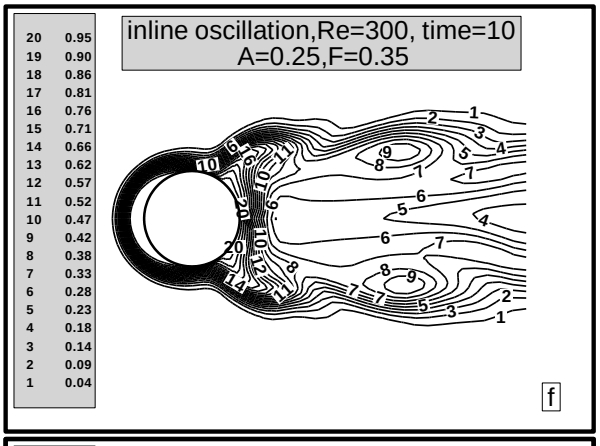
20 0.95
19 0.90
18 0.86
17 0.81
16 0.76
15 0.71
14 0.66
13 0.62
12 0.57
11 0.52
10 0.47
9 0.42
8 0.38
7 0.33
6 0.28
5 0.23
4 0.18
3 0.14
2 0.09
1 0.04
inline oscillation,Re=300, time=10
A=0.25,F=0.35
f

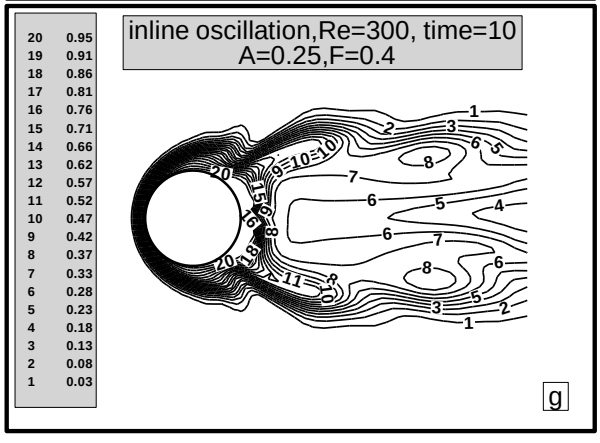
20 0.95
19 0.91
18 0.86
17 0.81
16 0.76
15 0.71
14 0.66
13 0.62
12 0.57
11 0.52
10 0.47
9 0.42
8 0.37
7 0.33
6 0.28
5 0.23
4 0.18
3 0.13
2 0.08
1 0.03
inline oscillation,Re=300, time=10
A=0.25,F=0.4
g

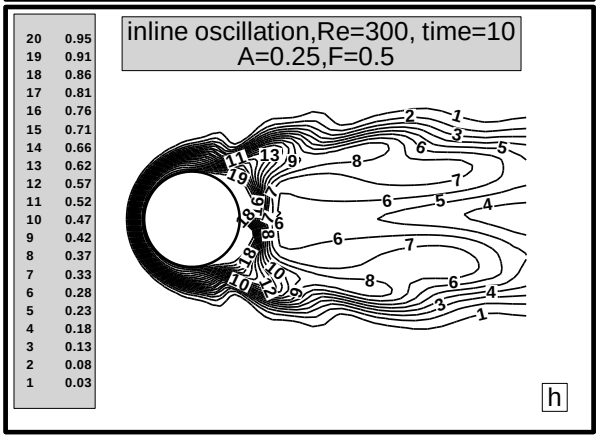
20 0.95
19 0.91
18 0.86
17 0.81
16 0.76
15 0.71
14 0.66
13 0.62
12 0.57
11 0.52
10 0.47
9 0.42
8 0.37
7 0.33
6 0.28
5 0.23
4 0.18
3 0.13
2 0.08
1 0.03
inline oscillation,Re=300, time=10
A=0.25,F=0.5
h

Fig.(٥-٢٩)Isothermal contours for inline oscillating cylinder at Re=٣٠٠ and A=٠.٢٥ with multi-frequency.

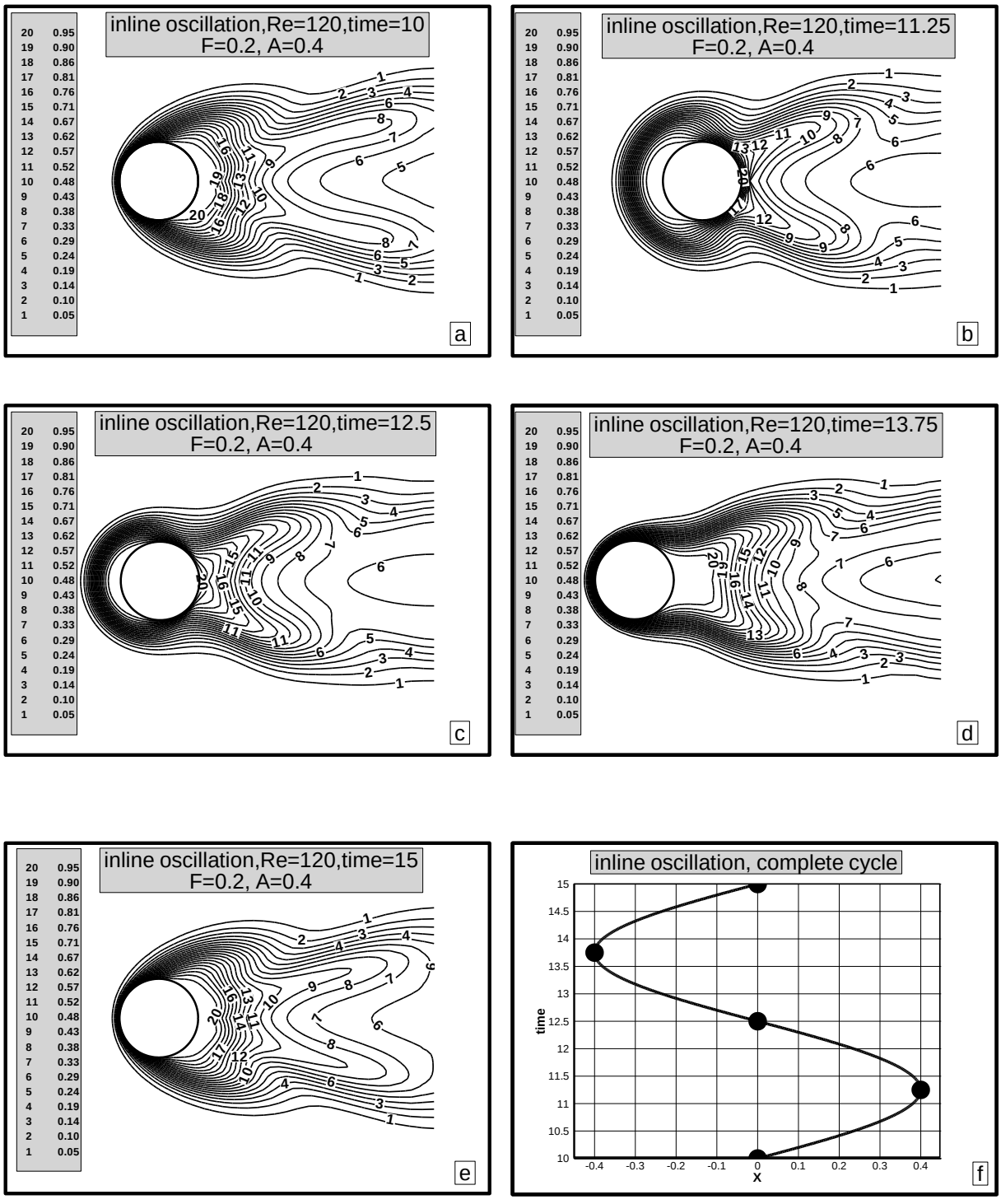

Fig.(٥-٣٠)Isothermal contours for inline oscillating cylinder at Re=٢٠٠,F=٠.٤ and A=٠.٤ for complete cycle

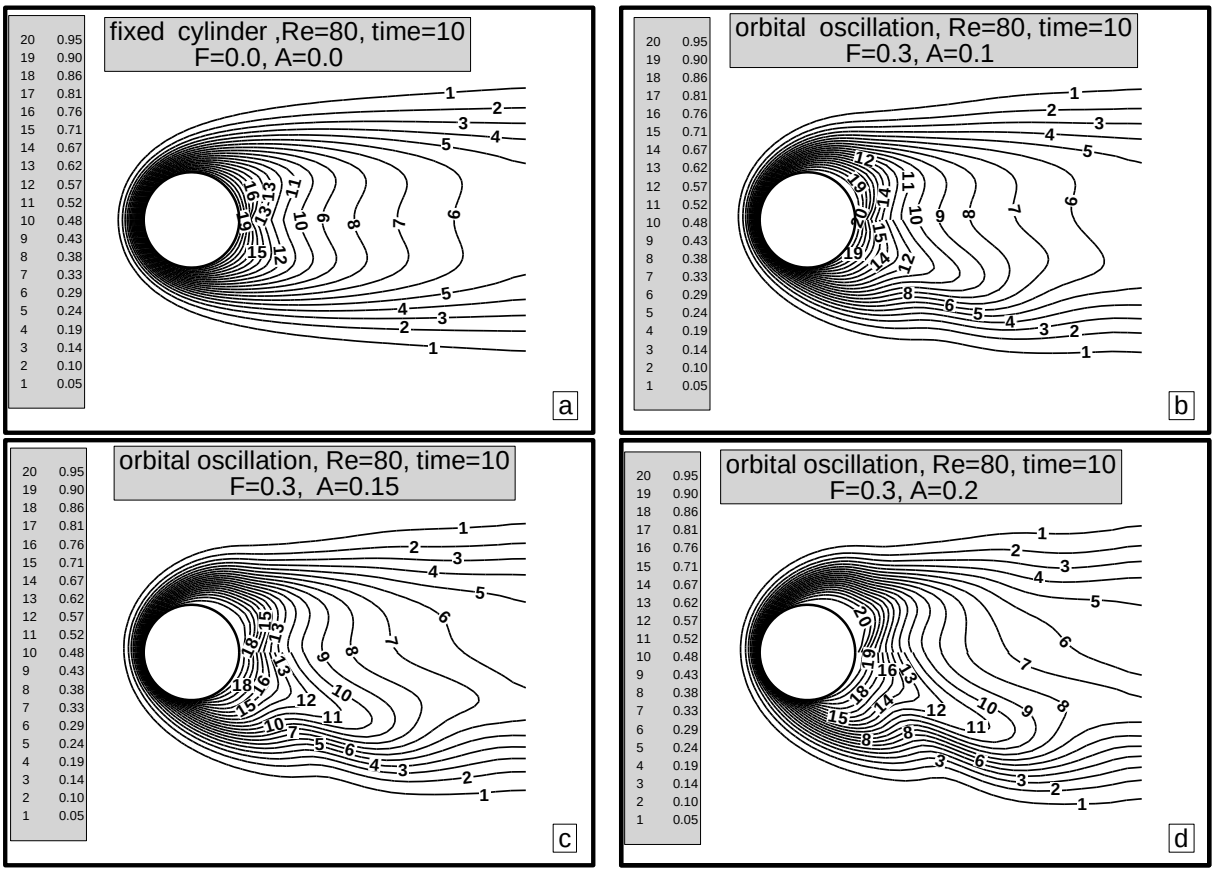

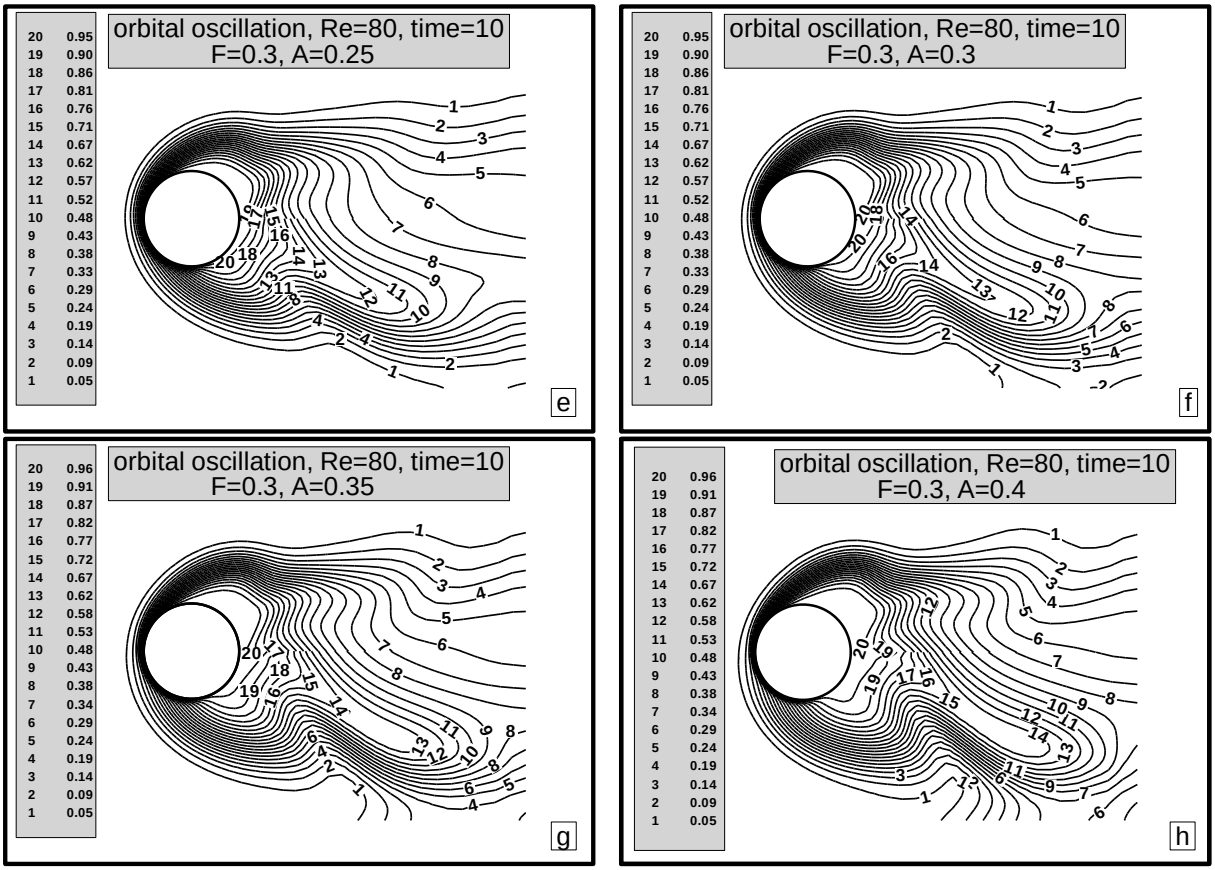

Fig.(٥-٣١)Isothermal contours for orbital oscillating cylinder at Re=٨٠ and F=٠.٣ with multi-amplitude.

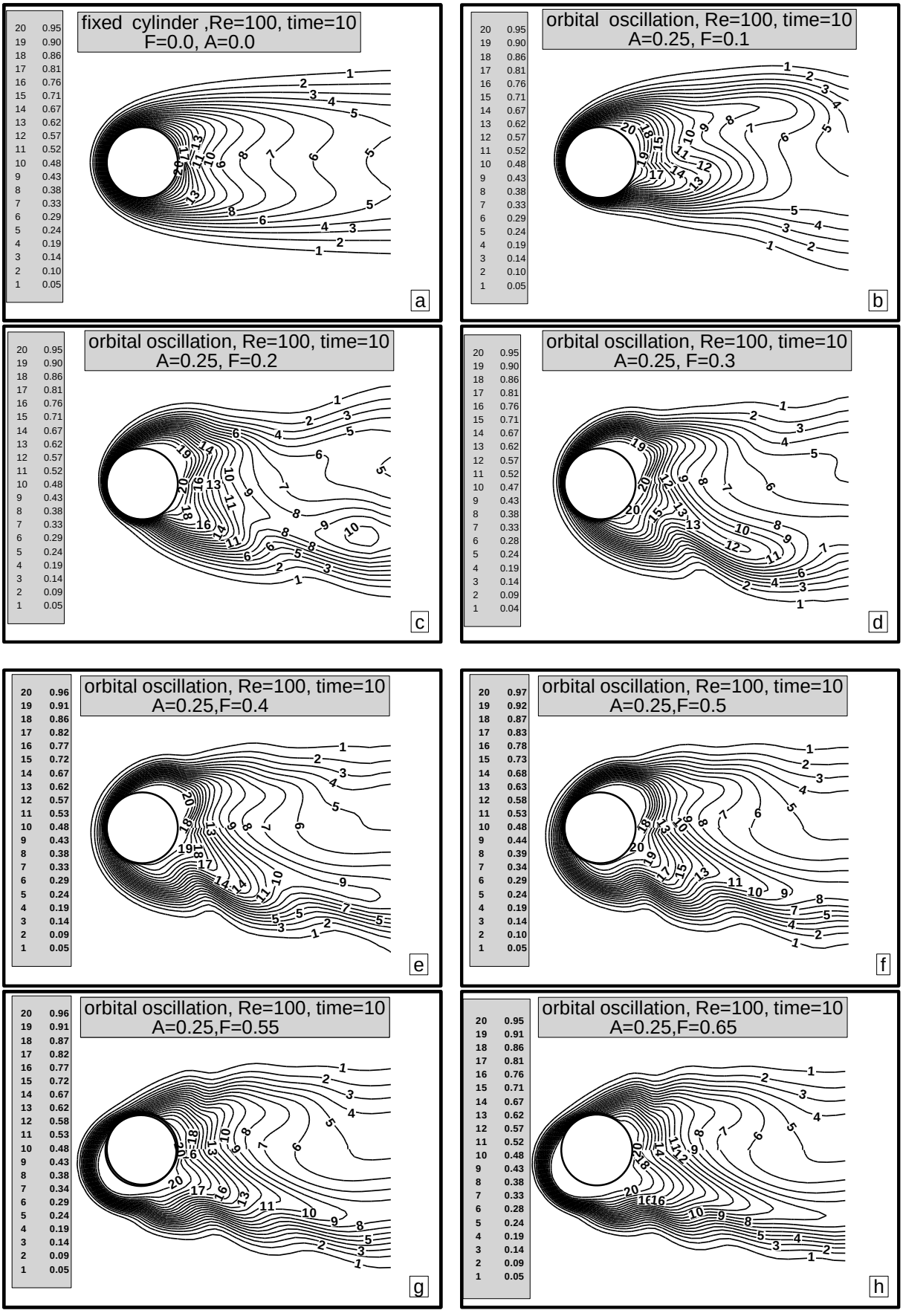

Fig.(٥-٣٢)Isothermal contours for orbital oscillating cylinder at Re=١٠٠ and A=٠.٢٥ with multi-frequency.

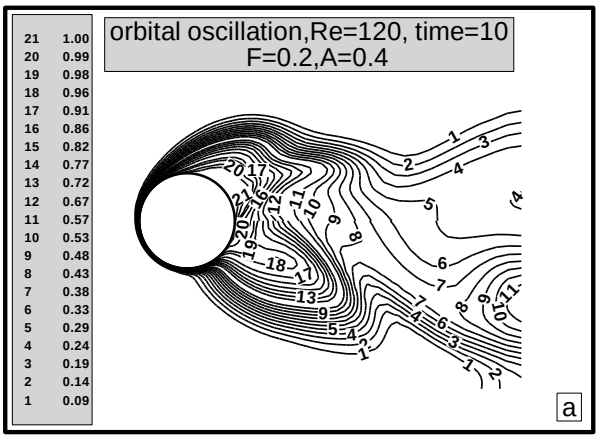
21 1.00
20 0.99
19 0.98
18 0.96
17 0.91
16 0.86
15 0.82
14 0.77
13 0.72
12 0.67
11 0.57
10 0.53
9 0.48
8 0.43
7 0.38
6 0.33
5 0.29
4 0.24
3 0.19
2 0.14
1 0.09
orbital oscillation,Re=120, time=10
F=0.2,A=0.4
a

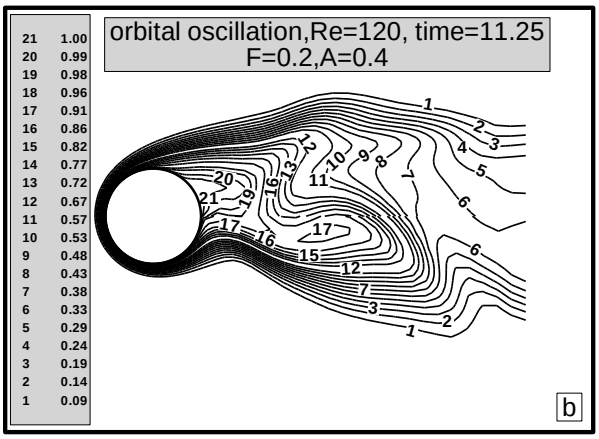
21 1.00
20 0.99
19 0.98
18 0.96
17 0.91
16 0.86
15 0.82
14 0.77
13 0.72
12 0.67
11 0.57
10 0.53
9 0.48
8 0.43
7 0.38
6 0.33
5 0.29
4 0.24
3 0.19
2 0.14
1 0.09
orbital oscillation,Re=120, time=11.25
F=0.2,A=0.4
b

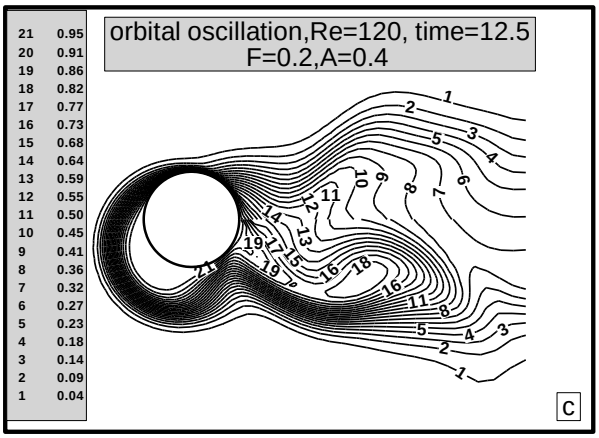
21 0.95
20 0.91
19 0.86
18 0.82
17 0.77
16 0.73
15 0.68
14 0.64
13 0.59
12 0.55
11 0.50
10 0.45
9 0.41
8 0.36
7 0.32
6 0.27
5 0.23
4 0.18
3 0.14
2 0.09
1 0.04
orbital oscillation,Re=120, time=12.5
F=0.2,A=0.4
c

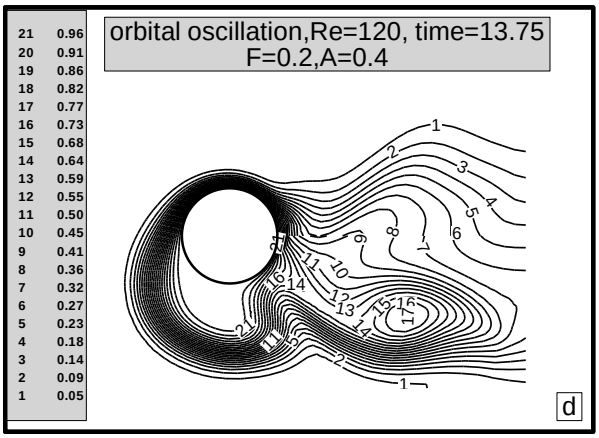
21 0.96
20 0.91
19 0.86
18 0.82
17 0.77
16 0.73
15 0.68
14 0.64
13 0.59
12 0.55
11 0.50
10 0.45
9 0.41
8 0.36
7 0.32
6 0.27
5 0.23
4 0.18
3 0.14
2 0.09
1 0.05
orbital oscillation,Re=120, time=13.75
F=0.2,A=0.4
d

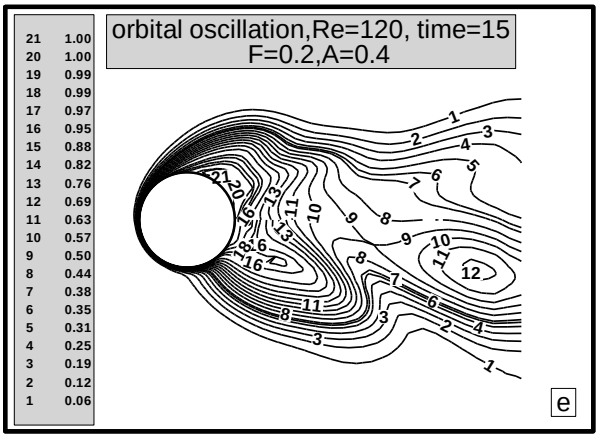
21 1.00
20 1.00
19 0.99
18 0.99
17 0.97
16 0.95
15 0.88
14 0.82
13 0.76
12 0.69
11 0.63
10 0.57
9 0.50
8 0.44
7 0.38
6 0.35
5 0.31
4 0.25
3 0.19
2 0.12
1 0.06
orbital oscillation,Re=120, time=15
F=0.2,A=0.4
e

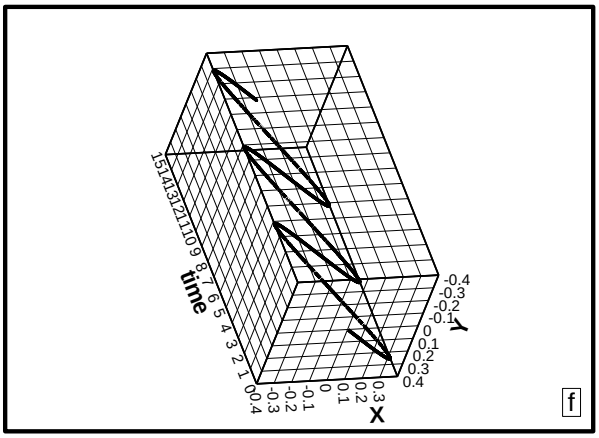
time
X
Y
f

Fig.(٥-٣٣)Isothermal contours for orbital oscillating cylinder at Re=١٢٠,F=٠.٢ and A=٠.٤ for complete cycle

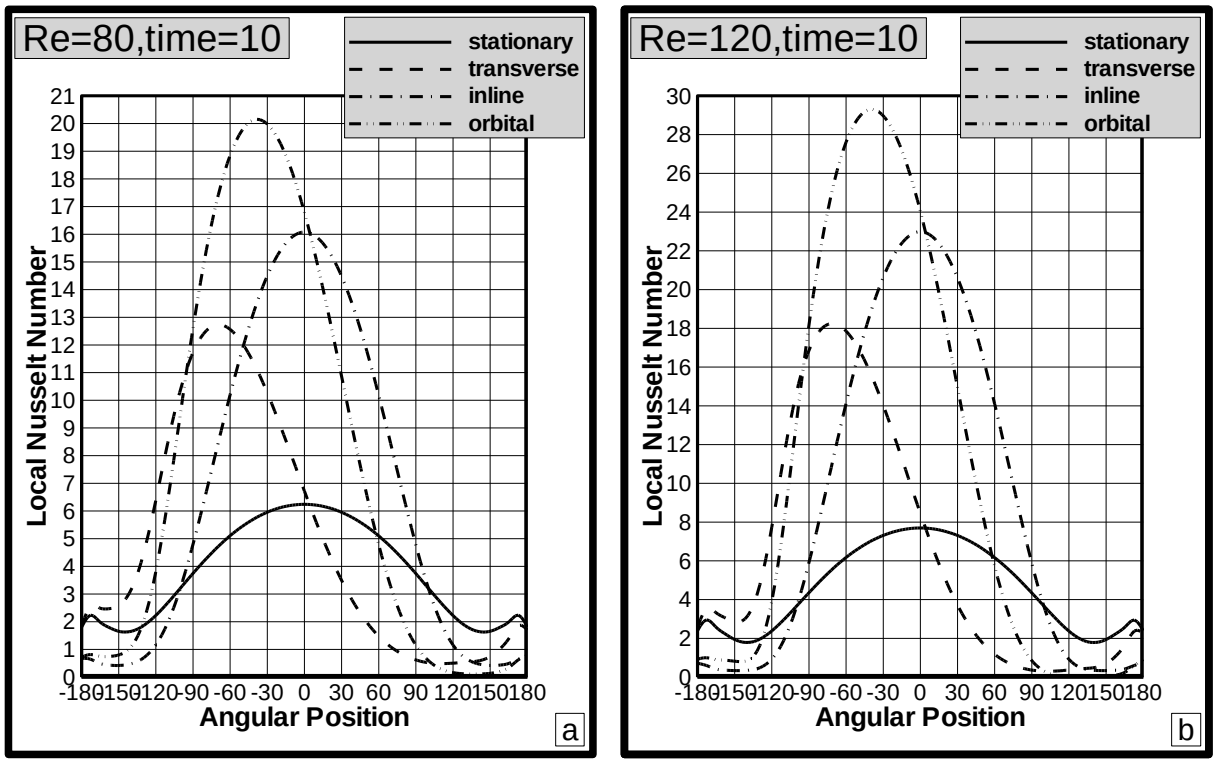

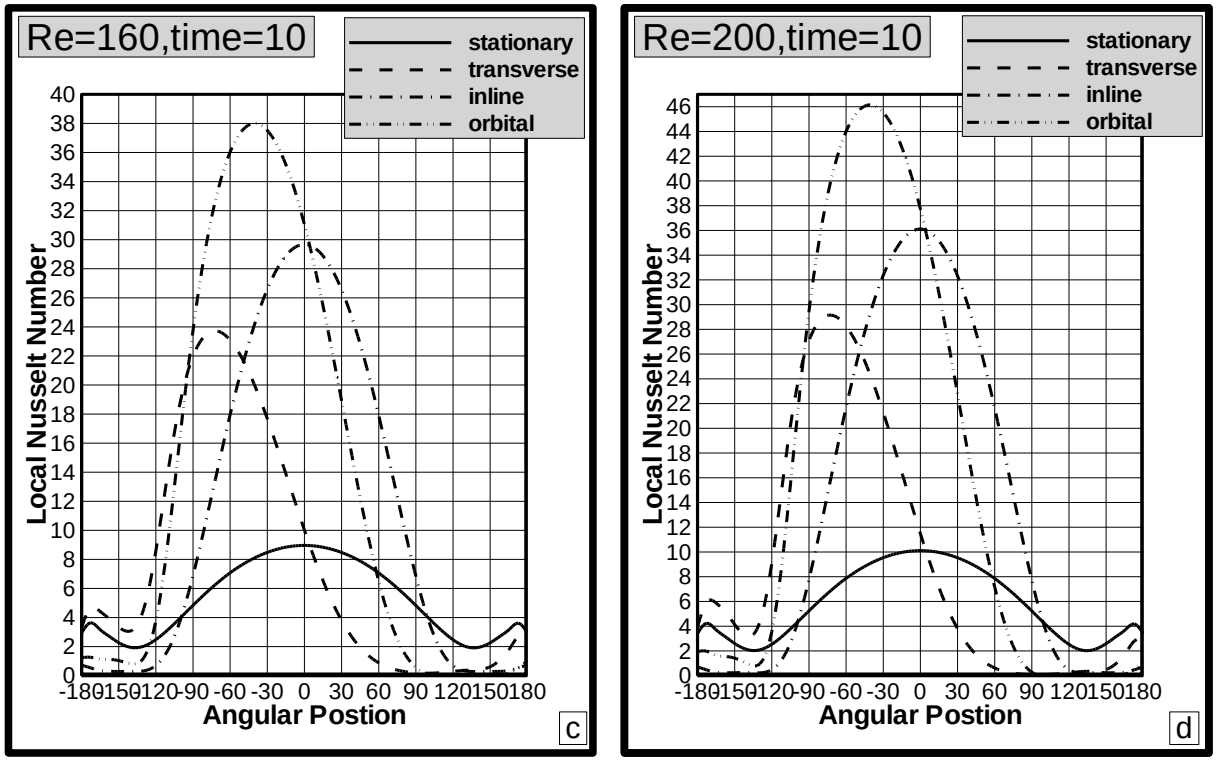

Fig.(٥-٣٤)Local Nusselt number distribution on the cylinder surface for different Reynolds number and different case of cylinder oscillation with F=٠.٢ and A=٠.٢.

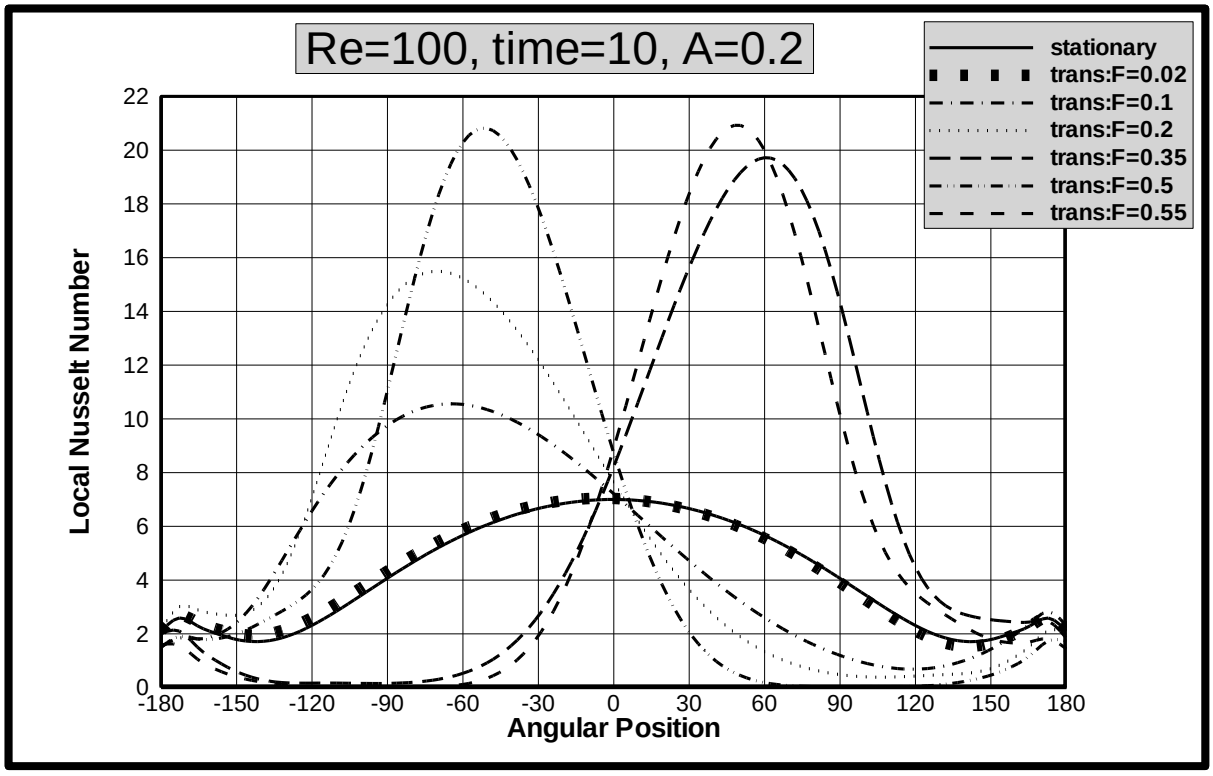

Fig.(٥-٣٥)Local Nusselt number distribution on the cylinder surface for Reynolds number=١٠٠ with constant amplitude(A=٠.٢) and different frequency (transverse).

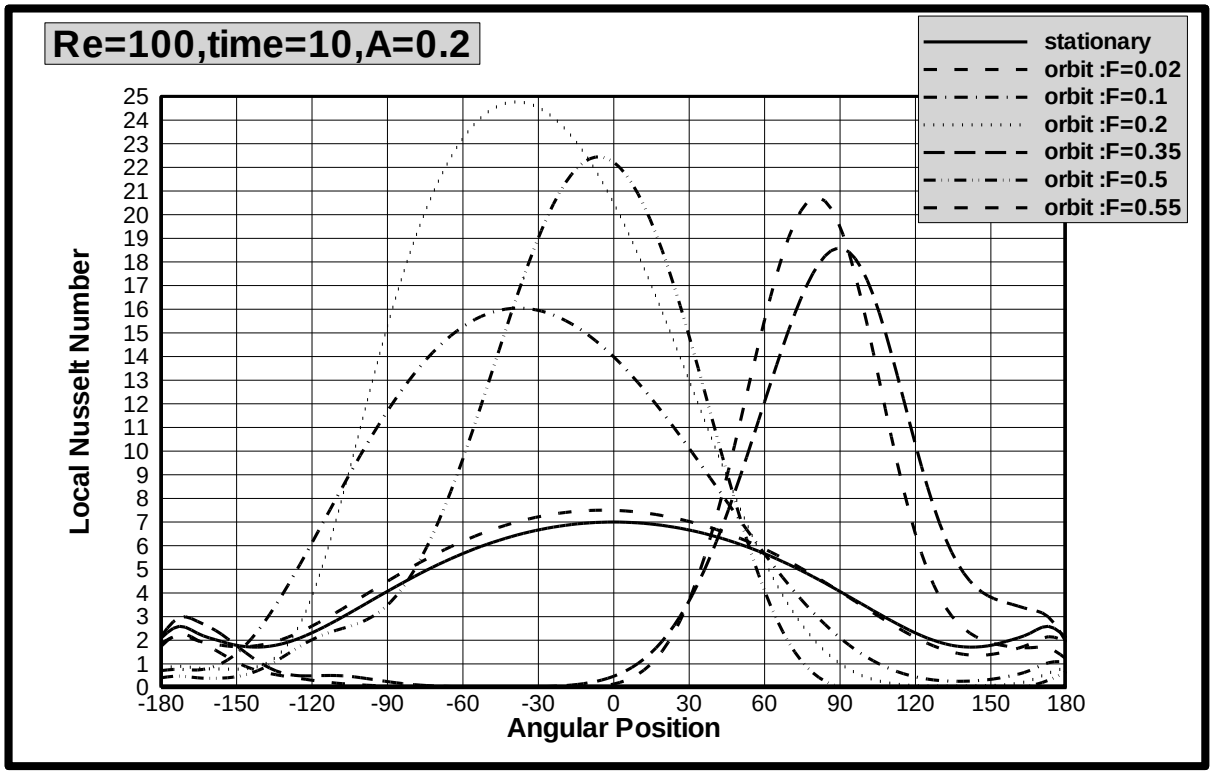

Fig.(٥-٣٦)Local Nusselt number distribution on the cylinder surface for Reynolds number=١٠٠ with constant amplitude(A=٠.٢) and different frequency (orbital).

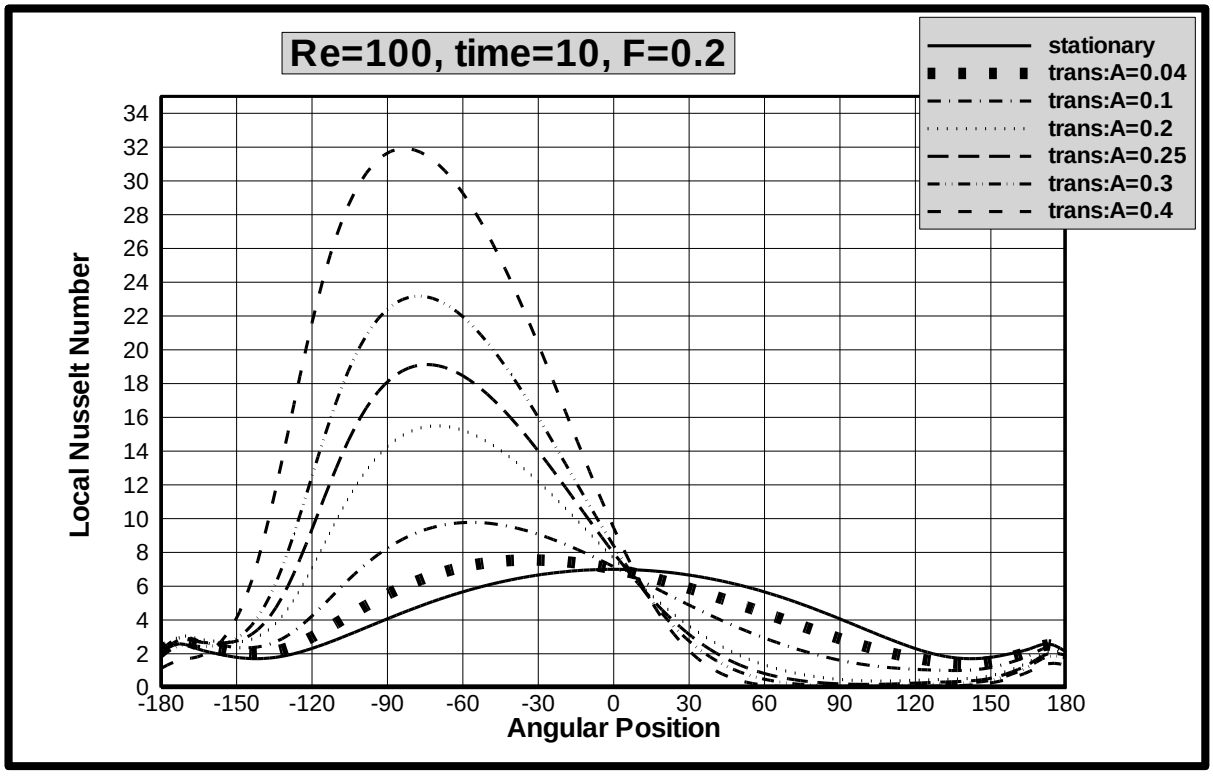

Fig.(٥-٣٧)Local Nusselt number distribution on the cylinder surface for Reynolds number=١٠٠ with constant frequency(F=٠.٢) and different amplitude (transverse).

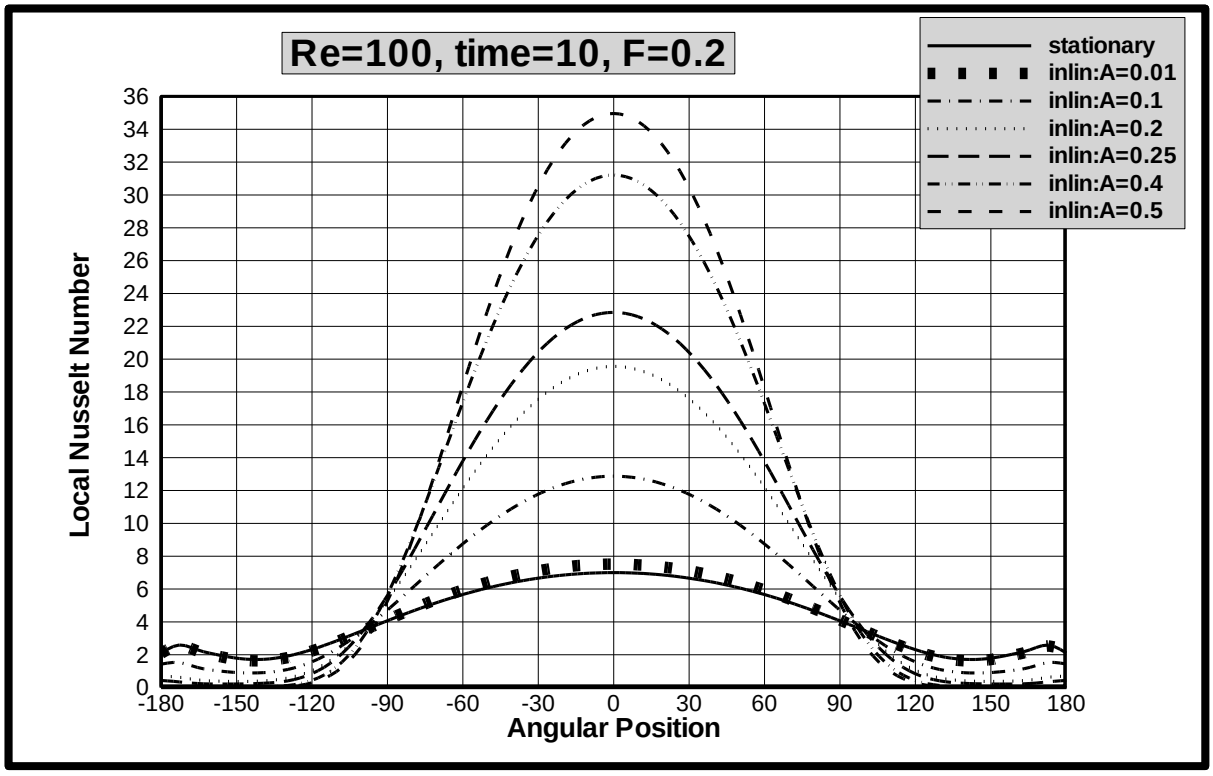

Fig.(٥-٣٨)Local Nusselt number distribution on the cylinder surface for Reynolds number=١٠٠ with constant frequency(F=٠.٢) and different amplitude (inline).

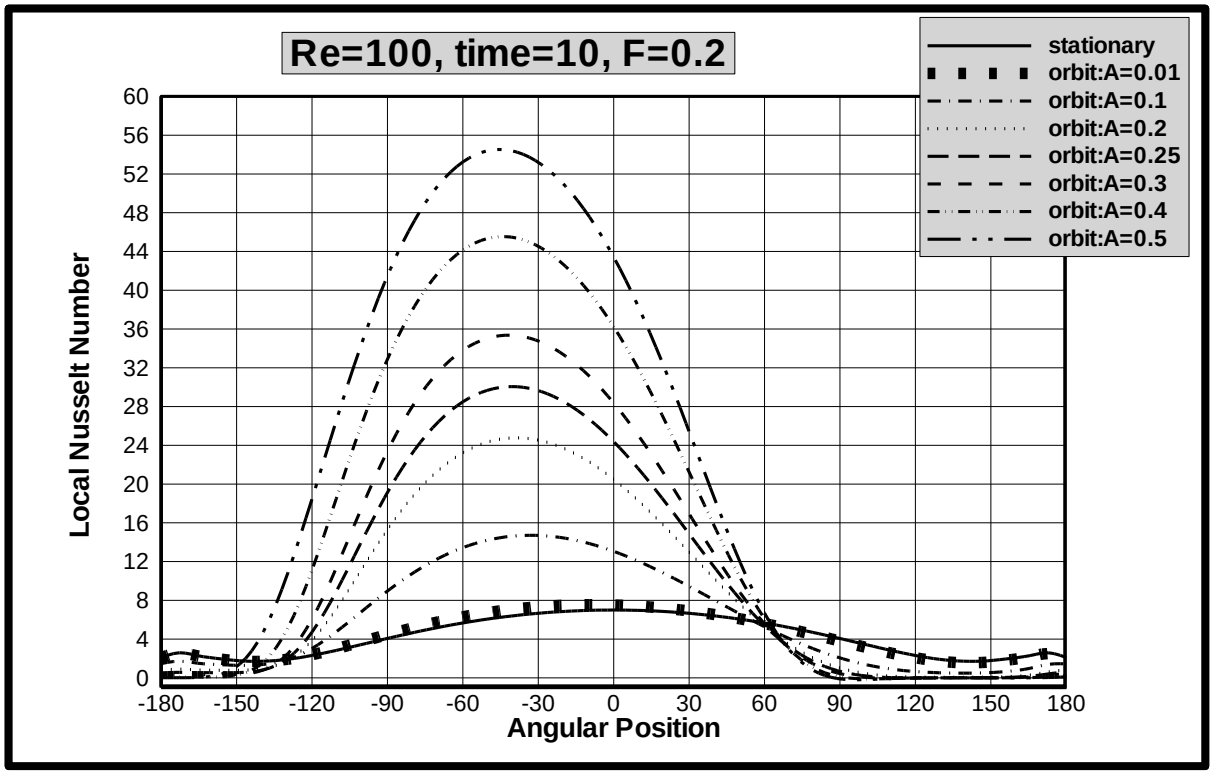

Fig.(٥-٣٩)Local Nusselt number distribution on the cylinder surface for Reynolds number=١٠٠ with constant frequency(F=٠.٢) and different amplitude (orbital).

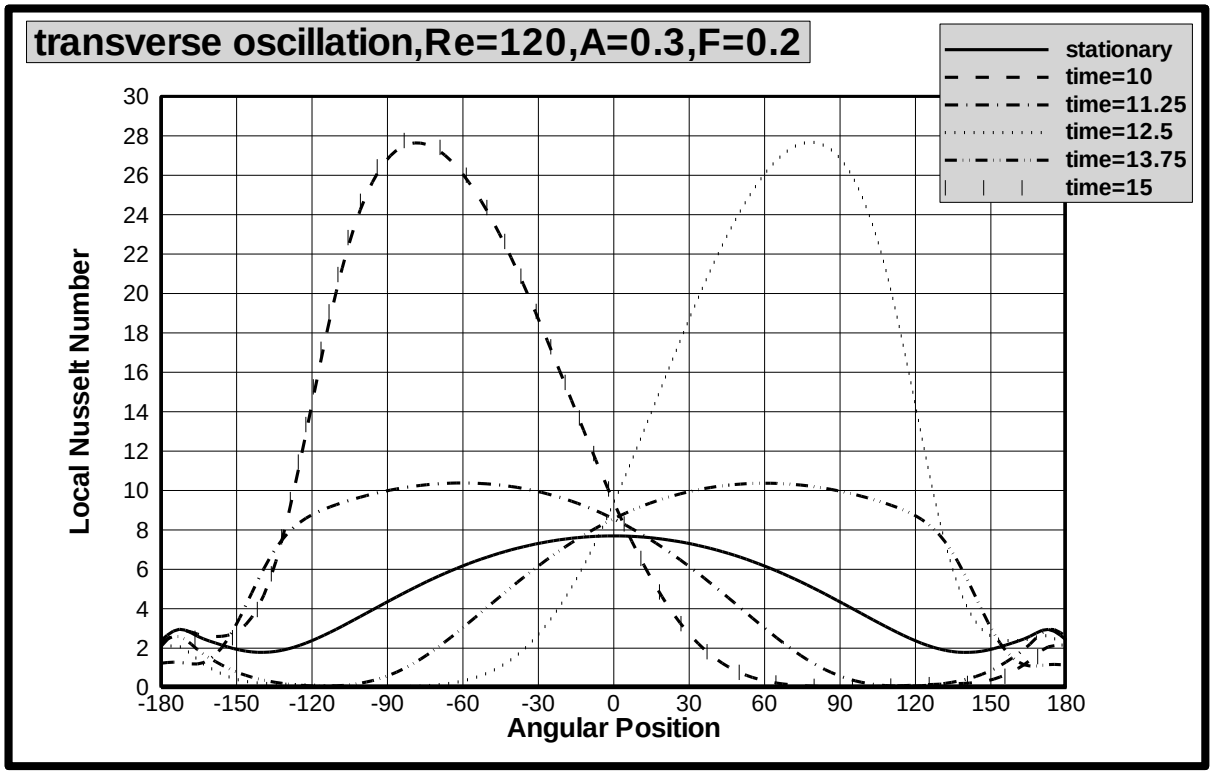

Fig.(٥-٤٠)Local Nusselt number distribution on the cylinder surface for Reynolds number=١٢٠ with constant frequency and amplitude(F=٠.٢,A=٠.٣)for complete cycle(transverse)

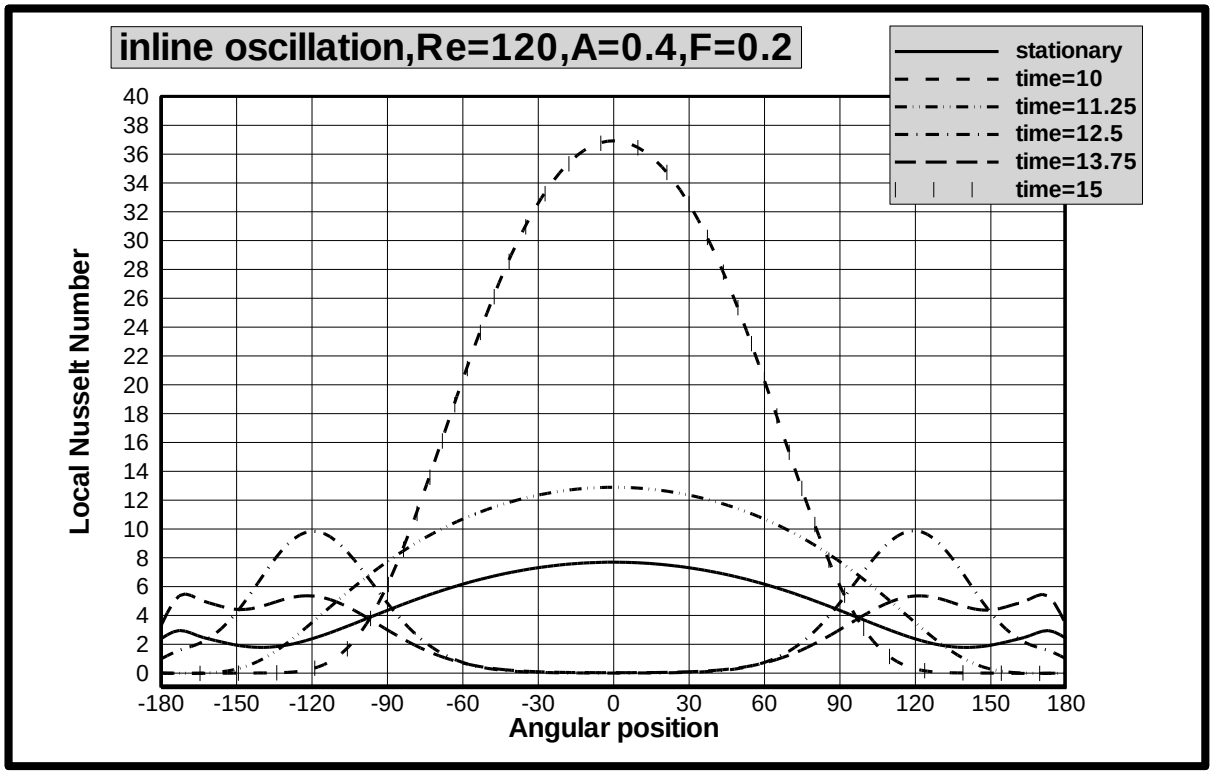

Fig.(٥-٤١)Local Nusselt number distribution on the cylinder surface for Reynolds number=١٢٠ with constant frequency and amplitude(F=٠.٢,A=٠.٤)for complete cycle(inline)

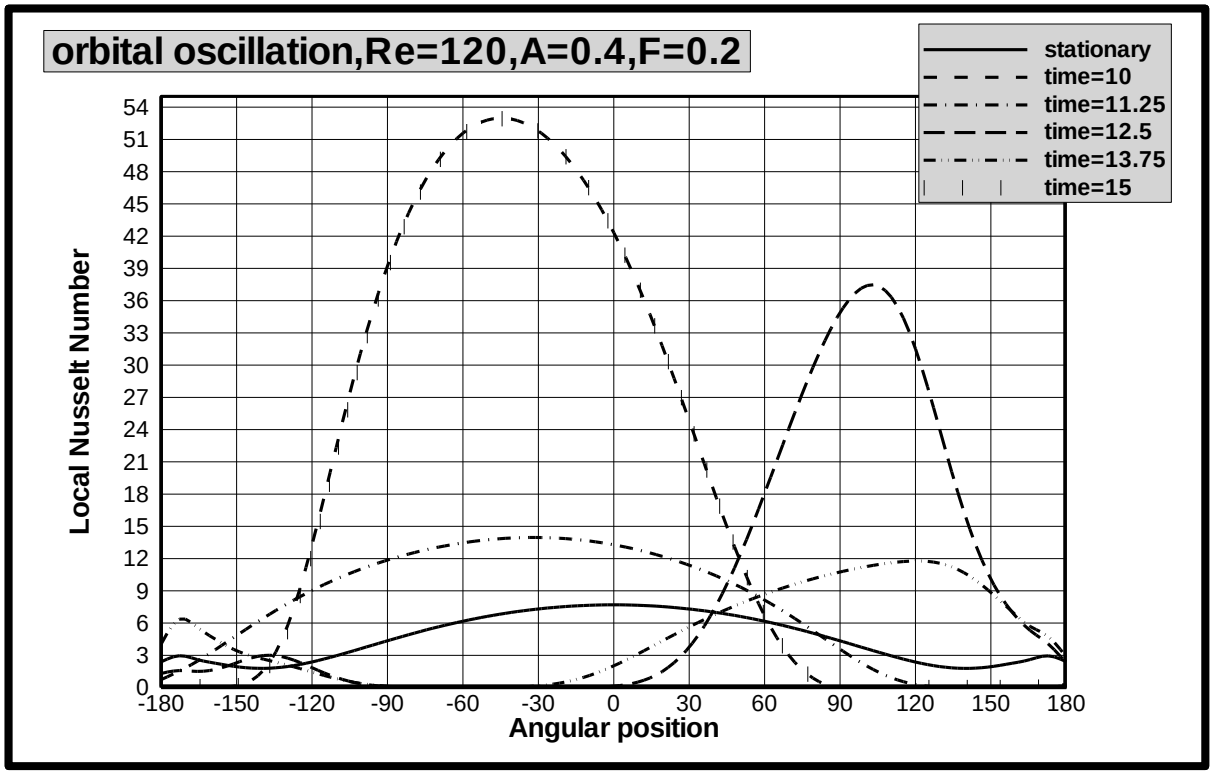

Fig.(٥-٤٢)Local Nusselt number distribution on the cylinder surface for Reynolds number=١٢٠ with constant frequency and amplitude(F=٠.٢,A=٠.٤)for complete cycle(orbital)

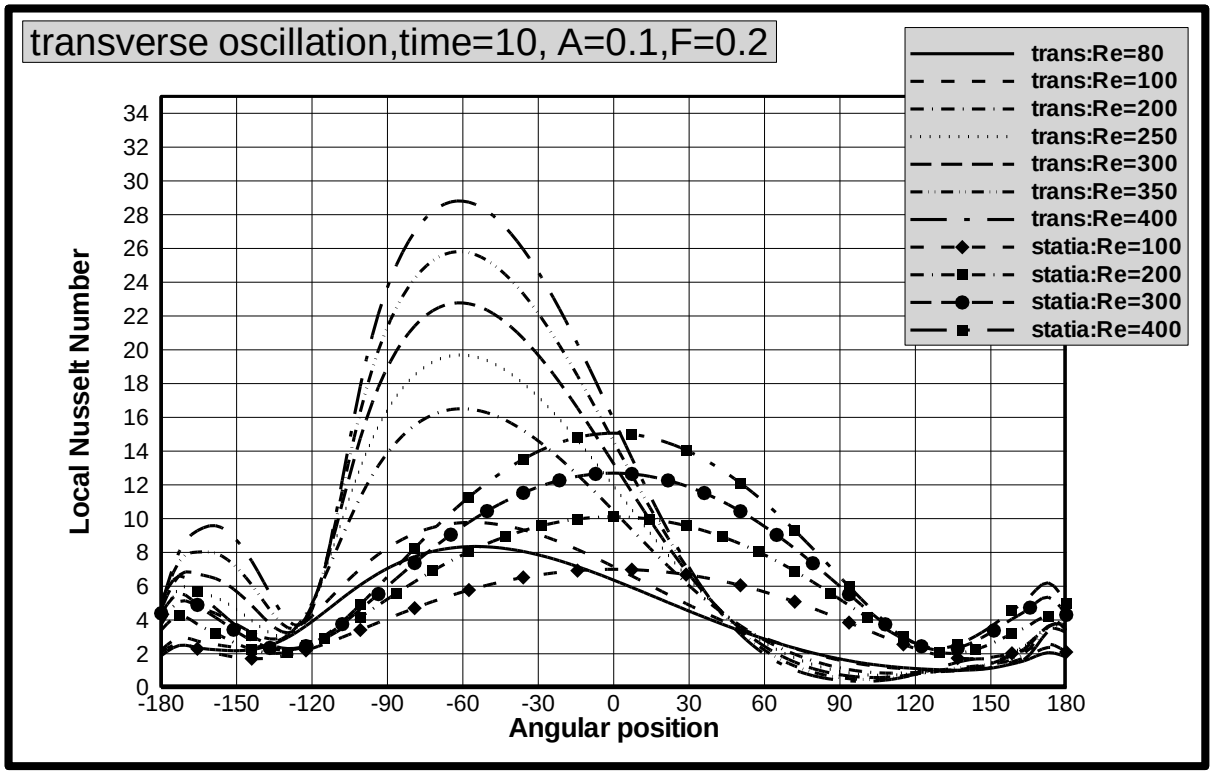

Fig.(٥-٤٣)Local Nusselt number profiles on the stationary and oscillating cylinder surface for multi-Reynolds with constant frequency and amplitude(F=٠.٢,A=٠.١)(transverse)

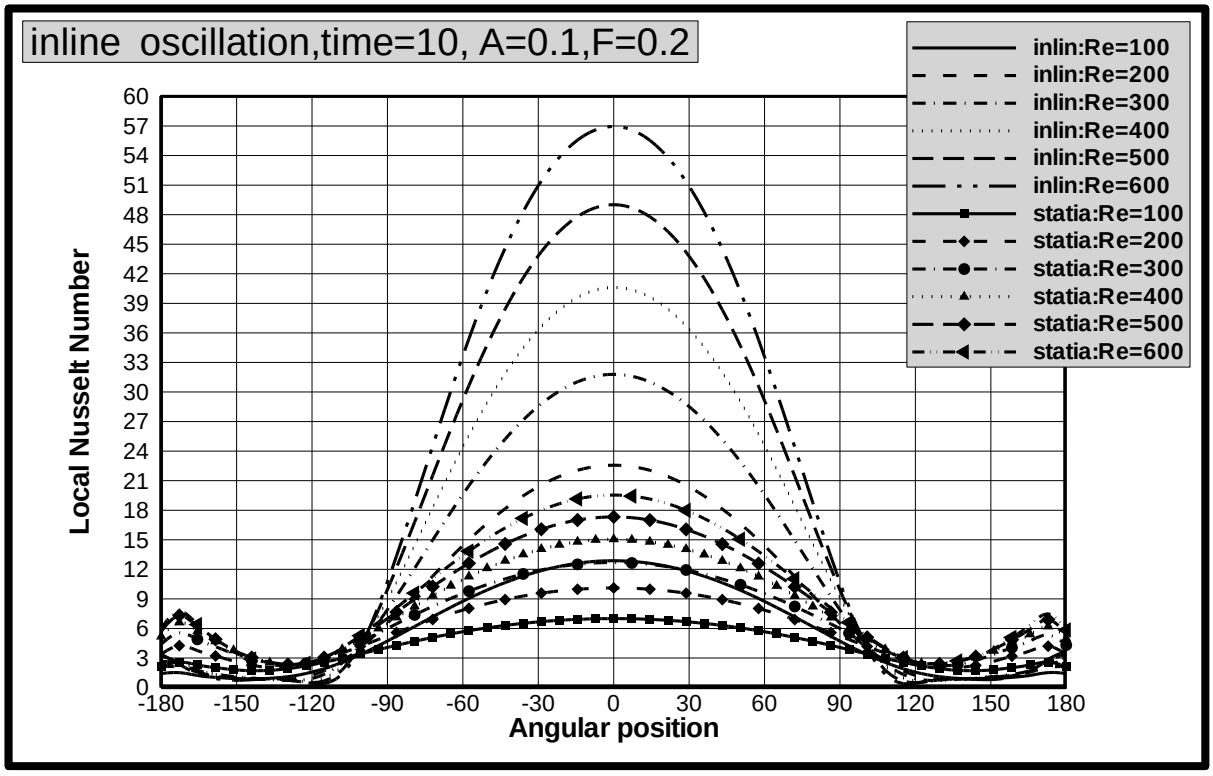

Fig.(٥-٤٤)Local Nusselt number profiles on the stationary and oscillating cylinder surface for multi-Reynolds with constant frequency and amplitude(F=٠.٢,A=٠.١)(inline)

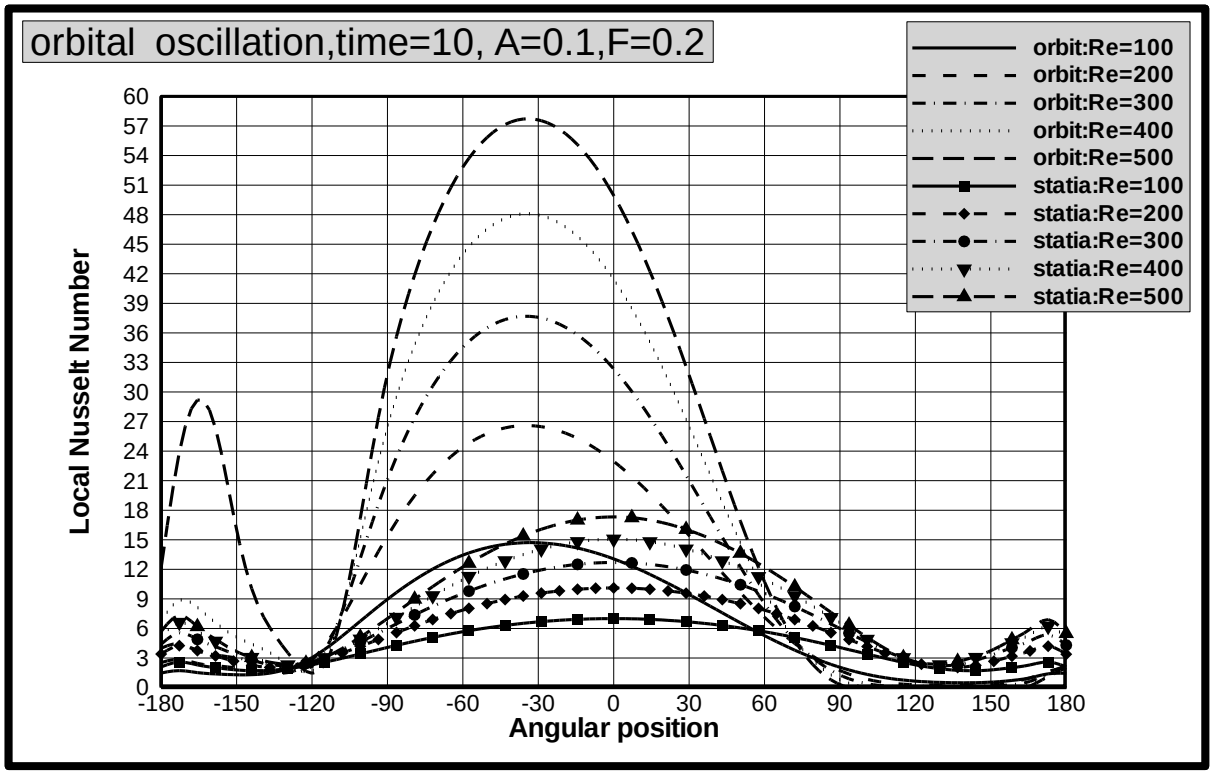

Fig.(٥-٤٥)Local Nusselt number profiles on the stationary and oscillating cylinder surface for multi-Reynolds with constant frequency and amplitude(F=٠.٢,A=٠.١)(orbital)

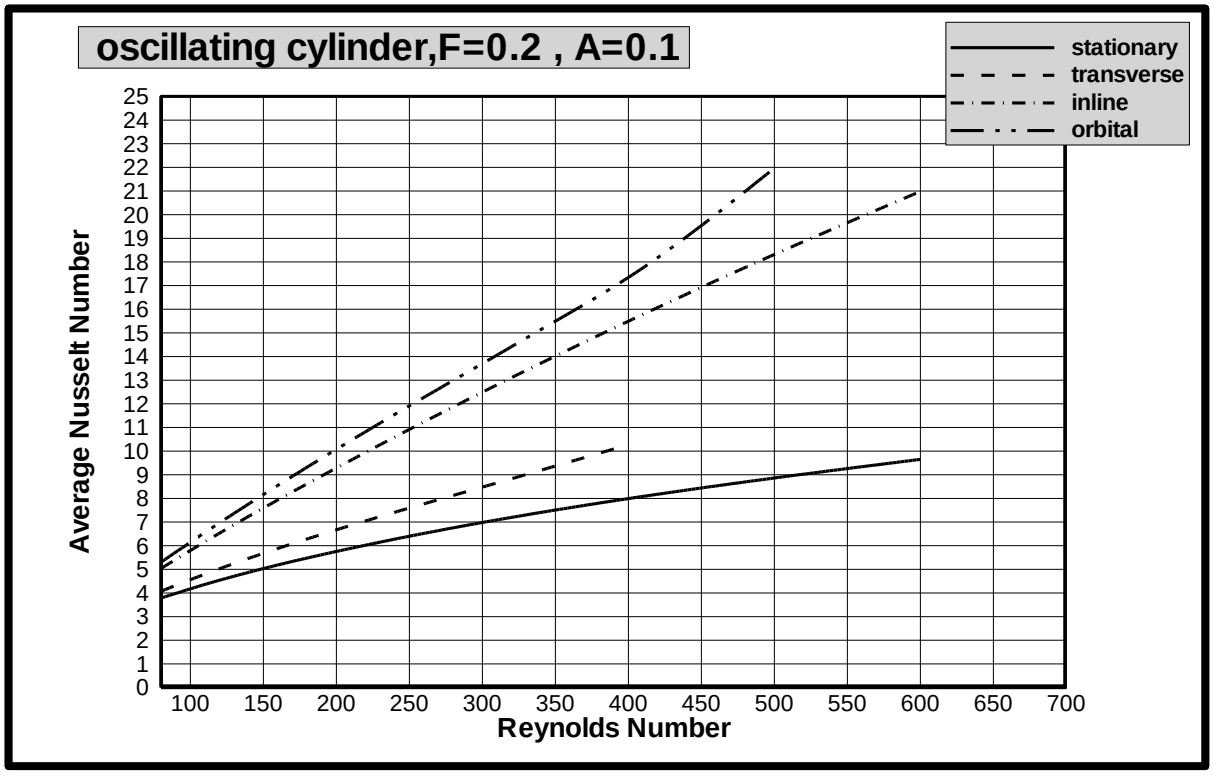

Fig.(٥-٤٦)Variation of average Nusselt number for stationary cylinder and oscillating cylinder in three direction(transverse, inline and orbital)

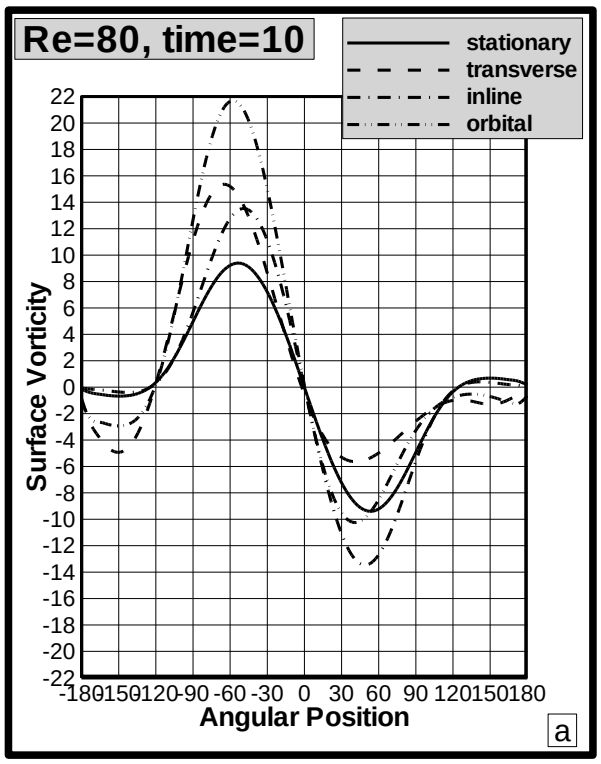
Re=80, time=10
stationary
transverse
inline
orbital
Surface Vorticity
Angular Position
a

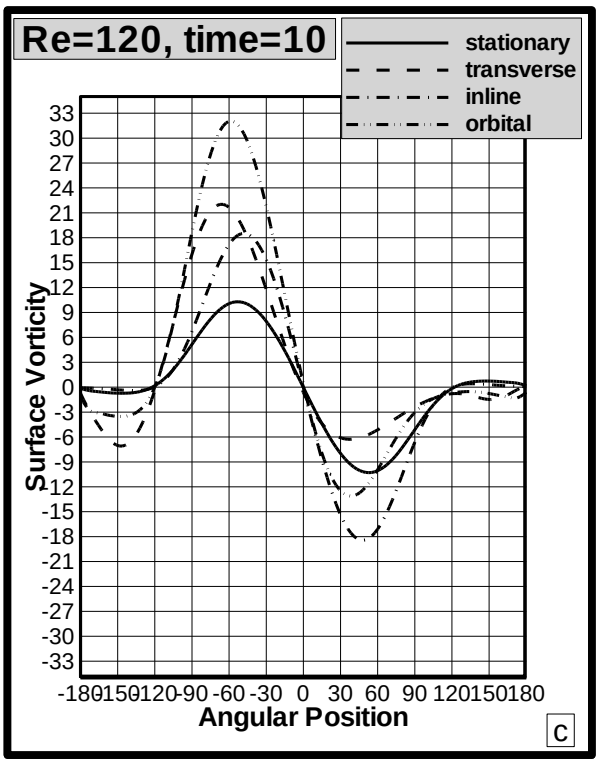
Re=120, time=10
stationary
transverse
inline
orbital
Surface Vorticity
Angular Position
c

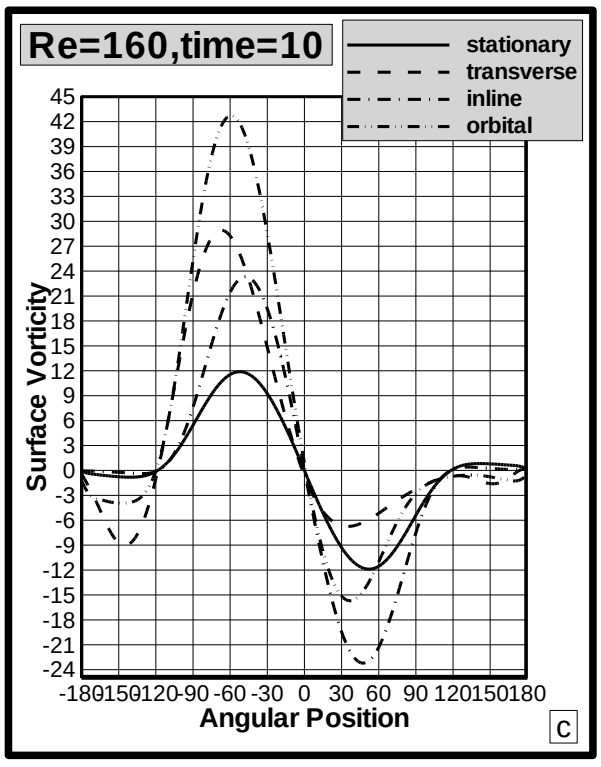
Re=160,time=10
stationary
transverse
inline
orbital
Surface Vorticity
Angular Position
c

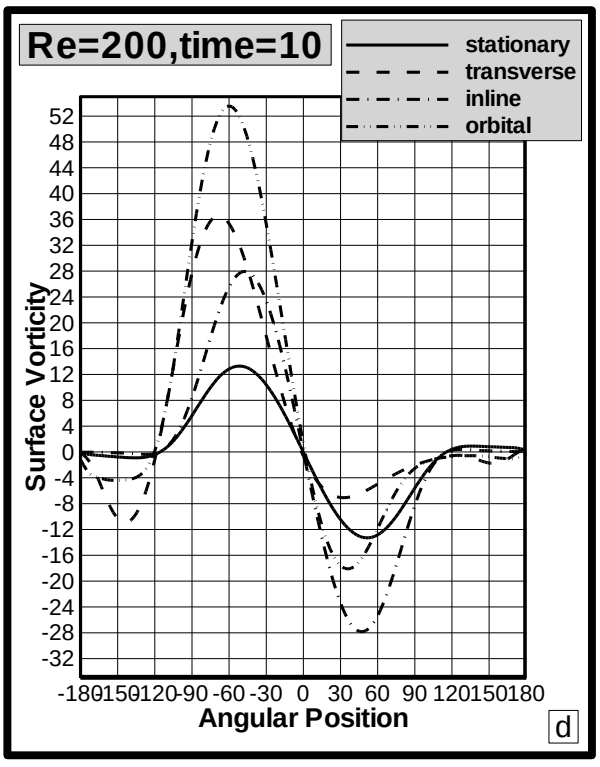
Re=200,time=10
stationary
transverse
inline
orbital
Surface Vorticity
Angular Position
d

Fig.(٥-٤٧)Surface vorticity distribution on the cylinder surface for different Reynolds number and different cases of cylinder oscillation at F=٠.٢ and A=٠.٢

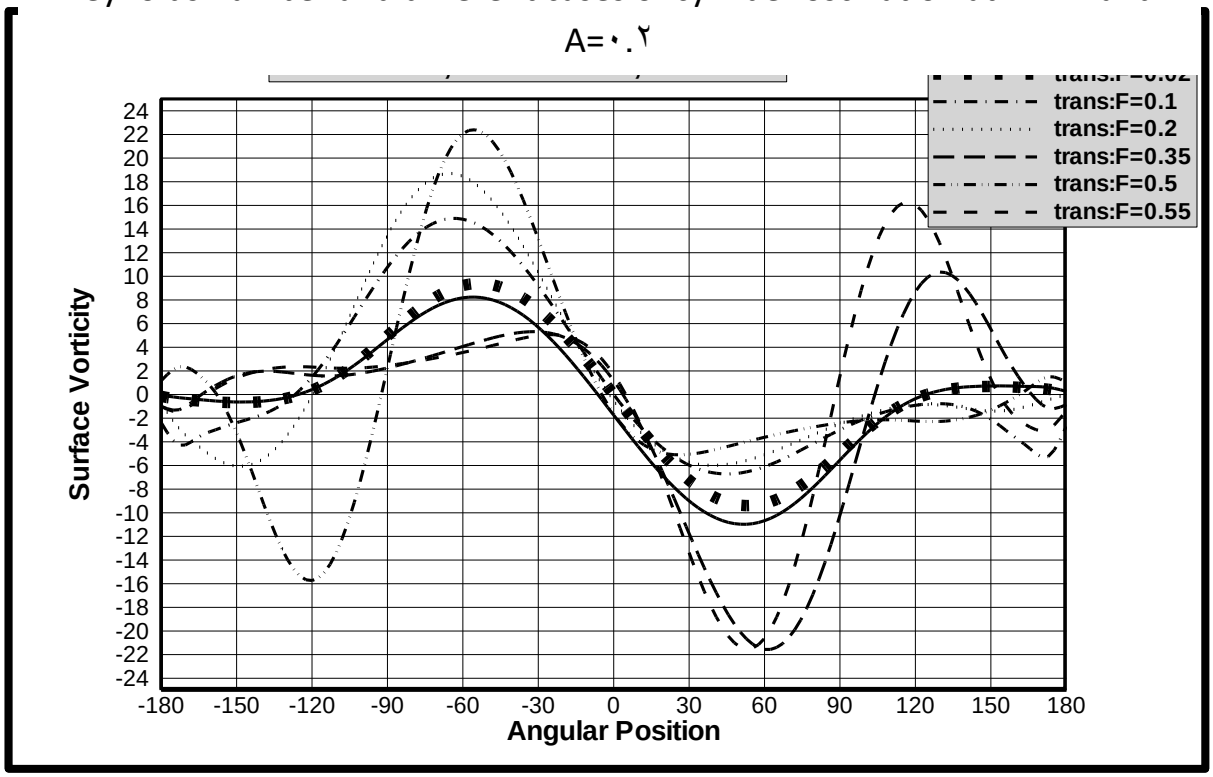

Fig.(٥-٤٨) Surface vorticity on the cylinder for Reynolds number =١٠٠ with constant amplitude (A=٠.٢)and different frequency(transverse).

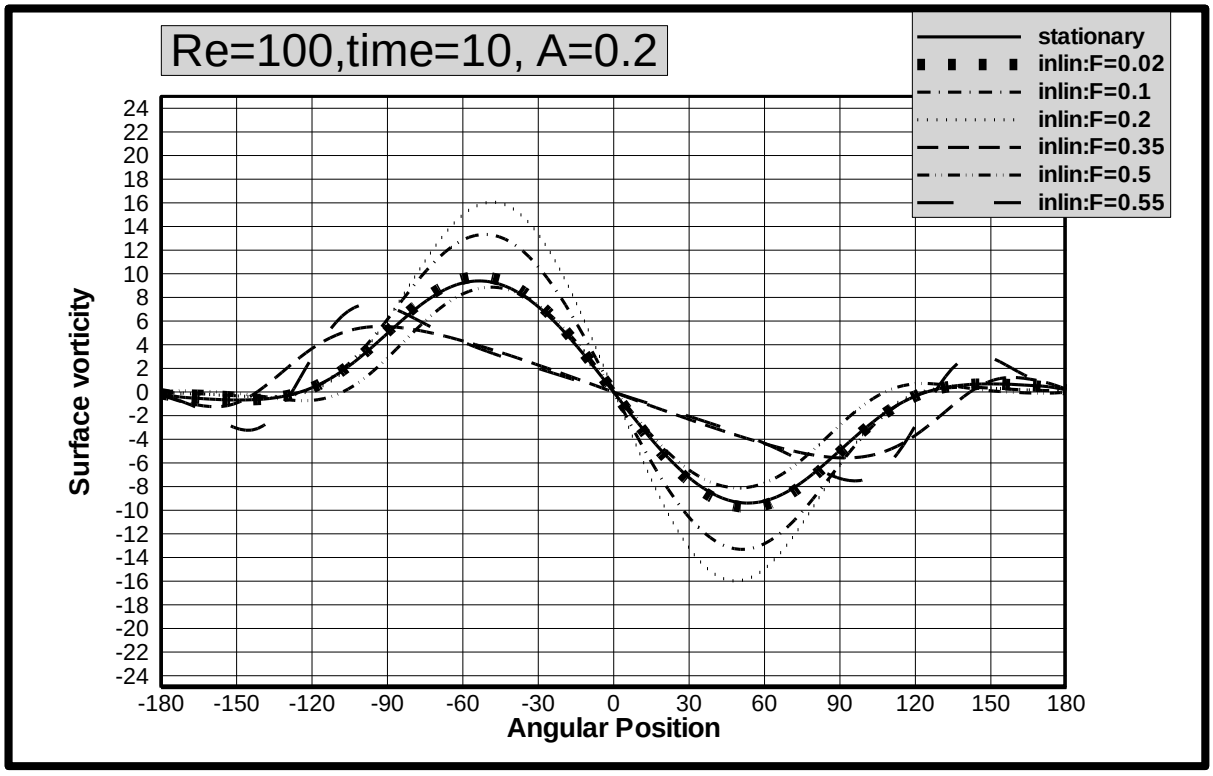

Fig.(٥-٤٩) Surface vorticity on the cylinder for Reynolds number =١٠٠ with constant amplitude (A=٠.٢)and different frequency(inline)

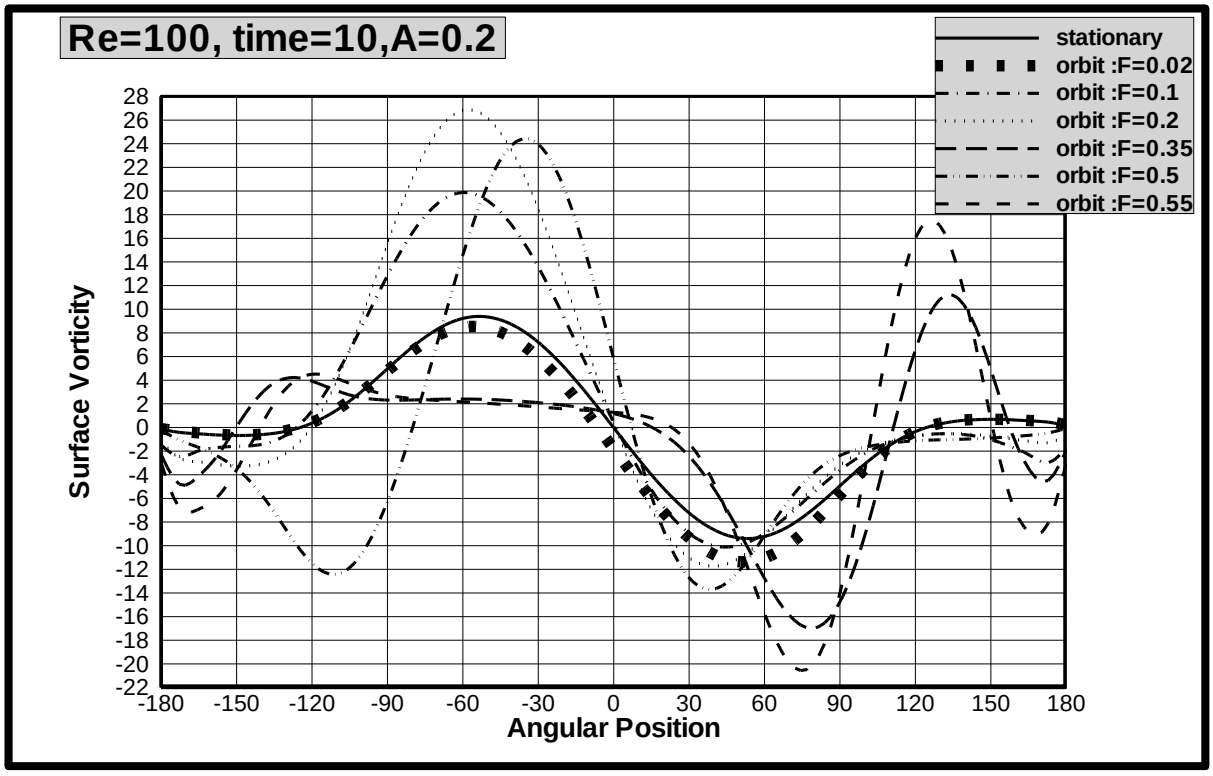

Fig.(٥-٥٠)Surface vorticity on the cylinder for Reynolds number =١٠٠ with constant amplitude (A=٠.٢)and different frequency(orbital)

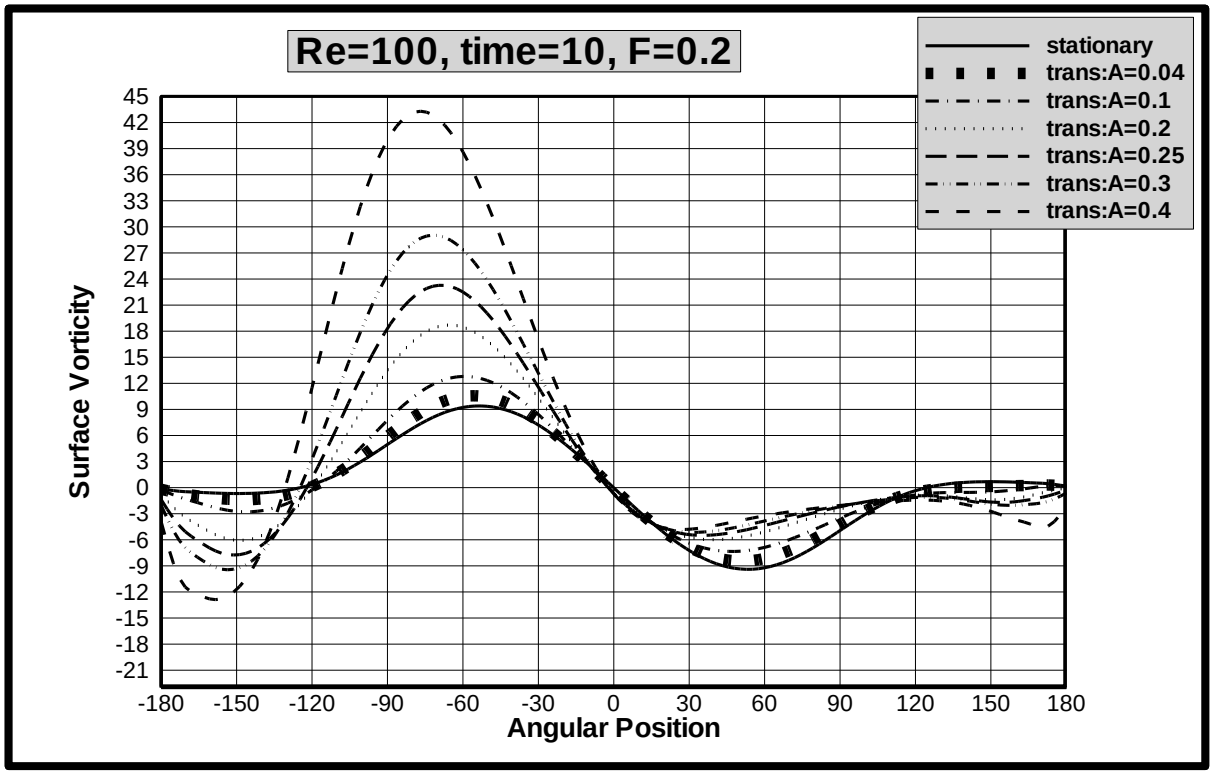

Fig.(٥-٥١)Surface vorticity on the cylinder for Reynolds number =١٠٠ with constant frequency(F=٠.٢)and different amplitude(transverse)

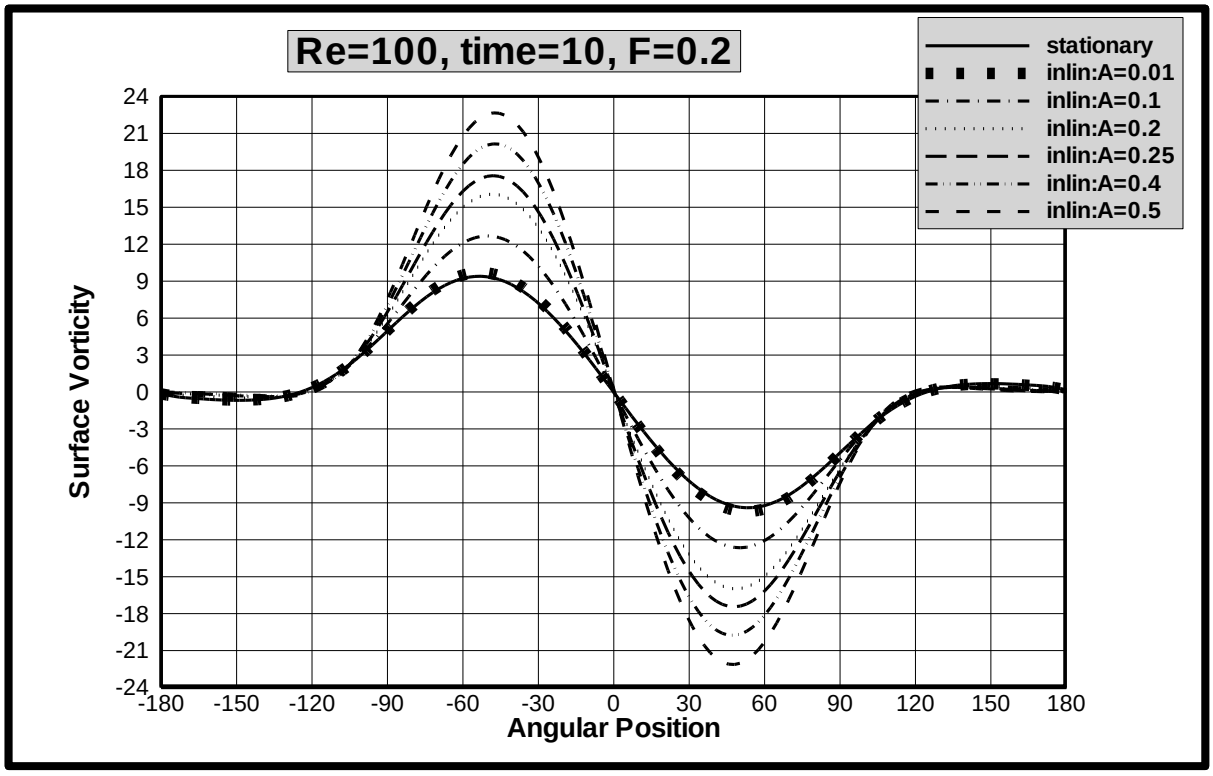

Fig.(٥-٥٢) Surface vorticity on the cylinder for Reynolds number =١٠٠ with constant frequency(F=٠.٢)and different amplitude(inline)

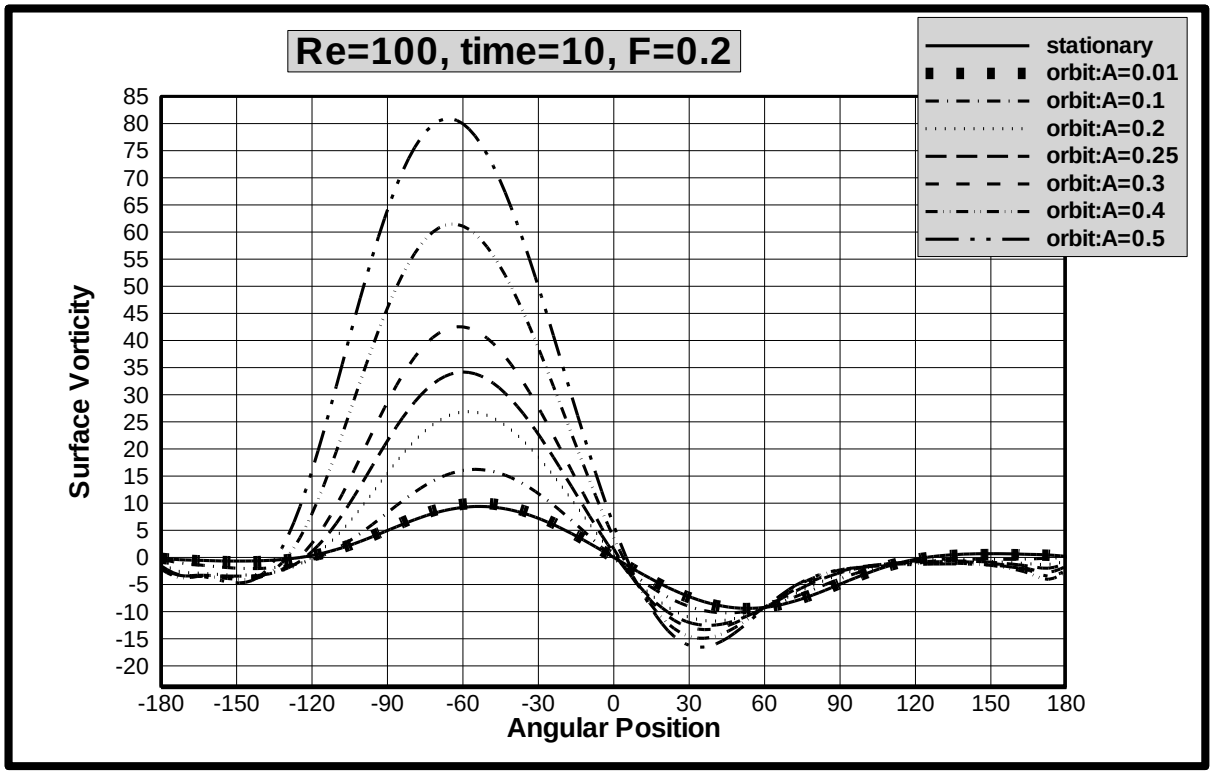

Fig.(٥-٥٣)Surface vorticity on the cylinder for Reynolds number =١٠٠ with constant frequency(F=٠.٢)and different amplitude(orbital)

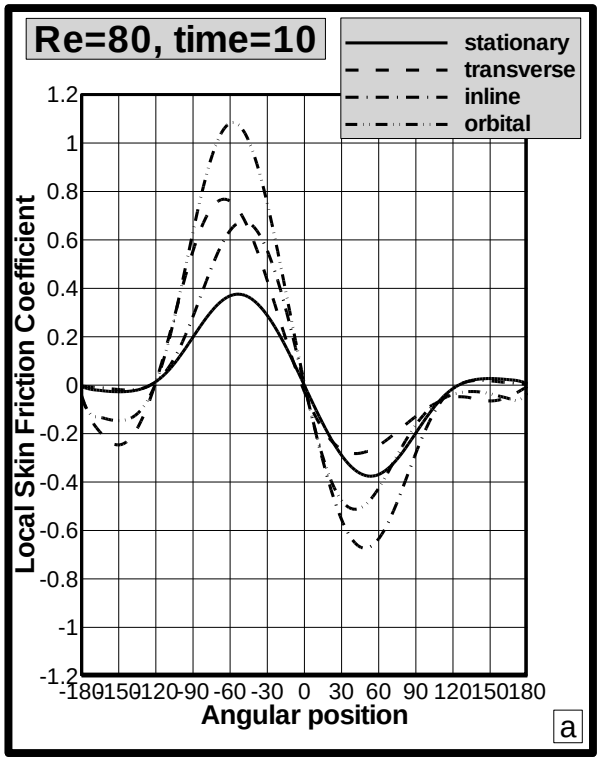
Re=80, time=10
stationary
transverse
inline
orbital
Local Skin Friction Coefficient
1.2
1
0.8
0.6
0.4
0.2
0
-0.2
-0.4
-0.6
-0.8
-1
-1.2
-180 -150 -120 -90 -60 -30 0 30 60 90 120 150 180
Angular position
a

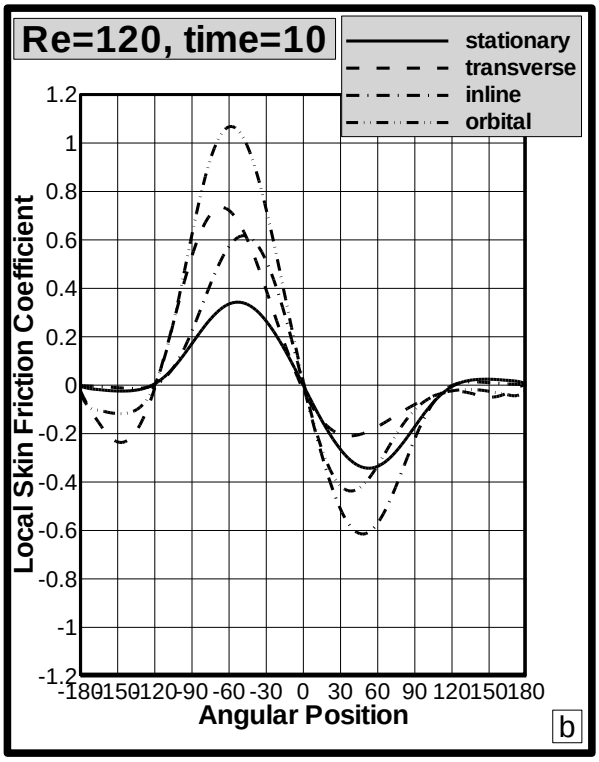
Re=120, time=10
stationary
transverse
inline
orbital
Local Skin Friction Coefficient
1.2
1
0.8
0.6
0.4
0.2
0
-0.2
-0.4
-0.6
-0.8
-1
-1.2
-180 -150 -120 -90 -60 -30 0 30 60 90 120 150 180
Angular Position
b

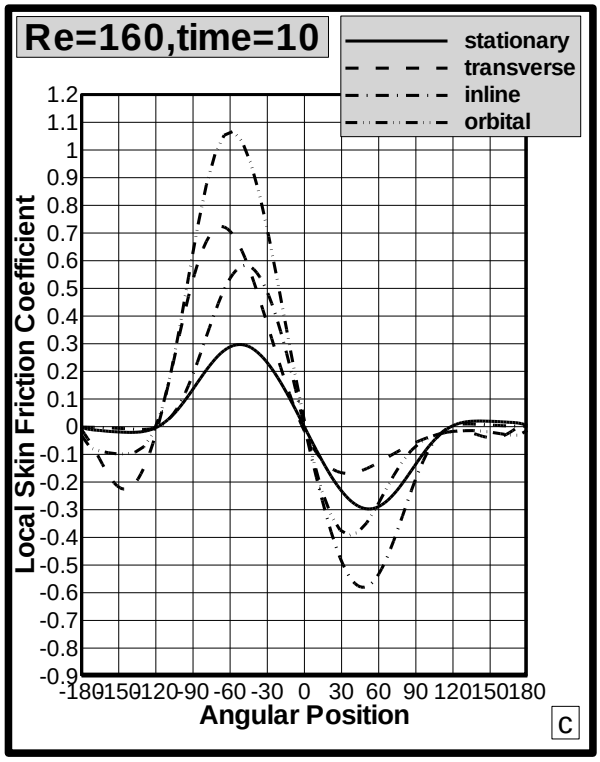
Re=160,time=10
stationary
transverse
inline
orbital
Local Skin Friction Coefficient
1.2
1.1
1
0.9
0.8
0.7
0.6
0.5
0.4
0.3
0.2
0.1
0
-0.1
-0.2
-0.3
-0.4
-0.5
-0.6
-0.7
-0.8
-0.9
-180 -150 -120 -90 -60 -30 0 30 60 90 120 150 180
Angular Position
c

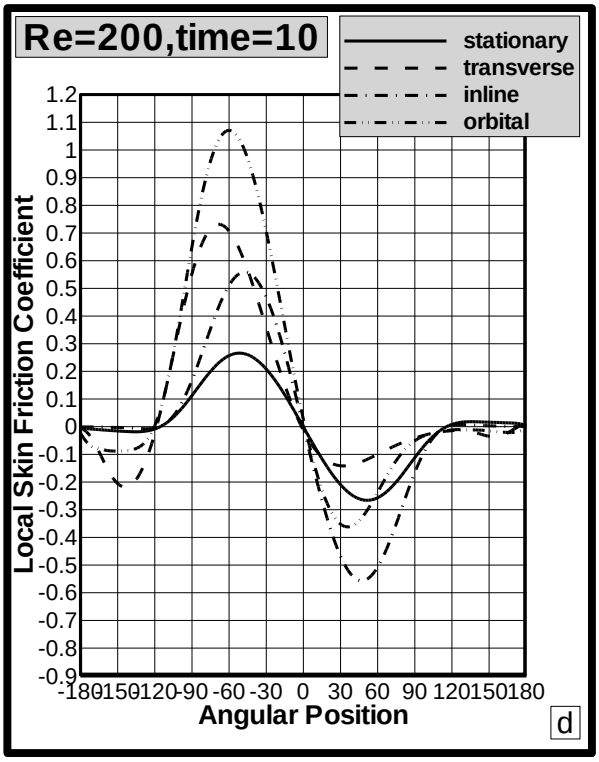
Re=200,time=10
stationary
transverse
inline
orbital
Local Skin Friction Coefficient
1.2
1.1
1
0.9
0.8
0.7
0.6
0.5
0.4
0.3
0.2
0.1
0
-0.1
-0.2
-0.3
-0.4
-0.5
-0.6
-0.7
-0.8
-0.9
-180 -150 -120 -90 -60 -30 0 30 60 90 120 150 180
Angular Position
d

Fig.(٥-٥٤)Local Skin Friction Coefficient distribution on the cylinder surface for different Reynolds number and different cases of cylinder oscillation at F=٠.٢ and A=٠.٢

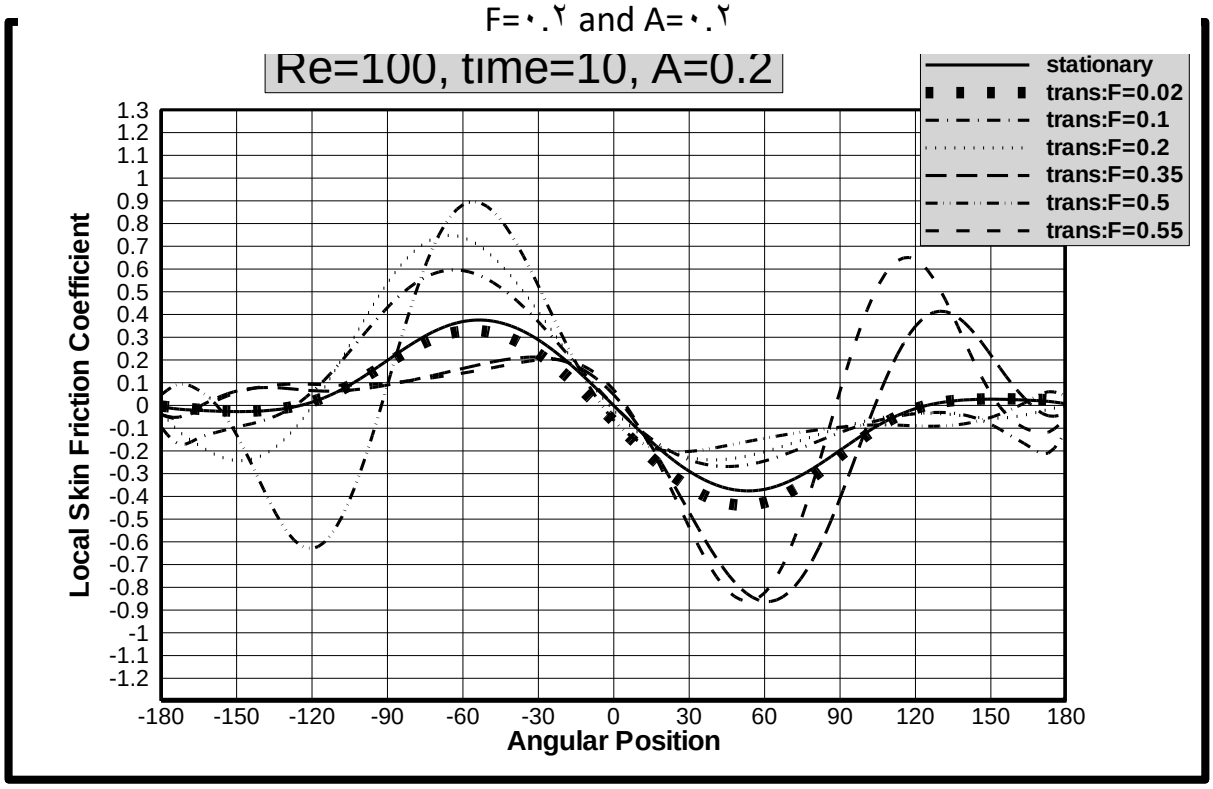

Fig.(٥-٥٥)Local skin friction coefficient distribution on the cylinder for Reynolds number =١٠٠ with constant amplitude (A=٠.٢)and different frequency(transverse)

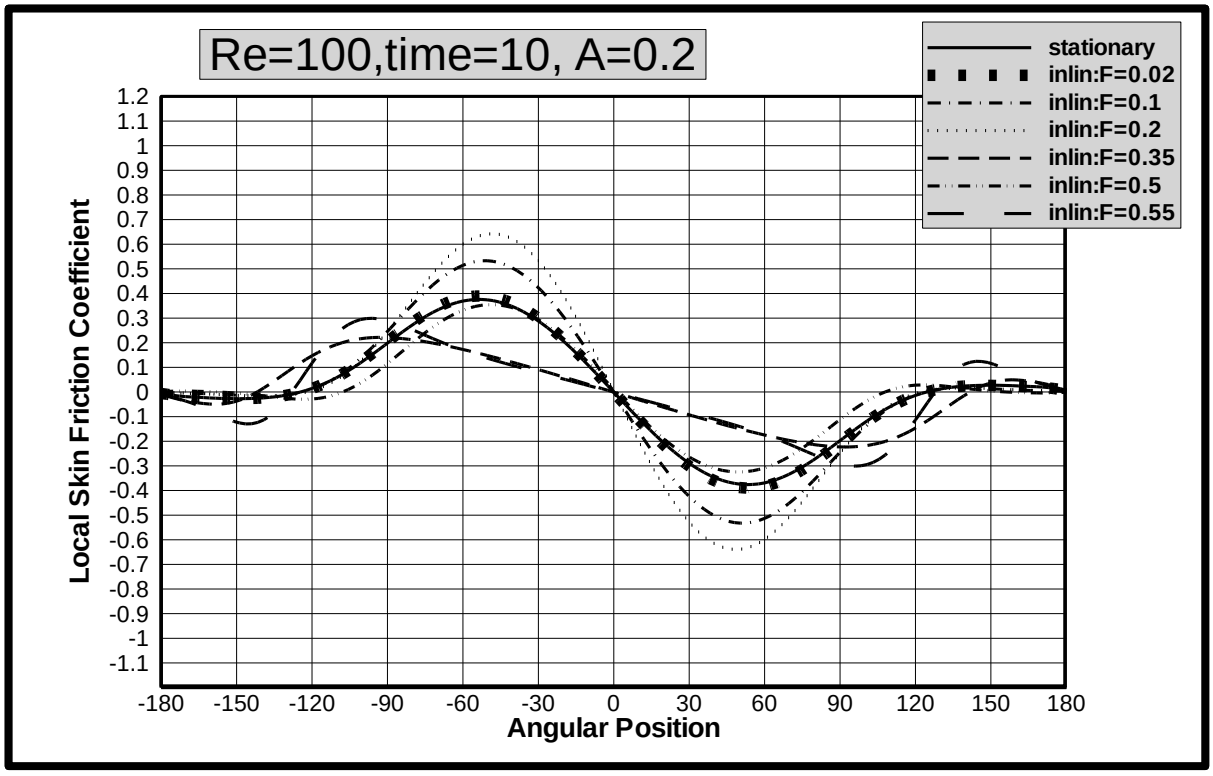

Fig.(٥-٥٦) Local skin friction coefficient distribution on the cylinder for Reynolds number =١٠٠ with constant amplitude (A=٠.٢)and different frequency(inline)

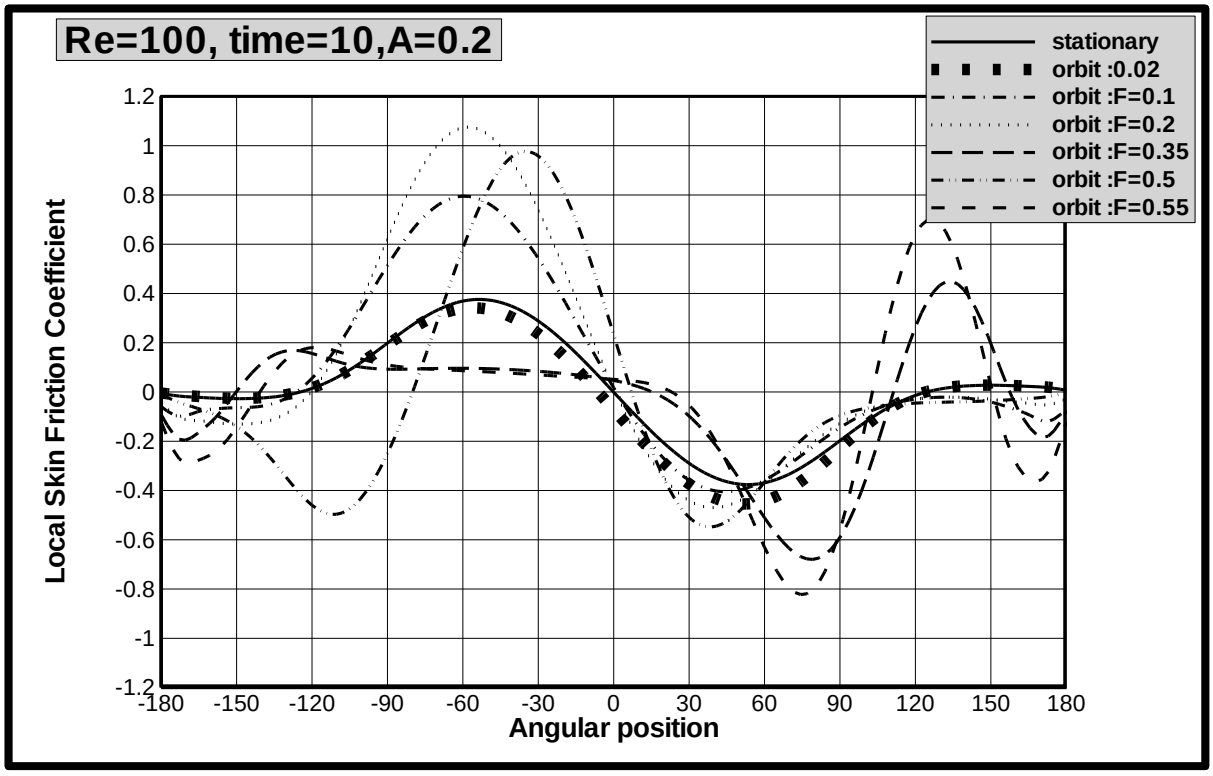

Fig.(٥-٥٧) Local skin friction coefficient distribution on the cylinder for Reynolds number =١٠٠ with constant amplitude (A=٠.٢)and different frequency(orbital)

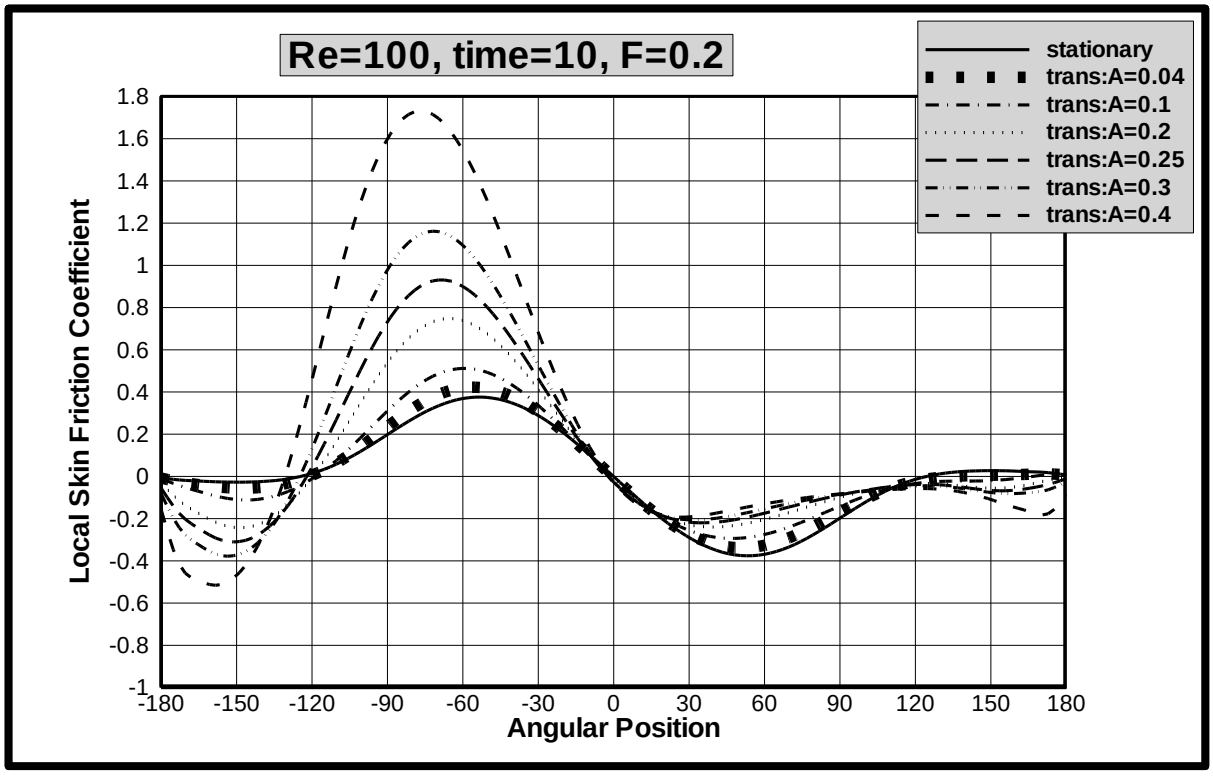

Fig.(٥-٥٨) Local skin friction coefficient distribution on the cylinder for Reynolds number =١٠٠ with constant frequency (F=٠.٢)and different amplitude(transverse)

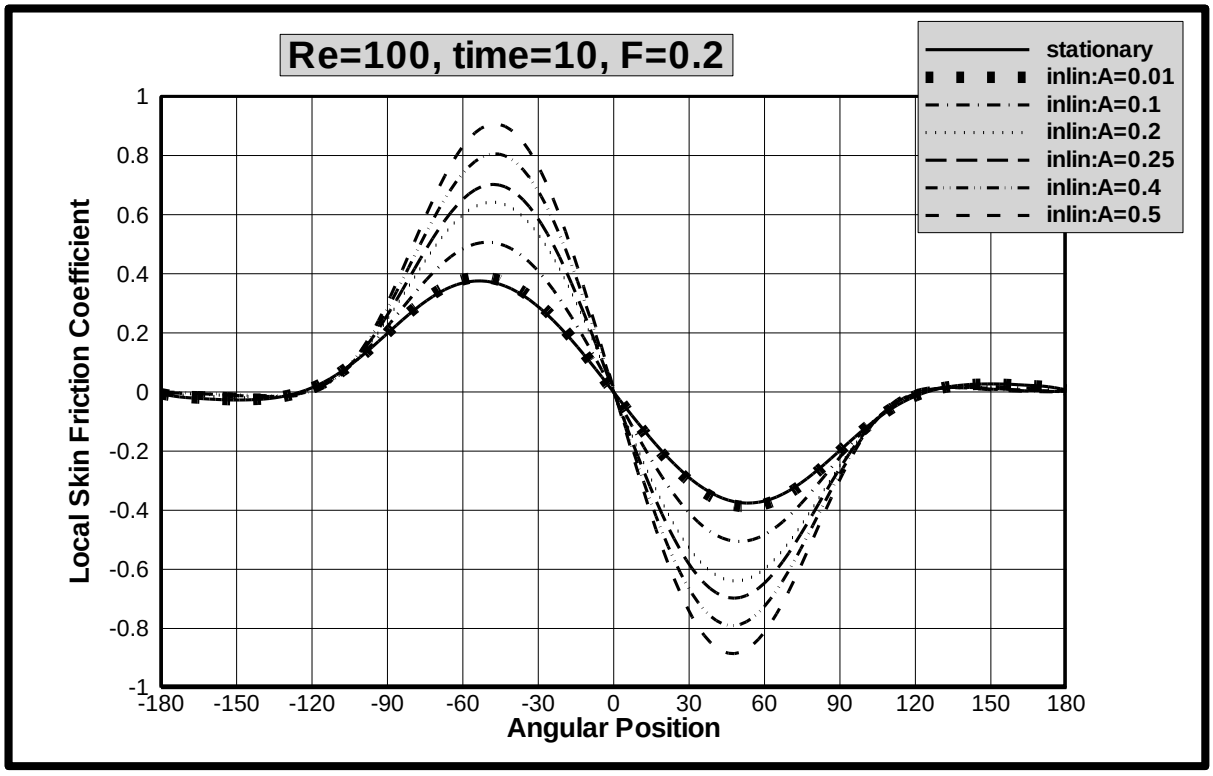

Fig.(٥-٥٩) Local skin friction coefficient distribution on the cylinder for Reynolds number =١٠٠ with constant frequency (F=٠.٢)and different amplitude(inline)

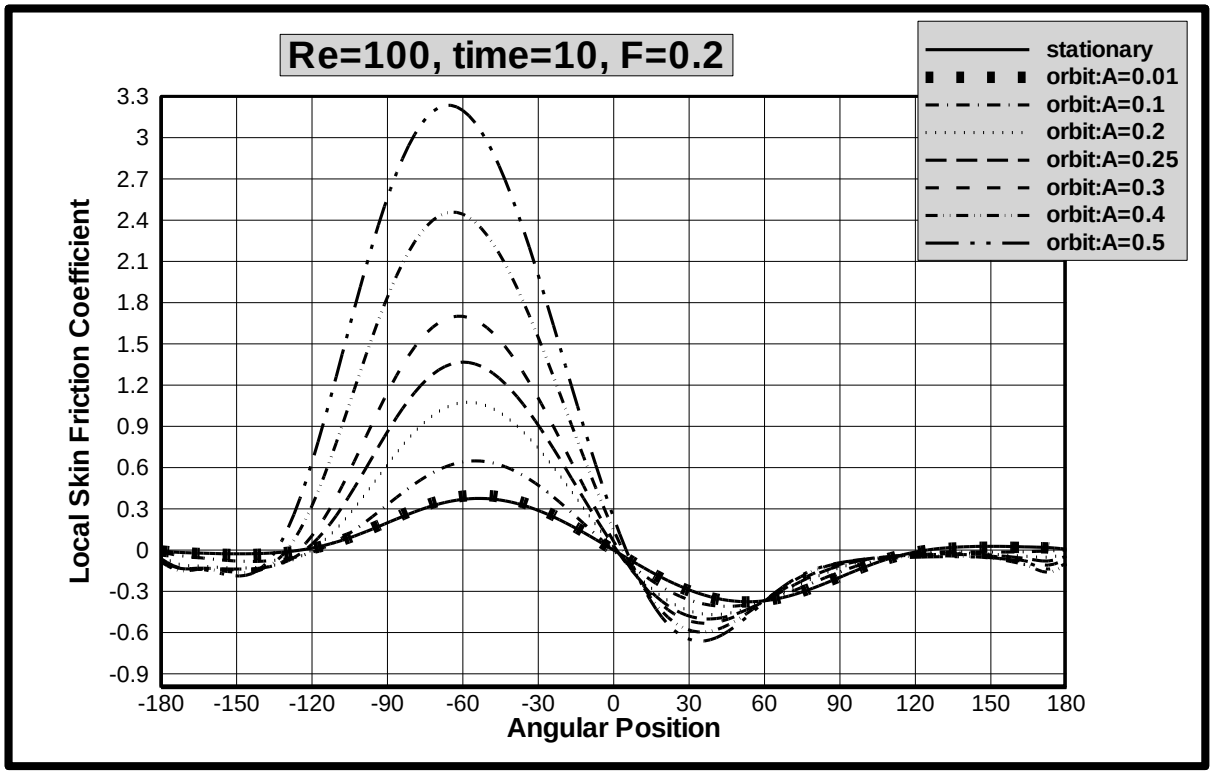

Fig.(٥-٦٠) Local skin friction coefficient distribution on the cylinder for Reynolds number =١٠٠ with constant frequency (F=٠.٢)and different amplitude(orbital)

CONCLUSIONS AND SUGGESTIONS FOR FUTURE WOEK

٦.١ Conclusions

A numerical, finite difference with time dependent grid approach has been utilized for solving the governing equations for forced convection around an isothermal surface of circular cylinder in cross flow. The cylinder oscillating in three direction transverse, inline and orbital. The results for local Nusselt number and local skin friction are obtained for Pr=٠.٧ (air). The ranges of Reynolds, reduced frequency and dimensionless amplitude are(٨٠ to ٦٠٠),(٠.٠ to ٠.٧)and(٠.٠ to ٠.٩)respectively. From these results, the following conclusions can be drawn:

١. The use of a time dependent grid technique leads to a successful finite difference simulation of moving boundary problems(oscillating cylinder in a viscous fluid).
٢. The interaction between the oscillation cylinder and vortex shedding from the cylinder dominates the state of the wake.
٣. For the range of conditions of this investigation, some of the local Nusselt numbers and the local skin friction coefficients were up to about ٧٨ percent and ٧٥ percent larger during oscillations than when the cylinder was at rest.

٤. For the range of conditions of this investigation, the oscillating velocity(that depends on reduced frequency "F" and dimensionless amplitude "A")of the cylinder is the major factor in the enhance of local Nusselt number and local skin friction. Also, the local Nusselt number is greater in case of orbital oscillating when compared with other cases.

٥. At the conditions used in the study, the entrainment process of the free stream into the wake is main reason to increase heat transfer rate.

٦. The large increase in heat transfer from the surface of oscillating cylinder can be correlated with the observation of vortices rolling-up close the base of the cylinder. The increase in heat transfer is believed to be result of energetic fluid of the vortices scrubbing away the normally stagnant and poor heat convecting fluid which normally resides at the base of the cylinder.

٧. The use of forced oscillation cylinder is a good method of enhancing heat convection from a heated cylinder.

٦.٢ Suggestions for Future Work

Following the conclusion of the present study, it becomes apparent that several important issues requires further investigation. The following points are suggested for future work:

١. The numerical work on forced convection around oscillating cylinder should be extended to study, the effect of oscillation on mixed and free convection heat transfer from heated cylinder.

٢. Solving the same problem by using another models such primitive variable or vorticity-velocity model .

٣. studying the effect of oscillation on multi-cylinder(tube bundle) and in multi configurations (such staggered or inline cylinders).

٤. Solving the same problem with higher frequency, amplitude and Reynolds number going to the turbulent flow regions.

٥. Investigating the effect of oscillating cylinder on the characteristic of compressible fluid.

References

١. **Shih,T.M.,** *"Numerical Heat Transfer."* Hemisphere publishing corporation, Washington, ١٩٨٤.

٢. **Mahfouz,F.M.** and **Badr,H.M.,** "Forced Convection from a Rotationally Oscillating Cylinder Placed in a Uniform Stream. " International Journal of Heat and Mass Transfer, Vol.٤٣,PP.٣٠٩٣-٣١٠٤,٢٠٠٠

٣. **Blevins,R.D.,** *"Flow-Induced Vibration."* ١st Ed., Van Nostrand Reinhold, New York,١٩٧٧.

٤. **Fu,W.-S.** and **Yang, S.-J.,** "Heat Transfer Induced by a Body Moving in Opposition to a Flowing Fluid. " International Journal of Heat and Mass Transfer, Vol.٤٤, PP.٨٩-٩٨,٢٠٠١.

٥. **Dennis,S.C.** and **Chang,G-Z,** "Numerical Solution for Steady Flow Past a Circular Cylinder at Reynolds Numbers up to ١٠٠." Journal of Fluids Mechanics,Vol.٤٢,Part ٣,PP.٤٧١-٤٨٩,١٩٧٠

٦. **Jain,P.C.** and **Goel,B.S.,** "Shedding of Vortices behind a Circular Cylinder." Journal of Computers and Fluids, Vol.٤,PP.١٣٧-١٤٢,١٩٧٦.

٧. **Jain,P.C.** and **Goel,B.S.,** "A Numerical Study of Unsteady Laminar Forced Convection From a Circular Cylinder. " Journal of Heat Transfer, Vol.٩٨,PP.٣٠٣-٣٠٧,١٩٧٦.

٨. **Patel,V.A.,** "Time-Dependent Solutions of The Viscous Incompressible Flow Past a Circular Cylinder by Method of Series Truncation." Journal of Computers and Fluids, Vol.٤,PP.١٣-٢٧,١٩٧٦.

٩. **Lin,C.L.,Pepper,D.W.** and **Lee,S.C.,** "Numerical Methods for Separated Flow Solutions around a Circular Cylinder." AIAA Journal, Vol.١٤ , No.٧ , PP. ٩٠٠-٩٠٧,١٩٧٦.

١٠. **Tuann,S.** and **Olson,M.D.,** "Numerical Studies of The Flow around a Circular Cylinder by a Finite-Element Method." Journal of Computers and Fluids,Vol.٦,PP.٢١٩-٢٤٠,١٩٧٨.

١١. **Ta Phuoc Loc** and **Bouard,R.,** "Numerical Solution of The Early Stage of The Unsteady Viscous Flow around a Circular Cylinder; a Comparison with Experimental Visualization and Measurements." Journal of Fluid Mechanics, Vol.١٦٠,PP.٩٣-١١٧,١٩٨٥.

١٢. **Karniadakis,G.,E.,** "Numerical Simulation of Forced Convection Heat Transfer from a Cylinder in Cross-Flow." International Journal of Heat and Mass Transfer, Vol.٣١,No.١,PP.١٠٧-١١٨,١٩٨٨.

١٣. **Rumsey,C.L.,** "Details of The Computed Flow Field over a Circular Cylinder at Reynolds Number ١٢٠٠." Journal of Fluids Engineering, Vol.١١٠ ,PP. ٤٤٦-٤٥٢,١٩٨٨.

١٤. **Chun,W.** and **Boehm,R.F.,** "Calculation of Forced Flow and Heat Transfer around a Cylinder in Cross Flow." Journal of Numerical Heat Tansfer,Vol.١٥,PP.١٠١-١٢٢,١٩٨٩.

١٥. **Lange,C.F.,Durst,F.** and **Breuer,M.,** " Momentum and Heat Transfer from Cylinders in Laminar Cross Flow at $١٠^{-٤} \leq Re \leq ٢٠٠$. "International Journal of Heat and Mass Transfer, Vol.٤١,PP.٣٤٠٩-٣٤٣٠,١٩٩٨.

١٦. **Baranyi,L.,** "Computation of Unsteady Momentum and Heat Transfer from a Fixed Circular Cylinder in Laminar Flow." Journal of Computational and Applied Mechanics,Vol.٤,No.١,PP.١٣-٢٥,٢٠٠٣.

١٧. **Hurlbut,S.E.,Spaulding,M.L.** and **White,F.M.,** "Numerical Solution for Laminar Two-Dimensional Flow about a Cylinder Oscillating in a Uniform Stream." Journal of Fluids Engineering,Vol.١٠٤,PP.٢١٤-٢٢٠, ١٩٨٢.

١٨. **Lecointe,Y.** and **Piquet,J.,** "On The Use of Several Compact Methods for The Study of Unsteady Incompressible Viscous Flow round a Circular Cylinder." Journal of Computers and Fluids,Vol.١٢,No.٤,PP.٢٥٥-٢٨٠, ١٩٨٤.

١٩. **Chilukuri,R.,** "Incompressible Laminar Flow Past a Transversely Vibrating Cylinder." Journal of Fluids Engineering,Vol.١٠٩,PP.١٦٦-١٧١,١٩٨٧.

٢٠. **Ongoren,A.** and **Rockwell,D.,** "Flow Structure from an Oscillating Cylinder; Part١:Mechanisms of Phase Shift and Recovery in The near Wake." Journal of Fluid Mechanics,Vol.١٩١,PP.١٩٧-٢٢٣,١٩٨٨.

٢١. **Ongoren,A.** and **Rockwell,D.,** "Flow Structure from an Oscillating Cylinder; Part٢:Mode Competition in The near Wake." Journal of Fluid Mechanics, Vol.١٩١,PP.٢٢٥-٢٤٥,١٩٨٨.

٢٢. **Lecointe,Y.** and **Piquet,J.,** "Flow Structure in The Wake of an Oscillating Cylinder." Journal of Fluids Engineering,Vol.١١١,PP.١٣٩-١٤٨,١٩٨٩.

٢٣. **Mittal,S.,Ratner,A.,Hastreiter,D.**and **Tezduyar,T.E.,** "Space-Time Finite Element Computation of Incompressible Flows with Emphasis on Flow

Involving Oscillating Cylinders." International Video Journal of Engineering Research,Vol.١,PP.٨٣-٩٦,١٩٩١.

٢٤. **Mittal,S.** and **Tezduyar,T.E.,** "A Finite-Element Study of Incompressible Flow Past Oscillating Cylinders and Aerofoils." International Journal of Numerical Methods in Fluids,Vol.١٥,PP.١٠٧٣-١١١٨,١٩٩٢.

٢٥. **Mittal,S.**and **Kumar,V.,** "Finite-Element Study of Vortex-Induced Cross-Flow and In-Line Oscillations of a Circular Cylinder at Low Reynolds Numbers." International Journal For Numerical Methods in Fluids,Vol.٣١, PP.١٠٨٧-١١٢٠,١٩٩٩.

٢٦. **Blackburn,H.M.** and **Henderson,R.D.,** "A Study of Two-Dimensional Flow past an Oscillating Cylinder." Journal of Fluid Mechanics,Vol.٣٨٥, PP.٢٥٥-٢٨٦,١٩٩٩.

٢٧. **Mittal,S.** and **Kumar,V.,** "Flow-Induced Vibrations of a Light Circular Cylinder at Reynolds Numbers $١٠^{٣}$to$١٠^{٤}$." Journal of Sound and Vibration, Vol.٢٤٥,No.٥,PP.٩٢٣-٩٤٦,٢٠٠١.

٢٨. **Sreenivasan,K.** and **Ramachandran,A.,** "Effect of Vibration on Heat Transfer from Horizontal Cylinder to a Normal Air Stream." International Journal of Heat and Mass Transfer, Vol.٣,PP.٦٠-٦٧,١٩٦١.

٢٩. **Kezios,S.P.** and **Prasanna,K.V.,** "Effect of Vibration on Heat Transfer from a Cylinder in Normal Flow." Journal of Heat Transfer, ASME Paper No.٦٦-WA/HT-٤٣,١٩٦٦.As cited in ref.[٣٩]

٣٠. **Saxena,U.C.** and **Laird, A.D.K.,** "Heat Transfer from a Cylinder Oscillating in a Cross Flow." Journal of Heat Transfer, Vol.١٠٠,PP.٦٨٤-٦٨٩,١٩٧٨.

٣١. **Michaelides,E.E., Chang,Y.** and **Bosworth,R.T.,** "Heat Transfer Coefficients and Friction Factors for Banks of Flexible Vibrating Tubes in Cross Flow."٨^{th} International Heat Transfer Conference,Vol.٦,PP.٢٧٥٧-٢٧٦٢, ١٩٨٦.

٣٢. **Chang,Y.,Beris,A.N.**and **Miachaelides,E.E.** "A Numerical Study of Heat and Momentum Transfer for Flexible Tube Bundles in Cross Flow." International Journal of Heat and Mass Transfer, Vol.٣٢ ,No.١١, PP.٢٠٢٧-٢٠٣٦,١٩٨٩.

٣٣. **Karanth,D.,Rankin,G.W.** and **Sridhar,K.,** "A Finite Difference Calculation of Force Convective Heat Transfer from Oscillating Cylinder." International Journal of Heat and Mass Transfer,Vol.٣٧,No.١١,PP.١٦١٩-١٦٣٠,١٩٩٤. As cited in ref.[٣٩].

٣٤. **Cheng,C.H.,Chen,H.N.**and **Aung,W.,** "Experimental Study of the Effect of Transverse of Oscillation on Convection Heat Transfer from a Circular Cylinder." Journal of Heat Transfer,Vol.١١٩,PP.٤٧٤-٤٨٢,١٩٩٧.As cited in ref.[٣٩].

٣٥. **Cheng,C.H.** and **Hong,J.L.,** "Numerical Prediction of lock-on Effect on Convective Heat Transfer from a Transversely Oscillating Circular Cylinder." International Journal of Heat and Mass Transfer, Vol.٤٠,No.٨,PP.١٨٢٥-١٨٣٤,١٩٩٧.

٣٦. **Park,H.G.,** "A Study of Heat Transfer Processes in The Wake of a Stationary and Oscillating Circular Cylinder Using Digital Particle Velocimetry/thermometry." Ph.D. Thesis, California Institute of Technology,١٩٩٨.

٣٧. **Gau,C.,Wu,J.M.** and **Liang,C.Y.,** "Heat Transfer Enhancement and Vortex Flow Structure over a Heated Cylinder Oscillating in The Cross Flow Direction." Journal of Heat Transfer,Vol.١٢١,PP.٧٨٩-٧٩٥,١٩٩٩.As cited in ref.[٣٩].

٣٨. **Fu,W.S.** and **Tong,B.H.,** "Numerical Investigation of Heat Transfer from a Heated Oscillating Cylinder in a Cross Flow. " International Journal of Heat and Mass Transfer, Vol.٤٥,PP.٣٠٣٣-٣٠٤٣,٢٠٠٢.

٣٩. **Pottebaum,T.S.,** "The Relationship between Near-Wake Structure and Heat Transfer for an Oscillating Circular Cylinder in Cross-Flow." Ph.D Thesis, California Institute of Technology, Pasadena, California,٢٠٠٣.

٤٠. **Fu,W.S.** and **Tong,B.H.,** "Numerical Investigation of Heat Transfer Characteristics of The Heated Blocks in The Channel with a Transversely Oscillating Cylinder. " International Journal of Heat and Mass Transfer,Vol.٤٧,PP.٣٤١-٣٥١,٢٠٠٤.

٤١. **Ferziger,J.H.** and **Peric,M.,** *"Computational Methods for Fluid Dynamics."* ٣rd ed.,Springer-Verlag,Berlin,٢٠٠٢.

٤٢. **Thompson,J.F., Thames,F.C.,**and **Mastin,C.W.,** "Automatic Numerical Generation of Body-Fitted Curvilinear Coordinate System for Field containing any Number of Arbitrary Two-Dimensional Bodies." Journal of Computational Physics,Vol.١٥,PP.٢٩٩-٣١٩,١٩٧٤.

٤٣. **Tannehill,J.C. Holst,T.L.** and **J.V. Rakich** "Numerical Computation of Two-Dimensional Viscous Blunt Body Flows with an Impinging Shock." AIAA Journal, Vol.١٤,No.٢,PP.٢٠٤-٢١١,١٩٧٦.

٤٤. **Steger,J.L.** and **Bailey,H.E.,** "Calculation of Transonic Aileron Buzz." AIAA Journal ,Vol.١٨,No.٣,PP.٢٤٩-٢٥٥,١٩٨٠.

٤٥. **Hindman,R.G.,Kutler,P.**and **Anderson,D.A.,** "Two-Dimensional Unsteady Euler-Equation Solver for Arbitrarily Shaped Flow Regions." AIAA Journal, Vol.١٩,No.٤,PP.٤٢٤-٤٣١,١٩٨١.

٤٦. **Chyu,W.J.,Davis,S.S.** and **Chang,K.S.,** "Calculation of Unsteady Transonic Flow over an Airfoil." AIAA Journal, Vol.١٩,No.٦, PP.٦٨٤-٦٩٠,١٩٨١.

٤٧. **Patanker,S.V.,** *"Numerical Heat Transfer and Fluid Flow."* Hemisphere, Washington,D.C.,١٩٨٠.

٤٨. **Michael,S. Pantazopoulos,** "Vortex-Induced Vibration Parameters; Critical Review." Offshore Technology,ASME,OMAE,Vol.١,PP.١٩٩-٢٥٥,١٩٩٤.

٤٩. **Schlichting,H.,** *"Boundary-Layer Theory."* ٦th ed., McGraw-Hill, New York, ١٩٦٨.

٥٠. **Yuan,S.W.,** *"Foundation of Fluid Mechanics."* Prentice-Hall, New Delhi, India,١٩٧٦.

٥١. **Iatridis,L.M.,** "A Theoretical Study of Buoyancy Driven Circulation in a Liquid Drop." M.Sc. Thesis, University of Liverpool,١٩٨٧.

٥٢. **Bose,T.K.,** *"Computational Fluid Dynamics."* ١st Ed., Wiley, New Delhi, India,١٩٨٨.

٥٣. **Anderson,Dale,A.,John,C.,Tannehill** and **Richard,H.,Pletcher,** *"Computational Fluid Mechanics and Heat Transfer."* ٢nd Ed. McGraw-Hill,NewYork,١٩٩٧.

٥٤. **Roache,P.J.,** *"Computational Fluid Dynamics."* Hermosa, Albuquerque, New Mexico,١٩٧٢.

٥٥. **Pozrikidis,C.,** *"Introduction to Theoretical and Computational Fluid Dynamics."* Oxford University Press, Inc.,١٩٩٧.

٥٦. **Hoffmann,K.A.,** *"Computational Fluid Dynamics for Engineers."* Engineering Education System,Austin,Texas,١٩٨٩.

٥٧. **Launder,B.E.** and **Massey,T.H.,** "The Numerical Prediction of Viscous Flow and Heat Transfer in Tube Banks." Journal of Heat Transfer,Vol.١٠٠, PP.٥٦٥-٥٧١,١٩٧٨.

٥٨. **Papantonis,D.E.** and **Athanassiadis,N.A.,** " A Numerical Procedure for Generation of Body-Fitted Coordinate Systems with Direct Determination of Grid Points on The Boundary." International Journal of Numerical Methods in Fluids,Vol.٥,PP.٢٤٥-٢٥٥,١٩٨٥.

٥٩. **Fletcher,C.A.,** *"Computational Techniques for Fluid Dynamics,*Vol.٢; *Specific Techniques for Different Flow Categories."* Springer-Verlag, Berlin,١٩٨٨.

٦٠. **Anderson, John D.,Jr.,** *"Computational Fluid Dynamics; The Basics with Applications."* McGraw-Hill, New York,١٩٩٥.

٦١. **Thames,F.C., Thompson,J.F., Mastin,W.C.** and **Walker,R.L.,** "Numerical Solutions for Viscous and Potential Flow about Arbitrary Two-Dimensional Bodies Using Body Fitted Coordinate Systems." Journal of Computational Physics,Vol.٢٤,PP.٢٤٥-٢٧٣,١٩٧٧.

٦٢. **Steger,J.L.,** "Implicit Finite Difference Simulation of Flow about Arbitrary Two-Dimensional Geometries." AIAA Journal, Vol.١٦,No.٧,PP.٦٧٩-٦٨٦, ١٩٧٨.

٦٣. **Petrovic,Z.** and **Stupar,S.,** *"Computational Fluid Dynamics One."* Mechanical Engineering Faculty, Belgrade,١٩٩٦.

٦٤. **Broughton,R.C.** and **Oliver,A.J.,** "A Numerical Model for Convection in Complex Geometries and its Application to Buoyancy Flow in a Power Cable." ٨^{th} International Heat Transfer Conferences,Vol.٢,PP.٤٤٧-٤٥١,١٩٨٦.

٦٥. **Rangwalla,A.A.** and **Munson,B.R.,** "Numerical Solution for Viscous Flow for Two-Dimensional Domains Using Orthogonal Coordinate Systems." Journal of Computational Physics,Vol.٧٠,PP.٣٧٣-٣٩٦,١٩٨٧.

٦٦. **Thompson,J.F.,Warsi,Z.U.A** and **Mastin,C.W.,** "Boundary Fitted Coordinate Systems for Numerical Solutions of Partial Differential Equations-a Review." Journal of Computational Physics,Vol.٤٧,PP.١-١٠٨,١٩٨٢.

٦٧. **Thompson,J.F.,Warsi,Z.U.A.** and **Mastin,C.W.,** *"Numerical Grid Generation Foundation and Applications."* North-Holland,١٩٨٥.

٦٨. **Roache,P.J.** and **Mueller,T.J.,** "Numerical Solutions of laminar Separated Flows." AIAA Journal, Vol.٨,No.٣,PP.٥٣٠-٥٣٨,١٩٧٠.

٦٩. **Hornbeck,R.W.,** *"Numerical Marching Techniques for Fluid Flows with Heat Transfer."* NASA SP-٢٩٧, Washington,D.C.,١٩٧٣.

٧٠. **Incropera, F.P.** and **Dewitt, D.P.,** *"Fundamentals of Heat and mass Transfer."* ٤th Ed., John Wiley and Sons, New York, ١٩٩٦.

٧١. **Cebeci,T.** and **Bradshaw,P.,** *"Physical and Computational Aspects of Convective Heat Transfer."* Springer-Velag, New York,١٩٨٤.

٧٢. **Chapra,S.C.** and **Canale,R.P.,** *"Numerical Methods for Engineers."* ٢nd ed., McGraw-Hill, New York,١٩٨٨.

٧٣. **Baek,S.J.** and **Sung,H.J.,** "Numerical Simulation of The Flow behind a Rotary Oscillating Circular Cylinder." Physics of Fluids,Vol.١٠,No.٤, PP.٨٦٩-٨٧٦,١٩٩٨.

٧٤. **Waqar Ahmed,K, "**Modeling of Fluid Flow and Heat Transfer for Optimization Pin-Fin Heat Sink." Ph.D. Thesis, University of Waterloo, Waterloo, Ontario, Canada, ٢٠٠٤

٧٥. **Baranyi,L. "**Numerical Simulation of Flow Past A Cylinder in Orbital Motion." Journal of Computational and Applied Mechanics, Vol.٥,No.٢, PP.٢٠٩-٢٢٢,٢٠٠٤